Synthesis, structure and catalytic activity of new lanthanide alkynylamidinates

Dissertation

zur Erlangung des akademischen Grades

doctor rerum naturalium

(Dr. rer. nat.)

von **M.Sc. Farid Mohamed Ahmed Sroor**

geb. am 01.04.1982 in Sohag

genehmigt durch die Fakultät für Verfahrens- und Systemtechnik
der Otto-von-Guericke-Universität Magdeburg

Gutachter:
Prof. Dr. rer. nat. habil. Frank T. Edelmann
Prof. Dr. rer. nat. habil. Peter W. Roesky
PD Dr. rer. nat. habil. Edgar Haak

eingereicht am: 01.04.2015
Promotionskollqium: 27.05.2015

Table of Contents

Acknowledgments		I
Abbreviations		II
Abstract		III
1.	**Introduction**	1
2.	**Results and discussion**	9
2.1.	Synthesis and structural characterization of new lithium amidinate and guanidinates	9
2.1.1.	A new lithium alkynylamidinates	9
2.1.2.	New lithium guanidinate	15
2.2	Synthesis and structural characterization of lanthanide(III)-bis(amidinate) complexes	18
2.2.1.	Lanthanide(III)-bis(cyclopropylethinylamidinate) complexes	18
2.2.2.	A europium(III)-bis(cyclopropylethinylamidinate) complex	24
2.2.3.	A cerium(III)-bis(diiminophosphinate) complex	26
2.2.4.	A holmium(III)-(amidinatoguanidinate) complex	28
2.3.	Synthesis and structural characterization of lanthanide(III)-tris(amidinate) complexes	30
2.3.1.	Lanthanide(III)-tris(cyclopropylethinylamidinate) complexes	30
2.3.2.	Lanthanide(III)-tris(propiolamidinate) complexes	36
2.4.	Lanthanide(III)-bis(cyclopropylethinylamidinato)amide complexes	40
2.5.	Synthesis and structural characterization of (COT)lanthanide(III) amidinate complexes	45
2.5.1.	Synthesis and structure of (COT)Ln[μ-*c*-C_3H_5-C≡C-C$(NR)_2]_2$Li(S) complexes	45
2.5.2.	Synthesis and structure of (μ-η^8:η^8-COT)[Ce{*c*-C_3H_5-C≡C-C$(NR)_2\}_2]_2$ complexes	48
2.5.3.	Synthesis and structure of [(COT)Ln(μ-*c*-C_3H_5-C≡C-C$(NR)_2)]_2$ complexes	53
2.5.4.	Synthesis and structure of (COT)Ho[*c*-C_3H_5-C≡C-C$(NR)_2$](THF) complexes	62
2.5.5.	Synthesis and structure of [(μ-η^8:η^8-COT){Nd(*c*-C_3H_5-C≡C-C$(NR)_2$)(μ-Cl)$\}_2]_4$	64
2.6.	Catalytic activity of lanthanide(III) amidinate complexes	68
2.6.1.	Catalytic activity of lanthanide(III)-bis(cyclopropylethinylamidinate) complexes	68
2.6.2.	Catalytic activity of lanthanide(III)-tris(cyclopropylethinylamidinate) complexes	74
3.	**Summary**	78
4.	**Experimental section**	89
5.	**Crystal data and refinement details**	114
6.	**References**	139
7.	**List of publications**	147

Acknowledgments

All the gratitude and special appreciation are to my supervisor Prof. Dr. Frank T. Edelmann for his time and his generosity. He has been a tremendous mentor for me. I would like to thank him for encouraging my research and for allowing me to grow as a research scientist. I was proud to work in his research group under his guidance. Special thanks to him for allowing me to express my own ideas in the thesis.

A special thanks to my family. Words cannot express how grateful I am with my mother and my beloved wife "Shaimaa" for all of the sacrifices that they have made on my behalf. Their prayer for me was what sustained me thus far. They were always the biggest supporting icons to overcome all the difficulties.

I gratefully acknowledge the financial support of the German Academic Exchange Service (DAAD) and the Egyptian Ministry of Higher Education and Scientific Research (MHESR).

Special thanks are due to Dr. Volker Lorenz for his help in the review of the thesis as well as the measuring of the IR spectra.

I am also very appreciate and thankful to Frau Dr. Liane Hilfert for measuring the NMR spectra and for her long time in the discussion with me about the results.

I would especially like to thank Dr. Cristian G. Hrib for the X-ray measurements and for his time in the discussion as well.

Thanks are also due to Frau Dr. Sabine Busse and Frau Beatrice Häusler for their efforts in the measurements of the mass spectrum and elemental analysis. I am deeply thankful to Frau Sabine Hentschel for her kindness and generousity with me in the NMR analysis. I express my warm thanks and profound gratitude to Mr. Marcel Kühling for his kind help during the course of my study.

I would like to express my deepest appreciation to the committee members:

Prof. Dr. Lothar Mörl, Institut für Apparate-und Umwelttechnik der Otto-von-Guericke-Universität Magdeburg.

Prof. Dr. Frank T. Edelmann, Chemisches Institut der Otto-von-Guericke-Universität Magdeburg.

Prof. Dr. Peter W. Roesky, Institut für Anorganische Chemie des Karlsruher Institut für Technologie.

PD Dr. Edgar Haak, Chemisches Institut der Otto-von-Guericke-Universität Magdeburg.

I am very thankful to the office of ″Büro für Gleichstellungsfragen″ of the Otto-von-Guericke-Universität Magdeburg for the financial support in the last three months of the course of my study.

In this opportunity I would like to express my sincere gratitude to all of my Egyptian and Arabic colleagues in Magdeburg who supported me throughout the course of my thesis.

″Gedruckt mit Unterstützung des Deutschen Akademischen Austauschdienstes″

List of Abbreviations

Me	methyl group (CH_3)
Et	ethyl group (CH_2CH_3)
^{i}Pr	*iso*-propyl group ($CH(CH_3)_2$)
^{t}Bu	*tert*-butyl group ($C(CH_3)_3$)
R	alkyl or other organic group
Cy	cyclohexyl group (C_6H_{11})
Ph	phenyl group
Ar	aromatic group
Cp	cyclopentadienyl (η^5-C_5H_5)
Cp′	substituted cyclopentadienyl
Cp*	pentamethylcyclopentadienyl (η^5-C_5Me_5)
COT	cyclooctatetraenyl group (C_8H_8)
COT″	1,4-bis(trimethylsilyl)cyclooctatetraenyl group
Ln	group 3 or lanthanide metal
THF	tetrahydrofuran
Et_2O	diethyl ether
DME	1,2-dimethoxyethane
DMSO	dimethylsulfoxide
TMS	tetramethylsilane
NMR	nuclear magnetic resonance
HSQC	heteronuclear single quantum correlation
MS	mass spectrometry
IR	infrared
EI	electron ionization
δ	chemical shift
ppm	parts per million
s	singlet
d	doublet
t	triplet
q	quartet
o	ortho
m	meta
p	para
et al.	and others
e. g.	for example

Abstract

The main goal of this Ph.D. thesis was to investigate the synthesis, structural characterization and catalytic activity of new lanthanide alkynylamidinate complexes. Chapter 1 gives an overview of the general aspects and properties of lanthanide elements, as well as a brief description of the main synthetic approaches and properties of lanthanide amidinate and guanidinate chemistry. The second Chapter, "Results and Discussion", is subdivided in six subtitles and describes the major results of the Ph.D. thesis. The Ph.D. work started with the synthesis and investigation of a series of new lithium-cyclopropylethinylamidinates and lithium-propiolamidinates. Moreover, an unprecedented bulky amidino-guanidinate ligand was prepared by reaction of *n*-butyllithium and *N*,*N*′-dicyclohexylcarbodiimide in a 1:2 molar ratio. With these monoanionic amidinate and guanidinate ligands several new lanthanide bis- and tris(amidinate) complexes could be synthesized. The reactions of lanthanide bis(cyclopropylethinylamidinate) complexes with $KN(SiMe_3)_2$ in a 1:1 molar ratio afforded a series of new lanthanide bis-(cyclopropylethinylamidinato)amide complexes. Novel types of lanthanide half-sandwich complexes consisting of cyclopropylethinylamidinate and cyclooctatetraenyl (= COT) ligands have been prepared *via* different synthetic routes. A series of solvated, unsolvated and inverse sandwich complexes have been prepared and fully characterized. The last part of the PhD work deals with the catalytic activity of the new lanthanide bis- and tris(cyclopropylethinylamidinate) complexes towards C–C and C–N bond formation. The lanthanide bis(cyclopropylethinylamidinate) complexes were found to be extremely active precatalysts for the guanylation of substituted aniline derivatives with both *N*,*N*′-diisopropylcarbodiimide and *N*,*N*′-dicyclohexylcarbodiimide. In contrast, the use of the new homoleptic lanthanide tris(cyclopropylethinylamidinate) complexes as catalysts for the addition of terminal acetylenes to *N*,*N*′-diisopropylcarbodiimide and *N*,*N*′-dicyclohexylcarbodiimide appears to be quite limited. Chapter 3 contains the summary of the PhD thesis and Chapter 4 describes the experimental part of the PhD work. The crystal data and refinement details are summarized in Chapter 5.

Abstrakt

Ziel der vorliegenden Dissertation war die Synthese, strukturelle Charakterisierung und katalytische Aktivität von neuen Lanthanoid-Alkinylamidinat-Komplexen. Kapitel 1 gibt einen Überblick über allgemeine Aspekte und Eigenschaften der Lanthanoidelemente, sowie die wichtigsten Synthesemethoden und Eigenschaften von Lanthanoid-Amidinaten und -Guanidinaten. Das zweite Kapitel, "Results and Discussion", ist in sechs Unterabschnitte unterteilt und beschreibt die wichtigsten Ergebnisse dieser Dissertation. Am Beginn der Arbeiten standen die Synthese und Charakterisierung einer Reihe von neuen Lithium-cyclopropylethinylamidinaten und Lithium-proiolamidinaten. Darüber hinaus konnte ein neuartiger raumerfüllender Amidinoguanidinat-Ligand durch Reaktion von *n*-Butyllithium mit *N,N'*-Dicyclohexylcarbodiimid im Molverhältnis 1:2 dargestellt werden. Mit diesen monoanionischen Amidinat- und Guanidinat-Liganden konnte eine Reihe neuer Lanthanoid-bis- und -tris(amidinato)-Komplexe synthetisiert werden. Reaktionen der Lanthanoid-bis(cyclopropylethinylamidinato)-Komplexe mit $KN(SiMe_3)_2$ im Molverhältnis 1:1 lieferten neue Lanthanoid-bis(cyclopropylethinylamidinato)amido-Komplexe. Neuartige Lanthanoid-Halbsandwich-Komplexe mit Cyclopropylethinylamidinat- und Cyclooctatetraenyl-Liganden (= COT) konnten nach unterschiedlichen Syntheserouten erhalten werden. Solvatisierte, unsolvatisierte und auch inverse Sandwich-Komplexe konnten dargestellt und vollständig charakterisiert werden. Der letzte Teil der vorliegenden Dissertation befasst sich mit der katalytischen Aktivität der neuen Lanthanoid-bis- und -tris(amidinato)-Komplexe bei der Knüpfung von C-C- und C-N-Bindungen. Die Lanthanoid-bis(cyclopropylethinylamidinato)-Komplexe erwiesen sich als hoch aktive Präkatalysatoren für die Guanylierung von substituierten Anilinderivaten mit *N,N'*-Diisopropylcarbodiimid und *N,N'*-Dicyclohexyl-carbodiimid. Dagegen erwies sich die Eignung der neuen homoleptischen Lanthanoid-tris(cyclopropylethinylamidinato)-Komplexe als Katalysatoren für die Addition terminaler Alkine an *N,N'*-Diisopropylcarbodiimid und *N,N'*-Dicyclohexylcarbodiimid als eher begrenzt. Kapitel 3 gibt eine Zusammenfassung der Ergebnisse, und Kapitel 4 enthält den Experimentellen Teil der Dissertation. Angaben zu Kristalldaten und Strukturverfeinerungen sind im Kapitel 5 zusammengefasst.

1. Introduction

1.1. General aspects and properties of lanthanide elements

The lanthanide metals (Ln) consist of the series of 14 4f elements ranging from cerium (Ce) to lutetium (Lu). Scandium (Sc), yttrium (Y) and lanthanum (La), the metals of group 3, have chemistry similar to the lanthanide metals. Therefore, the lanthanide and group 3 elements are often collectively known as the rare-earth metals [1]. Note that the "rare earths" are not rare in terms of relative abundance in the earth crust [2]. The general electronic configuration of the lanthanide is [Xe] $4f^n5d^16s^2$ with n = 0 (La) to 14 (Lu). The 4f valence orbitals of the lanthanides don't protrude significantly beyond the filled $5s^2$ and $5p^6$ orbitals. As a result, the 4f electrons are commonly thought to be unavailable for bonding, and ligand field effects are not found [3, 4]. Consequently, the chemistry of the lanthanides is believed to be predominantly ionic and governed more by electrostatic factors and steric properties than by filled orbital considerations [5]. The 14 elements of the lanthanide series represent the largest subgroup in the periodic table. The chemistry of lanthanide differs considerably from that of the d-transition metal ions. Some general principles of organo-d-transition metal chemistry don't apply in organolanthanide chemistry, such as σ-donor/π-acceptor metal ligand bonding, the 18-electron rule, the formation of stable M=O, M=N or M≡N multiple bonds, as well as direct M–M bonds, which is a very common phenomenon in d-transition metal compounds [5, 22]. The most stable oxidation state for the lanthanides is Ln^{3+} [1]. Besides the ubiquitous oxidation state Ln^{3+}, the neighboring oxidation states Ln^{2+} and Ln^{4+} are also encountered. Cerium is unique in that it also possesses an easily accessible tetravalent oxidation state Ce^{4+} (f^0). Stable divalent lanthanide ions are *e.g.* Sm^{2+} (f^6), Eu^{2+} (f^7) and Yb^{2+} (f^{14}), Table 1. Although the oxidation state +4 has been encountered with some metals throughout the lanthanide elements series, for example, the ions Ce^{4+} (f^0, orange–yellow or purple), Pr^{4+} (f^1, colorless), Nd^{4+} (f^2, blue–violet), Tb^{4+} (f^7, colorless), and Dy^{4+} (f^8, orange–yellow) (Table 1). The chemistry of Ce^{4+} is the most common for the oxidation state +4 of lanthanides [6 – 10]. The very high positive normal potentials of the tetravalent lanthanide ions Pr^{4+}, Nd^{4+}, Tb^{4+}, and Dy^{4+} (*e.g.* Pr: +2.86 V) make them very strong oxidizing agents, whereas the Ce^{4+} ion is readily available in aqueous solution (E Ce^{3+}/Ce^{4+} = +1.44 V in 2M H_2SO_4, 1.61 V in 1M HNO_3, and 1.70 V in 1M $HClO_4$), so that the chemistry of organolanthanides in the oxidation state +4 remains totally limited to cerium(IV) [6, 7, 11 – 18]. Owing to their oxidation potential, cerium +4 complexes are widely used in various areas of chemistry and technology. Important fields of application include organic synthesis, bioinorganic chemistry, materials

science, and industrial catalysis (automotive three-way catalyst, oxygen storage) [1, 19, 20]. More recently, soluble cerium +4 compounds are increasingly employed for the production of ceria nanoparticles. Consequently, there is a constant demand for new, well-defined cerium +4 species [21, 23]. Unfortunately, the synthesis of such Ce^{4+} complexes is highly dependent on the choice of solvent, reaction temperature and the oxidant. It is interesting to note that all three oxidation state $Ln^{2+,\ 3+,\ 4+}$ are never observed for the same lanthanide metal [22]. Consequently, the highly important mechanistic steps of oxidative addition and reductive elimination found in d-transition metal compounds can not occur with lanthanide metals as they would involve $M^{2+\rightarrow4+}$ or $M^{4+\rightarrow2+}$ transformations, respectively [1]. The decrease of the ionic radii in the series $La^{3+} > Ce^{3+} > Pr^{3+} > \cdots\cdot > Yb^{3+} > Lu^{3+}$ is known as the lanthanide contraction, which refers to the shielding of 4f electrons by the $5s^2$ and $5p^6$ orbitals. The lanthanide contraction causes the lanthanide ions to have similar but not identical properties and is the main reason why the separation of the lanthanide metals can be possible [5, 22, 24].

Table 1 Possible oxidation states for lanthanide elements.

Ce	Pr	Nd	Pm	Sm	Eu	Gd	Tb	Dy	Ho	Er	Tm	Yb	Lu
–	–	–	–	+2	+2	–	–	–	–	–	+2	+2	–
+3	+3	+3	+3	+3	+3	+3	+3	+3	+3	+3	+3	+3	+3
+4	+4	+4	–	–	–	–	+4	+4	–	–	–	–	–

Coordination numbers in the range of 6 – 12 are preferred for the lanthanide ions and the coordination number 8 is typical for many lanthanide ions [1, 25]. According to Pearson´s hard-soft-acid-base (HSAB) concept, the lanthanide metal ions are considered as hard acids and prefer coordination to hard ligands, such as O- or N-donors, while coordination of softer ligands containing *e.g.* phosphorus or sulfur donors are disfavored [22]. The pronounced oxophilicity makes organometallic compounds of the rare-earth metals very sensitive towards water and air. The NMR spectroscopy parameters are the most important indicators for solution structure determination in the lanthanide organometallic chemistry. The lanthanide metals in the trivalent state Ln^{3+} are paramagnetic for all configurations from $4f^1$ to $4f^{13}$. Thus it is not surprising that many researchers have chosen the NMR analysis to investigate the chemistry of the diamagnetic Sc^{3+}, Y^{3+}, La^{3+}, Yb^{3+} , Lu^{3+} and Ce^{4+} structures. The elements Sc^{3+}, Y^{3+}, La^{3+} and Yb^{2+} are also accessible to direct observation by heteronuclear NMR spectroscopy [26].

1.2. Organolanthanide Chemistry

In the year 1954, Wilkinson and Birmingham reported the preparation of the first lanthanide tris(cyclopentadienyl) derivatives, Cp_3Ln (cyclopentadienyl abbreviated as Cp) [27]. However, the organometallic chemistry of the rare-earth metals has slowly developed relative to that of other metals. Despite the early discovery of organolanthanide compounds, the development of this new area of organometallic chemistry was slow because of the extreme sensitivity of these organometallic compounds towards traces of moisture and air. Moreover, it was thought that these organometallic compounds were ionic and represented just trivalent analogues of alkali and alkaline earth metal organometallic compounds [26]. Around 1970 the development of dry-box techniques and single-crystal X-ray diffraction made the rigorous exclusion of air and moisture during preparation and characterization of lanthanide complexes possible. Further, progress of organolanthanide chemistry came in the early 1980s because of their rich and interesting chemistry and by the discovery of the high potential of organolanthanide chemistry as reagents in organic chemistry, such as catalytic alkene hydrogenation, hydroamination and polymerization at very high rates as very active homogeneous catalysts [22]. Until the early 1970s the chemistry of lanthanides had been limited to π-bonded organometallic compounds such as lanthanide tris(cyclopentadienyls), Cp_3Ln [27] and tris(indenyls) [28] as well as cyclooctatetraene complexes [29]. In addition, some homoleptic compounds, such as $Li[LnPh_4]$ [30 – 32] and $Sc(CCPh)_3$, were reported [30]. Tsutsui and Ely reported the preparation of lanthanide bis(cyclopentadienyl) derivatives, Cp_2LnR (R = alkyl, aryl or alkynyl) [33, 34 – 36]. Since then, the derivatives of tris(cyclopentadienyl), bis(cyclopentadienyl) (Cp_2LnR), 1,3-bis(trimethylsilyl)cyclopentadienyl (Cp''), and pentamethylcyclopentadienyl (Cp^*) type complexes, sandwich structures and metallocenes, have attracted most attention in organolanthanide chemistry (Scheme 1).

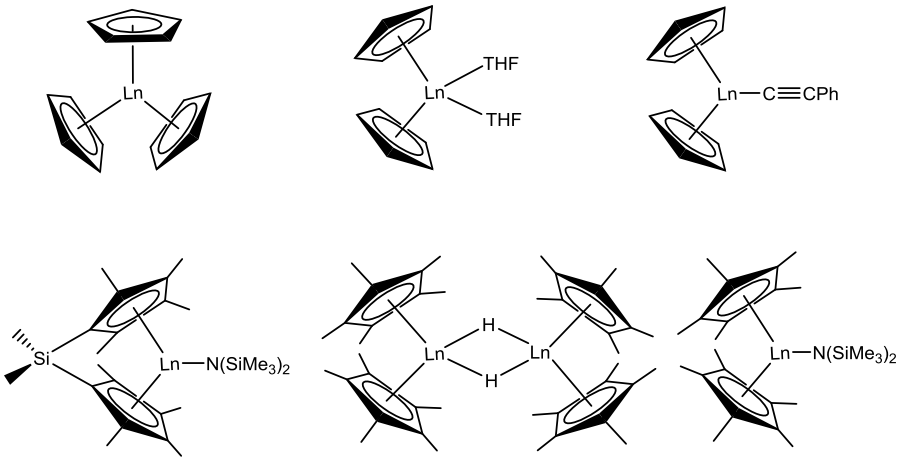

Scheme 1 Examples of lanthanide cyclopentadienyl complexes.

The large flat cyclooctatetraenyl ligand ($C_8H_8^{2-}$, commonly abbreviated as COT) is one of the carbocyclic ring systems which play an important role in organolanthanide chemistry for more than five decades. Streitwieser *et al.* reported the first anionic sandwich complexes of the type $[Ln(COT)_2]^-$ [37], as well as the dimeric mono(cyclooctatetraenyl) lanthanide(III) chlorides, $[(COT)Ln(\mu\text{-}Cl)(THF)_2]_2$ which are important starting materials in the organolanthanide chemistry containing COT ligands [38] (Scheme 2).

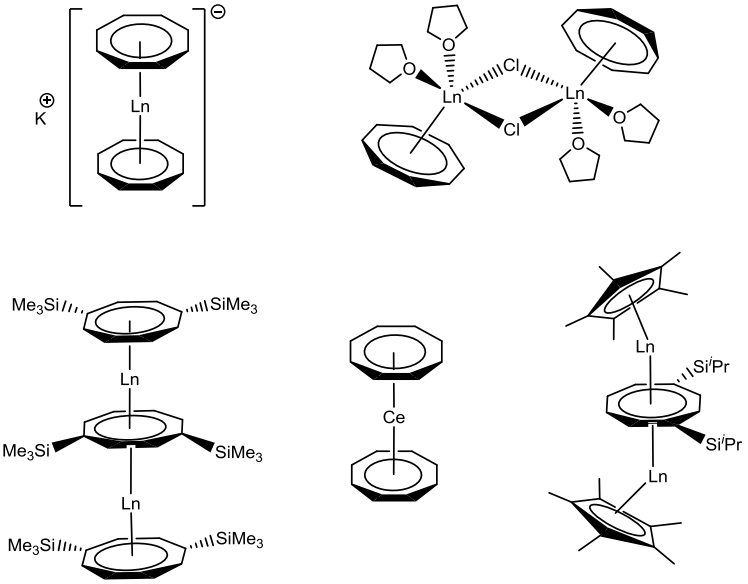

Scheme 2 Examples of lanthanide COT complexes.

1.3. Lanthanide amidinate and guanidinate chemistry

As outlined above, the lanthanide ions prefer coordination to hard base ligands such as oxygen or nitrogen donors. Consequently, the amidinates and guanidinates are considered as analogues of cyclopentadienyl ligands [22]. The anions of amidines and guanidines are among the very few ligands which stabilize lanthanide compounds in all possible oxidation states (II, III and IV). There are four main synthetic approaches for preparation of amidinate complexes (Scheme 3) [39 – 42];

I) The first method is the insertion of a σ-alkyl group of an organometallic fragment M–R into the C=N double bond of carbodiimides. These reactions can be carried out under mild conditions affording amidinates in high yields.

II) The second method involves deprotonation of an amidine by a metal alkyl. This method is used mainly for the preparation of alkali, alkaline-earth metal and transition metal amidinate complexes.

III) The third method is the reaction of anhydrous metal halides of transition metals, lanthanides, or actinides with amidinate salts of alkali and alkaline-earth metals.

IV) The fourth method is the reaction of metal bis(trimethylsilyl)amides with alkyl or aryl cyanides. This method is used as a general method for the synthesis of *N*,*N*′-bis(trimethylsilyl)benzamidinate complexes.

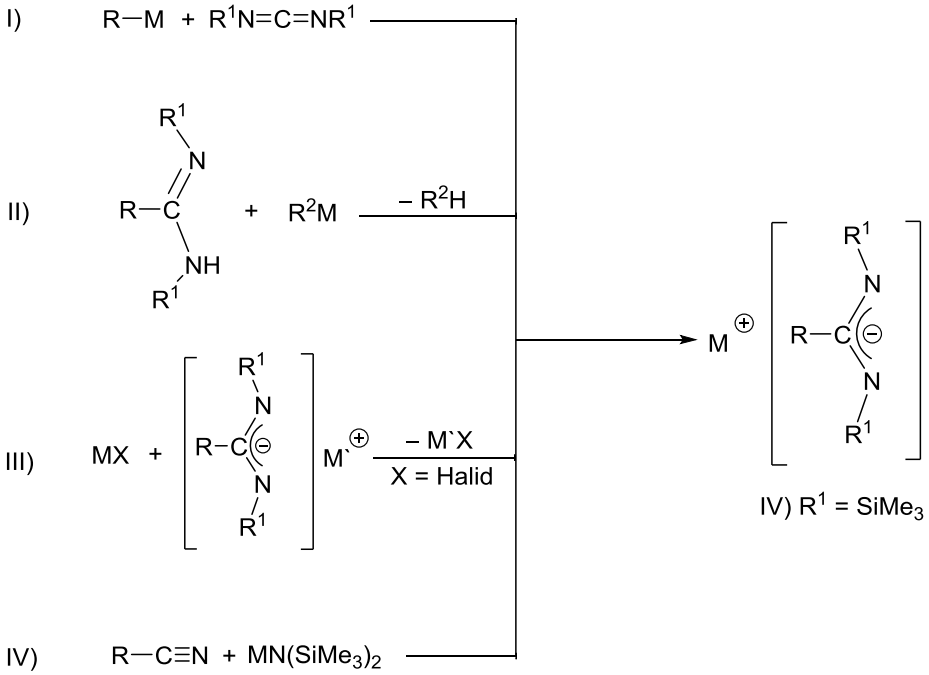

Scheme 3 Main synthetic approaches to amidinate complexes.

Generally, the amidinate anions are considered as nitrogen analogues of the carboxylate anions. They can be C_1-symmetric ($R_1 \neq R_2$) or C_2-symmetric ligands ($R_1 = R_2$). Some examples of C_1-symmetric amidinate ligands are shown in Scheme 4. The most common type of amidinate anions are the C_2-symmetric ligands [43, 44].

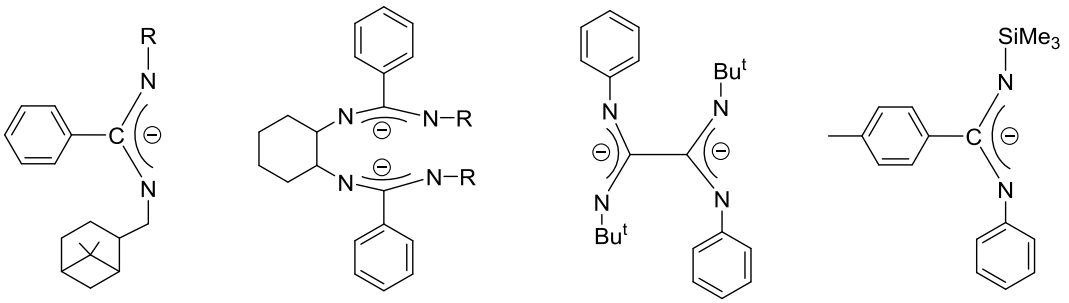

Scheme 4 Examples of C_1-symmetric amidinate ligands.

The steric factors of the substituents on the carbon and nitrogen atoms of amidinate ligands are governed in the coordination mode of the NCN unit of the amidinate. Bulky substituents on the carbon atom make the lone pairs of the nitrogen atoms oriented to form a chelating coordination mode, while small substituents make amidinate ligand more easily adapt a bridging coordination mode (Scheme 5) [45 – 49].

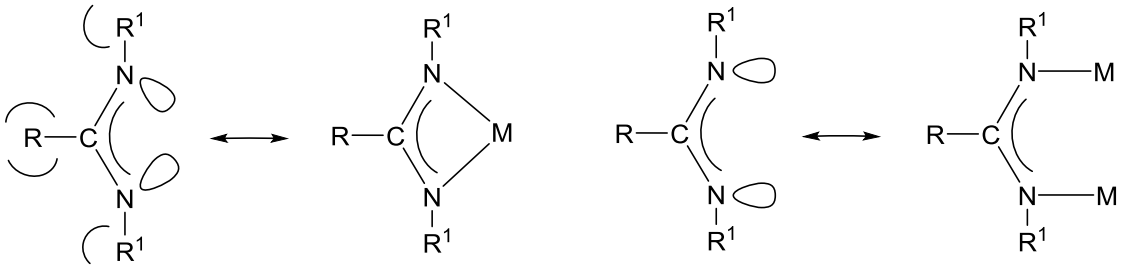

Scheme 5

The bridging coordination mode is very familiar in d-transition metal amidinate complexes and is well established in "paddlewheel" complexes of the type M_2(amidinate)$_4$ [50]. In contrast, this type of coordination mode has not been achieved in lanthanide coordination chemistry because this type of coordination mode requires direct bonding between the lanthanide ions (Ln – Ln), which has never been realized in lanthanide chemistry [22]. The size of the four-membered M(NCN) ring and the values of the C–N and M–N bond lengths as well as the NCN, NMN and CNM angles mainly depend on the type of the substituents on the

carbon and the nitrogen atoms as well as the atomic radius of the corresponding metal ion [22]. In Figure 1, a diagram illustrates the bond lengths and angles of amidinate complexes depending on the corresponding metal ion. The bond lengths of C–N_1 and C–N_2 are equal (π-delocalization) ranging in average from 1.299 to 1.360 Å, while the bond lengths of M–N_1 or M–N_2 are in the range from 2.061 to 2.636 Å according to the metal ion size. The bond angles of N_1CN_2 increase parallel to the increasing in the atomic radius of the metal ion, while the bond angles of N_1MN_2 decreased by increasing of the atomic radius of the metal ion [51 – 56].

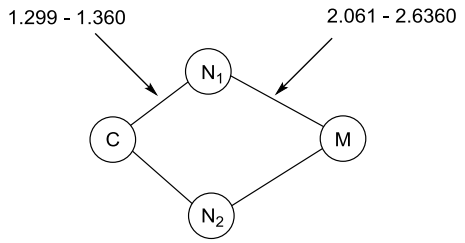

M	N_1CN_2 angle / deg.	N_1MN_2 angle / deg.
–	125.7	-
Li, Na, K	116 - 119	63 - 67
transiton-metals	109 - 121	59 - 69
Ln, Ac	114 - 123	53 - 59

Figure 1 Average bond lengths and bond angles of metal amidinate complexes.

The closely related guanidinate ligands contain an R_2N substituent at the central carbon atom of the NCN unit (Scheme 6). In the year 1970, Lappart *et al.* investigated the coordination chemistry of guanidinate anions and prepared the first transition metal guanidinate complexes. The general main synthetic approaches for the preparation of guanidinate complexes are:

i) Insertion of carbodiimides into a metal–nitrogen bond.

ii) Deprotonation of a guanidine by a metal alkyl.

iii) Reaction of halides of transition metals, lanthanides, or actinides with alkali or alkaline-earth guanidinate complexes [57 – 65].

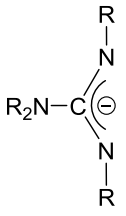

Guanidinates

Scheme 6 General representation of guanidinate ligands

The general aspects, properties and features of amidinates such as the coordination modes, the π-delocalization between C–N_1 and C–N_2, and the influence of substituents on the nitrogen atoms are also found in the chemistry of guanidinate anions. A series of reviews covered the continuing success in the applications of lanthanide amidinate and guanidinate complexes [22, 39, 66 – 68]. Historically, the first literature report on the use of lanthanide amidinate complexes as catalysts appeared in 2002, when Shen and co-workers discovered new homoleptic lanthanide amidinates and their catalytic activity for the ring-opening polymerization of ε-caprolactone at room temperature [69]. Since then, the rare-earth metal complexes became highly efficient homogeneous catalysts, such as for polymerization of olefins and dienes [22, 70, 71], the ring-opening polymerization of cyclic esters [72], the hydroamination of olefins [73] as well as the guanylation of amines [74 – 78]. Moreover, certain alkyl-substituted lanthanide tris(amidinates) and tris(guanidinates) were found to be highly volatile and promising precursors for atomic layer deposition (ALD) and metal–organic chemical vapor deposition (MOCVD) processes in materials science, such as the production of lanthanide nitride thin layers and lanthanide oxides (Ln_2O_3) [22, 39]. The coordination chemistry, synthesis and applications of both d-transition metal and lanthanide amidinate and guanidinate complexes have been reviewed recently by Edelmann [22, 40]. It should be noted that the d-transition metal amidinate and guanidinate complexes made significant progress in many new applications in the last few years [79 – 90].

2. Results and Discussion

2.1. Synthesis and structural characterization of new lithium amidinate and guanidinate ligands

Amidinate and guanidinate ligands have proven to be extremely versatile ligands for the preparation of a wide range of main group, d-transition metal, and f-block elements [91]. Among the classes of compounds reported to date, especially lithium amidinate and guanidinate salts function as useful reagents in salt metathesis reactions with metal halides and related precursors [91]. A potentially useful variation of amidinates is the bonding of alkynyl groups to the central carbon atom in the NCN unit to give alkynylamidines of the type RC≡C–C(=NR′)(NHR′). A considerable number of coordination compounds of alkynylamidinate ligands with lanthanide ions have appeared within the last years [92 – 96].

2.1.1. Synthesis and structure of new lithium alkynylamidinates.

The alkynylamidinates are well established as valuable reagents for the preparation of many of heterocycles, and a special group of alkynylamidinates have been found to be useful antitussives [97]. More recently, alkynylamidinates have attracted considerable attention because of their diverse applications in biological and pharmacological systems [97]. The most common synthetic approach to amidinate ligands is the insertion of carbodiimides, R–N=C=N–R, into M–C bonds. In 2012, it has been reported that lithium-trimethylsilylethynylamidinates can be prepared by the reaction between *N*,*N*′-diisopropylcarbodiimide or *N*,*N*′-dicyclohexylcarbodiimide and lithium-trimethylsilylacetylide in diethyl ether [98].

Using the straightforward reaction shown in Scheme 7, a series of six new lithium-cyclopropylethynylamidinates, Li[*c*-C_3H_5-C≡C-C(NR)$_2$]·S (**1a**: R = ^{i}Pr, S = THF, **1b**: S = Et_2O, **1c**: S = DME; R = cyclohexyl (Cy), **2a**: S = THF, **2b**: S = Et_2O, **2c**: S = DME) have obtained by *in situ* deprotonation of commercially available cyclopropylacetylene with ^{n}BuLi followed by treatment with either *N*,*N*′-diisopropylcarbodiimide or *N*,*N*′-dicyclohexylcarbodiimide. A solution of cyclopropylacetylene in THF, diethyl ether, or DME (= 1,2-dimethoxyethane) was cooled to –20 °C and treated slowly with an equimolar amount

of *n*-butyllithium. After stirring for 15 min at –20 °C, *N*,*N*′-diisopropylcarbodiimide was added in a 1:1 molar ratio. The reaction mixture was stirred for 10 min at –20 °C, and then warmed to room temperature and stirred for 1 hour. The solvent was removed under vacuum to a small volume. The resulting solution was stored at –25 °C in a freezer to obtain colorless crystals of **1a** in 78% yield, **1b** in 75% yield, or **1c** in 73% yield.

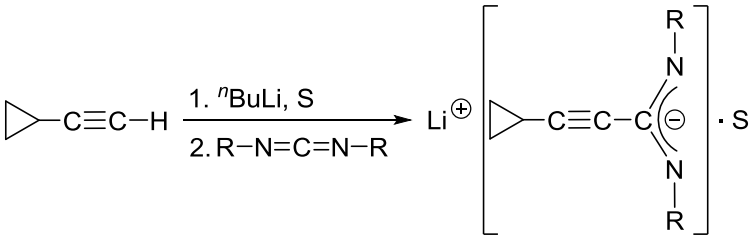

1a: R = ^{i}Pr, S = THF, 78% yield
1b: R = ^{i}Pr, S = Et_2O, 75% yield
1c: R = ^{i}Pr, S = DME, 73% yield
2a: R = *c*-C_6H_{11} (= Cy), S = THF, 80% yield
2b: R = *c*-C_6H_{11} (= Cy), S = Et_2O, 82% yield
2c: R = *c*-C_6H_{11} (= Cy), S = DME, 87% yield

Scheme 7

All three compounds **1a**, **1b**, and **1c** are very moisture-sensitive crystals and freely soluble in the respective donor solvents as well as partially soluble in *n*-pentane. The compounds **2a**, **2b**, and **2c** have been prepared by the same procedures of preparation like **1a**, **1b**, and **1c**, respectively, by using *N*,*N*′-dicyclohexylcarbodiimide instead of *N*,*N*′-diisopropylcarbodiimide affording **2a** in 80% yield, **2b** in 82% yield, and **2c** in 87% yield. The new lithium-cyclopropylethynylamidinates **1a-c** and **2a-c** have been fully characterized by spectroscopic methods and elemental analysis. Crystals of the THF adducts **1a** and **2a** were found to be suitable for single-crystal X-ray diffraction studies. NMR measurements of all the new lithium-cyclopropylethynylamidinates were carried out in THF-d_8 except for **2b**, which was measured in C_6D_6 at 25 °C. In the IR spectrum, a strong band in the range 2214 – 2224 cm^{-1} could be assigned to the C≡C stretching vibration [95]. A medium strong intensity band in the range of 1592 – 1644 cm^{-1} can be attributed to the antisymmetric valence vibrations of the C=N group in the NCN units in the cyclopropylamidinate moieties [99]. A dimeric structure is in fact a common feature in this class of compounds and most of the previously

reported lithium amidinates are dimers in the solid state. The mass spectra of **1a-c** and **2a-c** exhibited only fragments of the monomeric species. The ^{1}H NMR spectra of the new lithium-cyclopropylethynylamidinates **1a-c** and **2a-c** are collected in Table 2. Notable are the significant spectroscopic features of the ^{13}C NMR shifts of the alkyne carbon atoms in the compounds. The ^{13}C NMR spectroscopic data of the recently described trimethylsilylethynylamidinates Li[Me_3Si-C≡C-C($N^iPr)_2$] and Li[Me_3Si-C≡C-C$(NCy)_2$] have been reported. The ^{13}C shifts of the acetylenic carbon atoms appear at δ = 98.5 and 96.5 ppm in Li[Me_3Si-C≡C-C$(NCy)_2$] [98]. The low intensity of the latter signals is indicative of the carbon atom directly bonded to the amidinate group. For **1a-c** and **2a-c**, the ^{13}C NMR signals of the acetylenic carbon atoms which are attached to the amidinate group are very similar, falling in the narrow range of δ = 96.8(**2c**) – 99.2(**2b**) ppm. In contrast, the ^{13}C NMR signals of the acetylenic carbon atoms bearing the cyclopropyl substituent are shifted by 25–30 ppm to higher field, being observed in the very narrow range of δ = 68.6 (**2b**) – 69.4 (**2c**) ppm [97]. This very significant shift could be ascribed to the well known electron-donating ability of the cyclopropyl group to an adjacent electron-deficient center. The latter signals are similar to the ^{13}C NMR spectra which have been reported for cyclopropyl-2-propionic acid, *c*-C_3H_5-C≡C-COOH (δ = 68.1 and 96.8 ppm) [100].

Table 2 ^{1}H NMR spectra of lithium-cyclopropylethynylamidinate **1a-c** and **2a-c**

δ (ppm) / Comp.	C**H**, *c*-C_3H_5	C**H**$_2$, *c*-C_3H_5	C**H**, ^{i}Pr	C**H**, Cy	C**H**$_3$, ^{i}Pr	C**H**$_2$, Cy
1a	0.81 – 1.04	0.30, 0.41	3.37 – 3.45	–	0.64	–
1b	0.99	0.64, 0.78	3.74 – 3.81	–	0.99	–
1c	2.09	1.39, 1.52	4.46 – 4.52	–	1.71	–
2a	1.27 – 1.35	0.61, 0.78	–	3.27 – 3.33	–	1.01– 1.67
2b	0.82 – 89	0.41, 0.68	–	3.66 – 3.99	–	0.94 – 2.27
2c	1.38 – 1.45	0.86, 0.92	–	3.37 – 3.44	–	1.12 – 1.79

Both THF adducts **1a** and **2a** were structurally characterized by single-crystal X-ray diffraction. In both **1a** and **2a**, the X-ray diffraction study revealed the presence of dimeric

ladder-type molecular structures in the solid state (Figures 2 and 3). The amidinate moieties serve as a chelate ligand with one lithium ion to form two planar four-membered LiNCN rings which are bonded on either side to a central planar four-membered Li_2N_2 ring. The lithium ions are four-coordinate in pseudo-tetrahedral geometry. Therefore, the lithium atoms are coordinated to both nitrogen atoms of the NCN amidinate unit and one nitrogen atom of the other amidinate ligand, as well as, the oxygen atom of the THF ligand [98, 99]. The metric parameters of both structures are very typical for related amidinate compounds and are not exceptional. Selected bond lengths and bond angles for both **1a** and **2a** are collected in Table 3.

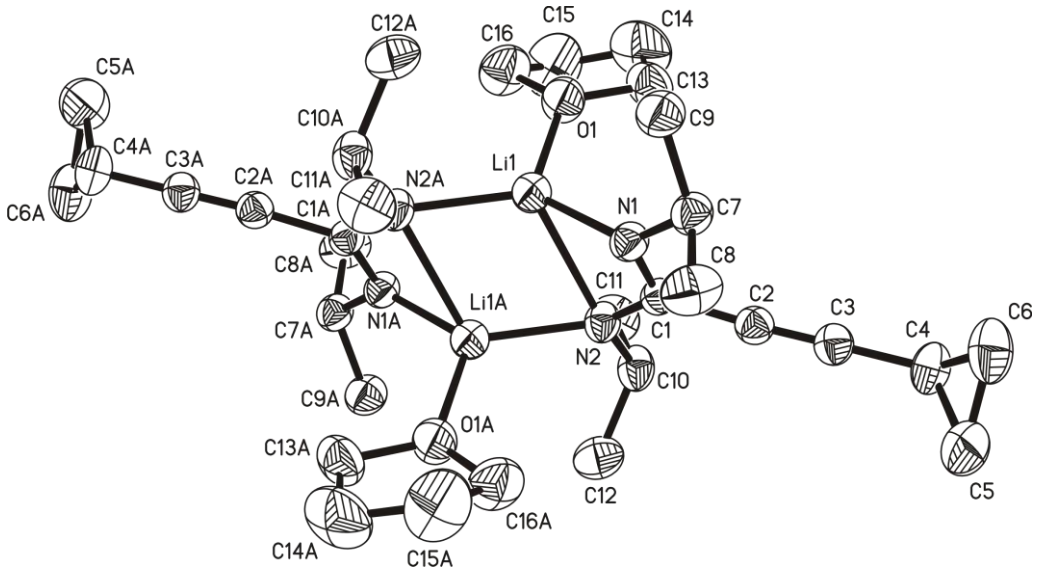

Figure 2. Molecular structure of $\{Li[c\text{-}C_3H_5\text{-}C{\equiv}C\text{-}C(N^iPr)_2]\cdot THF\}_2$ (**1a**)

The bond lengths of the C–N bonds in the amidinate moieties (e.g. C(1)–N(1) 1.318(2) and C(1)–N(2) 1.329(2) Å in **1a** and C(1)–N(1) 1.314(2) and C(1)–N(2) 1.341(2) Å in **2a**) indicate uniform π-delocalization.

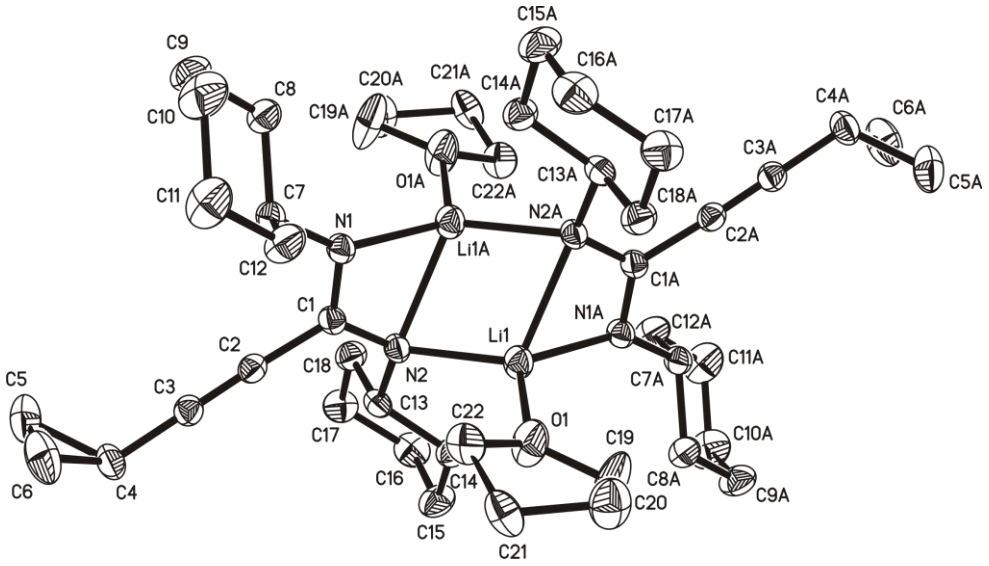

Figure 3. Molecular structure of {Li[*c*-C_3H_5-C≡C-C(NCy)$_2$]·THF}$_2$ (**2a**)

Table 3 Selected bond lengths (Å) and bond angles (°) for **1a** and **2a**

Compound / Bond lengths and angles	**1a**	**2a**
C(1)–N(1)	1.318(2)	1.314(2)
C(1)–N(2)	1.329(2)	1.341(2)
N(1)–Li(1) (Li(1) #1 in **2a**)	1.975(3)	1.986(3)
N(2)–Li(1)	2.336(4)	2.052(3)
N(2)–Li(1)#1	2.041(3)	2.245(3)
Li(1)–O(1)	1.893(3)	1.887(13)
C(2)–C(3)	1.193(2)	1.193(3)
N(1)–C(1)–N(2)	118.91(15)	118.91(14)
N(1)–Li(1)–N(2)	63.20(10)	–
N(1)#1–Li(1)–N(2)#1	–	65.10(10)
N(2)#1–Li(1)–N(2)	112.29(14)	109.66(14)
Li(1)#1–N(2)–Li(1)	67.71(14)	70.34(14)

In a similar way, Li[Ph-C≡C-C(NCy)$_2$] was prepared in a straightforward manner according to Scheme 8 by *in situ* deprotonation of phenylacetylene with ^{n}BuLi at –20 °C in THF or Et$_2$O followed by addition of *N,N′*-dicyclohexylcarbodiimide. After 10 min, the reaction mixture was warmed to room temperature and stirred for 2 hours at room temperature. The solvent was removed under vacuum affording white solids of Li[Ph-C≡C-C(NCy)$_2$] ·S (**3a**: S = THF) in excellent yield (88%) or (**3b**: S = Et$_2$O) in moderate yield (76%).

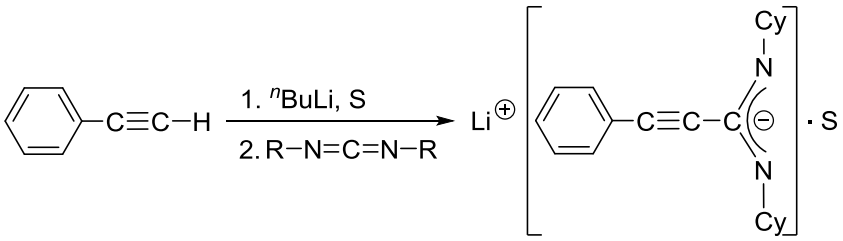

3a: S = THF, 88% yield
3b: S = Et$_2$O, 76% yield

Scheme 8

In 2008, the compound Li[Ph-C≡C-C(N^{i}Pr)$_2$] has been reported to be suitable ligand for the prepration of d-transition metal complexes containing bridging alkynylamidinate ligand [46]. Moreover, the same ligand has been used in the synthesis of the unsolvated homoleptic Ce(III) complex [Ph-C≡C-C(N^{i}Pr)$_2$]$_3$Ce [95]. Both alkynylamidinates **3a** and **3b** have been fully characterized by spectroscopic methods and elemental analysis. In addition, compound **3a** has been investigated by single-crystal X-ray diffraction. The IR spectra showed a medium band at 2217 cm^{-1} which could be assigned to C≡C in **3a**, while it appears at 2211 cm^{-1} as weak band in **3b**. The C=N stretching vibrations of the NCN unit of amidinate moieties was observed at 1610 cm^{-1} as very strong band in **3a** and at 1592 cm^{-1} as strong band in **3b** [95]. The NMR spectra were recorded in toluene-d_8 and C_6D_6 for **3a** and **3b**, respectively. The ^{1}H and ^{13}C NMR analyses were in good agreement with the formation of Li[Ph-C≡C-C(NCy)$_2$]. All protons and carbons have been observed except for the carbon atom of the NCN unit and one carbon atom of the two acetylenic carbon atoms in **3b**.

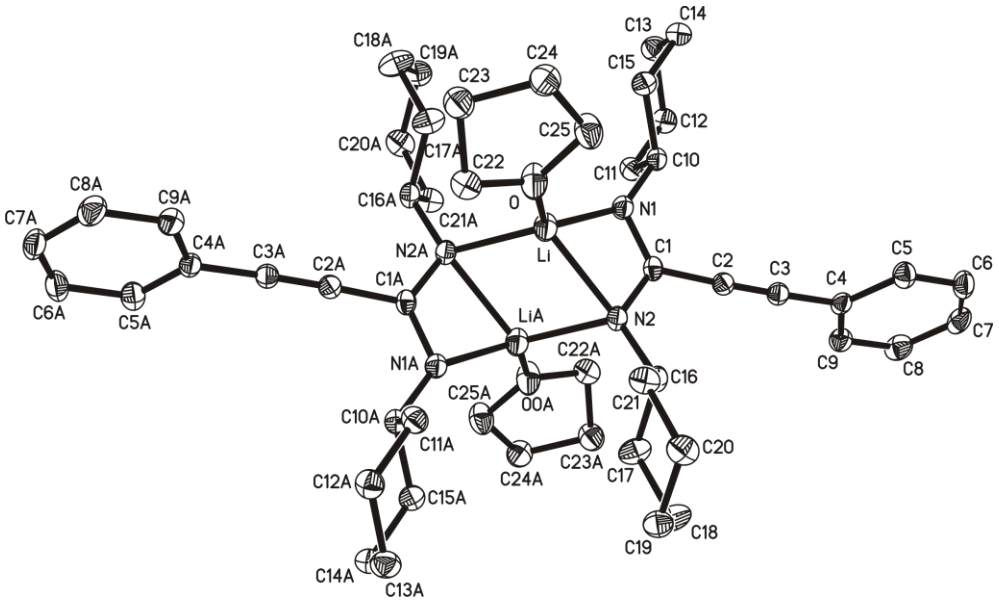

Figure 4. Molecular structure of {Li[Ph-C≡C-C(NCy)$_2$]·THF}$_2$ (**3a**)

A saturated solution of compound **3a** in THF was kept at 5 °C affording block-like single-crystals. Figure 4 depicts the molecular structure of dimeric **3a**. In the solid state, Li[Ph-C≡C-C(NCy)$_2$] crystallizes in the triclinic space group P-1 with one molecule in the unit cell. The bond lengths and bond angles are in good agreement with similar structures of amidinate ligands. The N(1)–C(1) and N(2)–C(1) distances are 1.3201(13) and 1.3407 (12) Å respectively, to indicate uniform π-delocalization. The distances N(1)–Li and N(2)–Li are 2.031(2) and 2.188(2) Å. The C≡C bond length is 1.2018(18) Å. The bond angles of N(1)–C(1)–N(2) and N(1) –Li–N(2) are 118.89(8)° and 65.67(6)°, respectively.

2.1.2. Synthesis and structure of new lithium guanidinate.

An unprecedented bulky lithium guanidinate salt has also been prepared in the course of this work. A reaction between *N*,*N*′-dicyclohexylcarbodiimide and ^{n}BuLi in a 2:1 molar ratio, respectively, in THF afforded Li[^{n}Bu-C(=NCy)(NCy)C(NCy)$_2$]·THF (**4**) in moderate yield 60% (Scheme 9). This guanidinate salt has partial solubility in THF, Et$_2$O, DME, toluene, and *n*-pentane. The new bulky amidino-guanidinate **4** has been fully characterized by spectroscopic methods and elemental analysis to confirm the product as shown in Scheme 72. Deuterated DMSO-d_6 (DMSO = dimethyl sulfoxide) was found to be the best solvent for

measuring the NMR spectra of Li[^{n}Bu-C(=NCy)(NCy)C(NCy)$_2$]·THF, Table 4. Unlike most of the reported lithium guanidinates and amidinates, which are dimers in the solid state, the mass spectrum of Li[^{n}Bu-C(=NCy)(NCy)C(NCy)$_2$]·THF showed only the fragments for the monomeric compound.

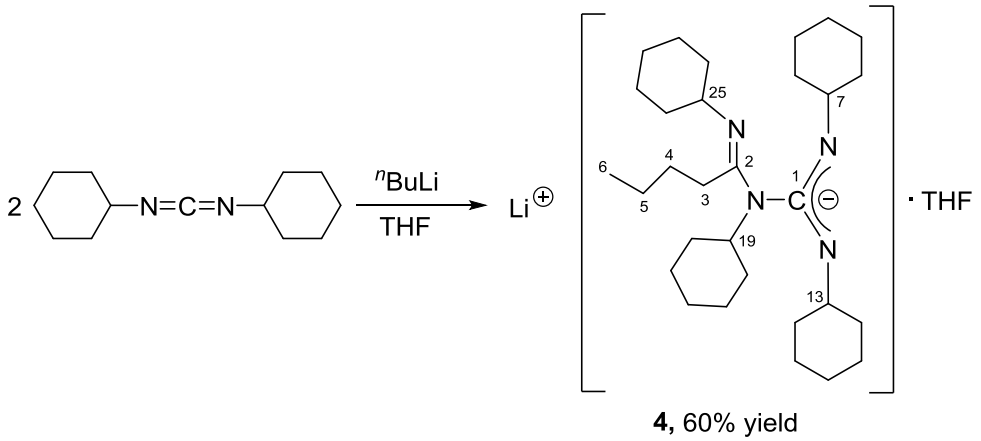

4, 60% yield

Scheme 9

Table 4 ^{1}HNMR and ^{13}CNMR spectra of Li[^{n}Bu-C(=NCy)(NCy)C(NCy)$_2$]·THF (**4**)

δ(ppm) NMR	C$_3$**H**$_2$	C$_4$**H**$_2$	C$_5$**H**$_2$	C$_6$**H**$_3$	C$_7$**H**	C$_{13}$**H**	C$_{19}$**H**	C$_{25}$**H**	
^{1}HNMR	2.5	2.09	1.84	0.85	3.04	3.2	3.84	3.60	
δ(ppm) NMR	C1	C2	C3	C4	C5	C6	C7, C13	C19	C25
^{13}CNMR	155.3	145.1	34.5	30.7	29.5	13.8	54.2	55.4	49.3

Interestingly, the same reaction in Et_2O gave a mixture of guanidinate and amidinate salts, Li[^{n}Bu-C(=NCy)(NCy)C(NCy)$_2$] and Li[^{n}Bu-C(NCy)$_2$], respectively, as illustrated in Scheme 10. This reaction was investigated by treatment *in situ* with $HoCl_3$ dissolved in THF to give {^{n}Bu-C(=NCy)(NCy)C(NCy)$_2$}Ho{^{n}Bu-C(NCy)$_2$}(μ-Cl)$_2$Li(THF)$_2$ which will be discussed in more detail in the section of lanthanide(III) bis(amidinate) and bis(guanidinate) complexes.

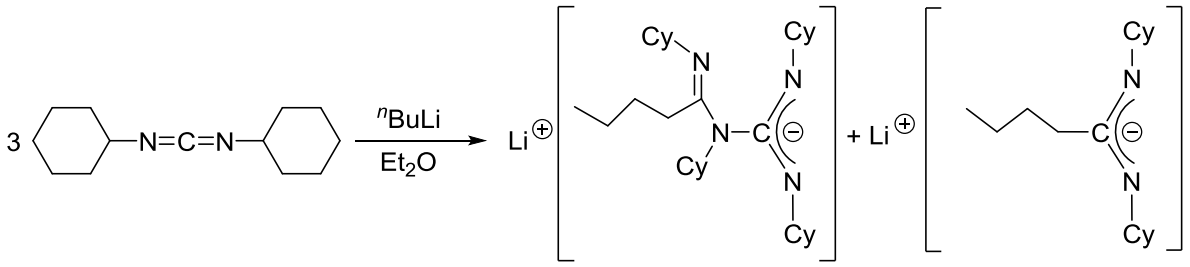

Scheme 10

All of the previously described lithium alkynylamidinates and lithium guanidinates have been used as precursors for the synthesis of heteroleptic and homoleptic lanthanide complexes, as well as in the preparation of novel lanthanide COT half-sandwich complexes.

2.2. Synthesis and structural characterization of lanthanide(III) bis(amidinate) and bis(guanidinate) complexes

Over the past decades, the monoanionic amidinate and guanidinate moieties, as some of the important non-cyclopentadienyl ligands, have been used in organolanthanide chemistry as ancillary ligands, due to their strong binding to the lanthanide metals and tunable electronic and steric factors. In addition to structural interests, rare-earth amidinate complexes have great versatility in materials and chemical applications. The lanthanide amidinate complexes have witnessed rapid progress and have been proven to be very efficient homogeneous catalysts/pre-catalysts in organic transformation and polymerizations *e.g.* for the guanylation of amines or ring–opening polymerization reaction of lactones. Lanthanide alkynylamidinate complexes have been found to be efficient and versatile catalysts *e.g.* for C–C and C–N bond formation, addition of C–H, N–M, and P–H bonds to carbodiimides as well as ε-caprolactone polymerization [101 – 108].

2.2.1. Lanthanide(III) bis(cyclopropylethinylamidinate)

The 1:2 reactions between anhydrous $CeCl_3$ with **1a** and **2a** as well as a reaction of $NdCl_3$ with **2a** were carried out in THF solution at 65 °C for 2 h followed with stirring at room temperature and gave the chloro-functional lanthanide(III) bis(cyclopropylethynylamidinate) complexes $[\{c\text{-}C_3H_5\text{-}C{\equiv}C\text{-}C(NR)_2\}_2Ln(\mu\text{-}Cl)(THF)]_2$ (**5**: Ln = Ce, R = ^{i}Pr; **6**: Ln = Ce, R = Cy; **7**: Ln = Nd, R = Cy). They were isolated in moderate (**5**: 62%, **6**: 55%) to good (**7**: 85%) isolated yields, as shown in Scheme 11.

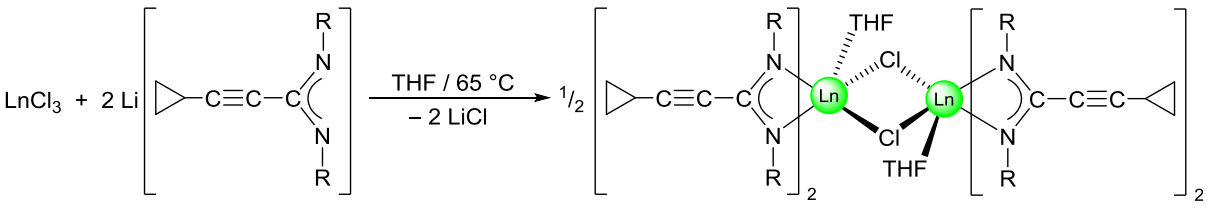

1a: R = ^{i}Pr
2a: R = *c*-C_6H_{11} (= Cy)

5: Ln = Ce, R = ^{i}Pr, 62% yield
6: Ln = Ce, R = Cy, 55% yield
7: Ln = Nd, R = Cy, 85% yield

Scheme 11

The cerium compounds **5** and **6** were isolated from *n*-pentane solution as exceedingly air- and moisture-sensitive complexes. All three complexes were isolated in the form of needle-like crystals, with the cerium complexes **5** and **6** being bright yellow and the neodymium complex **7** dark green. X-ray diffraction studies showed that all three complexes are chloro-bridged dimers; therefore the reactions can be formulated as shown in Scheme 11.

All three compounds **5**, **6** and **7** have been investigated by IR spectra and elemental analysis as well as ^{1}H and ^{13}C NMR. IR spectra show strong bands in the range of 2221 – 2227 cm^{-1}. They could be assigned to the C≡C stretching vibration, whereas a medium strong intensity bond, which appears at around 1610 cm^{-1} can be attributed to the C=N in the NCN units of amidinate ligands [95, 99]. Despite the paramagnetic nature of the Ce^{3+} and Nd^{3+} ions, NMR spectra of the compounds **5** – **7** could be obtained. However, the ^{1}H NMR signals showed little or no indication of the presence of THF ligands. In general, bis(amidinato) and bis(guanidinato) lanthanide chloride complexes are known in three different types [22, 40]: (i) THF-solvated monomers $L_2LnCl(THF)$ [109, 110]; (ii) "ate" complexes such as $L_2Ln(\mu\text{-}Cl)_2Li(THF)_2$ [111 – 115]; and (*c*) chloro-bridged dimers $[L_2Ln(\mu\text{-}Cl)]_2$ (L = amidinate or guanidinate anion) [116 – 119]. The complexes **5** and **6** form bright yellow needle-like crystals and complex **7** dark green needle-like crystals, which were obtained by slow cooling of saturated solutions in *n*-pentane to –30 °C. They were all found to be suitable for single-crystal X-ray diffraction. The X-ray studies releaved that **5** – **7** have dimeric structures of the type $[\{c\text{-}C_3H_5\text{-}C{\equiv}C\text{-}C(NR)_2\}_2Ln(\mu\text{-}Cl)(THF)]_2$ (**5**: Ln = Ce, R = ^{i}Pr; **6**: Ln = Ce, R = Cy; **7**: Ln = Nd, R = Cy) with two μ_2-bridging chloro ligands. The molecular structures of **5** and **6** are depicted in Figure 5, whereas the molecular structure of **7** is shown in Figure 6.

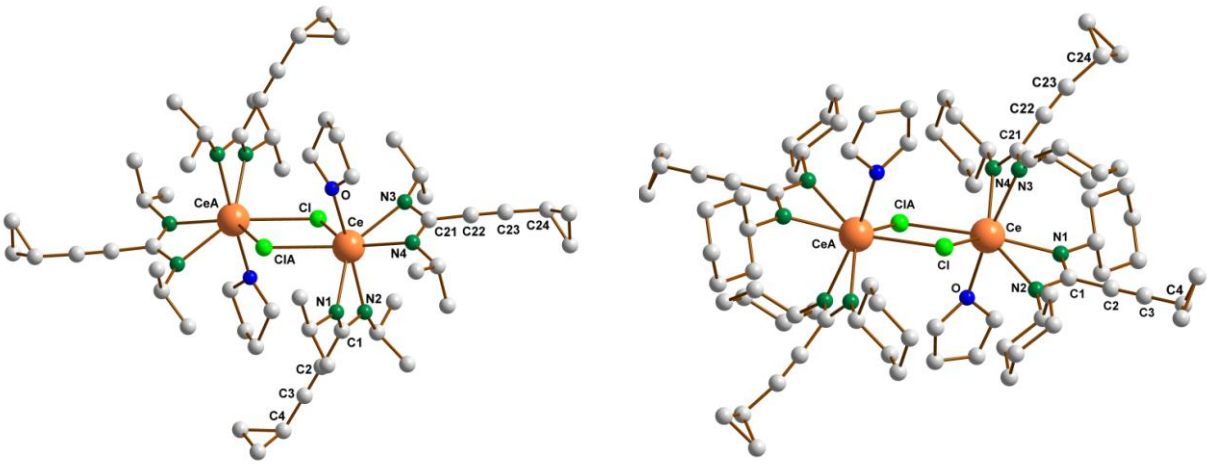

Figure 5. Molecular structures of [{*c*-C_3H_5-C≡C-C(N^iPr)$_2$}$_2$Ce(μ-Cl)(THF)]$_2$ (**5**) (left) and [{*c*-C_3H_5-C≡C-C(NCy)$_2$}$_2$Ce(μ-Cl)(THF)]$_2$ (**6**) (right)

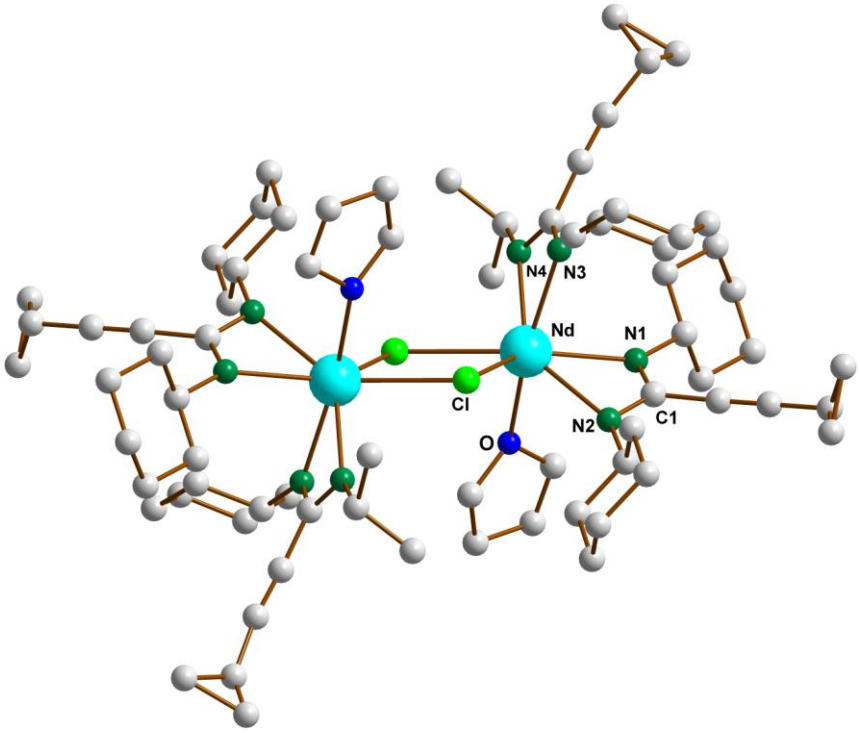

Figure 6. Molecular structure of [{*c*-C_3H_5-C≡C-C(NCy)$_2$}$_2$Nd(μ-Cl)(THF)]$_2$ (**7**)

The lanthanide ions (Ce or Nd) are coordinated by four nitrogen atoms of the bis(amidinate) ligand, two chlorine atoms and one oxygen atom of the THF molecule, thus resulting in a coordination number of seven. The new complexes **5** – **7** are centrosymmetric dimers of the

type $[L_2Ln(\mu\text{-}Cl)(THF)]_2$ with a planar four-membered Ln_2Cl_2 (Ln = Ce or Nd) ring as the central structural unit. The complexes **5 – 7** crystallize in triclinic P-1 (**5**) and monoclinic $P2_1/c$ (**6** and **7**) space groups. According to the angles of M–Cl–M with 106.59(3)° (**5**), 105.722(14)° (**6**) and 106.12(2)° (**7**), as well as Cl–M–Cl, 73.41(3)° (**5**), 74.272(14)° (**6**) and 73.88(2)° (**7**), the Ln_2Cl_2 unit is rhomb-shaped. Generally, the lanthanide amidinate and guanidinate complexes have relative small N–Ln–N bite angles. The N–Ln–N angles in the complexes **5** – **7** are significantly smaller than the N–Y–N angles which were published for $[\{(Me_3Si)_2NC(N^iPr)_2\}_2Y(\mu\text{-}Cl)]_2$ [111]. The angles of the N–Ln–N units of the new complexes are collected in Table 5.

Table 5 Selected angles (°) of the N–Ln–N units of **5** – **8**

Angles (°) \ Complex	**5**	**6**	**7**	**8**
N(1)–Ln–N(2)	54.14(9)	53.42(6)	54.12(7)	57.70(13)
N(3)–Ln–N(4)	53.93(9)	54.05(6)	54.93(7)	57.45(12)

The Ln–N bond lengths of all complexes are nearly equal in a range of 2.461 – 2.582 Å. The lengths of the amidinate N–C bonds in all new complexes have similar values, indicating the negative charge delocalization within the NCN fragments (average C–N = 1.33 Å). The Ln–Cl distances in all new complexes **5** – **7** (average Ln–Cl = 2.828 Å) have a value close to that published for $[\{(Me_3Si)_2NC(N^iPr)_2\}_2Nd(\mu\text{-}Cl)]_2$ [117]. The bond lengths of the triple bonds in the cyclopropylethynyl units are 1.189(5) Å for C(5)–C(3) and 1.191(5) Å for C(22)–C(23). The single crystal X-ray diffraction data of bond lengths and angles for **6** compared to **5** show that the different substituents on the amidinate N atoms (^{i}Pr *vs.* Cy) have no significant impact on the structural parameters. Surprisingly, when a similar reaction between $HoCl_3$ with **2a** was carried out in THF, the "ate" complexe, $[\{c\text{-}C_3H_5\text{-}C{\equiv}C\text{-}C(NCy)_2\}_2Ho(\mu\text{-}Cl)_2Li(THF)(Et_2O)]$ was isolated as shown in Scheme 12.

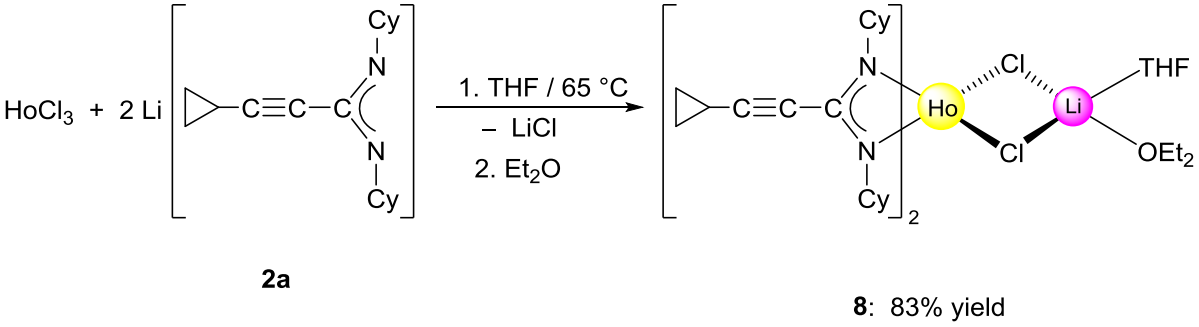

2a

8: 83% yield

Scheme 12

The formation of the "ate" complex **8** could be attributed to the smaller size of the holmium ion as compared to Ce and Nd. The reaction of $HoCl_3$ with 2 equiv. of **2a** in THF at 65 °C for 3 hours followed with stirring over night afforded the bright yellow "ate" complex [*c*-C_3H_5-C≡C-C(NCy)$_2$]$_2$Ho(μ-Cl)$_2$Li(THF)(Et_2O) (**8**) in high yield 83% after recrystallization from diethyl ether as exceedingly air- and moisture-sensitive complex. The Ho^{3+} ion has highly paramagnetic properties, therefore it was impossible to obtain interpretable NMR spectra for **8**. However, compound **8** has been characterized by IR spectroscopy and elemental analysis as well as single-crystal X-ray diffraction. The IR spectrum shows a strong band at 2227 cm^{-1} assigned to the C≡C stretching vibration, whereas a medium strong intensity band at around 1629 cm^{-1} can be attributed to the C=N vibration in the NCN units of the amidinate ligands [95, 99]. The X-ray diffraction study clearly established the presence of an "ate" complex formed by coordination of lithium chloride to monomeric {*c*-C_3H_5-C≡C-C(NCy)$_2$}$_2$HoCl. In this case, the {[*c*-C_3H_5-C≡C-C(NCy)$_2$]$_2$Ho(μ-Cl)}$^-$ portion of the structure is best described as having a distorted *pseudo*-octahedral geometry defined by the four nitrogen atoms of the two amidinate ligands and the two chlorine atoms. Surprisingly, the tetrahedral coordination sphere of Li is supplemented by both THF and Et_2O, apparently as a result of the reaction having been carried out in THF and the product recrystallized from diethyl ether. The molecular structure of **8** is depicted in Figure 7.

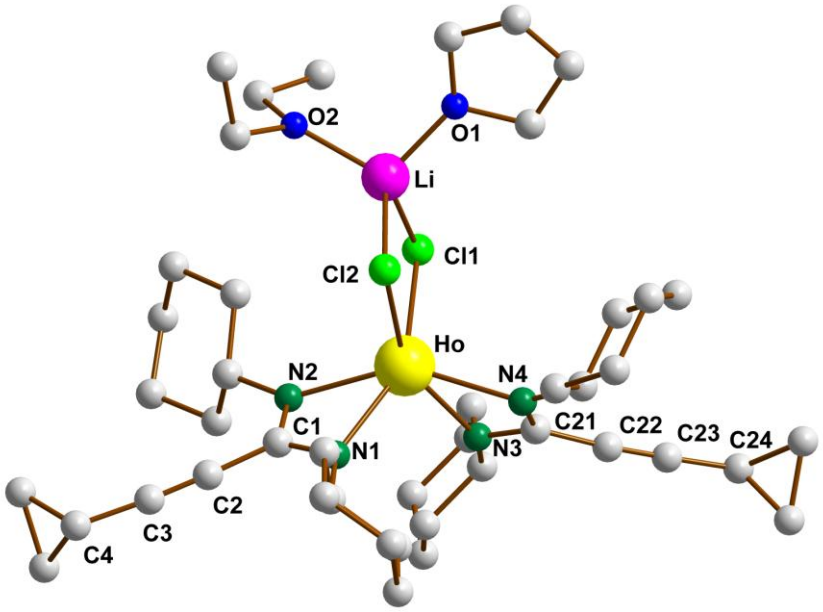

Figure 7. Molecular structure of [*c*-C_3H_5-C≡C-C(NCy)$_2$]$_2$Ho(μ-Cl)$_2$Li(THF)(Et_2O) (**8**)

Complex **8** crystallizes in the monoclinic space group $P2_1/c$. According to the angles Ho–Cl–Li with 88.8(3)° and Cl–Ho–Cl with 83.70(5)° the Ho_2Cl_2 unit is rhomb-shaped. The Ho–N bond lengths is (average Ho–N = 2.342 Å) and the Ho–Cl bond is (average Ho–Cl = 2.652 Å). On the other hand, the N–Ho–N bite angles are larger than those in **6** and **7** (Table 5). The molecular structure of **8** is very similar to previously published lanthanide(III) bis(amidinate) or bis(guanidinate) "ate" complexes such as [2,4,6-$(CF_3)_3C_6H_2C(NSiMe_3)_2$]$_2$Nd($\mu$-Cl)$_2$Li(THF)$_2$ or [$(Me_3Si)_2NC(N^iPr)_2$]$_2$Ln(μ-Cl)$_2$Li(THF)$_2$ (Ln = Nd, Yb, Lu) [111 – 115]. The average Ln–N bond length in all four lanthanide bis(cyclopropylethynylamidinate) complexes, **5 – 8** decrease in the row Ce (2.512 Å) > Nd (2.478 Å) > Ho (2.341 Å) [163, 164]. In accordance, the average N–Ln–N angles show an increase in the order Ce (53.89°) > Nd (54.52°) > Ho (57.60°) as shown in Table 5.

All the new complexes **5**, **6**, **7** and **8** have been tested as useful catalysts in the reaction of *p*-phenylenediamine with 2 equiv. of *N*,*N*′-diisopropylcarbodiimide to afford the corresponding guanidine derivatives. This will be discussed in detail in the section describing the catalytic activity of lanthanide(III) amidinates (Section 2.6.1.).

2.2.2. Europium(III) bis(cyclopropylethynylamidinate)

An attempt to prepare a new europium(II) amidinate complex using cyclopropylethynylamidinate as ligand, led to the surprising result that the Eu(II) ion was oxidized to give a Eu(III) complex. The reaction between $EuI_2(THF)_2$ and **2a** was carried out in a molar ratio 1:2 in THF at room temperature and afforded the Eu(III) cyclopropylethynylamidinate complex $[c\text{-}C_3H_5\text{-}C{\equiv}C\text{-}C(NCy)_2]Li[c\text{-}C_3H_5\text{-}C{\equiv}C\text{-}C(NCy)_2]_2Eu(\mu\text{-}I)_2Li(THF)_2$ (**9**) amidinate as product according to Scheme 13.

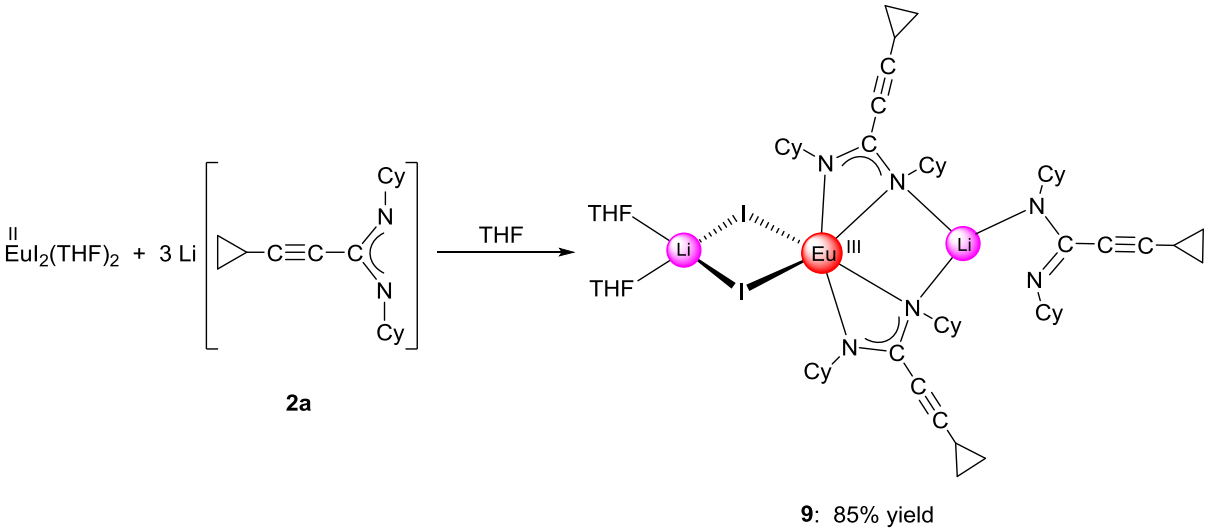

Scheme 13

The europium compound **9** was isolated from *n*-pentane as yellow solid. Needle-like single-crystals were obtained at 5 °C in 85% yield. Compound **9** was also structurally characterized through X-ray diffraction as shown in Figure 8. In the ^1H NMR spectra of **9** the protons of the cyclopropyl group are shifted to high magnetic field. The CH_2 protons in the $c\text{-}C_3H_5$ groups were observed at $\delta = -1.75$ and -2.40 ppm and the CH protons were observed at $\delta = -3.18$ ppm, whereas the protons of THF have not been observed. Only the carbon atoms of the cyclopropyl group and CH_2 units of the cyclohexyl groups have been observed in the ^{13}C NMR spectrum. This could be attributed to the strong paramagnetic nature of the europium(III) ion.

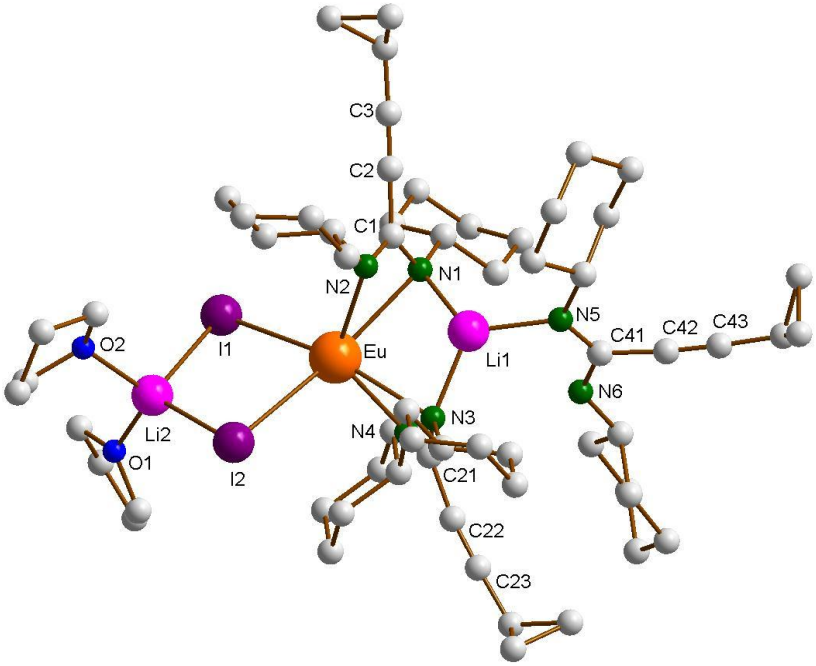

Figure 8. Molecular structure of [*c*-C_3H_5-C≡C-C(NCy)$_2$]Li[*c*-C_3H_5-C≡C-C(NCy)$_2$]$_2$Eu(μ-I)$_2$Li(THF)$_2$ (**9**)

The europium ion is coordinated by four nitrogen atoms of the chelating amidinate ligands and two iodine atoms, thus resulting in coordination number of six. The complex **9** crystallizes in the monoclinic space group $P2_1/c$. The most interesting features of **9** are the two unsymmetrically bridging amidinate ligands and the presence of two differently coordinated lithium ions, three-coordinated lithium bonded to three nitrogen atoms from three different amidinate ligands and four-coordinated lithium bonded to two THF molecules and two iodine atoms. The Eu–N bond length (average 2.588 Å) is close to the Ln–N distances observed in complexes **5**, **6** and **7**. Interestingly, the distance Eu–Li(1) (3.006(6) Å) is shorter than the bond lengths Eu–I1 (3.2240(9) Å) and Eu–I2 (3.2321(6) Å). The presence of two different coordination modes for the lithium ions, Li1 and Li2, can be attributed to the Li1 (3.006(6) Å) ion which is closer to the Eu ion than Li2 (3.2240(9) Å) as well as the Li1 encapsulated between the two nitrogen atoms N1 and N3 to have only one free coordination place for N5 atom. The three-coordinated lithium ion is coordinated by N5 with a bond length Li1–N5 2.004(7) Å. The bond length of C41–N6 1.356(5) Å is shorter than a single bond

indicating localization of the π-bond between C41 and N6 atoms. The bond length of triple bond C2–C3 is 1.198(5) Å. The angles N1–Eu–N3 (82.48(9)°), N1–Li1–N3 (118.4(3)°) and Eu–N1–Li1 (78.3(2)°) result in distorted rhombus shape. With 51.34(9)° and 52.21(9)° the N–Eu–N angles are smaller than the corresponding N–Ln–N angles in **5** – **8**.

2.2.3. A cerium(III)-bis(diiminophosphinate)

A new monomeric Ce(III)-diiminophosphinate complex $[Ph_2P(NSiMe_3)_2]_2Ce(\mu\text{-}Cl)_2Li(THF)_2$ (**10**) has also been synthesized. The starting material $Li[Ph_2P(NSiMe_3)_2]$ was prepared according to the literature method [120, 121].

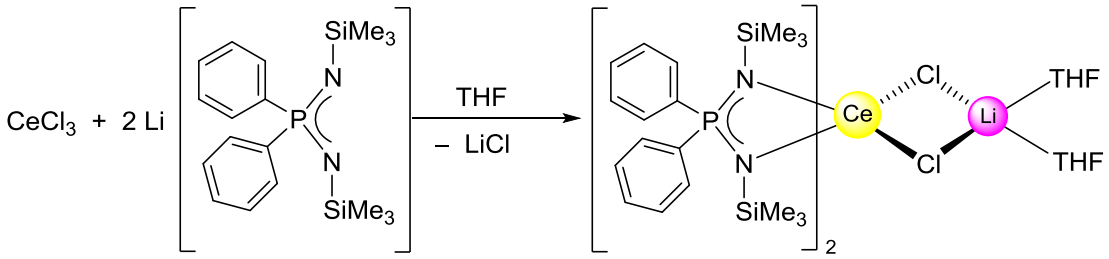

10: 78% yield

Scheme 14

According to Scheme 14, a suspension of anhydrous $CeCl_3$ in THF was added to a solution of $Li[Ph_2P(NSiMe_3)_2]$ in THF. The reaction mixture was stirred over night at room temperature. The product **10** was extracted as a golden-yellow solution in *n*-pentane. Complex **10** was isolated as exceedingly air- and moisture-sensitive bright yellow, block-like crystals at 5 °C in 78% yield. The new compound $[Ph_2P(NSiMe_3)_2]_2Ce(\mu\text{-}Cl)_2Li(THF)_2$ (**10**) has been fully characterized by spectroscopic methods, elemental analysis and single-crystal X-ray diffraction. The molecular structure of **10** is in good agreement with related structures such as $[Ph_2P(NSiMe_3)_2]_2Sm(\mu\text{-}I)_2Li(THF)_2$ [122]. The IR spectrum showed a medium band at 1180 and 1116 cm^{-1} which can be assigned to the PNSi unit. The strong bands can be attributed to the $SiMe_3$ groups which appear at 1246, 933 and 840 cm^{-1}. The ^1H NMR spectrum of **10** shows multiple sets of signals due to the phenyl group and the coordinated THF molecules. Due to the paramagnetic nature of Ce(III) ion, the protons of the $Si(CH_3)_3$ groups appear as singlets at high magnetic field at $\delta = -6.50$ ppm. The X-ray study revealed that, unlike the

previous Ce(III) complexes **5** and **6**, the presence of the "ate" complex $[Ph_2P(NSiMe_3)_2]_2Ce(\mu\text{-}Cl)_2Li(THF)_2$ (**10**). The cerium(III) ion is coordinated with four nitrogen atoms of the diiminophosphinate ligands and two chlorine atoms, giving a formal coordination number of six as shown in Figure 9.

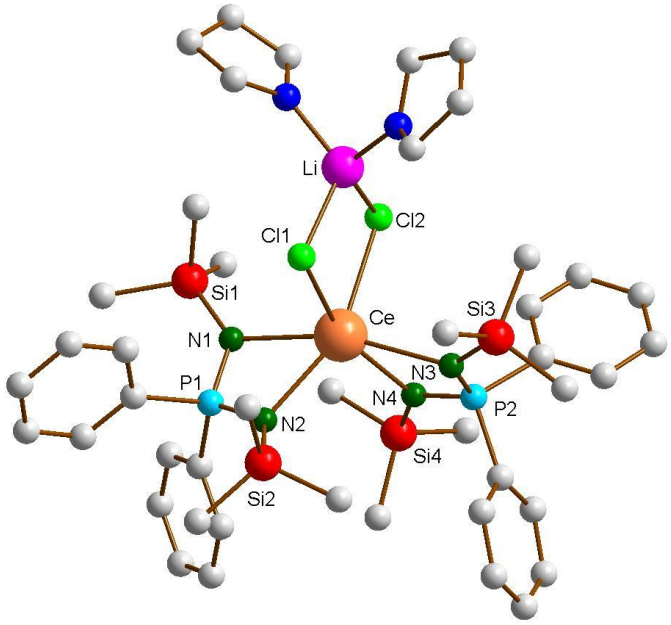

Figure 9. Molecular structure of $[Ph_2P(NSiMe_3)_2]_2Ce(\mu\text{-}Cl)_2Li(THF)_2$ (**10**)

Compound **10** crystallizes in the monoclinic space group $P2_1/n$ with one molecule of the complex in the unit cell. The average Ce–N bond distance (2.551 Å) is almost identical compared to the Ce–N distances in **5** and **6**. Likewise, the Ce–Cl distance (average 2.810 Å) is very similar. The bond lengths P1–N1 (1.593(2) Å), P1–N2 (1.594(2) Å), P2–N3 (1.597(2) Å) and P2–N3 (1.593(2) Å) are almost equal, confirming the delocalization of the negative charge in the N1–P1–N2 and N3–P2–N4 units, respectively. The bond angles N1–Ce–N2 (60.96(7)°) and N3–Ce–N4 (60.80(7)°) in **10** are longer than those observed in **5** and **6**. The bond angles Ce–Cl1–Li, Cl1–Li–Cl2, and Cl1–Ce–Cl2 are 39.80(10)°, 97.7(2)° and 79.01(3)°, respectively, to form the distorted rhomb-shaped CeCl1LiCl2 unit.

2.2.4. A holmium(III)-(amidinatoguanidinate) complex

In a straightforward manner according to Scheme 15, the treatment of *N*,*N*′-dicyclohexylcarbodiimide with ^{n}BuLi in Et_2O followed by *in situ* addition of anhydrous $HoCl_3$ in THF and recrystallization from *n*-pentane resulted in formation of the unexpected holmium-(amidinatoguanidinate) complex [^{n}Bu-C(=NCy)(NCy)C(NCy)$_2$]Ho[^{n}Bu-C-(NCy)$_2$](μ-Cl)$_2$Li(THF)$_2$ (**11**) in 71% yield as shown in Scheme 15.

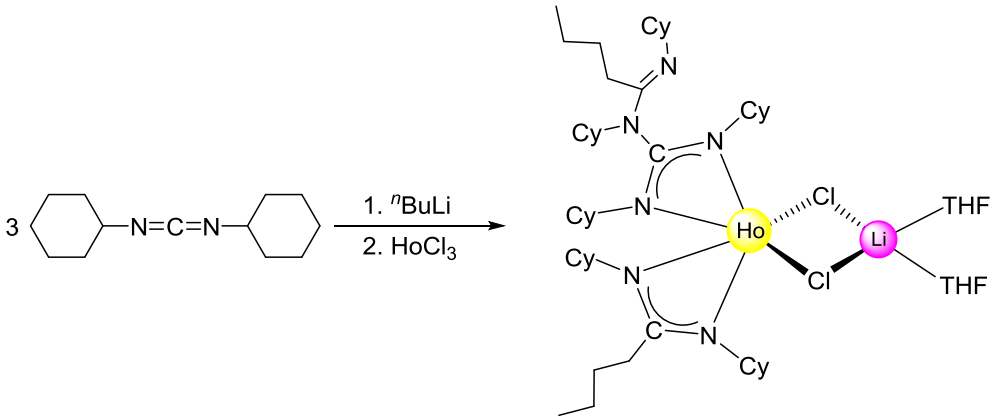

11: 71% yield

Scheme 15

The mixture of amidinate and guanidinate ligands was further demonstrated by the serendipitous isolation of the complex **11**, while the treatment of *N*,*N*′-dicyclohexylcarbodiimide with ^{n}BuLi in THF afforded only a guanidinate ligand, Li[^{n}Bu-C(=NCy)(NCy)C(NCy)$_2$] (**4**) as shown in Scheme 9. Compound **11** was fully characterized by spectroscopic methods, elemental analysis and single-crystal X-ray diffraction. Owing to the highly paramagnetic nature of Ho^{3+}, it was impossible to obtain NMR signals for **11**. Complex **11** crystallizes in the triclinic space group P-1 with two molecules in the unit cell. The X-ray study revealed the presence of an "ate" complex type in **11**.The molecular structure is shown in Figure 10. The bimetallic complex **11** consists of the central holmium atom which is coordinated by two bridging chloride ligands, one chelating guanidinate ligand and one chelating amidinate ligand. The Ho atom lies in the CN3 plan of the chelating guanidinate ligand. Within the chelating NCN units of the amidinate and the guanidinate ligands, the C–N distances are nearly equal (average C–N = 1.332 Å), indicating π electron delocalization within these units. The C2–N3 bond length is 1.403 Å, whereas the C2–N4 bond length is

1.273 Å, indicating a localization of π-electron density between C2 and N4 atoms. The Ho–N distances (average 2.341 Å) are agreement with related amidinate and guanidinate complexes. The Ho–Cl and Li–Cl bond distances as well as the Cl1–Ho–Cl2 and Ho–Cl–Li bond angles show that the HoCl1LiCl2 unit is rhomb-shaped.

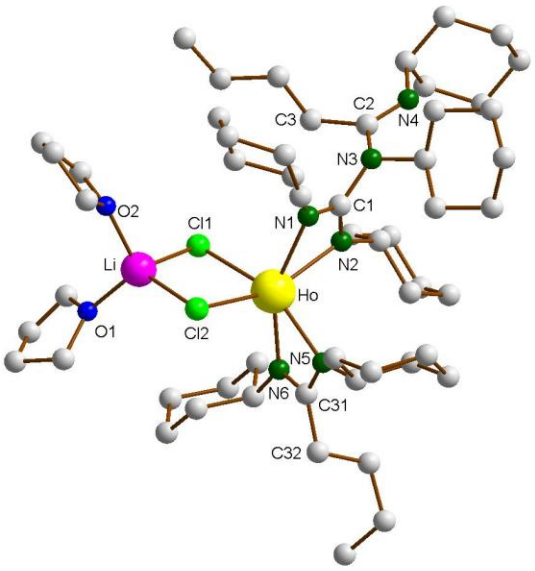

Figure 10. Molecular structure of [^{n}Bu-C(=NCy)(NCy)C(NCy)$_2$]Ho[^{n}Bu-C(NCy)$_2$](μ-Cl)$_2$Li(THF)$_2$ (**11**)

The orientation of the [^{n}Bu-C(=NCy)(NCy)] group relative to the HoNCN plane is approximately perpendicular, similar to that found earlier for this type of ligands [111, 124, 125]. The bond angles N1–Ho–N2 (57.03(11)°) and N5–Ho–N6 (57.38(11)°) are almost identical with those found in compound **8**.

2.3. Synthesis and structural characterization of lanthanide(III) tris(amidinate) complexes

A first application of lanthanide amidinate complexes, their catalytic activity for the ring-opening polymerization (ROP) of ε-caprolactone at room temperature, was discovered by using homoleptic lanthanide(III) tris(amidinate) complexes [69, 126]. Moreover, a high catalytic activity of homoleptic lanthanide(III) tris(amidinate) compounds has been found for the polymerization of other polar monomers such as trimethylene carbonate (TMC), L-lactide and methylmethacrylate (MMA) [22]. In the year 2003, Gordon *et al.* first reported that pure rare-earth metals can be deposited by using volatile homoleptic metal amidinato complexes of the type $Ln[RC(NR')_2]_3$ (R = Me, ^{t}Bu; R′ = ^{i}Pr, ^{t}Bu) and molecular hydrogen gas as the reactants [40, 127, 128]. By now the homoleptic lanthanide complexes have been shown to be valuable precursors in materials science and nanotechnology [22].

2.3.1. Lanthanide(III) tris(cyclopropylethynylamidinate)

The reaction of anhydrous $LnCl_3$ (Ln = Nd, Sm or Ho) with **1a**, as well as the reaction of anhydrous $SmCl_3$ with **2a** in a 1:3 molar ratio using THF as solvent at 65 °C for 3 hours followed with stirring at room temprature over night afforded a series of new lanthanide tris(cyclopropylethynylamidinates), $[c\text{-}C_3H_5\text{-}C{\equiv}C\text{-}C(NR)_2]_3Ln$ (**12**: Ln = Nd, R = ^{i}Pr; **13**: Ln = Sm, R = ^{i}Pr; **14**: Ln = Sm, R = cyclohexyl (Cy); **15**: Ln = Ho, R = ^{i}Pr) were isolated as illustrated in Scheme 16. All these homoleptic lanthanide amidinate species are air- and moisture-sensitive. They are highly soluble in common non-protic solvents, including THF, diethyl ether, toluene and *n*-pentane. The products were isolated in moderate (**12**: 54%, **13**: 55%), (**15**: 45%) to good (**14**: 79%) yields as unsolvated complexes in the form of brightly colored crystals (**12**: green, **13**: yellow, **14**: yellow, **15**: yellow).

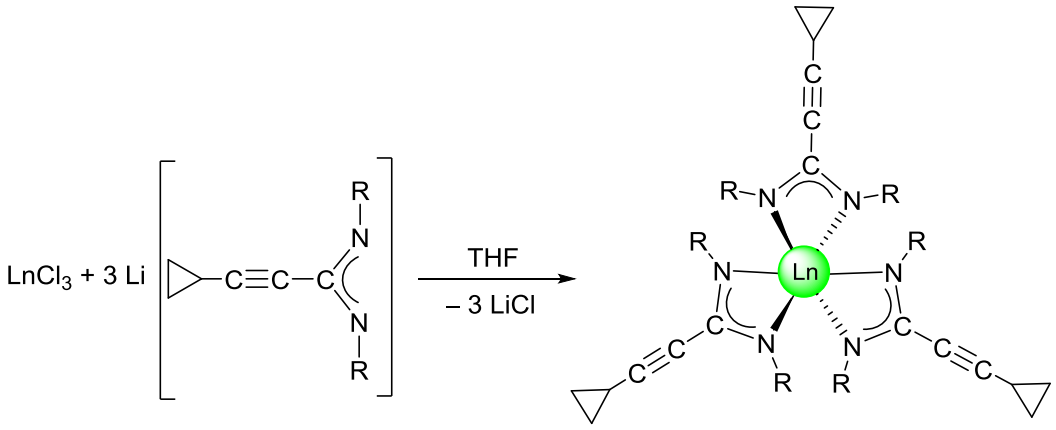

1a: R = ^{i}Pr
2a: R = *c*-C_6H_{11} (= Cy)

12: Ln = Nd, R = ^{i}Pr, 54% yield
13: Ln = Sm, R = ^{i}Pr, 55% yield
14: Ln = Sm, R = Cy, 79% yield
15: Ln = Ho, R = ^{i}Pr, 45% yield

Scheme 16

The structure of the new unsolvated lanthanide(III) tris(cyclopropylethynylamidinate) complexes **12** – **15** was supported by elemental analysis and spectroscopic methods. In the IR spectra, there are strong absorption bands of the C=N stretch at 1591 – 1612 cm^{-1}, which are consistent with the delocalized π-bond of the NCN unit [95, 129], whereas medium bands at 2220 – 2227 cm^{-1} can be assigned to C≡C vibrations. The mass spectra of **13**, **14** and **15** showed the molecular ion with low relative intensity, whereas the mass spectrum for **12** showed the molecule without two isopropyl groups. Meaningful NMR spectroscopic data were available for compounds **12**, **13** and **14**, whereas the strongly paramagnetic nature of the Ho^{3+} ion prevented the measurement of an interpretable ^{1}H NMR spectrum, although a ^{13}C NMR spectrum of **15** could be obtained. Unlike the previously described solvated complexes **5**, **6** and **7**, the NMR spectra of the unsolvated complexes **12** – **14** were easier interpretable. Deuterated benzene, C_6D_6, was found to be the suitable solvent for measuring the NMR spectra of these homoleptic complexes. In the ^{1}H NMR, by comparison between the complexes **12** and **13**, the protons of CH in the isopropyl group appear at high field at δ = 22.3 ppm in **12** (Figure 11) whereas in **13** they appear at δ 3.60 ppm (Figure 12), and the protons of the CH_3 group appear at δ = – 3.55ppm in **12** while they appear in **13** at δ = – 0.47 ppm. Obviously, this difference in the field shift can be attributed to the stronger paramagnetic nature of Nd^{3+} ion than that of the Sm^{3+} ion.

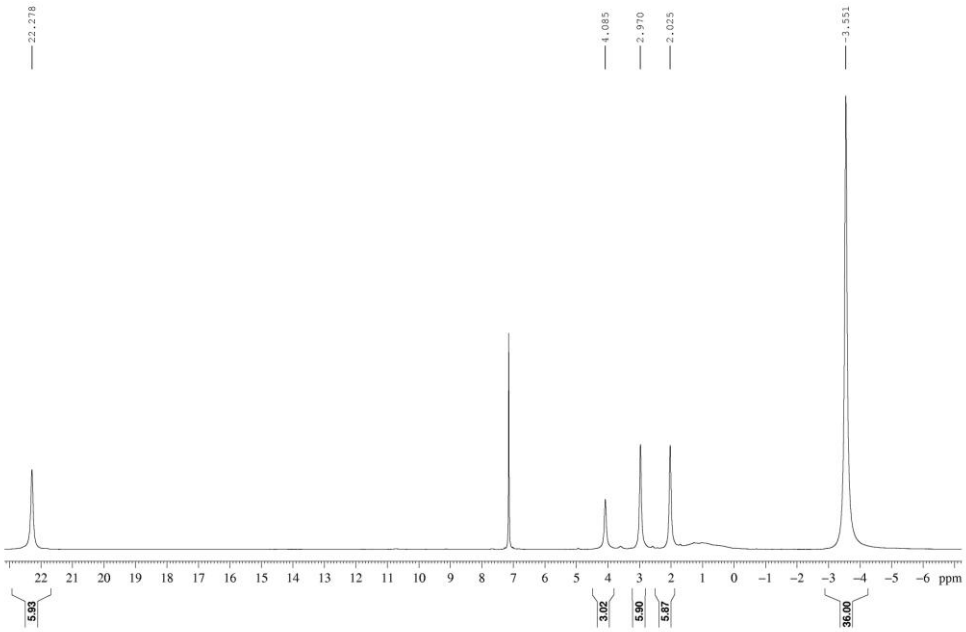

Figure 11. ^{1}H NMR spectrum (400 MHz, C_6D_6, 25 °C) of [*c*-C_3H_5-C≡C-C(N^{i}Pr)$_2$]$_3$Nd (**12**).

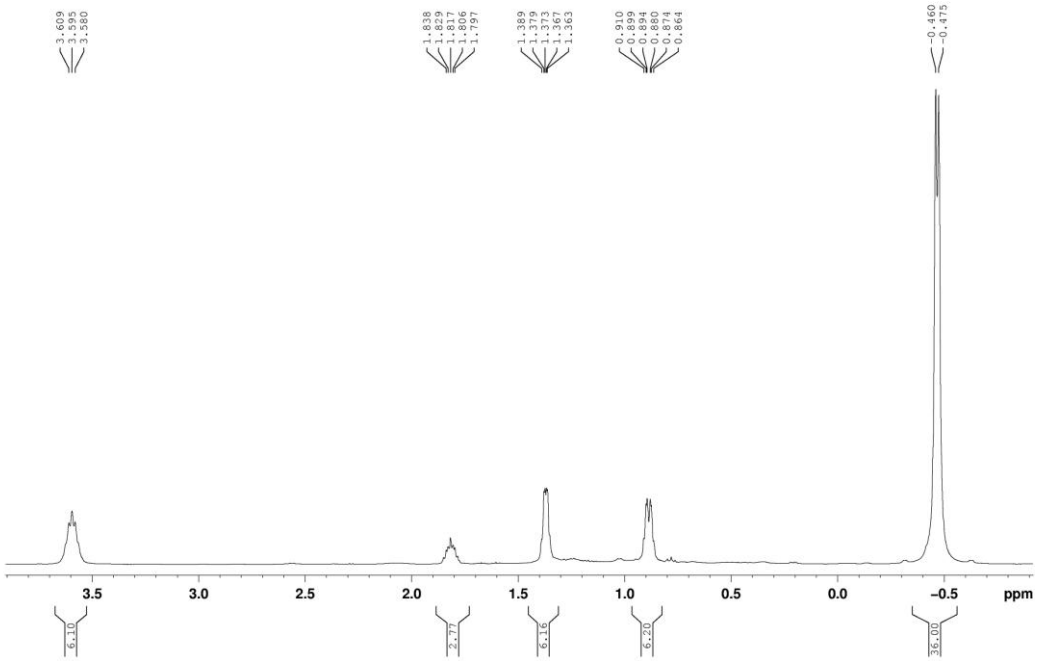

Figure 12. ^{1}H NMR spectrum (400 MHz, C_6D_6, 25 °C) of [*c*-C_3H_5-C≡C-C(N^{i}Pr)$_2$]$_3$Sm (**13**).

The ^{1}H NMR spectrum of [*c*-C_3H_5-C≡CC(NCy)$_2$]$_3$Sm (**14**) confirmed the formulation as an unsolvated homoleptic samarium complex. As shown in Figure 13, all the protons of **14** are clearly observed and are in a good agreement with the expected composition of **14**. Since they have the same lanthanide ion, a comparison between the spectra of complexes **13** and **14** showed the CH protons of the cyclohexyl group to appear at δ = 3.40 ppm in **14** which is very close to the signal observed for the CH protons of the isopropyl group in **13** (δ = 3.60 ppm).

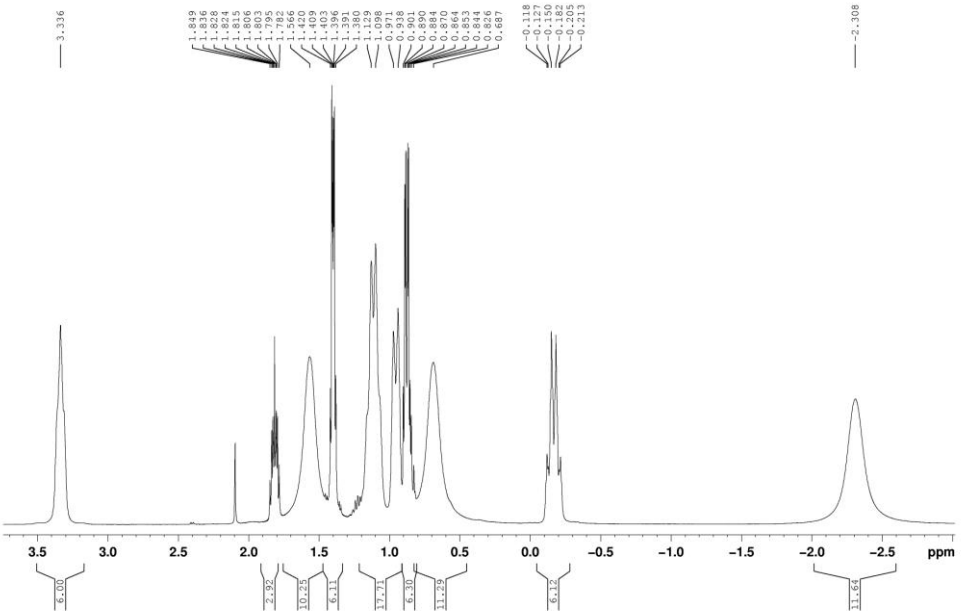

Figure 13. ^{1}H NMR spectrum (400 MHz, C_6D_6, 25 °C) of [*c*-C_3H_5-C≡C-C(NCy)$_2$]$_3$Sm (**14**).

Remarkable low-field shifts are observed in the ^{13}C NMR spectra for the central carbon atoms of the amidinate N–C–N linkage (**12**, δ = 228.6 ppm; **13**, δ = 201.6 ppm; **14**, δ = 201.9 ppm; **15**, δ = 224.8 ppm). These values show the pronounced tendency of the Nd^{3+}, Sm^{3+} and Ho^{3+} ions to act as intramolecular shift reagents. The carbon atoms of CH in the isopropyl or the cyclohexyl groups were observed at varying values depending on the type of the substituent, isopropyl or cyclohexyl, and the nature of lanthanide ion. The CH signal of the isopropyl groups in **12** was observed at δ = 65.3 ppm (Figure 14) whereas in the samarium the comparable signal for **13** was observed at δ = 48.3 ppm (Figure 15).

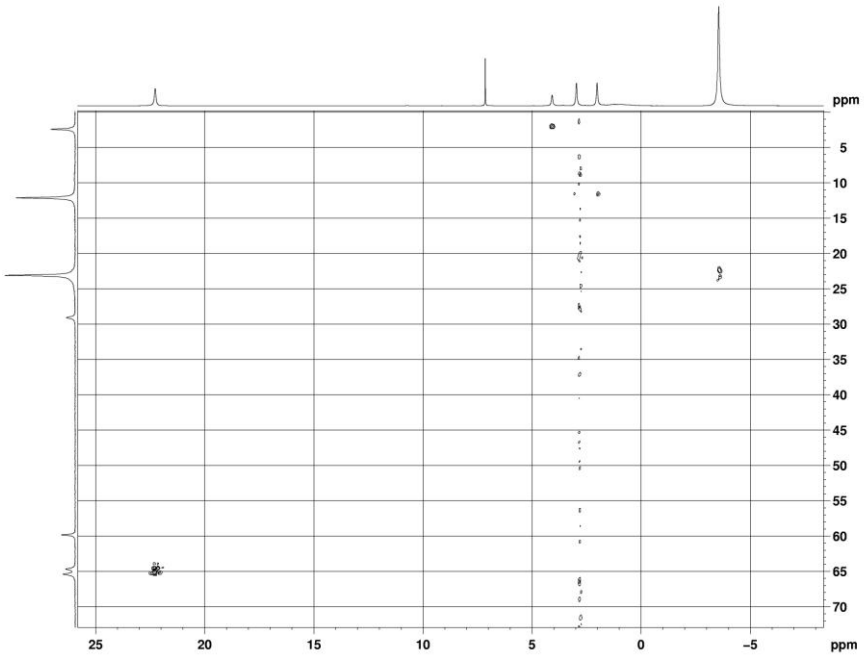

Figure 14. HSCQ spectrum (400 MHz, C_6D_6, 25 °C) of [*c*-C_3H_5-C≡C-C(N^{i}Pr)$_2$]$_3$Nd (**12**).

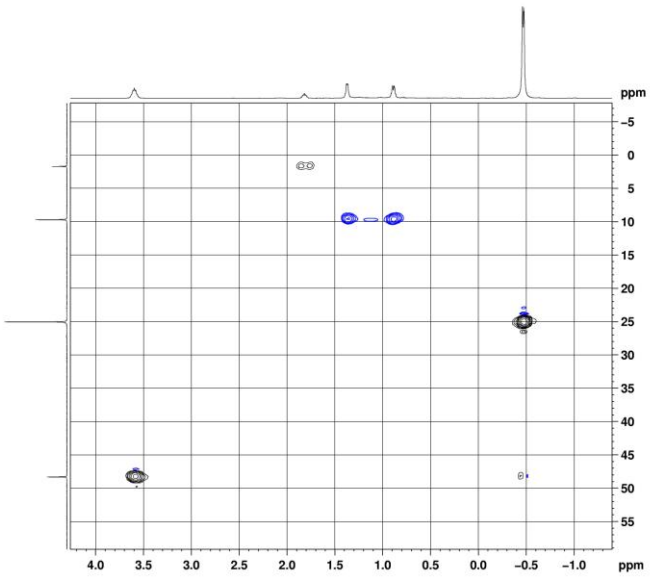

Figure 15. HSQC spectrum (400 MHz, C_6D_6, 25 °C) of [*c*-C_3H_5-C≡C-C(N^{i}Pr)$_2$]$_3$Sm (**13**).

Despite the fact that protons of the CH-isopropyl and CH-cyclohexyl groups in **13** and **14**, respectively, are very close together in the ^{1}H NMR spectra, the ^{13}C NMR spectra showed that

the carbon signal of CH-cyclohexyl of **14** has shifted to high field to appear at δ = 56.9 ppm (Figure 16) and the CH-isopropyl signal in **13** was observed at δ = 48.3 ppm.

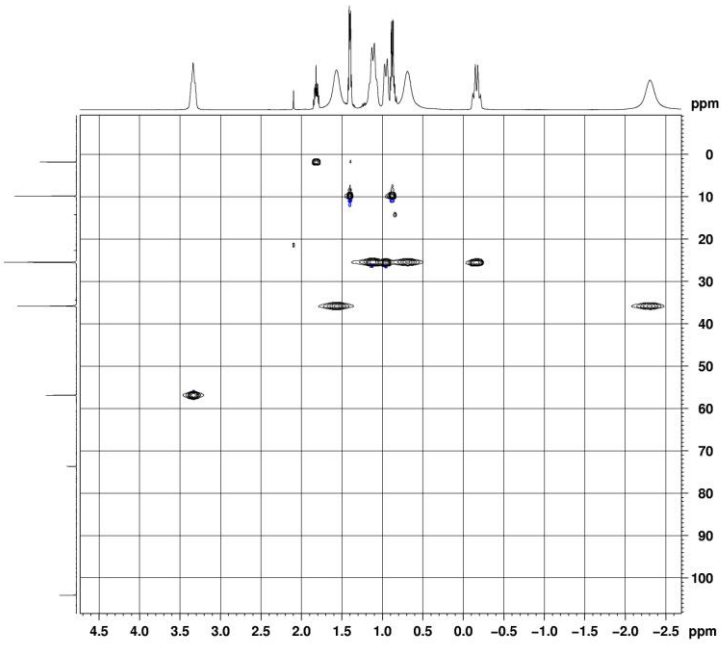

Figure 16. HSQC spectrum (400 MHz, C_6D_6, 25 °C) of [*c*-C_3H_5-C≡C-C(NCy)$_2$]$_3$Sm (**14**).

The molecular structure of [*c*-C_3H_5-C≡CC(N^{i}Pr)$_2$]$_3$Ho (**15**) was determined by single-crystal X-ray diffraction. Compound **15** crystallizes from *n*-pentane at −32 °C in the triclinic space group P-1 with one molecule in the unit cell. The molecular structure of **15** is shown in Figure 17. The central Ho atom is coordinated by three bidentate cyclopropylethynylamidinate ligands through the nitrogen atoms to form Ho–N–C–N units. The average bond distance of Ho–C to the N–C–N unit of the amidinate moiety is 2.76 Å, which indicates an η^3-allyl structure [130]. The C–N bond distances within the chelating N–C–N unit are nearly equal and their average value is 1.332 Å, which reflects the delocalization of the π-bonds in the NCN unit. The average Ho–N bond length is 2.356 Å, which is comparable with those of the analogues homoleptic complexes, [Ph-C(NCy)$_2$]$_3$Sm (2.42 Å) and [Ph-C(NSiMe$_3$)$_2$]$_3$Eu (2.48 Å) [99].

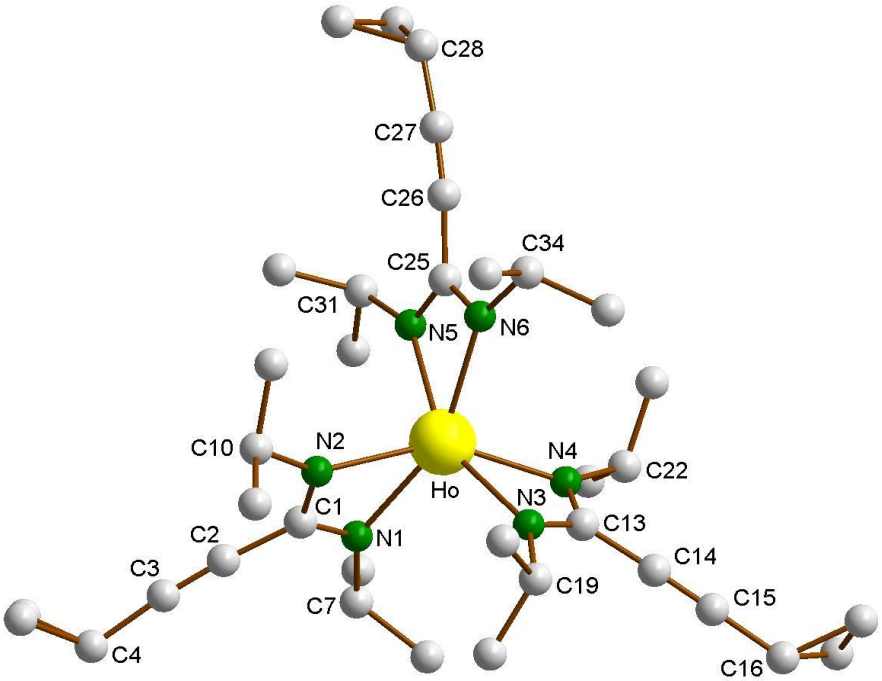

Figure 17. Molecular structure of [*c*-C_3H_5-C≡CC(N^{i}Pr)$_2$]$_3$Ho (**15**).

The three four-membered rings HoNCN are planar and are twisted by 0.71 Å with respect to each other. The average N–Ho–N angle is 57.3 (9)° which similar to analogous compounds [132, 136]. The N–C–N angles in the NCN units are nearly equal, and the average value is 116.8 (3)°.

The new complexes **12**, **13**, **14** and **15** have been found to show catalytic activity in the reaction of alkynes with *N*,*N*′-diisopropylcarbodiimide or *N*,*N*′-dicyclohexylcarbodiimide to give the corresponding alkynylamidines. This will be discussed in detail in the section describing the catalytic activity of lanthanide(III) amidinate (Section 2.6.2.).

2.3.2. Lanthanide(III) tris(propiolamidinates)

A series of homoleptic lanthanide(III) tris(propiolamidinates) were prepared in a straightforward manner according to Scheme 17. The reaction of a solution of anhydrous $LnCl_3$ (Ln = Ce, Nd, Sm or Ho) with **3a** in a 1:3 molar ratio by using THF as solvent afforded a series of new lanthanide tris(propiolamidinate), [Ph-C≡C-C(NCy)$_2$]$_3$Ln (**16**: Ln = Ce; **17**: Ln = Nd; **18**: Ln = Sm; **19**: Ln = Ho). The products were isolated in moderate (**16**: 61%, **17**: 56% and **18**: 59% to high **19**: 89%) yields as unsolvated complexes in the form of brightly colored crystals (**16**: orange, **17**: pale green, **18**: yellow, **19**: bright yellow).

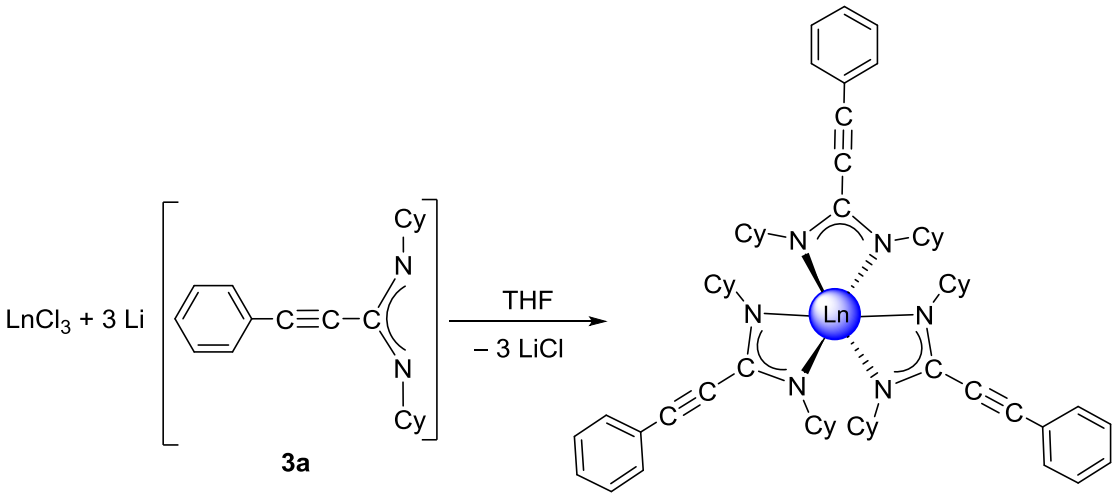

Scheme 17

The new unsolvated lanthanide tris(propiolamidinate) complexes, [Ph-C≡C-C(NCy)$_2$]$_3$Ln (**16** – **19**) have been fully characterized by spectroscopic methods and elemental analysis. Unfortunately, attempted recrystallization of complexes **16** and **19** from various solvents such as toluene, pentane, THF or diethyl ether did not provide single-crystals suitable for X-ray diffraction. Only on one occasion, well-formed crystals of **19** obtained from *n*-pentane could be successfully subjected to X-ray diffraction, but the crystal quality was too poor to allow full refinement of the crystal structure. The NMR spectra were in good agreement with those of similar unsolvated homoleptic lanthanide amidinate complexes, [Ph-C≡C-C(N^{i}Pr)$_2$]$_3$Ce [95] and [Ph-C(NCy)$_2$]$_3$Ln (Ln = Pr, Nd or Sm) [99]. Due to the paramagnetic nature of Ho^{3+} ion, it was impossible to obtain NMR spectra for **19**. According to the ^{1}H–^{13}C correlation (HSQC) technique, the protons of CH in the cyclohexyl group observed at three different positions, δ = 9.49, 3.76 and 3.56 ppm in **16** (Figure 18) and at δ = 18.33, 3.77 and 3.57 ppm in **17** (Figure 19) are in agreement with the CH-protons in the complex [Ph-C(NCy)$_2$]$_3$Ln (Ln = Pr or Nd), whereas the CH-protons of *c*-C_6H_{11} in **19** (Figure 20) appear at δ 3.71 and 3.30 ppm [99]. The protons of the phenyl group appear in the range of δ = 7.40 – 9.41 ppm [95, 99].

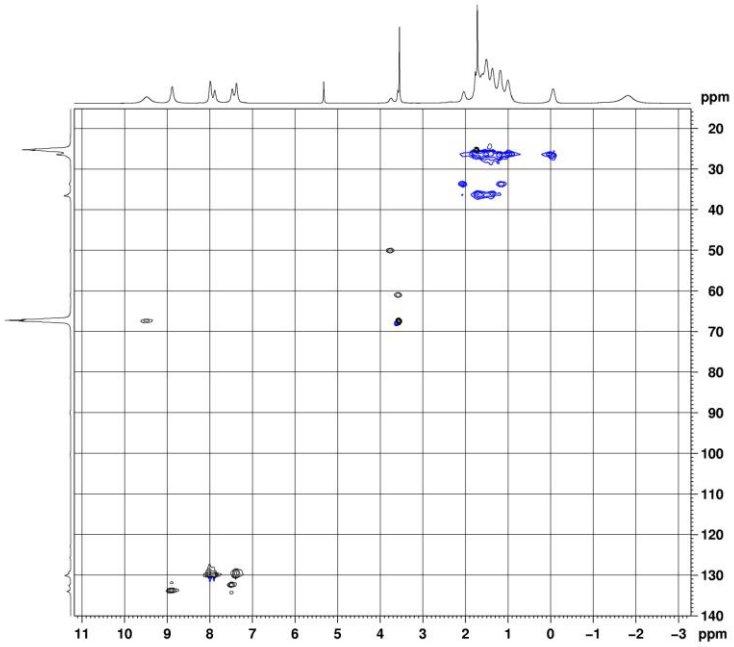

Figure 18. HSQC spectrum (400 MHz, THF-d_8, 25 °C) of [Ph-C≡C-C(NCy)$_2$]$_3$Ce (**16**).

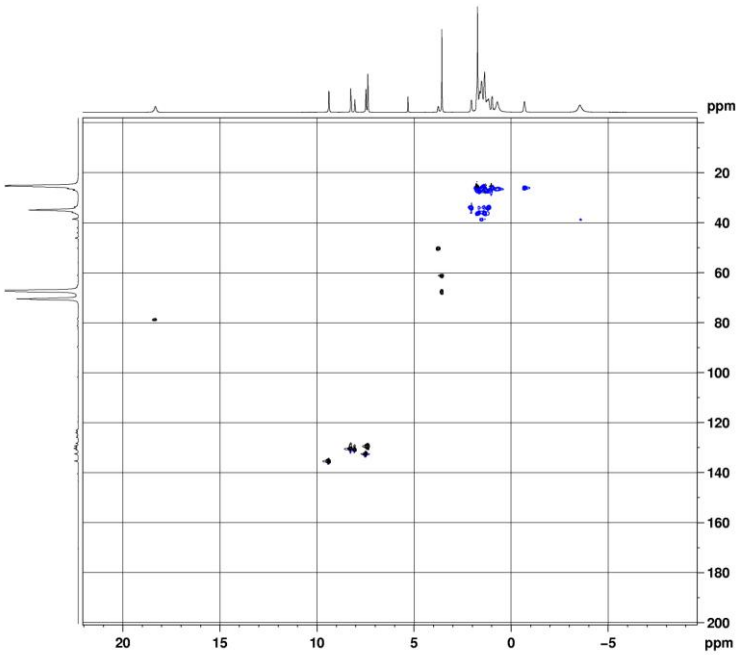

Figure 19. HSQC spectrum (400 MHz, THF-d_8, 25 °C) of [Ph-C≡C-C(NCy)$_2$]$_3$Nd (**17**).

The ^{1}H NMR spectra showed the highly paramagnetic properties for the complexes of cerium **16** and neodymium **17** as compared the samarium complex **18**. On the other hand, the $^{13}C\{^{1}H\}$ NMR spectra showed that the carbons of the phenyl groups were observed in the range of δ = 125 – 140 ppm. The carbon atoms of the CH of the cyclohexyl groups were observed at δ = 67.1, 61.1 and 56.3 ppm in **16**, and at δ = 78.5, 61.1 and 50.0 ppm in **17**, whereas in **18** they were observed at δ = 59.5 and 57.4 ppm. The carbon atoms of the CH_2 in the cyclohexyl group appear in the same range at δ = 25.7 – 36.5 ppm for all of three complexes.

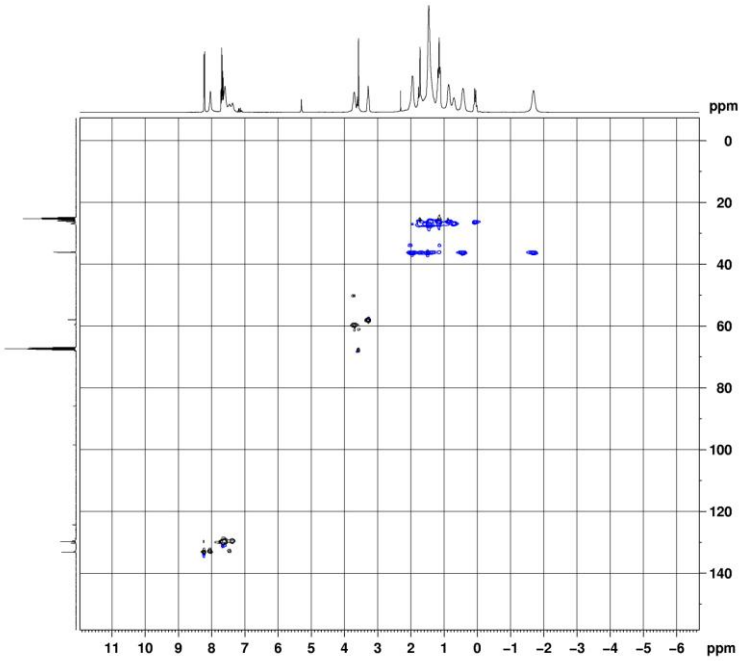

Figure 20. HSQC spectrum (400 MHz, THF-d_8, 25 °C) of [Ph-C≡C-C(NCy)$_2$]$_3$Sm (**18**).

2.4. Synthesis and structural characterization of lanthanide(III) bis(amidinato) amide complexes

Recently, alternative ligand environments other than cyclopentadienyl, such as amidinates, guanidinates and β-diketimines [22, 40, 131] have been developed to form lanthanide complexes as efficient homogenous catalysts. Some of these complexes have been found to show exciting reactivity. For example, Shen *et al*. reported that lanthanide bis(guanidinate) diisopropylamido complexes are highly active initiators for the polymerization of *ε*-caprolactone and methyl methacrylate (MMA) [117]. Piers *et al.* discovered that β-diketiminato scandium methyl complexes are efficient precatalysts for ethylene polymerization [132]. Most recently, Roesky *et al.* reported that β-diketiminate rare-earth borohydride complexes have high catalytic activity toward the ring-opening polymerization of *ε*-caprolactone and trimethylene carbonate [133], and they also discovered the first chiral lutetium bis(benzamidinato) amide complexes and their catalytic activity towards hydroamination reactions [73].

Amination of the lanthanide bis(amidinate) complexes, **5**, **6**, **7** and **8** with 2 equivalents (1 equivalent in case of **8**) of $KN(SiMe_3)_2$ in THF afforded new unsolvated lanthanide bis(amidinato) amide complexes $[c\text{-}C_3H_5\text{-}C{\equiv}C\text{-}C(NR)_2]_2LnN(SiMe_3)_2$ (**20**: Ln = Ce, R = ^{i}Pr; **21**: Ln = Ce, R = Cy; **22**: Ln = Nd, R = Cy; **23**: Ln = Ho, R = Cy). These complexes were isolated in low yields in the case of complexes **20** and **21** (17% and 28%, respectively) to moderate isolated yields in **22** and **23** (39% and 42%, respectively) as shown in method (b) according to Scheme 74. Furthermore, the new complexes **20** – **23** could be prepared *via* a multi-component reaction as shown in Scheme 18 method (a). The reaction mixture containing $LnCl_3$ (Ln = Ce, Nd or Ho) and **1a** or **2a** as well as $KN(SiMe_3)_2$ in a 1:2:1 molar ratio, respectively, in THF afforded the complexes **20** – **23** in moderate to good isolated yields (**20**: 37%, **21**: 52%, **22**: 67% and **23**: 56% yields). The structures of the complexes **20** – **23** were confirmed by elemental analysis and spectroscopic techniques as well as single-crystal X-ray diffraction for **22** and **23**. In the IR spectra, the methyl groups in the $SiMe_3$ groups absorb at 2926, 2850, 1469, 834 and 700 cm^{-1}. The bands at 1638, 1595, 1469 and 1450 cm^{-1} can be attributed to the chelating N–C–N units. The IR spectra of **1a** or **2a** exhibit no emission at 1683 cm^{-1} but an intensive line at 1384 cm^{-1} or at 1393 cm^{-1} [99].

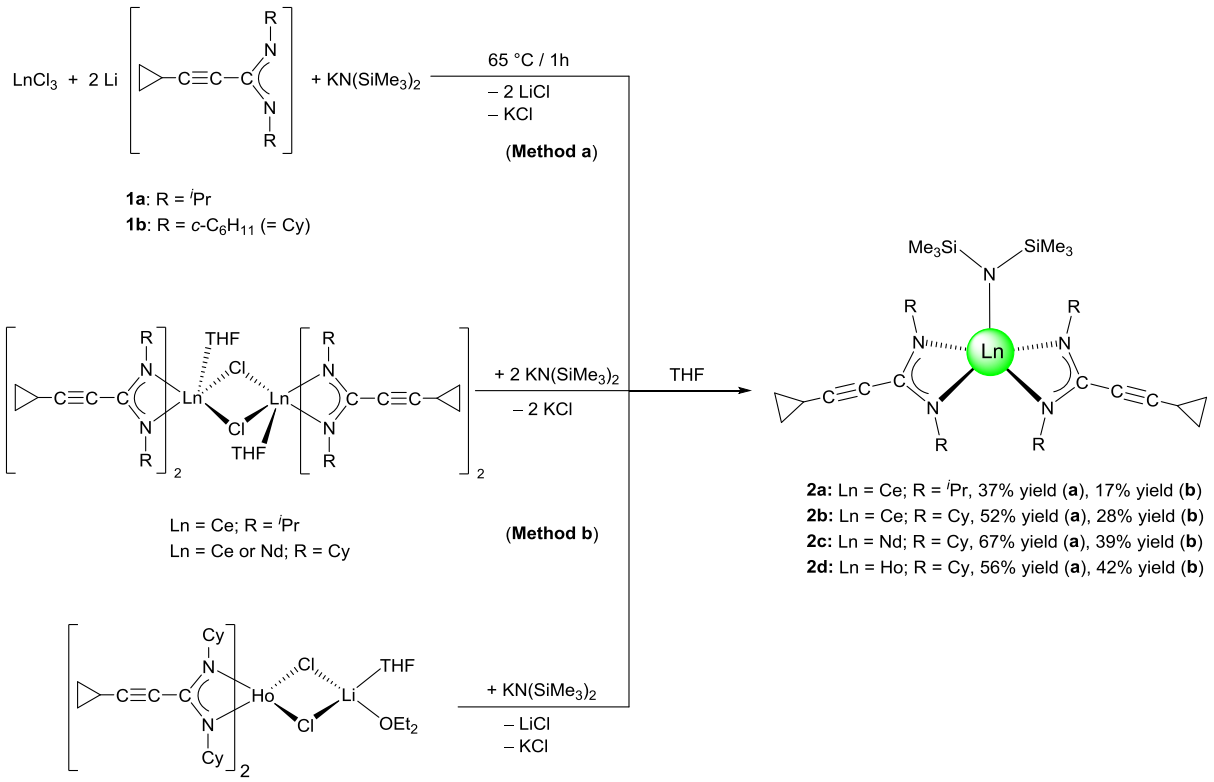

Scheme 18

NMR data confirmed that the compounds **20**, **21** and **22** are unsolvated complexes. In complex **20**, an ^{1}H NMR spectrum in C_6D_6 showed that the protons of the methyl groups in the two $Si(CH_3)_3$ moieties appear as a sharp singlet at $\delta = 0.04$ ppm. The CH_3 protons of the isopropyl groups appear as broad singlet of resonance at $\delta = -2.95$ ppm. The CH protons of the isopropyl groups appear at $\delta = 11.95$ ppm (Figure 21). The $^{13}C\{^{1}H\}$ NMR shows the carbon atoms of the CH of isopropyl groups at $\delta = 56.1$ ppm, whereas the CH_3 carbon atoms of the isopropyl groups appear at $\delta = 23$ ppm. The ^{29}Si NMR spectrum shows a signal at $\delta = -2.96$ ppm.

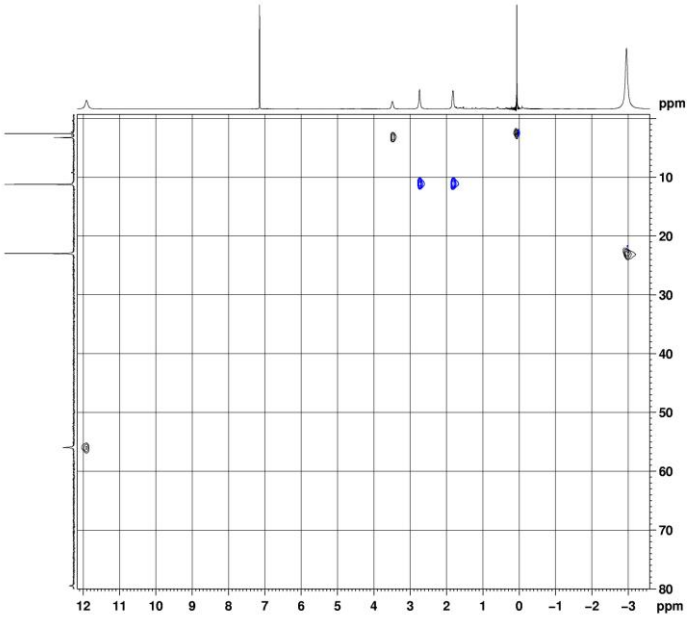

Figure 21. HSQC spectrum (400 MHz, C_6D_6, 25 °C) of [*c*-C_3H_5-C≡C-C(N^iPr)$_2$]$_2$CeN($SiMe_3$)$_2$ (**20**)

The room temperature ^1H and ^{13}C NMR spectra for **21** were in good agreement with the expected structure (Figure 22). The protons of CH in the cyclohexyl groups are observed at δ = 11.87 ppm and the protons of the methyl groups in $Si(CH_3)_2$ appear at δ = 0.05 ppm. The CH_2 protons of the cyclohexyl groups appear in the range from δ = 0.52 to δ = – 7.2 ppm. The carbon atoms of the CH of cyclohexyl groups are observed at δ = 65.0 ppm. The ^{29}Si NMR spectrum shows a singlet at δ = 1.92 ppm. Due to the stronger paramagnetic nature of the Nd^{3+} ion as compared to the Ce^{3+} ion, the protons of the CH of cyclohexyl in **22** are observed at δ = 25.85 ppm and the CH_2 protons in the range from δ = 0.34 to δ = – 13.50 ppm. The CH carbon atoms in the cyclohexyl groups appear at δ = 61.6 ppm. The ^{29}Si NMR spectrum of **22** a signal at δ = – 83 ppm. According to the highly paramagnetic nature of Ho^{3+} ion, it was impossible to obtain NMR spectra for **23**.

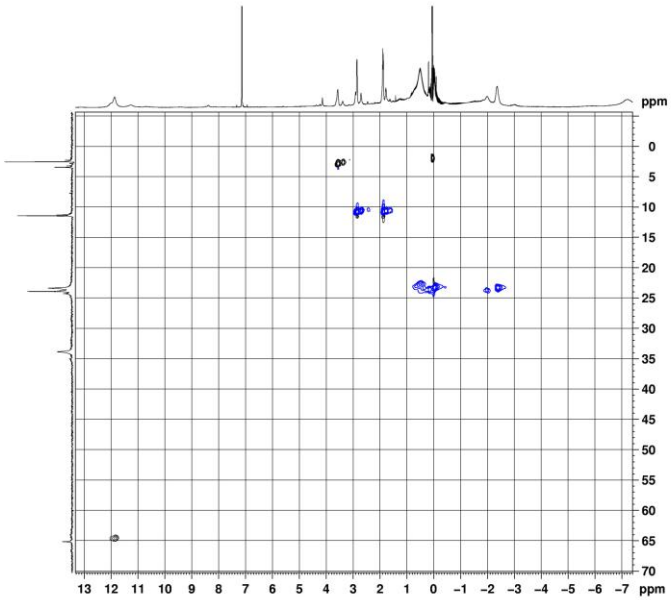

Figure 22. HSQC spectrum (400 MHz, C_6D_6, 25 °C) of [*c*-C_3H_5-C≡C-$C(NCy)_2]_2CeN(SiMe_3)_2$ (**21**)

Single-crystals of the compounds **22** and **23** were found to be suitable for single-crystal X-ray diffraction. The complexes **22** and **23** crystallize from *n*-pentane as monomeric structures with two molecules of **22** and one molecule of **23** in the unit cells in the orthorhombic space group Pbca in the solid state. The neodymium and holmium ions are coordinated by four nitrogen atoms of the two chelating amidinate ligands and the nitrogen atom of $N(SiMe_3)_2$ ligand. Thus the formal coordination number of the Ln^{3+} ions in **22** and **23** is five. The geometry around the Ln^{3+} ion (Nd in **22** and Ho in **23**) can be described as a *pseudo*-pyramidal with the four nitrogen atoms of the two chelating amidinate ligands forming the bottom, and the nitrogen atom of the $N(SiMe_3)_2$ group defining the vertex, as shown in Figure 23. The distances of Nd to the nitrogen atoms of the amidinate ligands in **22** are similar (average Nd–$N_{amidinate}$ = 2.426(2) Å). The Nd–N5 bond length is 2.323(2) Å, which is consistent with La–N in $La[CyNC(N(SiMe_3)_2)NCy](N(SiMe_3)_2)_2$ (2.377(3) Å and 2.382(3) Å) [134], and significantly longer than in previously characterized organolanthanide amide compound [{(*S*)-$PEBA\}_2Lu\{N(SiMe_3)_2\}$] ((*S*)-PEBA = (*S*,*S*)-*N*,*N*-bis-(1-phenylethyl)benzamidinate), (2.200 (7) Å) [73], if the difference in ionic radii between Nd^{3+} and Lu^{3+} ions is considered. Likewise, in complex **23** no difference between the bond lengths of the Ho–$N_{amidinate}$ bonds

has been observed (average Ho–$N_{amidinate}$ = 2.330(2) Å), whereas the bond length of Ho–N5 is 2.224(3) Å, which is very close to the Er–N σ-bond length in $(MeC_5H_4)_2ErNC_5H_{10}(HNC_5H_{10})$ (2.159(5) Å) [185].

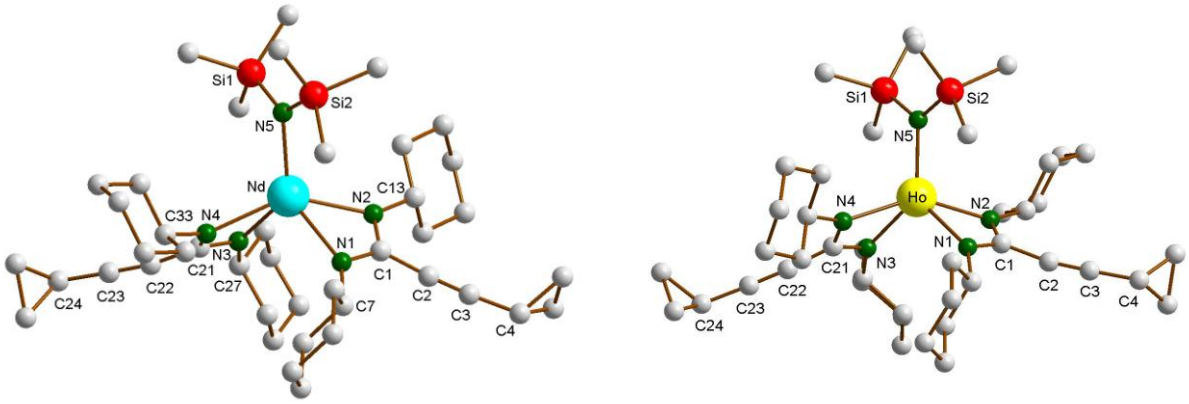

Figure 23. Molecular structures of $[c\text{-}C_3H_5\text{-}C{\equiv}C\text{-}C(NCy)_2]_2NdN(SiMe_3)_2$ (**22**) (left) and $[c\text{-}C_3H_5\text{-}C{\equiv}C\text{-}C(NCy)_2]_2HoN(SiMe_3)_2$ (**23**) (right).

The Nd–Si1 (3.452(9) Å) and Nd–Si2 (3.456(9) Å) distances in **22** are virtually identical, whereas there is a slight asymmetry in the Ho–N distances in **23** with Ho–Si1 (3.374(10) Å) and Ho–Si2 (3.430(9) Å) [73]. The C–N bond lengths in the NCN units of **22** and **23** complexes have similar values, indicating the negative charge delocalization within the NCN fragments (average C–N = 1.331(3) Å in **22** and 1.333(4) Å in **23**). The dihedral angle between the two planes Si1–N5–Si2 and C1–N5–C21 in **22** is 133.4° which is larger than that found in the complex $[(Me_3Si)_2NC(N^iPr)_2]_2YN^iPr_2$, 68.56° [117]. This can attributed to the steric hindrance of the cyclohexyl substituents on the nitrogen atoms with the amidinate moieties. The bond angles N1–Nd–N2 and N3–Nd–N4 in **22** are 55.50(7)° and 55.56(7)°, respectively, whereas the N1–Ho–N2 and N3–Ho–N4 bite angles in **23** are 59.20(8)° and 59.95(8)°, respectively. It can be seen in Figure 23 that the orientation of $N(SiMe_3)_2$ moieties relative to LnNCN (Ln = Nd or Ho) plane is approximately perpendicular. The average N–C–N bond angles in the amidinate moieties are 116.32(2)° in **22** and 116.05(4) in **23**.

2.5. Synthesis and structural characterization of (COT) lanthanide(III) amidinate complexes

The large flat cyclooctatetraenyl ligand ($C_8H_8^{2-}$, commonly abbreviated as COT) is an aromatic carbocyclic ring systems which plays a major role in organolanthanide and organoactinide chemistry. Lanthanide(II) cyclooctatetraenyl complexes of the type Ln(COT) (Ln = Eu or Yb) were reported as early as 1969 [135 – 137]. In the year 1970, Streitwieser *et al.* reported the first organolanthanide(III) complexes containing cyclooctatetraenyl as highly air-sensitive anionic sandwich complexes of the type $[Ln(COT)_2]^-$ [138 – 141], and in 1971 reported the dimeric mono(cyclooctatetraenyl) lanthanide(III) chlorides, $[(COT)Ln(\mu\text{-}Cl)(THF)_2]_2$ (Ln = Ce, Pr, Nd or Sm) [37, 38, 142 – 144]. Mono(cyclooctatetraenyl) lanthanide(III) halides of the type $[(COT)Ln(\mu\text{-}Cl)(THF)_2]_2$ are the most important precursors for the preparation of other half-sandwich complexes with cyclooctatetraenyl ligands [145, 146]. The coordinated THF cannot be removed from the solvates without extensive decomposition. The preparation of unsolvated organolanthanide half-sandwich complexes containing one COT ligand is, however, not always straightforward. In the year 1995 Schumann and Edelmann *et al.* reported a series of monomeric (cyclooctatetraenyl)lanthanide benzamidinates $(C_8H_8)Ln[4\text{-}RC_6H_4C(NSiMe_3)_2](THF)$ and the monomeric compounds $(C_8H_8)Ln[Ph_2P(NSiMe_3)_2](THF)$ [147]. Cloke *et al.* reported the first use of the 1,4-bis(trimethylsilyl)cyclooctatetraenyl dianion (= COT″) in organolanthanide chemistry [123, 148, 149].

2.5.1. Synthesis and structure of (COT)Ln[μ-*c*-C_3H_5-C≡C-$C(NR)_2]_2$Li(S)

The starting materials $[(COT)Ln(\mu\text{-}Cl)(THF)_2]_2$ (Ln = Pr or Nd) were prepared from anhydrous $LnCl_3$ and K_2COT according to the reported methods [38, 142 –144]. Treating a solution of the halide precursors $[(COT)Pr(\mu\text{-}Cl)(THF)_2]_2$ with **2a** as well as $[(COT)Nd(\mu\text{-}Cl)(THF)_2]_2$ with **1a** and **2a** in a 1:2 molar ratio, respectively, at room temperature afforded (COT)Ln[μ-*c*-C_3H_5-C≡C-$C(NR)_2]_2$Li(S) (**24**: Ln = Pr, R = Cy, S = Et_2O; **25**: Ln = Nd, R = ^{i}Pr, S = THF; **26**: Ln = Nd, R = Cy, S = THF) according to Scheme 19. Compounds **24** and **26** were isolated as pale green crystals by extraction and recrystallized in *n*-pentane at 5 °C, while **25** was extracted by toluene and recrystallized as bright yellow crystals using diethyl ether (Et_2O) at 5 °C. The yield was good (**25**: 64%) to moderate (**24**: 53%) (**26**: 41%).

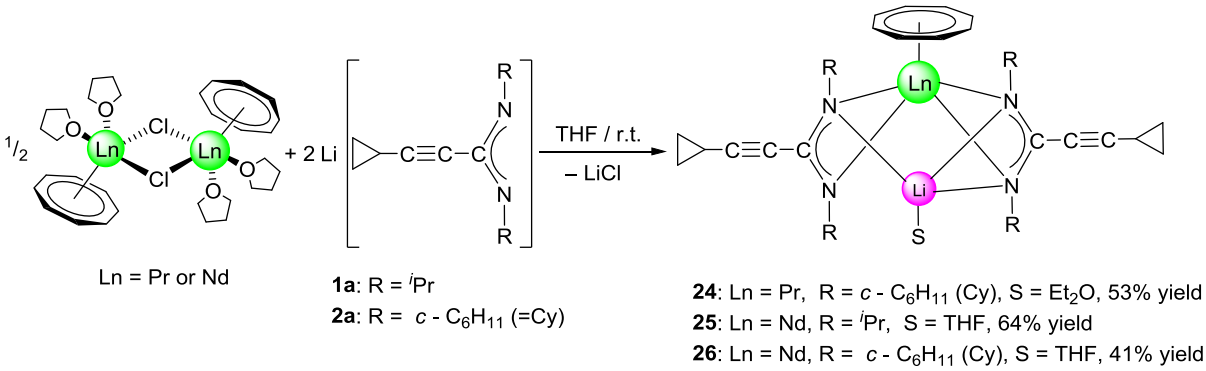

Scheme 19

All three compounds **24 – 26** were investigated by IR, mass spectra, elemental analysis, and NMR spectra. Crystals of **24** and **25** were found to be suitable for single-crystal X-ray diffraction. In the IR spectra, a strong band in the range of 2217 – 2226 cm^{-1} could be assigned to the C≡C stretching vibration [95], while the bands in range of 1593 – 1635 cm^{-1} can be attributed to the C=N vibration in the NCN units of the amidinate moieties [99]. All protons and carbons in the complexes **24** and **26** have been observed in the NMR spectra. Due to the paramagnetic nature of the Nd^{3+} ion, the NMR resonances of **25** could not be assigned. 2D experiments of **24** and **25** showed that the protons of η^8-C_8H_8 ligand appear as multiplet in **24** at δ = 5.50 – 5.90 ppm, while in **26** they appear at high field as singlet at δ = – 11.56 ppm [147]. The CH protons of the cyclohexyl groups were observed at δ = 3.40 ppm in **24** and at δ = 32.80 ppm in **26**. The signals of the cyclopropyl group are shifted to high field in **26** compared to those were observed in the lithium salt of amidinate **2a** (δ = 7.56 ppm for (CH), δ = 6.15 and 4.55 ppm for (CH_2) groups). In the ^{13}C NMR spectrum, the signals of the COT ligand appear at δ = 128 ppm in **24**, while in **25** they appear at δ = 161 ppm. The CH carbons of the cyclohexyl groups appear at a similar value at δ = 61 ppm in both complexes **24** and **25**. The molecular structures of the complexes **24** and **25** were verified by single-crystal X-ray diffraction. The molecular structures of **24** and **25** are shown in Figures 24 and 25, respectively.

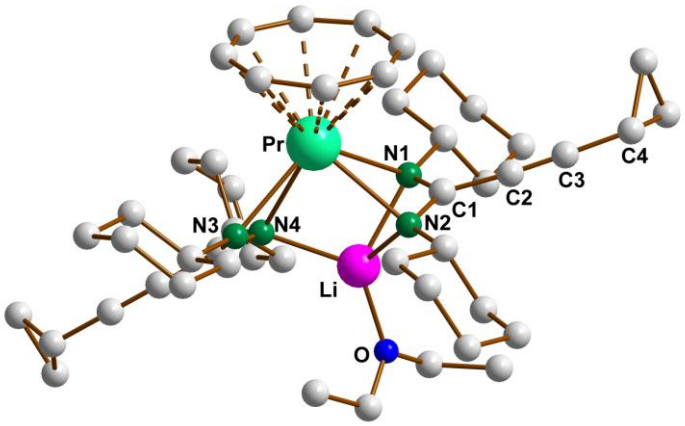

Figure 24. Molecular structure of (COT)Pr[μ-*c*-C_3H_5-C≡C-$C(NR)_2$]$_2$Li(Et_2O) (**24**)

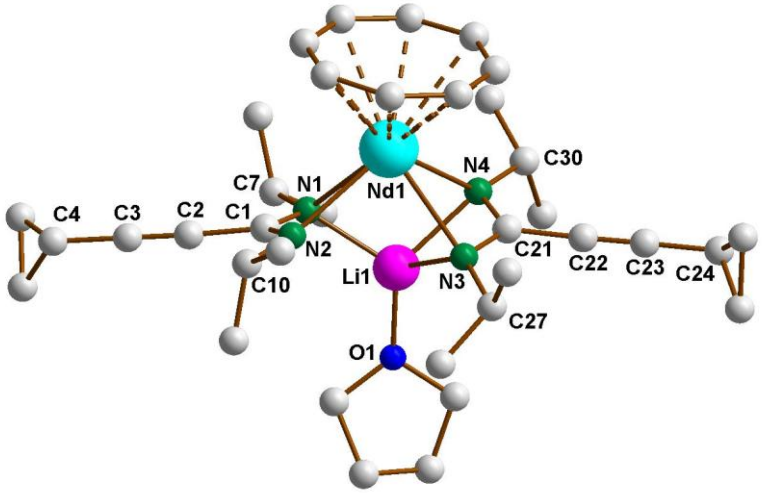

Figure 25. Molecular structure of (COT)Nd[μ-*c*-C_3H_5-C≡C-$C(NR)_2$]$_2$Li(THF) (**25**)

The crystal structures of **24** and **25** confirmed the presence of solvated half-sandwich complexes containing a COT ligand and two amidinate ligands, as well as a lithium atom coordinated with three nitrogen atoms of the amidinate ligands and one neutral ligand (Et_2O in **24** and THF in **25**). Complex **24** crystallizes from diethyl ether in the orthorhombic space group Pbca with one molecule in the unit cell. The praseodymium ion has a *pseudo*-tetragonal pyramidal coordination sphere consisting of one η^8-coordinated COT ring and four nitrogens

of the amidinate ligands. The Pr–N average distances are 2.633(2) Å which is significantly longer than that found in [4-$MeOC_6H_4C(NSiMe_3)_2]_3Pr$ (2.487(4) Å) [150] and (COT)Tm[$C_6H_5C(NSiMe_3)_2$](THF) (2.344(4) Å) [147]. The Pr–C distances to the η^8-coordinated COT are within a range from 2.697(3) to 2.743(3) Å. The Pr–(COT ring centroid) distance is 2.016 Å [151, 152]. The lithium atom is coordinated to three nitrogen atoms of the amidinate moieties with an average bond length of 2.129(5) Å, whereas the distance between the lithium atom and the fourth nitrogen atom Li–N3 (Figure 24) is 3.435 Å. The Li–O bond length of 1.894(5) Å. The N1–Pr–N2 and N3–Pr–N4 angles are 49.79(7)° and 52.39(7)°, respectively. The (COT ring centroid)–Pr–Li angle is 161.1° [151]. Despite the fact that complex **24** is insoluble in *n*-pentane, complex **25** was found to be soluble in *n*-pentane. Complex **25** crystallizes from *n*-pentane with two nearly identical crystallographically independent molecules in the asymmetric unit cell in the orthorhombic space group $P2_12_12_1$. Similar to **24**, the neodymium ion in **25** has a *pseudo*-tetragonal pyramidal coordination sphere consisting of one η^8-coordinated COT ring and four nitrogen atoms of the amidinate ligands. The average Nd1–N bond length of 2.619 Å which is significantly longer compared as to that found in (COT)Nd[$Ph_2P(NSiMe_3)_2$](THF) (2.473(3) Å) [147]. The bond length between the neodymium atom and the carbons of η^8-coordinated COT are in the range from 2.684(7) to 2.724(7) Å. The distance Nd1–(COT ring centroid) is 2.2002 Å, whereas in the second molecule it is 1.991 Å. The average bond length between lithium and the three nitrogen atoms of the amidinate ligands is 2.125(12) Å, whereas the distance between the lithium ion and the uncoordinated nitrogen atom Li1–N2 (Figure 25) is 3.247 Å. The bond length Li1–O1 is 1.875(13) Å. The N1–Nd1–N2 and N3–Nd1–N4 angles are 52.32(14)° and 49.78(16)°, respectively, and the angle (COT ring centroid)–Nd–Li is 163.7° [151]. In both complexes **24** and **25**, the bond length of C1–N1 (1.326(3) Å in **24** and 1.319(8) Å in **25**) and C1–N2 (1.338(3) in **24** and 1.331(7) Å in **25**) indicate the negative charge delocalization within the NCN fragments. The bond angles of N1–C1–N2 unit are 115.7(2)° in **24** and 118.3(6)° in **25**.

2.5.2. Synthesis and structure (μ-η^8:η^8-COT)[Ce{*c*-C_3H_5-C≡C-$C(NR)_2$}$_2$]$_2$

Known lanthanide triple-decker or tetra-decker sandwich complexes are mainly based on cyclooctatetraenyl ligands as middle-decks bridging two lanthanide ions as shown in Scheme 20 [153, 154]. The starting materials [(COT)Ln(μ-Cl)$(THF)_2]_2$ (Ln = Nd or Sm) have been

used in preparation of a neodymium triple-decker sandwich complex containing a planar $(C_8H_8)^{2-}$ ring sandwiched between twelve-membered $Si_4O_6Li_2$ inorganic rings in the complex $(\mu\text{-}\eta^8\text{:}\eta^8\text{-COT})[Nd\{(Ph_2SiO)_2O\}_2\{Li(THF)_2\}\{Li(THF)\}]_2$ [151] as well as in the preparation of the samarium triple-decker sandwich complex $(\mu\text{-}\eta^8\text{:}\eta^8\text{-COT})[Sm\{N(SiMe_3)_2\}_2]_2$ using the $[(Me_3Si)_2N]^-$ ligand as outer decks [152]. Encapsulation of a $(C_8H_8)^{2-}$ ring in a divalent lanthanide triple-decker sandwich complex was achieved by reaction of $[(Me_3Si)_2N]_2Ln(THF)_2$, $LnI_2(THF)_2$ and $K_2C_8H_8$ to give $(\mu\text{-}\eta^8\text{:}\eta^8\text{-COT})[Ln\{N(SiMe_3)_2\}(THF)_2]_2$ (Ln = Sm or Yb) [155].

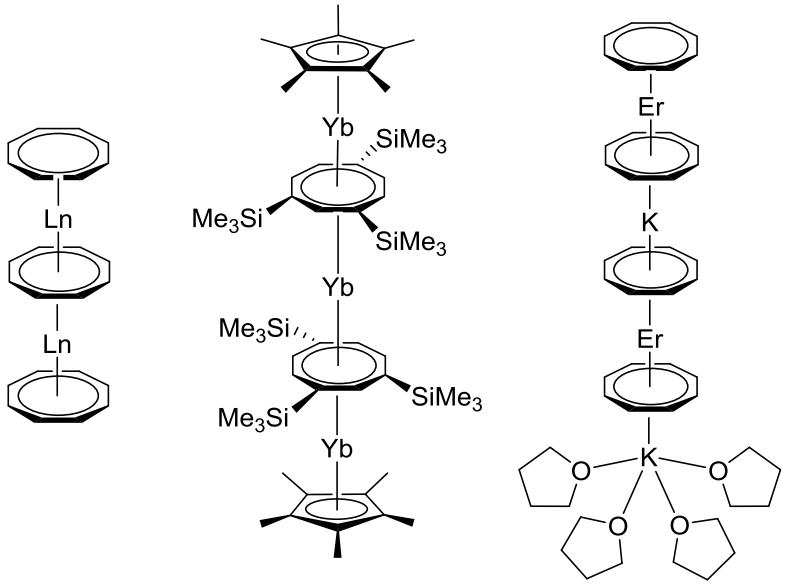

Scheme 20

An unprecedented synthetic route to unsolvated inverse sandwich bimetallic Ln(COT) complexes was reported within this work. The complexes $(\mu\text{-}\eta^8\text{:}\eta^8\text{-COT})[Ce\{c\text{-}C_3H_5\text{-}C{\equiv}C\text{-}C(NR)_2\}_2]_2$ (R = ^{i}Pr or Cy) were prepared by treatment of the dimers **5** and **6**, respectively, with $K_2C_8H_8$ in a 1:1 molar ratio at room temperature to afford $(\mu\text{-}\eta^8\text{:}\eta^8\text{-COT})[Ce\{c\text{-}C_3H_5\text{-}C{\equiv}C\text{-}C(NR)_2\}_2]_2$ (**27**: R = ^{i}Pr; **28**: R = Cy) as illustrated in Scheme 21. Both compounds **27** and **28** were extracted using *n*-pentane affording bright yellow crystals at 5 °C in 45% (**27**) and 49% (**28**) yields. The spectroscopic data and elemental analysis were consistent with the structures. Both complexes **27** and **28** were structurally characterized by single-crystal X-ray diffraction.

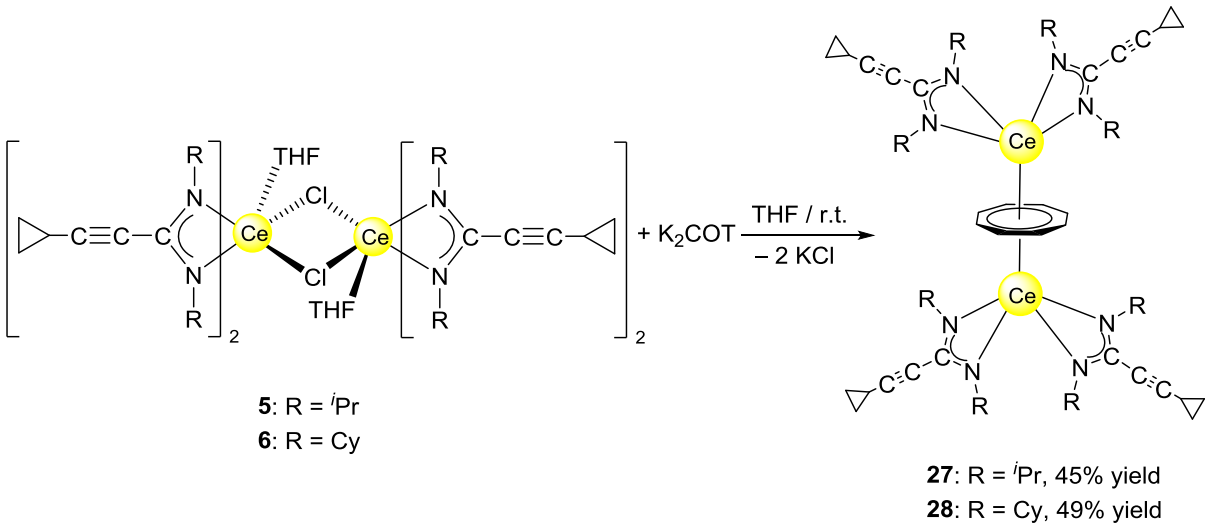

Scheme 21

In the ^{1}H NMR spectra of **27** and **28**, the influence of the paramagnetism of the Ce^{3+} ion on the protons of COT and the amidinate ligands is evident. Thus, the C_8H_8 protons in THF-d_8 solution have a chemical shift of δ = 1.15 ppm in **27** and at δ = 0.91 ppm in **28**. The CH protons of isopropyl groups in **27** appear at δ = 10.01 ppm, likewise, the CH protons of cyclohexyl groups in **28** appears at δ = 9.70 ppm. The CH protons of cyclopropyl groups were observed at the range δ = 0.81 – 1.04 and 1.27 – 1.35 ppm in **1a** and **2a**, respectively, and were found to appear at δ = 3.15 and 3.21 ppm in **27** and **28**, respectively. The carbon signals of the COT ligand are observed at δ = 107.7 ppm in **27** and at δ = 104.1 ppm in **28**. The CH carbons of the isopropyl groups are found at δ = 50 ppm in **1a**, whereas they are observed at δ = 58 ppm in **27**. Likewise, the CH carbons in cyclohexyl groups found at δ = 59 ppm in **2a**, whereas are observed at δ = 67 ppm in **28**. Single-crystals of both **27** and **28** were found to be suitable for single-crystal X-ray diffraction. These were obtained by cooling a saturated *n*-pentane solution at 5 C°. The compounds **27** and **28** crystallize in the monoclinic space groups C2/c and Pn with one molecule of **27** and two molecules of **28** in the unit cell. The crystal structure determination of **27** and **28** confirmed the presence of the unsolvated inverse sandwich structures in which a COT ligand is sandwiched between two trivalent cerium ions, and each of the cerium ions is attached to two bidentate amidinate ligands as shown in Figures 26 and 27. The coordination geometry around the cerium atoms can be described as distorted *pseudo*-tetragonal pyramidal. The Ce–C(COT) distances are ranging from 2.862(3) to 2.905(3) Å in **27** and from 2.872(4) to 2.908(4) Å in **28**. These values are well comparable to those found in (μ-η^8:η^8-COT)[Sm{N(SiMe$_3$)$_2$}$_2$]$_2$ (2.798(5) to 2.857(5) Å) [152] and in (μ-

η^8:η^8-COT)[Sm{N(SiMe$_3$)$_2$}(THF)$_2$]$_2$ (2.863(2) to 2.929(2) Å) [155]. In **27**, the bond lengths Ce1–(COT ring centroid) and Ce2–(COT ring centroid) are 2.220 and 2.244 Å, respectively [151, 155]. Due to the symmetry found in the complex **27**, the bond lengths of Ce1–N1 and Ce1–N1A have the same value of 2.521(2) Å, and likewise Ce1–N2 and Ce1–N2A are 2.478(2) Å. Similarly, the distances Ce2–N3, Ce2–N3A are 2.530(2) Å and Ce2–N4, Ce2–N4A are 2.453(2) Å (Figure 28 (left)). The Ce–N bond lengths are in good agreement with those found in complex **5**. As illustrated in Figure 28 (left), the distance between Ce1–Ce2 is 4.465 Å. The Ce1–(COT ring centroid)–Ce2 angle is 100.0°. The bond lengths N1–C1 and N2–C1 are 1.327(4) Å and 1.331(4), respectively, indicating negative charge delocalization within the NCN units.

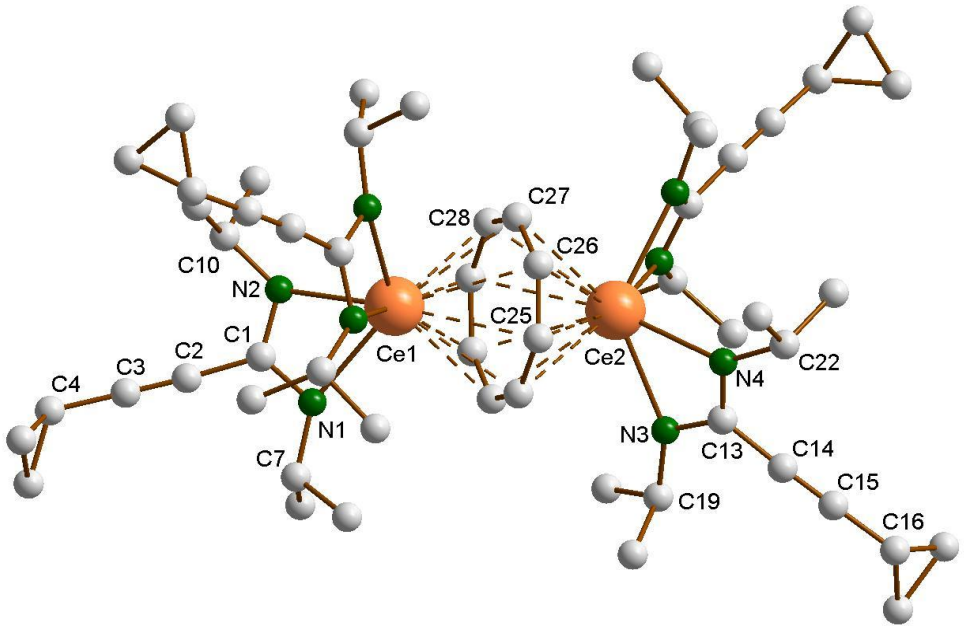

Figure 26. Molecular structure of (μ-η^8:η^8-COT)[Ce{*c*-C$_3$H$_5$-C≡C-C(N^{i}Pr)$_2$}$_2$]$_2$ (**27**)

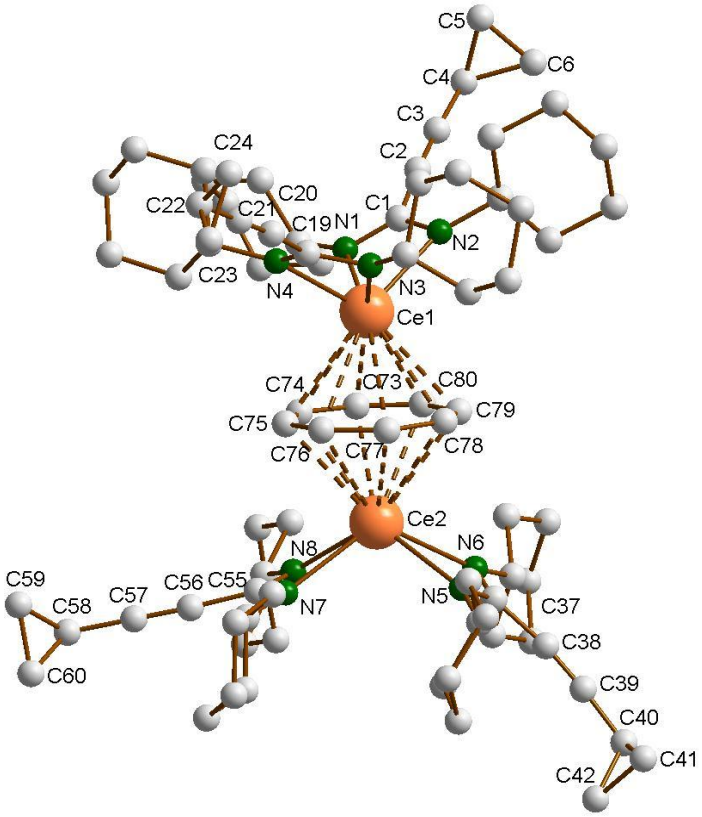

Figure 27. Molecular structure of (μ-η^8:η^8-COT)[Ce{*c*-C_3H_5-C≡C-$C(NCy)_2$}$_2$]$_2$ (**28**).

In the compound **28**, the bond lengths of Ce1–(COT ring centroid) and Ce2–(COT ring centroid) are 2.242 and 2.234 Å, respectively, [151, 155]. The Ce–N bond lengths are ranging from 2.438(4)° to 2.528(4)°, which is in good agreement with those found in compound **6**. Complex **28** has no symmetry like that found in complex **27**. As illustrated in Figure 28 (right), the distance between Ce1–Ce2 is 4.511 Å. The angle Ce1–(COT ring centroid)–Ce2 is 177.9°, whereas in the second molecule the Ce3–(COT ring centroid)–Ce4 is 178.7° [151]. In the complexes **27** and **28** no agostic interaction has been observed between Ce^{3+} and the outer decks of amidinate ligands although such interaction is found in (μ-η^8:η^8-COT)[Sm{$N(SiMe_3)_2$}$_2$]$_2$ [155].

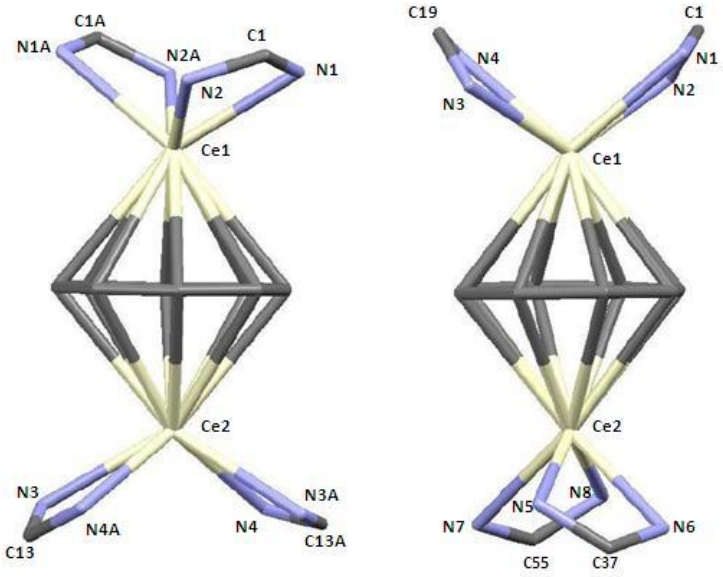

Figure 28. Capped-sticks views of the unit $\{(\mu\text{-}\eta^8\text{:}\eta^8\text{-COT})[Ce\{C(N)_2\}_2]_2\}$ of **27** (left) and **28** (right).

2.5.3. Synthesis and structure of $[(COT)Ln(\mu\text{-}c\text{-}C_3H_5\text{-}C{\equiv}C\text{-}C(NR)_2)]_2$

The preparation of the unsolvated half-sandwich complexes containing COT ligands is not always straightforward. Unlike the reaction of $[(COT)Pr(\mu\text{-Cl})(THF)_2]_2$ with **2a**, which afforded a solvated complex as shown in Scheme 19, treatment of $[(COT)Pr(\mu\text{-Cl})(THF)_2]_2$ with two equiv. of **1a** in THF at room temperature afforded the unusual complex $[(COT)Pr(\mu\text{-}c\text{-}C_3H_5\text{-}C{\equiv}C\text{-}C(N^iPr)_2)]_2$ (**29**) in 47% yield as shown in Scheme 22.

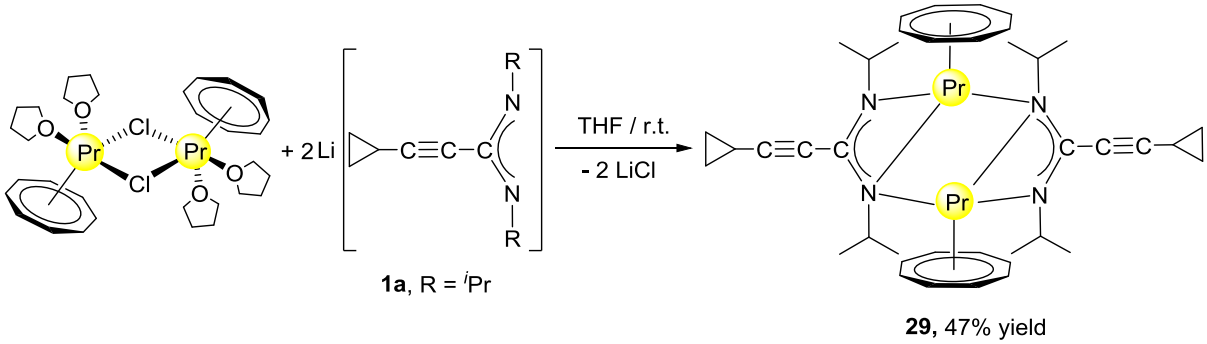

Scheme 22

The new unsolvated binuclear half-sandwich complex **29** has been fully characterized by spectroscopic and elemental analysis studies. Only on one occasion the well-formed crystals of **29** obtained from a saturated solution in toluene could be successfully subjected to X-ray diffraction, which provided the structure of **29** as a dimer as illustrated in Scheme 22. Unfortunately, the crystal quality was too poor to allow full refinement of the crystal structure. The NMR spectra in toluene-d_8 clearly indicated the absence of coordinated THF in the unsolvated half-sandwich complex **29** as shown in Figures 29 and 30. The CH protons of the isopropyl groups are shifted to δ = 10.57 ppm, which can be attributed to the paramagnetic nature of the Pr^{3+} ion. The singlet of η^8-C_8H_8 has shifted to high magnetic field and is observed at δ = – 4.63 ppm [147, 156]. Likewise, the CH_3 protons which were observed at δ = 0.65 ppm in **1a**, are strongly shifted to higher magnetic field at δ = – 10.24 ppm [147, 156]. All protons of the cyclopropyl groups showed a marked downfield shift as compared to **1a**. The CH protons of the *c*-C_3H_5 groups were found at a chemical shift δ = 0.81 – 1.04 ppm in **1a**, while they were observed at δ = 1.94 ppm in **29**. Likewise, the CH_2 protons were observed at δ = 0.34 – 0.49 and 0.28 – 0.32 ppm in **1a** and at δ = 1.70 and 1.22 ppm in **29**.

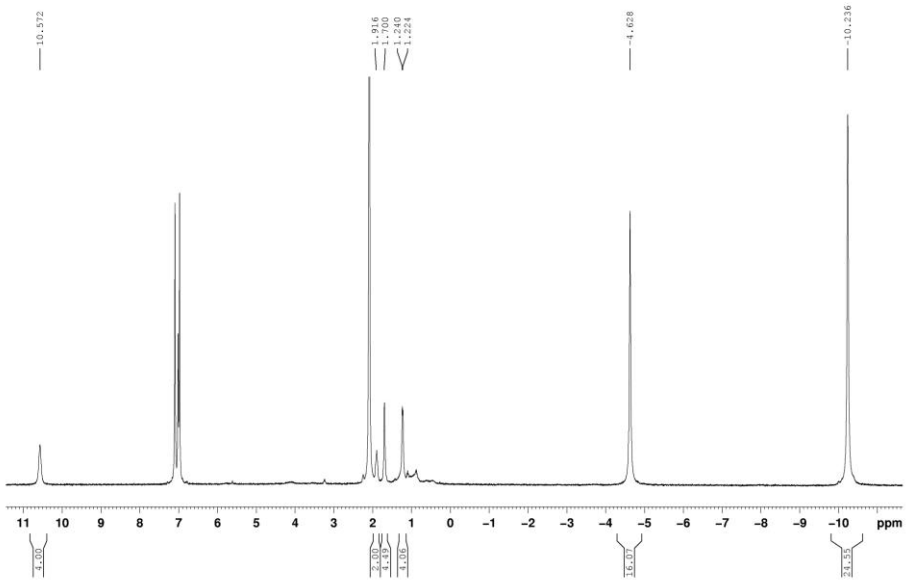

Figure 29. ^{1}H NMR spectrum (toluene-d_8, 25°C) of [(COT)Pr(μ-*c*-C_3H_5-C≡C-C(N^iPr)$_2$)]$_2$ (**29**)

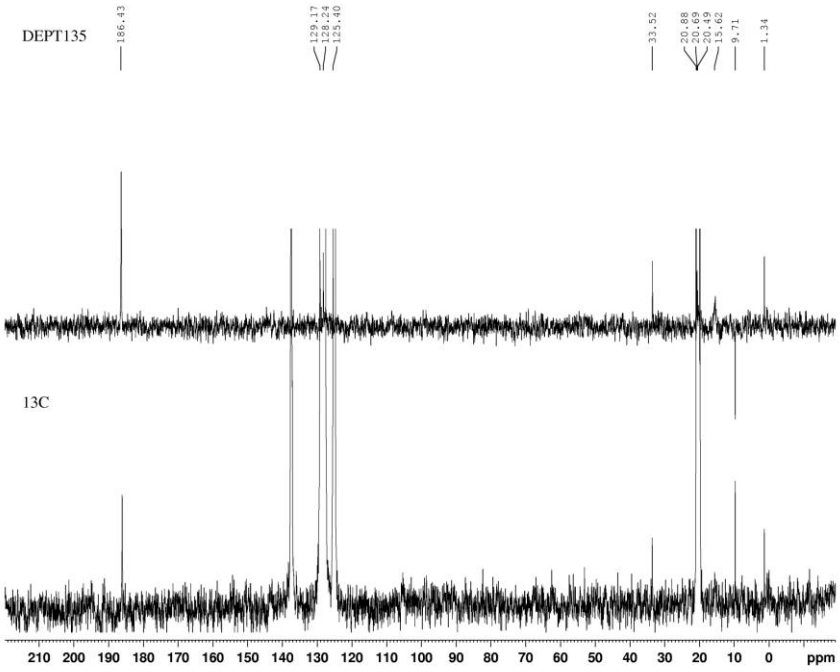

Figure 30. ^{13}C NMR and dept spectrum (toluene-d_8, 25°C) of [(COT)Pr(μ-*c*-C_3H_5-C≡C-C(N^{i}Pr)$_2$)]$_2$ (**29**)

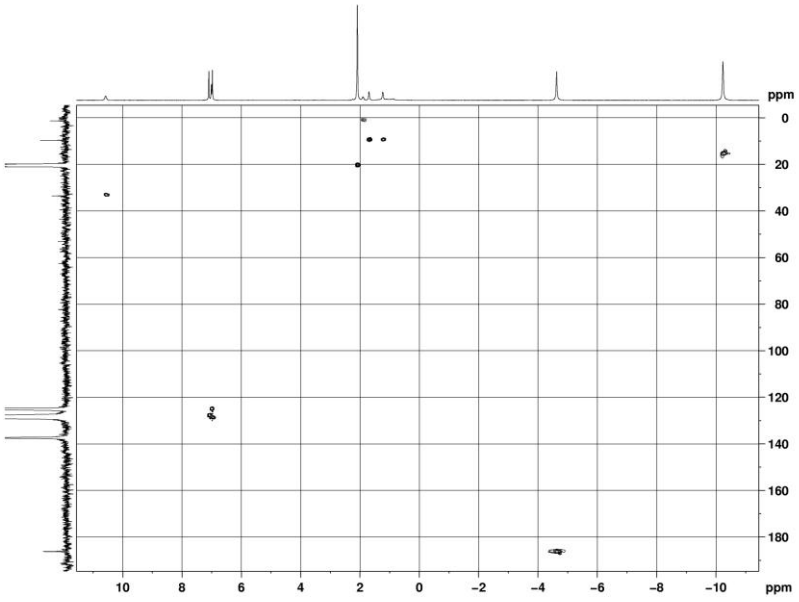

Figure 31. HSQC (H,C-correlation via ^1J (C, H)) spectrum in (toluene-d_8, 25°C) of [(COT)Pr(μ-*c*-C_3H_5-C≡C-C(N^{i}Pr)$_2$)]$_2$ (**29**)

The ^{13}C NMR and HSQC spectra of a **29** are shown in Figures 30 and 31. The influence of the paramagnetism of the Pr^{3+} ion on the carbons of complex **29** is evident. In comparison with the ^{13}C NMR spectrum of **1a**, the influence of the Pr^{3+} ion on the carbons of COT and isopropyl groups is higher than that found on the cyclopropyl group in **29**. Thus, the COT carbons have a chemical shift of δ = 186.1 ppm, and the CH carbons of the isopropyl groups were observed at δ = 33.5 ppm, while the CH_3 carbons were observed at δ = 15.6 ppm.

A series of solvated lanthanide half-sandwich complexes containing the bulky 1,4-bis(trimethylsilyl)cyclooctatetraenyl (COT″) ligand in combination with the chelating *N*,*N*′-bis(trimethylsilyl)diiminophosphinate [157] or aminotroponiminates [158] ligands have been reported in the literature *via* a one-pot reaction as shown in Scheme 23. The formation of monomeric solvated complexes in these reactions could be traced back to the high steric demand of the COT″ ligand as well as the steric bulk of the *N*,*N*′-bis(trimethylsilyl)diiminophosphinate or aminotroponiminate ligands.

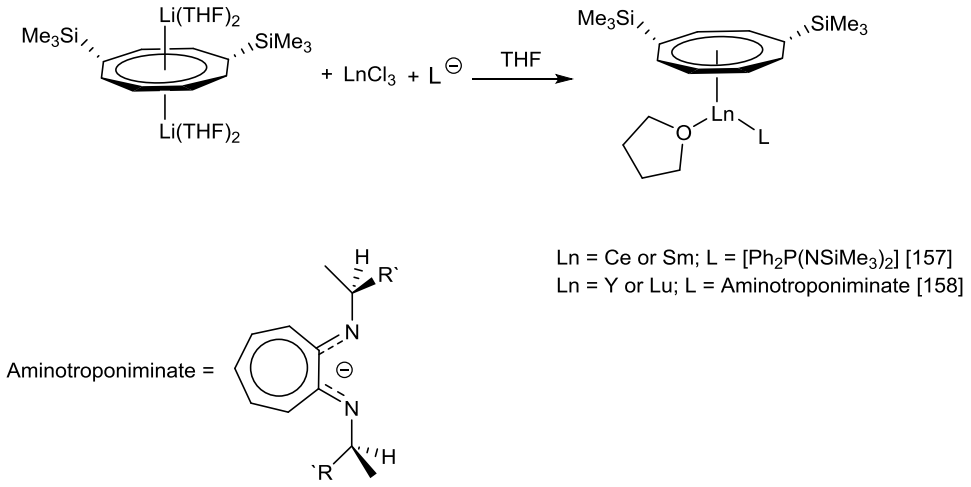

Scheme 23

In the course of this work, novel unsolvated lanthanide half-sandwich complexes have been prepared by reaction of anhydrous $LnCl_3$ with K_2COT and **1a** or **2a** *via* a one-pot reaction. A mixture of the cyclopropylethinylamidinate **1a** or **2a** and K_2COT dissolved in THF was added to a suspension of $LnCl_3$ (Ln = Ce or Nd) in THF in a 1:1:1 molar ratio as shown in Scheme 24. The reaction mixture was stirred for 12 h at room temperature. After evaporation of the solvent the product was extracted by using toluene to give the novel complexes $[(COT)Ln(\mu\text{-}c\text{-}C_3H_5\text{-}C{\equiv}C\text{-}C(NR)_2)]_2$ (**30**: Ln = Ce, R = ^{i}Pr; **31**: Ln = Ce, R = Cy; **32**: L= Nd, R = ^{i}Pr). Saturated solution of compounds **30** – **32** in toluene were kept at 5 °C affording **30** as dark-

green crystals (57% yield), **31** as green crystals (17% yield) and **32** as green crystals (43% yield). The unsolvated complexes are readily soluble in THF, Et_2O or toluene and insoluble in *n*-pentane. The new complexes **30** – **32** have been fully characterized by elemental analysis, spectroscopic methods and single-crystal X-ray diffraction.

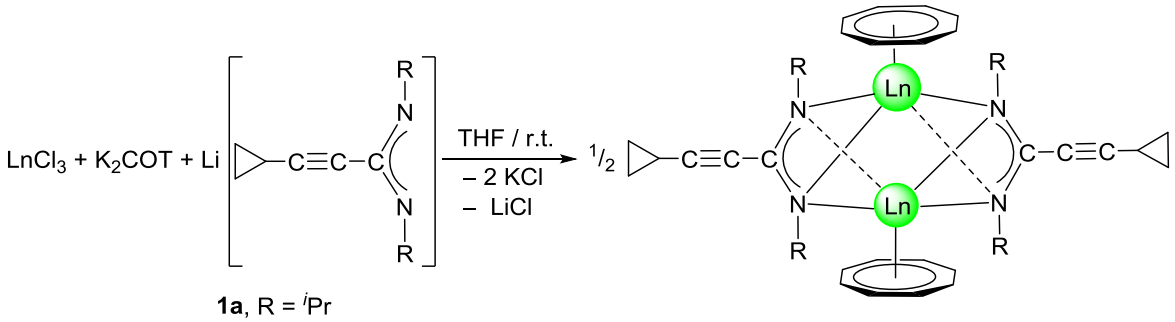

1a, R = ^{i}Pr
2a, R = *c* - C_6H_{11} (Cy)

30: Ln = Ce, R = ^{i}Pr, 57% yield
31: Ln = Ce, R = *c* - C_6H_{11} (Cy), 17% yield
32: Ln = Nd, R = ^{i}Pr, 43% yield

Scheme 24

The ^{1}H and ^{13}C NMR spectra of **30** – **32** indicated the presence of one COT and one cyclopropylethinylamidinate ligand for Ln atom. The protons of η^8-C_8H_8 were observed at δ = 0.91 – 1.53 and 0.93 – 1.87 ppm in **30** and **31**, respectively [147], whereas the η^8-C_8H_8 protons in **32** appear as singlet at δ = – 11.75 ppm [147, 159]. The COT carbons appear at δ = 108.6 and 115.3 ppm in **30** and **31**, respectively, while they appear at δ = 132.7 ppm in **32** [160 – 162]. Suitable single-crystals of **30**, **31** and **32** for X-ray diffraction studies were obtained from saturated solution in toluene at 5 °C. The compounds **30** and **32** crystallize in the monoclinic space group $P2_1/c$ and **31** in the monoclinic space group $P2_1/n$. Compounds **30** and **32** were found have two molecules in the unit cell, whereas **31** was found to crystallize with one molecule in the unit cell. The crystal structures of **30** and **32** showed a centrosymmetric dimeric structure in which the lanthanide ion is coordinated with one η^8-COT ring and three nitrogens of the two amidinate ligands. The coordination geometry around the cerium or neodymium atoms in **30** and **32** can be described as distorted *pseudo*-tetrahedral as shown in Figures 32 and 34. Unlike the complexes **30** and **32**, the X-ray diffraction study of **31** showed that the cerium atom in **31** is coordinated to one η^8-COT ring and four nitrogen atoms of the two amidinate ligands. Thus, the coordination geometry around the cerium atom in **31** can be described as distorted *pseudo*-tetragonal pyramidal as shown in

Figure 33. In **30**, the Ce–C(COT) distances range from 2.694(6) to 2.713(6) Å (average 2.704 Å) in good agreement with (μ-η^8:η^8-COT)[Sm{N(SiMe$_3$)$_2$}$_2$]$_2$ (2.798(5) to 2.857(5) Å) [152] and with (μ-η^8:η^8-COT)[Sm{N(SiMe$_3$)$_2$}(THF)$_2$]$_2$ (2.863(2) to 2.929(2) Å) [155]. The distances Ce–(COT ring centroid) have the same value of 1.992 Å. The Ce–N bond lengths are in the range between 2.625(5) and 2.647(5) Å (average 2.641 Å), whereas the distance of Ce–N2 (N2 is the fourth nitrogen atom which is not attached to the cerium atom) is 3.188 Å as illustrated in Figure 35(left). The Ce···Ce distance is 4.219 Å. The C1–N1 and C1–N2 bond lengths are 1.350(8) and 1.321(8) Å, respectively, indicating negative charge delocalization within the NCN fragments. The N–Ce–N and Ce–N–Ce bond angles are collected in Figure 35(left). Interestingly, compound **30** is centrosymmetric dimers of the type [(COT)LnL]$_2$ with a planar four-membered Ce1N1Ce1AN1A ring as the central structural unit with angles of 90.07° (Ce–N–Ce) and 89.93° (N–Ce–N), so that the Ce_2N_2 moiety has a rhomb-shaped geometry. The Nd–C(COT) distances in **32** are in the range between 2.658(5) to 2.679(5) Å (average 2.670 Å), in good agreement with the 2.852(3) to 2.928(3) Å range found in (μ-η^8:η^8-COT)[Nd{(Ph$_2$SiO)$_2$O}$_2${Li(THF)$_2$}{Li(THF)}]$_2$ [151]. Similar to **30**, the Nd–(COT ring centeroid) distances have value of 1.936 Å and 1.949 Å. The bond lengths of Nd–N range from 2.570(4) to 2.610(4) Å (average 2.587 Å), while the distance between Nd–N2 (N2 is the fourth nitrogen atom which is not attached to the neodymium atom) is 3.494 Å (Figure 35(right)). The Nd···Nd distance is 3.817 Å. The N–Nd–N and Nd–N–Nd bond angles in **32** are collected in Figure 35 (right). Similar to the structure of **30**, the dimeric **32** has a planar four-membered Nd1N1Nd1AN1A ring as the central structural unit with angles of 94.67° (Nd–N–Nd) and 85.33° (N–Nd–N) and the Nd_2N_2 unit is rhomb-shaped. The torsion angles of (COT ring centeroid)–Ce–Ce–(COT ring centeroid) and (COT ring centeroid)–Nd–Nd–(COT ring centeroid) in both complexes **30** and **32** are 180.0°.

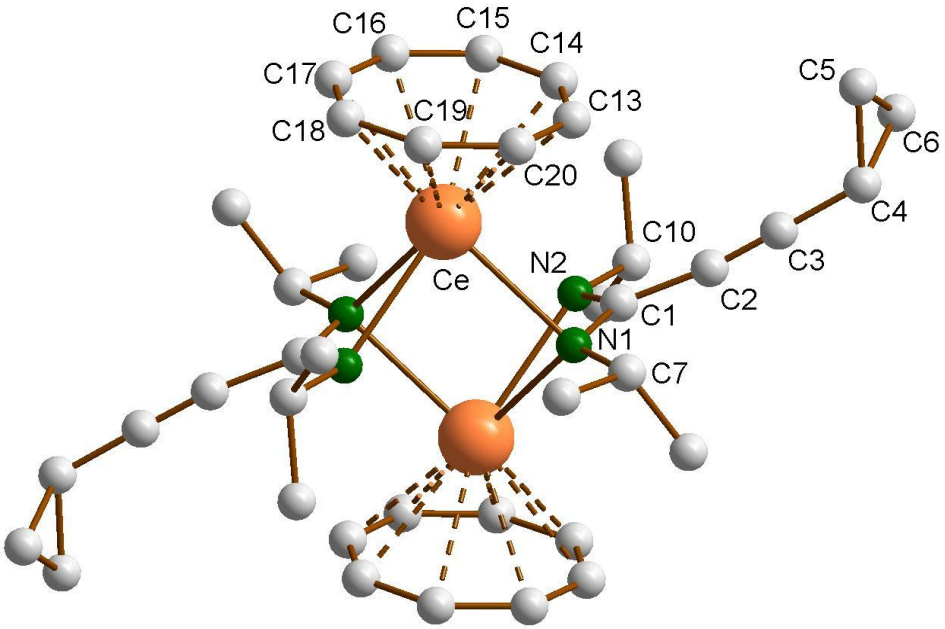

Figure 32. Molecular structure of [(COT)Ce(μ-*c*-C_3H_5-C≡C-C(N^iPr)$_2$)]$_2$ (**30**)

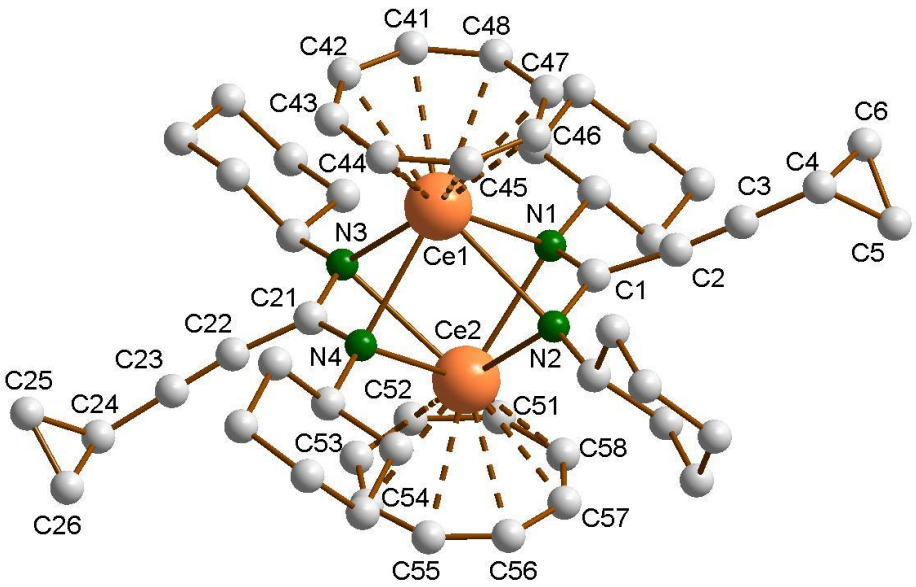

Figure 33. Molecular structure of [(COT)Ce(μ-*c*-C_3H_5-C≡C-C(NCy)$_2$)]$_2$ (**31**)

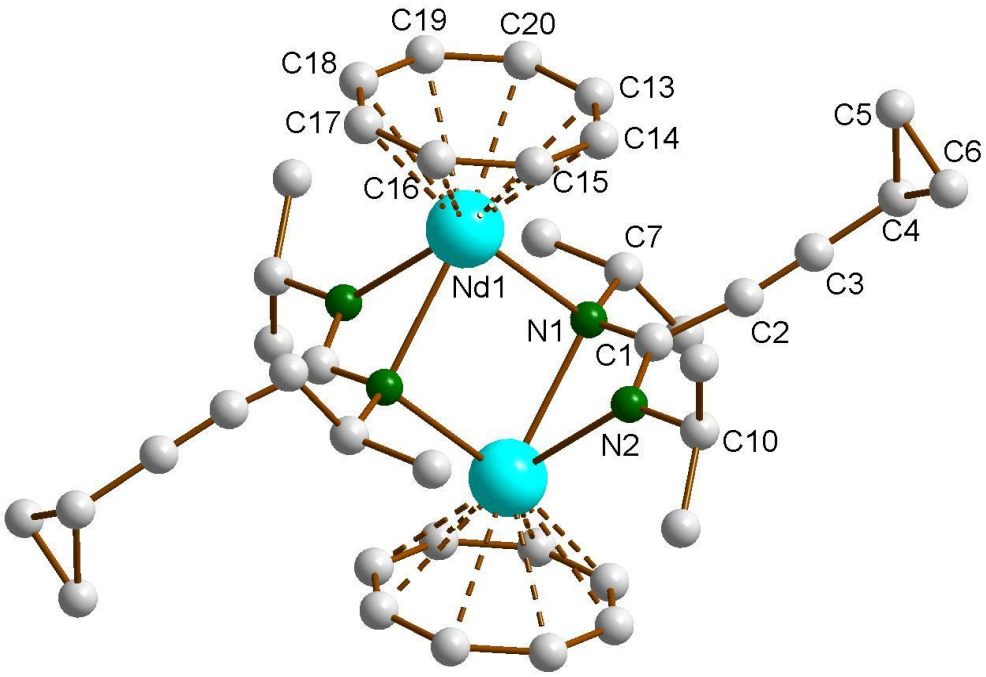

Figure 34. Molecular structure of [(COT)Nd(μ-*c*-C_3H_5-C≡C-C(N^iPr)$_2$)]$_2$ (**32**)

Due to the difference in ionic radii of Ce^{3+} and Nd^{3+}, slightly shorter bond distances are observed in **32** than in **30**. Interestingly, the analogue **30** and **32**, the complex **31** which has cyclohexyl groups on the nitrogen atoms comprises a different geometry. As shown in Figure 33, the cerium atoms are coordinated to the COT ring and four nitrogen atoms of amidinate ligands to give a distorted *pseudo*-tetragonal pyramidal geometry. In **31**, the Ce–C(COT) distances range from 2.693(4) to 2.721(4) Å (average 2.704 Å) [151, 152, 155]. The Ce–(COT ring centeroid) distance is 1.988 Å. The Ce–N bond lengths are in the range from 2.648(3) to 2.767(3) Å (average 2.711 Å). In comparison with **30**, the (COT ring centroid)–Ce–Ce–(COT ring centroid) torsion angle is 166.4°, which is smaller to that found in **30**. This can be traced back to the difference in the coordination mode in **31** as compared to that found in **30**. Surprisingly, the Ce···Ce distance in **31** (3.625 Å) is shorter than that observed in **30** (4.219 Å) with a difference of 0.594 Å. This can attributed to the difference in the substituents on the nitrogen atoms. Selected bond lengths, angles and torsion angles of the cerium half sandwich complexes **27**, **28**, **30** and **31** are collected in Table 6.

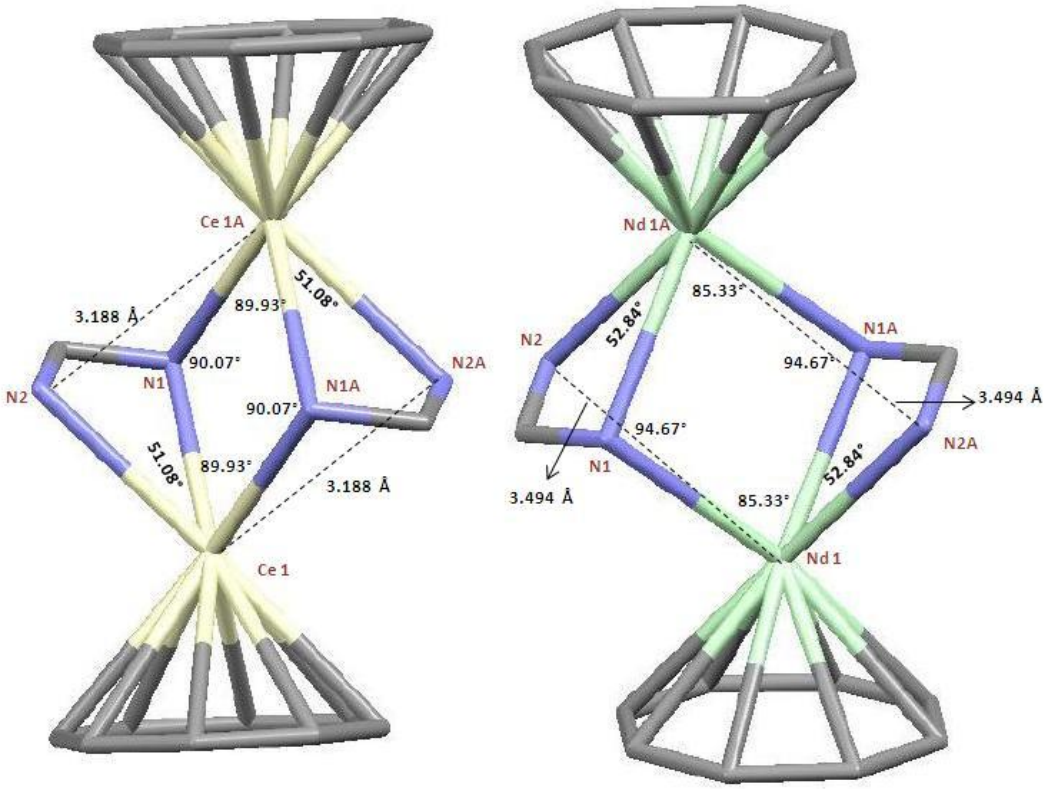

Figure 35. Capped-sticks views of the unit $[(COT)Ln(\mu\text{-}C(N)_2)]_2$ of **30** (left) and **32** (right).

Table 6 Selected bond lengths (Å), angles (°) and torsion angles (°) of **27** – **31**

Complex / Bond lengths and angles	**27**	**28**	**30**	**31**
Ce–C(COT) (average)	2.895	2.884	2.704	2.704
Ce–(COT ring centroid)	2.220, 2.244	2.242, 2.234	1.992	1.988
Ce···Ce (distance)	4.465	4.511	4.219	3.625
Ce–N (average)	2.499	2.485	2.641	2.711
Ce–COT–Ce	100.0	177.9, 178.7	–	–
COT–Ce–Ce–COT	–	–	166.4	180
(COT–COT) ring centroids, tilt angle	–	–	0	3.3

Table 6 shows the difference in bond lengths and angles of cerium complexes. The Ce–(COT ring centroid) distances in the centrosymmetric dimeric complexes **30** and **31** are shorter than

those found in the inverse sandwich complexes **27** and **28**. On the other hand, the bond lengths average of Ce–N in **27** and **28** is shorter than that observed in **30** and **31**.

2.5.4. Synthesis and structure of (COT)Ho[*c*-C_3H_5-C≡C-$C(NR)_2$](THF)

Unlike the compounds **30** – **32**, the smaller Ho^{3+} gave a different result. Treatment of a mixture of K_2COT and **1a** or **2a** with anhydrous $HoCl_3$ in a 1:1:1 molar ratio in THF as a one-pot reaction afforded the solvated half-sandwich complexes (COT)Ho[*c*-C_3H_5-C≡C-$C(NR)_2$](THF) (**33**: R = ^{i}Pr; **34**: R = Cy) as shown in Scheme 25. The monomeric complexes **33** and **34** were extracted with *n*-pentane or toluene and isolated in 48% and 30% yield, respectively.

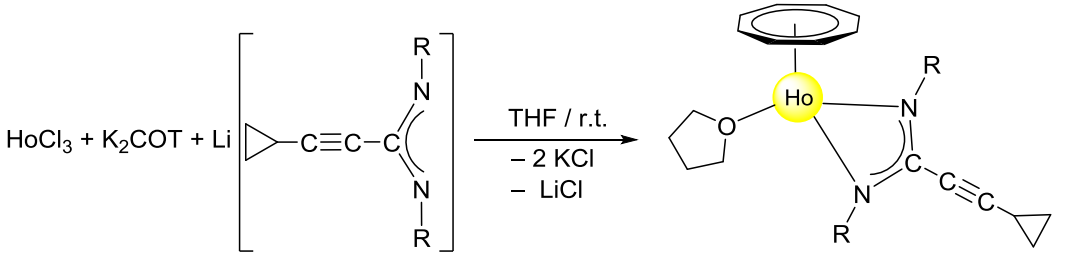

1a, R = ^{i}Pr
2a, R = *c* - C_6H_{11} (Cy)

33: R = ^{i}Pr, 48% yield
34: R = *c* - C_6H_{11} (Cy), 30% yield

Scheme 25

The new complexes **33** and **34** have been fully characterized by EI/mass, IR, and elemental analyses. In addition, single-crystals of **34** were found to be suitable for an X-ray diffraction study. The effect of the paramagnetism of Ho^{3+} ion prevented the measurement of NMR data. Both complexes **33** and **34** were characterized by an EI mass spectrum. The EI mass spectrum showed the molecule ion of **33** and its characteristic fragmentation. The EI mass spectrum of **34** showed the molecular ion of **34** without the coordinated THF molecule [147, 158]. Suitable single-crystals of **34** were obtained by recrystallization from *n*-pentane. The molecular structure of **34** was established by single-crystals X-ray diffraction as shown in Figure 36. Compound **34** crystallizes in the monoclinic space group $P2_1/n$ with one molecule in a symmetric unit cell. The holmium ion is coordinated with η^8-COT ring and two nitrogen atoms of the amidinate ligand as well as the oxygen atom of a neutral THF ligand. The coordination sphere around the Ho^{3+} ion can be described as *pseudo*-distorted tetrahedral fashion.

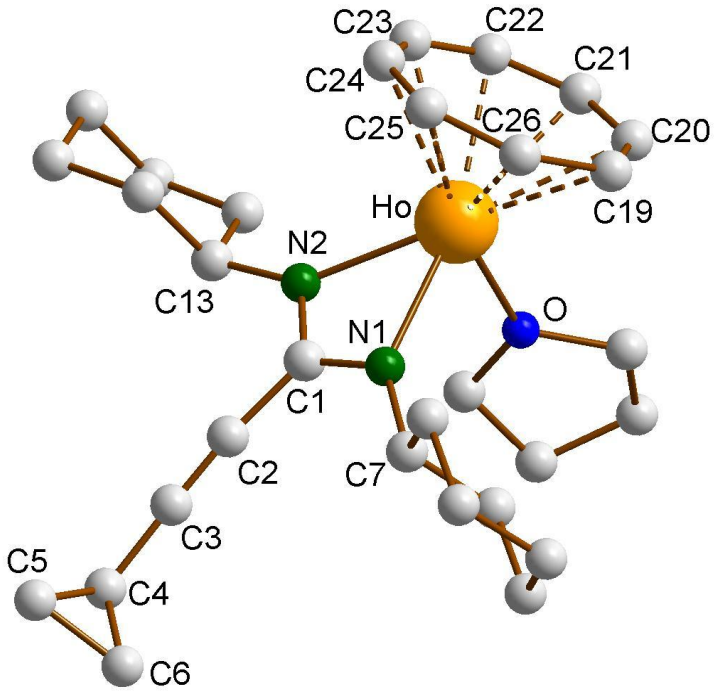

Figure 36. Molecular structure of (COT)Ho[*c*-C_3H_5-C≡C-C(NCy)$_2$](THF) (**34**)

The Ho–C(COT) distances, which range from 2.552(5) to 2.598(4) Å (average 2.568 Å) are in good agreement with those reported for (COT)Tm[$C_6H_5C(NSiMe_3)_2$](THF) (average 2.558 Å) [147] and [{η^8-1,4-$(Me_3Si)_2C_8H_6$}Y{(^{i}Pr)$_2$ATI}(THF)] (ATI = *N*-isopropyl-2-(isopropylamino)troponiminate, Scheme 23) (average 2.623 Å) [158]. The difference in the distances can attributed to the difference in the ionic radii according to Y>Ho>Tm. The Ho–(COT ring centeroid) distance is 1.821 Å [147, 158, 163]. Due to the smaller size of Ho^{3+}, the distance Ho–(COT ring centeroid) is significantly shorter than that observed in the compounds **27** – **31**. The bond lengths Ho–N1, Ho–N2 and Ho–O are 2.349(3), 2.342(3) and 2.397(2) Å, respectively, [153]. The C1–N1 and C1–N2 distances are 1.324(4) and 1.329(4) Å, respectively, indicating negative charge delocalization in NCN unit. The N1–Ho–N2 57.15(9)° angle is identical with that found in (COT″)Yb(^{DIPP}Form)(THF) (57.70(14)°) [153]. The bond angle (COT ring centroid)–Ho–C1 is 149.3°. The N1–Ho–O and N2–Ho–O angles are similar to each other 84.63(10)° and 84.13(9)°, respectively. The N1–C1–N2 bond angle is 115.5(3)°.

2.5.4. Synthesis and structure of $[(\mu\text{-}\eta^8\text{:}\eta^8\text{-COT})\{Nd(c\text{-}C_3H_5\text{-}C{\equiv}C\text{-}C(NCy)_2)(\mu\text{-}Cl)\}_2]_4$

A unique cyclic multidecker sandwich complex was prepared by reaction of anhydrous $NdCl_3$ with K_2COT and **2a** as one-pot reaction. According to Scheme 26, treatment of the mixture of K_2COT and **2a** with anhydrous $NdCl_3$ in THF afforded the unprecedented cyclic sandwich compound $[(\mu\text{-}\eta^8\text{:}\eta^8\text{-COT})\{Nd(c\text{-}C_3H_5\text{-}C{\equiv}C\text{-}C(NCy)_2)(\mu\text{-}Cl)\}_2]_4$ (**35**).

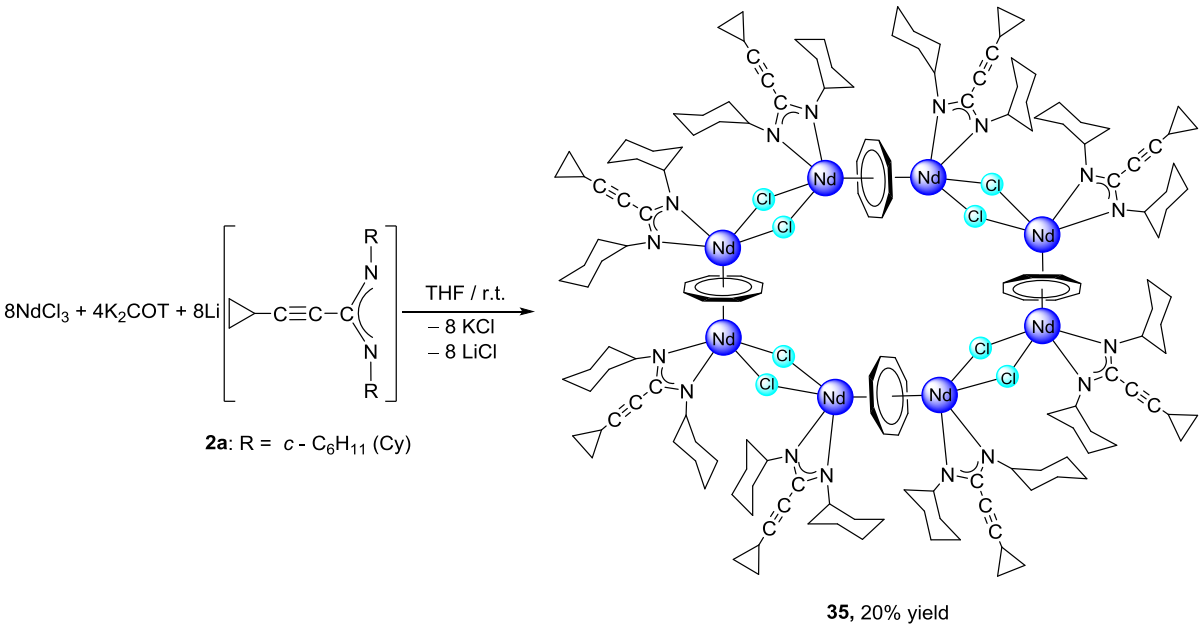

Scheme 26

The new compound **35** was extracted using toluene and isolated in the form of blue, needle-like crystals in 20% yield. Complex **35** was fully characterized by elemental analysis, spectroscopic methods and single-crystal X-ray diffraction. The NMR spectrum showed no resonances due to coordinated THF. In the ^{1}H NMR, the protons of η^8-C_8H_8 ligands appear at high field as singlet at δ = – 11.34 ppm [147]. The CH protons of the cyclohexyl groups include the appearance of two sets of resonances of equal intensity at δ = 3.61 and 3.35 ppm, which can be attributed to the paramagnetic nature of the Nd^{3+} ion. In comparison with the free ligand **2a**, the influence of the paramagnetism of the Nd^{3+} ion on the protons of the cyclopropyl protons is only weak. The CH protons of the *c*-C_3H_5 are observed at δ = 1.35 ppm, and the CH_2 groups at δ = 0.84 and 0.71 ppm. The ^{13}C NMR spectrum of **35** shows a resonance at δ = 133.7 due to the COT ring. Blue, needle-like single-crystals, grown by slow cooling of a saturated solution in toluene to 5 °C, were found to be suitable for X-ray

diffraction study. These crystals were found to contain six molecules of toluene per formula unit. Compound **35** crystallizes in the monoclinic space group C2/c with one molecule in the unit cell. The solid state structure of **35** revealed the presence of an unprecedented cyclic sandwich compound of the composition $[(\mu\text{-}\eta^8\text{:}\eta^8\text{-COT})\{Nd(c\text{-}C_3H_5\text{-}C{\equiv}C\text{-}C(NCy)_2)(\mu\text{-}Cl)\}_2]_4$, as shown in Figure 37.

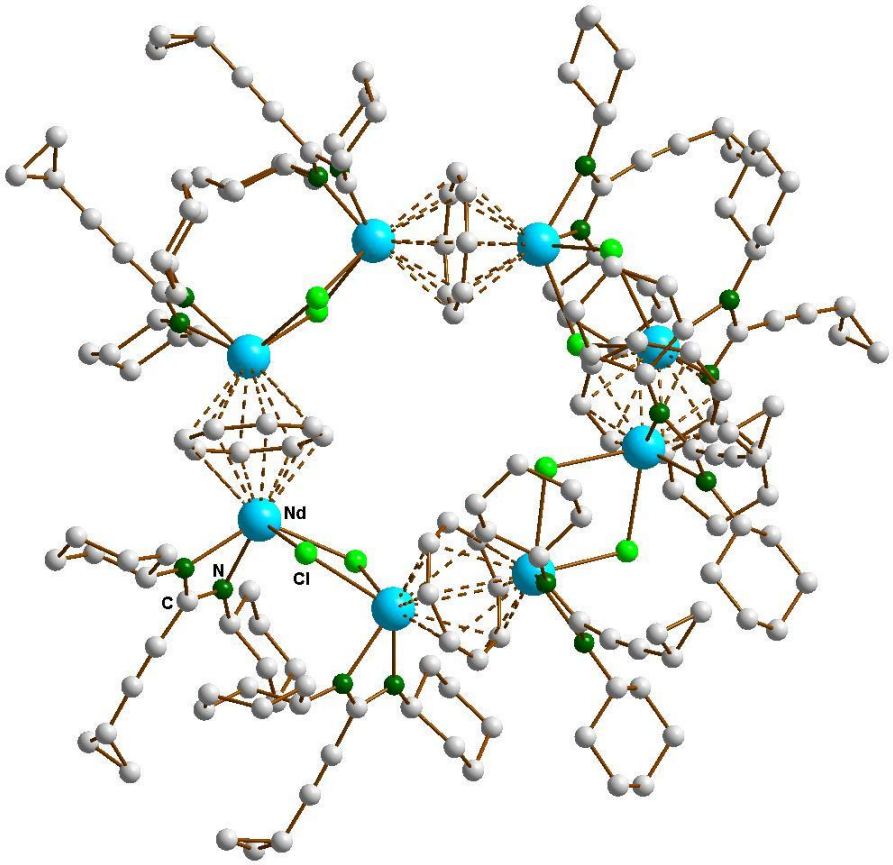

Figure 37. Molecular structure of $[(\mu\text{-}\eta^8\text{:}\eta^8\text{-COT})\{Nd(c\text{-}C_3H_5\text{-}C{\equiv}C\text{-}C(NCy)_2)(\mu\text{-}Cl)\}_2]_4$ (**35**)

The molecule consists of four COT rings sandwiched between eight Nd^{3+} ions, and each Nd^{3+} ion is bonded to one amidinate ligand and bridged by two chlorine atoms with the neighbouring Nd^{3+} atom (Figure 37). All four COT rings are η^8-coordinated to neodymium atom. The coordination sphere around the Nd^{3+} ion can be described as distorted *pseudo*-tetragonal pyramidal as shown in Figure 38.

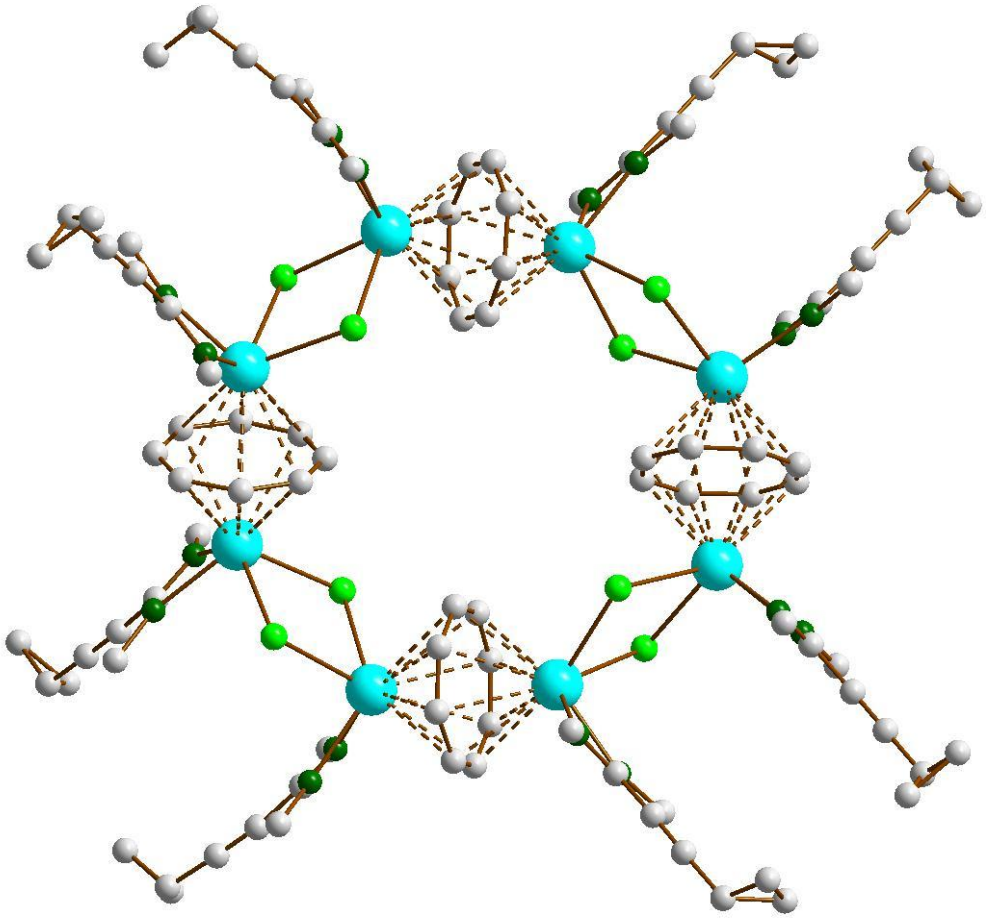

Figure 38. Molecular structure of (**35**) without cyclohexyl groups for clarity.

The average Nd–C(COT) distance range from 2.826 Å to 2.835 Å is similar to that found in (μ-η^8:η^8-COT)[Sm{N(SiMe$_3$)$_2$}$_2$]$_2$ with a range from 2.798(5) to 2.857(5) Å [152] and in (η^8-COT″)Nd((μ-η^8:η^8-COT″)Nd(η^8-COT″) with a range from 2.815(3) to 2.922(3) Å [164]. The Nd–(COT ring centroid) distances are ranging from 2.162 to 2.171 Å in good agreement with those found in (η^8-COT″)Nd(μ-η^8:η^8-COT″)Nd(η^8-COT″) (2.126 to 2.156 Å) [164]. The bond lengths of Nd–Cl are between 2.7655(11) and 2.8377(15) Å similar to Nd–Cl (from 2.822(1) to 2.8463(12) Å) in [(COT″)Nd(μ-Cl)(THF)]$_2$ [153]. The Nd–N bond lengths are ranging from 2.395(3) to 2.439(4) Å [147]. The Nd–(COT ring centeroid)–Nd (178.9°, 178.6° and 179.8°) angles are almost linear. The N–Nd–N angles range from 55.57(13)° to 56.19(12)° [147]. The unit NCN angles are between 115.0(4)° and 116.4(4)°. The Cl–Nd–Cl angles are ranging from 75.44(3)° to 77.36(3)°, and the Nd–Cl–Nd from 101.96(3)° to 104.02(4)° [153].

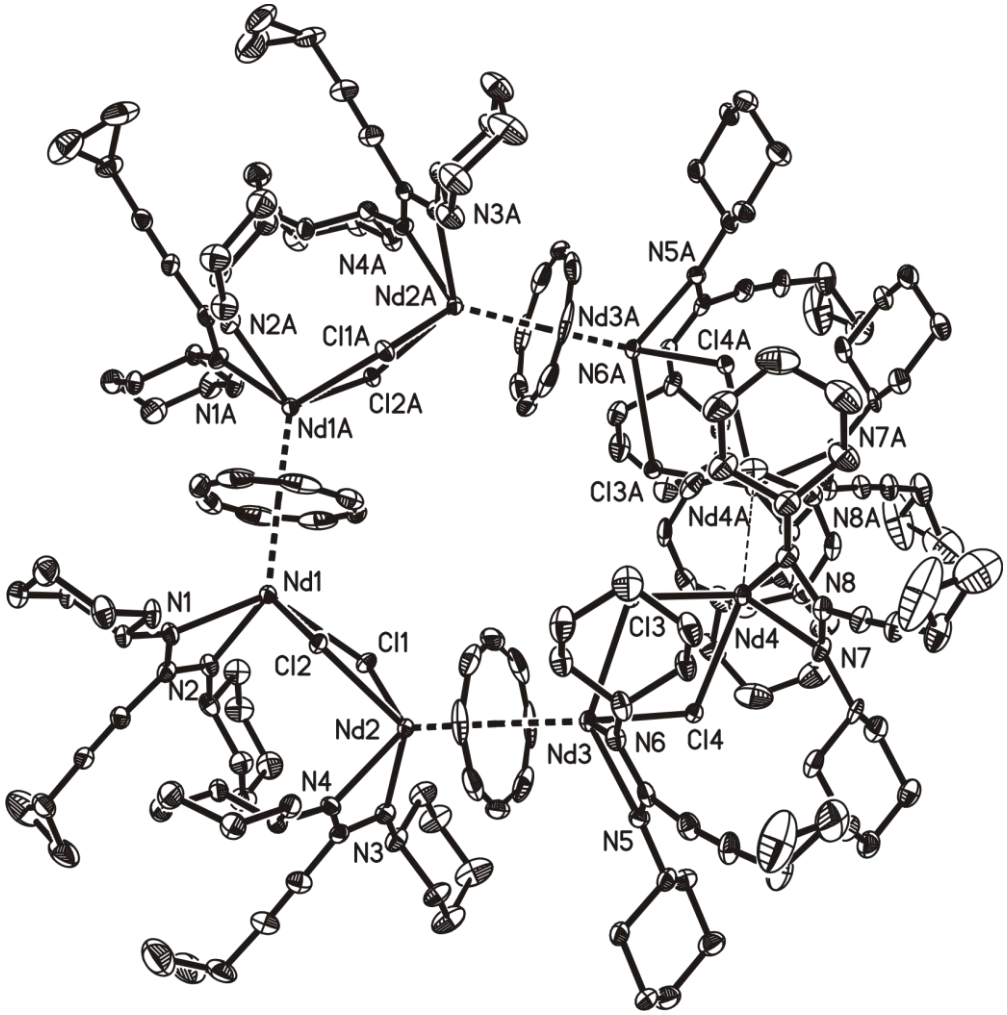

Figure 39. ORTEP view of $[(\mu\text{-}\eta^8\text{:}\eta^8\text{-COT})\{Nd(c\text{-}C_3H_5\text{-}C{\equiv}C\text{-}C(NCy)_2)(\mu\text{-}Cl)\}_2]_4$ (**35**)

Table 7 shows the difference in bond lengths and angles of neodymium complexes **25**, **32** and **35**.

Table 7 Selected bond lengths (Å) and angles (°) of **25**, **32** and **35**

Complex / Bond lengths and angles	**25**	**32**	**35**
Nd–C(COT) (average)	2.704	2.670	2.826 – 2.835
Nd–(COT ring centroid)	2.2002	1.936, 1.949	2.162 – 2.171
Nd–N (average)	2.619	2.587	2.395 – 2.439
Nd–COT–Nd	–	–	178.6, 178.9 and 179.8

2.6. Catalytic activity of lanthanide(III) amidinate complexes

As mentioned before, in 2002 Shen and co-workers reported new homoleptic lanthanide amidinates and their catalytic activity for the ring-opening polymerization (ROP) of ε-caprolactone at room temprature [69]. Thus far, the lanthanide amidinate and guanidinate complexes have witnessed rapid progress and have been proven to be very efficient homogeneous catalysts/precatalysts in organic transformations and polymerizations *e.g.* for the guanylation of amines or the ring–opening polymerization of lactones [22, 40]. The lanthanide amidinate complexes were found to effectively catalyze the addition of various primary and secondary amines as well as aromatic and aliphatic diamines to carbodiimides to afford the corresponding monoguanidine and biguanidine derivatives [40]. Guanidines are important structure motifs found in many biological and pharmaceutically active compounds [53, 54]. Lanthanide amidinate compounds were also found to be excellent precatalysts for the addition of terminal alkynes to carbodiimides yielding a series of propiolamidines [165 – 170].

2.6.1. Catalytic activity of lanthanide bis(cyclopropylethinylamidinates) (5 – 8)

In the course of this study the catalytic activity of the new lanthanide bis(cyclopropylethinylamidinate) complexes **5 – 8** has been investigated. The reaction between *p*-phenylendiamine and 2 equivalents of *N*,*N*′-diisopropylcarbodiimide to give the bis-guanylation product **36** was studied as an intial catalysis screening test for these complexes (Scheme 27). The results are listed in Table 8. All the reactions were carried out in THF solution at room temperature or at 60 °C for the fixed time of 15 or 30 min. The purity of the biguanidine derivative *N*,*N*′-1,4-phenylenebis(*N*,*N*′-diisopropylguanidine) (**36**) was checked by comparison of its NMR data (^{1}H and ^{13}C) with those reported in the previous litrature [171 – 173].

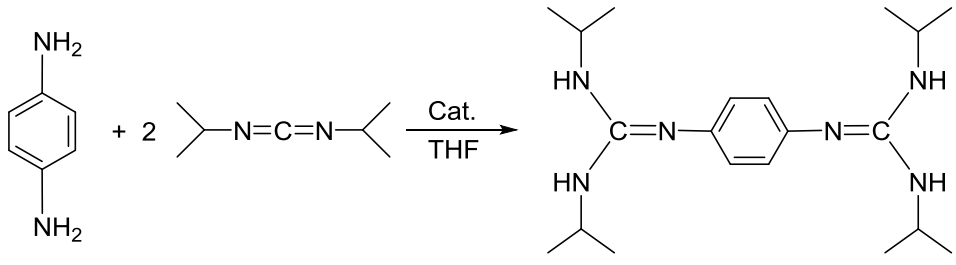

36

Scheme 27

It was surprising to find that all of the chloro-bridged dimers [{*c*-C_3H_5-C≡C-C(NR)$_2$}$_2$Ln(μ-Cl)(THF)]$_2$ (**5**: Ln = Ce, R = ^{i}Pr; **6**: Ln = Ce, R = Cy; **7**: Ln = Nd, R = Cy) and the "ate" complex [*c*-C_3H_5-C≡C-C(NCy)$_2$]$_2$Ho(μ-Cl)$_2$Li(THF)(Et_2O) (**8**) exhibited a high catalytic activity towards the reaction of amines with carbodiimides. By using the complexes **5 – 7** as precatalysts, the isolated yields of **36** were found to increase when the catalyst loading increased from 0.5 to 1.0 mol % (in the case of **7** no difference was observed, *cf.* Table 8). Only in the case of **8**, the isolated yields of **36** decreased by increasing the catalyst load from 0.5 to 1.0 mol %. The catalytic activity of complex **5** was almost equal to that of complex **6**, while the activity of **8** was somewhat lower than that of **5 – 7**. Especially the activity of **7** was found to be extremely high. For example, the yield of **36** could be as high as >99% at 60 °C and a catalyst loading of 0.5 % mol after 0.5 h (entry 7).

Table 8 Addition of 1,4-diaminobenzene to *N*,*N*′-diisopropylcarbodiimide catalyzed by the lanthanide bis(cyclopropylethinylamidinates) **5 – 8**

Entry[a]	Cat.	Catalyst loading (mol %)	Temp (°C)	Time (h)	Yield[b] of **36** (%)
1	**5**	0.5	60	0.5	92
2	**5**	1	60	0.5	98
3	**6**	0.5	60	0.5	92
4	**6**	1	60	0.25	>99
5	**7**	0.5	r.t.	0.5	92
6	**7**	1	r.t.	0.5	93
7	**7**	0.5	60	0.5	>99
8	**7**	1	60	0.5	>99
9	**8**	0.5	60	0.5	78
10	**8**	1	60	0.5	55
11	none	0	60	0.5	0

[a] In THF as solvent. [b] Isolated yield.

The most active complex, [{*c*-C_3H_5-C≡C-C(NCy)$_2$}$_2$Nd(μ-Cl)(THF)]$_2$ (**7**) was chosen as a precatalyst for further addition reactions of substituted anilines to *N,N'*-diisopropylcarbodiimide and *N,N'*-dicyclohexylcarbodiimide at 60 °C using a catalyst loading of 0.5 mol% in THF as solvent as shown in Scheme 28. Representative results are summarized in Table 9.

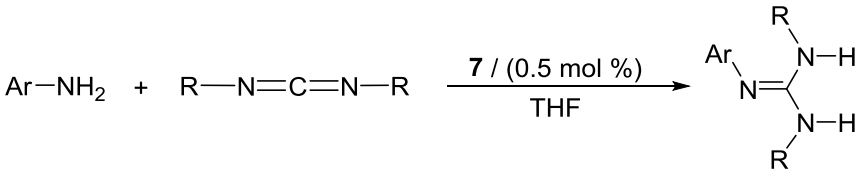

37 – 42

Scheme 28

All *N,N',N''*-trisubstituted guanidines and bis-guanidines listed in Table 9 are known compounds [174 – 183]. In the case of *o*- and *m*-phenylenediamine as substrates (Table 3), the yields obtained with *N,N'*-dicyclohexylcarbodiimides were lower than those obtained with *N,N'*-diisopropylcarbodiimide. It is, however, unlikely that with the guanidine units being in *p*- and *m*-positions the steric bulk of the substituents on the carbodiimides has a significant influence on the outcome of these reactions. Notable is the outcome of the analogous reactions of *o*-phenylenediamine with carbodiimides (Table 9, entries 5 and 6). It has been previously reported that the reaction of *o*-phenylenediamine with *N,N'*-diisopropylcarbodiimide in the presence of a titanacarborane monoamide catalyst (10 mol %) directly afforded the cyclic guanidine derivative *o*-$C_6H_4(NH)_2C{=}N^iPr$ [184]. However, under mild conditions, the intermediate mono-guanylation product **40** could be isolated in 59% yield. Thermal treatment of **40** at 140 °C for 30 h led to conversion into the cyclic guanidine *o*-$C_6H_4(NH)_2C{=}N^iPr$ (Scheme 29).

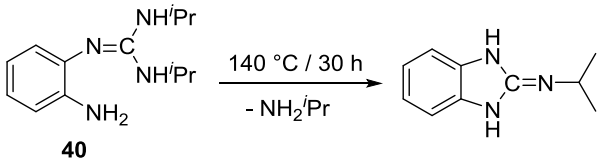

40

Scheme 29

This experiment implied that the catalyst might not be involved in the cyclization step [184]. In order to avoid subsequent cyclization in our study, the Ln-catalyzed reaction of *o*-phenylenediamine with *N,N'*-diisopropylcarbodiimide was carried out at room temperature. Quite remarkably, even with a catalyst loading as low as 0.5 mol %, the mono-guanylation

product **40** could be isolated after only 30 min in nearly quantitative yield (93%). Even at 60 °C, *N*,*N'*-dicyclohexylcarbodiimide did not react with *o*-phenylenediamine in the presence of **7**. This is in accordance with a previous report that the Ti-catalyzed formation of the cyclic guanidine *o*-$C_6H_4(NH)_2C{=}NCy$ requires rather harsh reaction conditions (140 °C/120 h) [184].

Table 9 Addition of primary amines to carbodiimides catalyzed by complex **7**

Entry[a]	R	Amines	Guanidines	Time (h)	Product	Yield %[b]
1	^{i}Pr	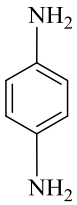	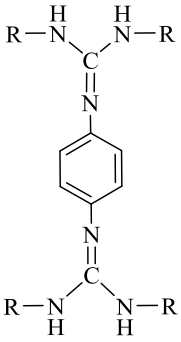	0.5	**36**	> 99
2	Cy			0.5	**37**	79
3	^{i}Pr	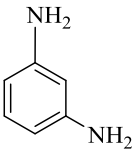	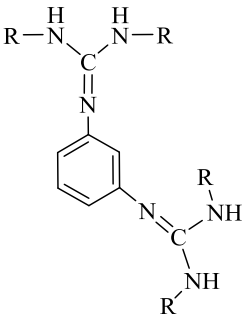	1	**38**	83
4	Cy			1	**39**	76
5	^{i}Pr	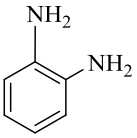	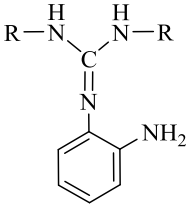	0.5	**40**	93[c]
6	Cy			2	–	Traces
7	^{i}Pr	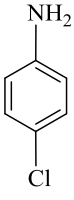	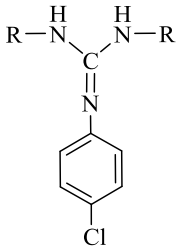	0.5	**41**	99
8	Cy			0.5	**42**	99

[a] General conditions: Solvent THF, temperature at 60 ºC and catalyst loading 0.5 mol %.
[b] Isolated yield. [c] Reaction carried out at room temperature.

Reactions of *p*-chloroaniline with both carbodiimides (Table 9, entries 7 and 8) provided the expected guanylation products **41** and **42** under the standard conditions in quantitative yields (99%), reflecting again the exceptionally high catalytic activity of the neodymium complex **7**. In both cases, quantitative conversion was observed after only 30 min. Both *p*-chlorophenyl-substituted guanidines could be easily isolated in a highly pure form by recrystallization from acetonitrile. In all cases (**36** – **42**), acetonitrile was found to be the solvent of choice for obtaining high-purity guanidine products. In addition to their ^{1}H and ^{13}C NMR data, the molecular structures of the trisubstituted guanidine products **40** and **41** were also authenticated by X-ray diffraction. The molecular structures are depicted in Figure 40.

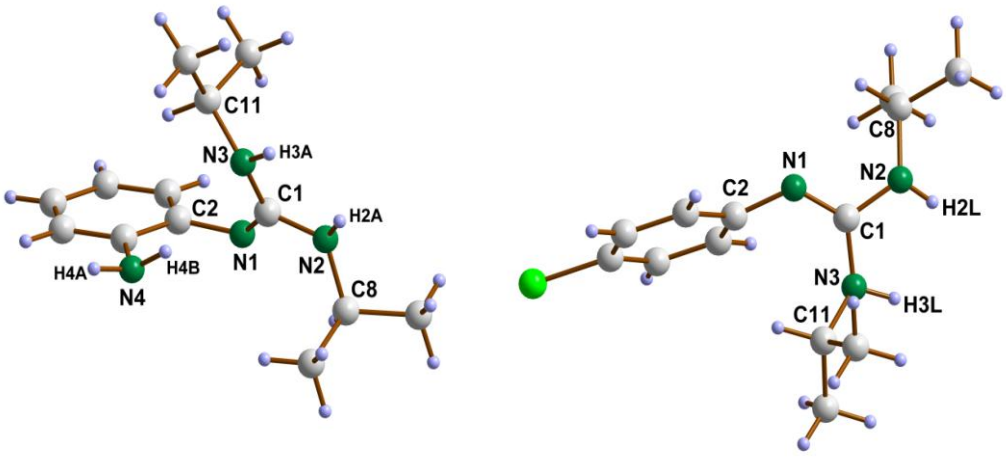

Figure 40. Molecular structures of 1,2-$C_6H_4(NH_2)[-N=C(NH^iPr)_2]$ (**40**) (left) and 1,4-$C_6H_4Cl[-N=C(NH^iPr)_2]$ (**41**) (right)

In both molecules the central structural unit comprises a CN_3 core with two distinctly different C-N bonds. Of particular interest is the structure of the *o*-phenylenediamine-derived compound *o*-$C_6H_4(NH_2)[N=C(NH^iPr)_2]$ (**40**). With 1.379(12) and 1.370(12) Å the C1–N2 and C1–N3 bond lenghts are consistent with the presence of C-NH single bonds, whereas the C1-N1 bond (1.301(12) Å) clearly has carbon-nitrogen double bond character. The CN_3 core is nearly planar. This is indicated by the N1–C1–N2, N1–C1–N3, and N2–C1–N3 angles of 119.35(9)°, 127.33(9)°, and 113.32(8), respectively. These values are in excellent agreement with those reported earlier for similar compounds [183, 184] as well as the molecular structure of the *p*-chlorophenyl derivative *p*-$C_6H_4Cl[-N=C(NH^iPr)_2]$ (**41**). As mentioned above, compound **40** itself is interesting as an intermediate in the formation of the cyclic guanidine derivative *o*-$C_6H_4(NH)_2C=N^iPr$ according to Scheme 92 [184]. Although the

distance H4B···N3 (Figure 40) is quite long (2.352 Å), it might be interesting to note that the N3–C1–N2 unit is not in a perpendicular arrangement with respect to the phenyl ring plane, but is tilted by 24.8° so that the ^{i}PrNH functionality bearing N3 is inclined toward the amino group in *ortho*-position.

According to the previous studies, the following mechanism for the Ln-catalyzed reaction of aromatic amines with *N,N'*-diisopropylcarbodiimide can be proposed (Scheme 30).

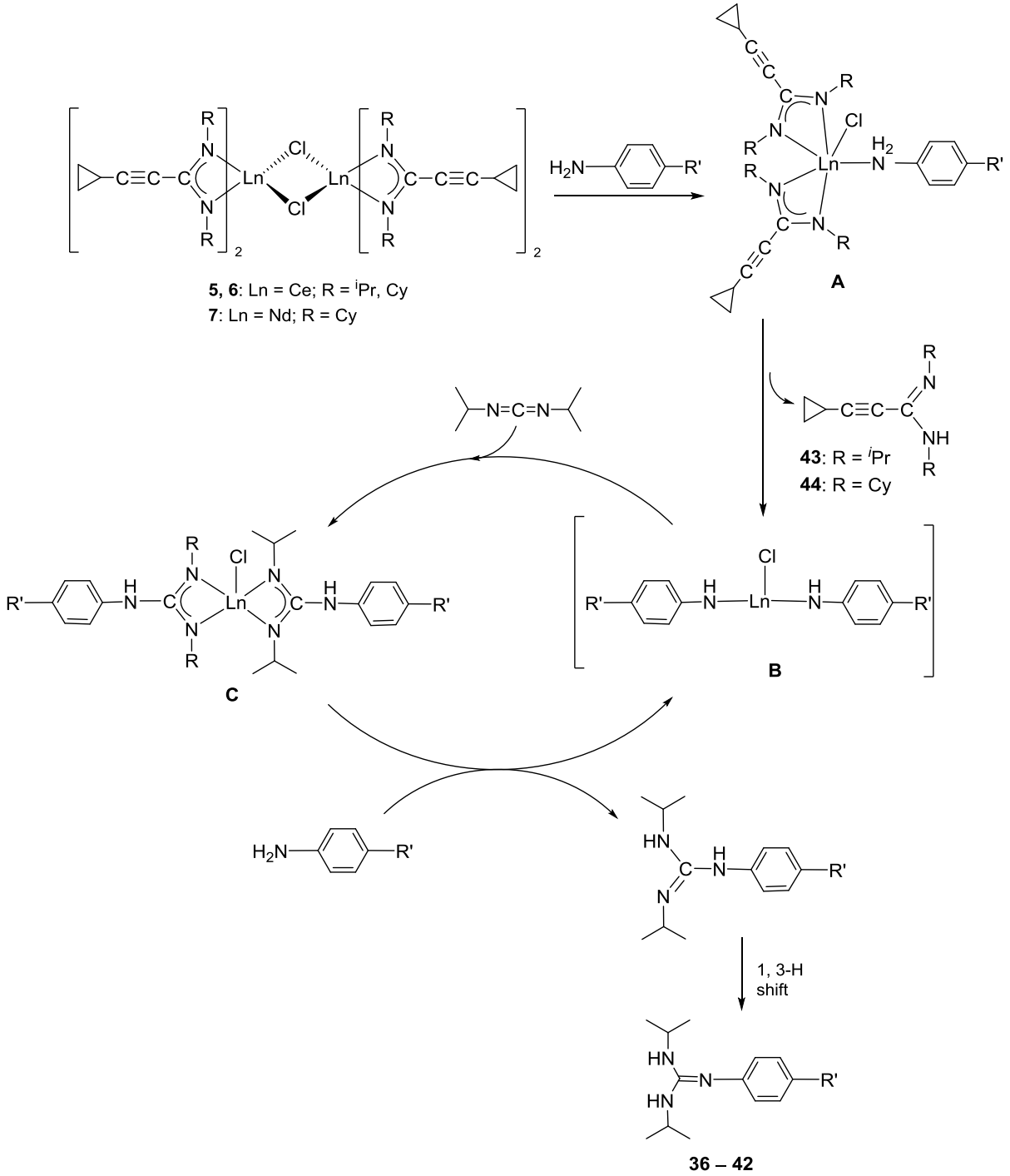

Scheme 30 Proposed mechanism of the Ln-catalyzed guanylation of aromatic amines.

In detail, it is safe to assume that the chloro-bridged dimer is first split into monomers upon addition of the aromatic amine to afford adduct **A**. As in previous cases, the catalytically active species should be a diamido complex **B**, which in this case could be generated by elimination of the free cyclopropylethinylamidines *c*-C_3H_5-C≡C-C(NHR)(=NR) (**43**: R = ^{i}Pr; **44**: R = Cy), Scheme 31. Preliminary positive proof for this assumption came from the independent preparation of *c*-C_3H_5-C≡C-C(NHCy)(=NCy) **44** by careful hydrolysis of **2a** in acetonitrile. Amidine **44** was identified by its ^{1}H and ^{13}C NMR data. A control NMR-tube reaction between **7** and *p*-chloroaniline in THF-d_8 clearly revealed the formation of free amidine **44**. Thus far, however, it was not possible to isolate an intermediate diamido complex of the type **B** from the reaction mixture. In the course of a closely related study by Xi *et al.*, a key intermediate with two bridging PhNH amido ligands, [{PhC(NAr)$_2$}$_2$Lu(μ-NHPh)]$_2$ (Ar = *p*-C_6H_4Me), could be isolated and structurally characterized [180]. In this case the amido intermediate was formed by elimination of the cyclopentadienyl ligand Cp′ from the precursor Cp'Lu[PhC(NAr)$_2$]$_2$ upon treatment with aniline. The following steps of the proposed catalytic cycle are well established through a variety of previous studies [170 – 180]. Subsequent insertion of the carbodiimide C=N bond into an Ln–N bond of the diamido species **B** could afford a bis(guanidinate)LnCl intermediate **C**, which upon reaction with the aromatic amine would release the trisubstituted guanidine product (**36 – 42**) and regenerate the amido complex **B**.

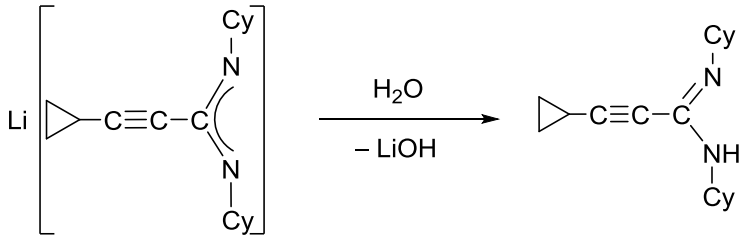

2a **44**

Scheme 31 Formation of free amidine **44** by controlled hydrolysis of **2a**.

2.6.2. Catalytic activity of lanthanide tris(cyclopropylethynylamidinates) (12 – 15)

The first synthesis of propiolamidines of the type R-C≡C-C(=NR')(NHR') was reported by Hou *et al*. in 2005 using rare-earth metal half-sandwich complexes [$Me_2Si(C_5Me_4)$(NPh)]Y-(CH_2SiMe_3)(THF)$_2$ as catalysts [106]. The catalytic activity of the new lanthanide tris-(cyclopropylethynylamidinates) **12** – **15** has been tested. The addition of phenylacetylene to 1 equivalent of *N*,*N*′-diisopropylcarbodiimide to give the propiolamidine **45** was studied as an

intial catalysis screening test for these complexes (Scheme 32). The results are listed in Table 10. All the reactions were carried out in THF solution at 60 °C for a fixed time 30 or 60 min. The known compound Ph-C≡C-C(=N^{i}Pr)(NH^{i}Pr) (**45**) was verified by comparison of its NMR spectra (^{1}H and ^{13}C) with those reported in the prevoius literature [165 – 170].

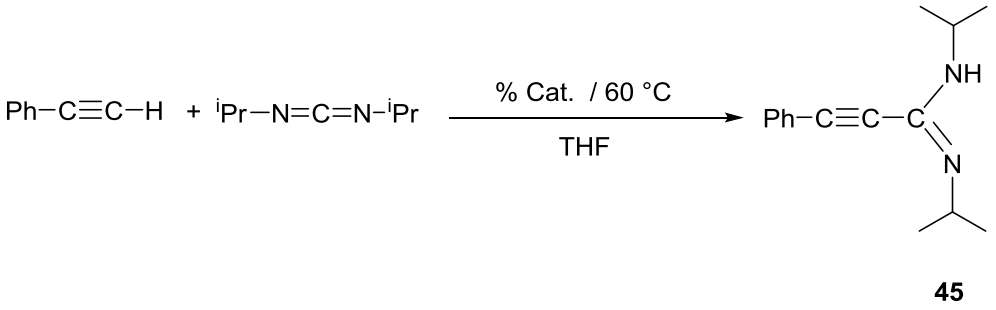

45

Scheme 32

Table 10 Addition of phenylacetylene to *N,N'*-diisopropylcarbodiimide catalyzed by the lanthanide-tris(cyclopropylethinylamidinates) **12 – 15**

Entry[a]	Cat.	Catalyst equiv. (mol %)	Time (h)	Yield[b] of **45** (%)
1	**12**	0.5	1	53
2	**12**	1	0.5	62
3	**13**	0.5	1	54
4	**13**	1	0.5	51
5	**14**	0.5	1	72
6	**14**	1	0.5	85
7	**15**	0.5	1	34
8	**15**	1	0.5	27
9	none	0	1	0

a General condition: THF as solvent at 60 °C.

b Isolated yield.

The isolated yields of **45** varied from 27 to 85% depending on the corresponding lanthanide metal. The catalytic activity of the samarium complex [*c*-C_3H_5-C≡C-C(NCy)$_2$]$_3$Sm (**14**) gave the highest yields (entry 5 and 6). By using the complexes **13** and **15** as precatalysts, the isolated yields of **45** were decreased when the catalyst loading increased from 0.5 to 1.0

mol%. Unlike in the cases of **12** and **14**, the isolated yields of **45** were increased by increasing the catalyst load from 0.5 to 1.0 mol %. The most active complex [*c*-C_3H_5-C≡C-$C(NCy)_2]_3Sm$ (**14**) was chosen as a precatalyst for further addition reactions of terminal alkynes to *N,N'*-diisopropylcarbodiimide and *N,N'*-dicyclohexylcarbodiimide at 60 °C using a catalyst loading of 1.0 mol % in THF as solvent as shown in Scheme 33. Representative results are summarized in Table 11.

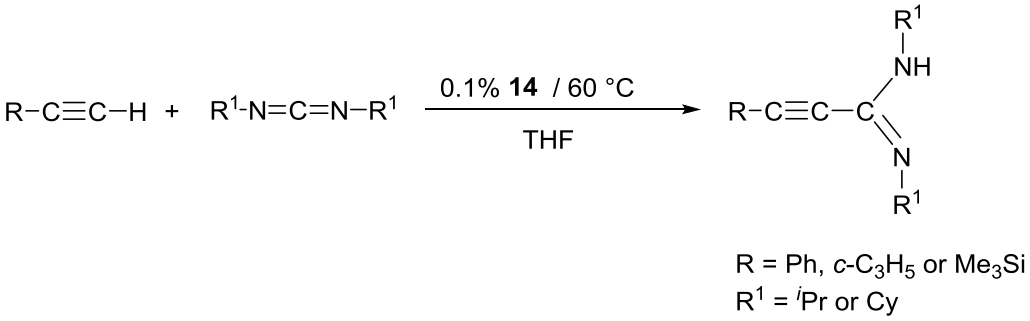

Scheme 33

Table 11 Catalytic addition of terminal alkynes to *N,N'*-diisopropylcarbodiimide catalyzed by **14**.

Entry[a,b]	R	R^1	Time (h)	Product	Yield[c] (%)
1	Ph	^{i}Pr	0.5	**45**	85
2	Ph	Cy	0.5	**46**	78
3	*c*-C_3H_5	^{i}Pr	0.5	–	traces
4	*c*-C_3H_5	Cy	1	**47**	48
5	Me_3Si	^{i}Pr	0.5	–	traces
6	Me_3Si	Cy	1	–	traces

[a] General condition: THF as solvent at 60 ºC. [b] All reactions carried out using 1.0 % mol of **14**.

[c] Isolated yield.

The reactions of phenylacetylene with both *N,N'*-diisopropylcarbodiimide and *N,N'*-dicyclohexylcarbodiimide gave good yields of the hydroacetylenation products **45** and **46**, while cyclopropylacetylene could be added only to *N,N'*-dicyclohexylcarbodiimide affording a moderate yield of propiolamidine **47**. In sharp contrast, virtually no reactions were observed when trimethylsilylacetylene was used. Thus the use of the new homoleptic lanthanide(III)

tris(cyclopropylethinylamidinates) as catalysts for the addition of terminal alkynes to carbodiimides appears to be quite limited. The molecular structure of the propiolamidine Ph-C≡C-C(NCy)(NHCy) (**46**) has been authenticated by single-crystal X-ray diffraction (Figure 41). The C≡C bond length in **46** is 1.195(3) Å, while the C1–N1 and C1–N2 distances (1.364(2) and 1.275(4) Å) correspond to standard C–N single and double bonds, respectively.

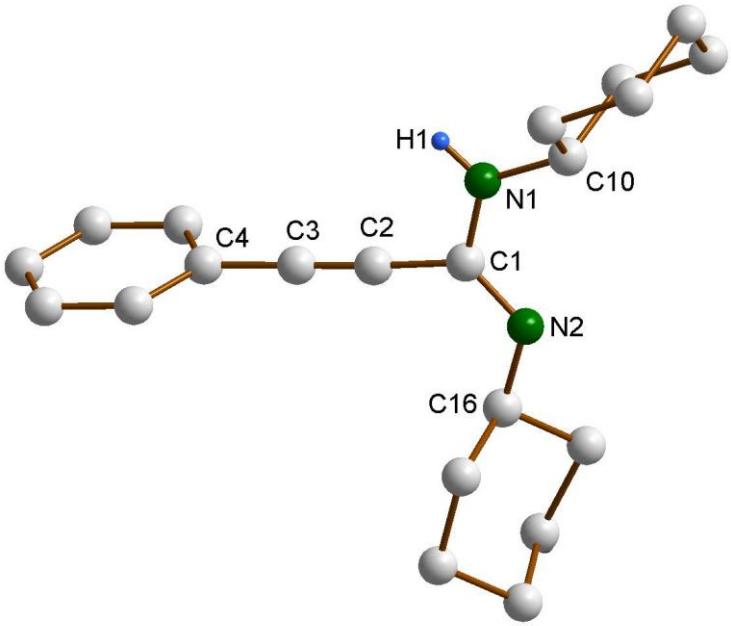

Figure 41. Molecular structure of Ph-C≡C-C(NCy)(NHCy) (**46**)

As in 4-ClC_6H_4-C≡C-C(N^{i}Pr)(NH^{i}Pr) and 2-ClC_6H_4-C≡C-C(N^{i}Pr)(NH^{i}Pr) [103], one cyclohexyl substituent points toward the alkynyl group and the other one away, resulting in a *transoid* conformation around the N–C–N unit. In contrast, a *cisoid* conformation (both substituents pointing toward the alkynyl group) has been reported for Ph-C≡C-C(N$C_6H_3{}^i Pr_2$-2,6)(NH$C_6H_3{}^i Pr_2$-2,6) [165] and Ph-C≡C-C(N$C_6H_3{}^i Pr_2$-2,6)(NH$C_6H_3Cl_2$-3,4) [168] which both contain bulky 2,6-diisopropylphenyl substituents.

3. Summary

The main goal of the present Ph.D. thesis was the investigation and structural characterization of new rare-earth metal alkynylamidinate and guanidinate complexes and their use as homogeneous catalysts for selected organic transformations. In the initial stage of the work a new type of alkynylamidinate ligands based on cyclopropylacetylene has been developed.

In a straightforward manner, a series of six new lithium-cyclopropylethinylamidinates, Li[*c*-C_3H_5-C≡C-C(NR)$_2$]·S (**1a**: R = ^{i}Pr, S = THF, **1b**: S = Et_2O, **1c**: S = DME; R = cyclohexyl (Cy), **2a**: S = THF, **2b**: S = Et_2O, **2c**: S = DME) have been obtained by *in situ* deprotonation of commercially available cyclopropylacetylene with ^{n}BuLi followed by treatment with either *N*,*N*′-diisopropylcarbodiimide or *N*,*N*′-dicyclohexylcarbodiimide. X-ray crystal structure determinations of **1a** and **2a** showed both compounds to adopt dimeric structures in the solid state (Figure 42).

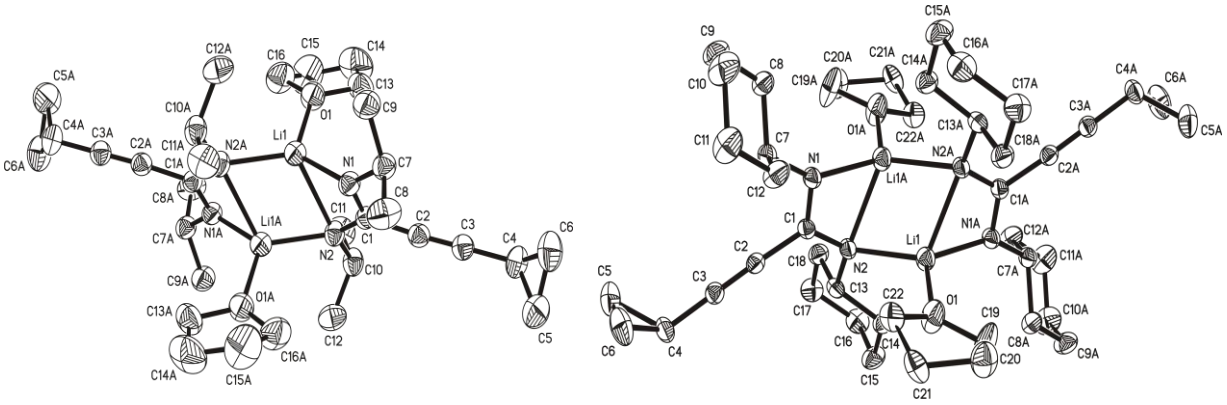

Figure 42. Molecular structures of **1a** (left) and **2a** (right)

In a similar manner, treatment of phenylacetylene with ^{n}BuLi at –20 °C in THF or Et_2O followed by addition of *N*,*N*′-dicyclohexylcarbodiimide afforded Li[Ph-C≡C-C(NCy)$_2$]·S (S = THF, **3a** (Figure 43)) (S = Et_2O, **3b**)

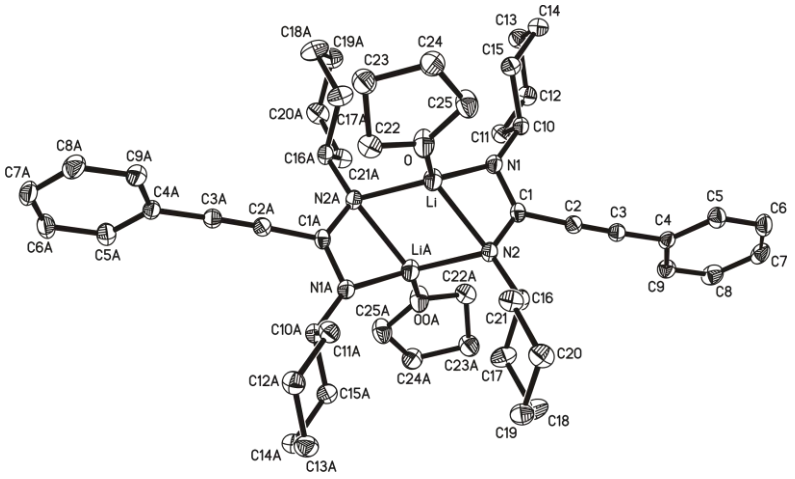

Figure 43. Molecular structure of **3a**

An unprecedented bulky lithium guanidinate was prepared by the reaction of *N*,*N*′-dicyclohexylcarbodiimide and ^{n}BuLi in a molar ratio of 2:1, respectively, in THF to give the amidino-guanidinate ligand, Li[^{n}Bu-C(=NCy)(NCy)C(NCy)$_2$]·THF (**4**).

Reactions of anhydrous lanthanide trichlorides, $LnCl_3$ (Ln = Ce, Nd, Ho), with 2 equiv. of the lithium-cyclopropylethinylamidinates, **1a** or **2a** afforded a series of new lanthanide bis(cyclopropylethinylamidinates). In the case of cerium and neodymium, the chloro-bridged dimers [{*c*-C_3H_5-C≡C-C(NR)$_2$}$_2$Ln(μ-Cl)(THF)]$_2$ (**5**: Ln = Ce, R = ^{i}Pr; **6**: Ln = Ce, R = Cy; **7**: Ln = Nd, R = Cy) were isolated, whereas holmium afforded the "ate" complex [*c*-C_3H_5-C≡C-C(NCy)$_2$]$_2$Ho(μ-Cl)$_2$Li(THF)(OEt$_2$) (**8**) (Figures 44 and 45).

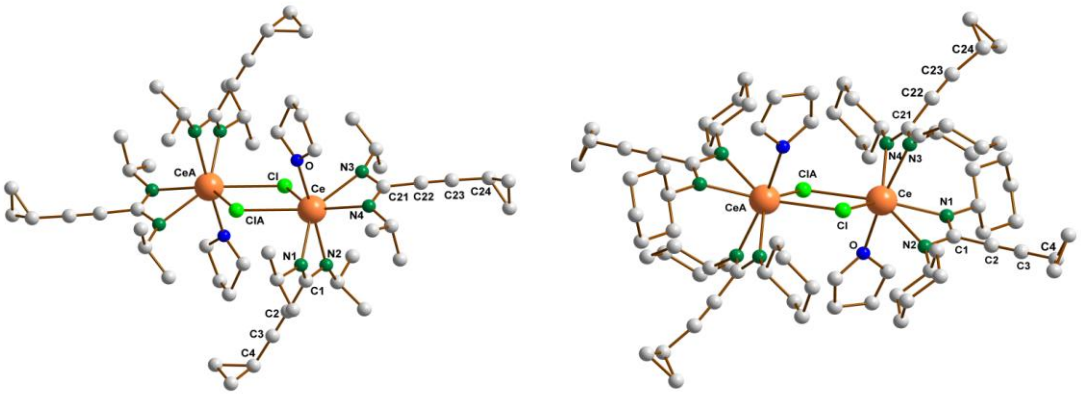

Figure 44. Molecular structures of **5** (left) and **6** (right)

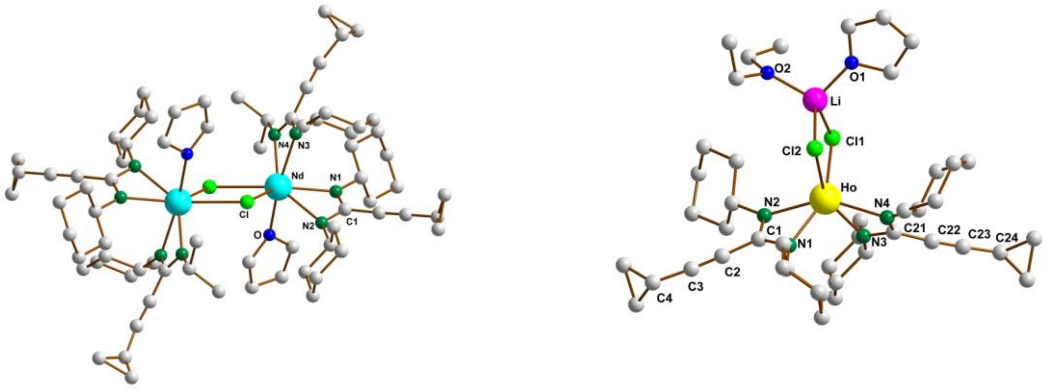

Figure 45. Molecular structures of **7** (left) and **8** (right)

In an attempt to prepare a new europium(II) amidinate complex, treatment of $EuI_2(THF)_2$ with **2a** in THF at room temperature gave the unusual Eu(III) cyclopropylethynylamidinate complex [*c*-C_3H_5-C≡C-C(NCy)$_2$]Li[*c*-C_3H_5-C≡C-C(NCy)$_2$]$_2$Eu(μ-I)$_2$Li(THF)$_2$ (**9**) (Figure 46).

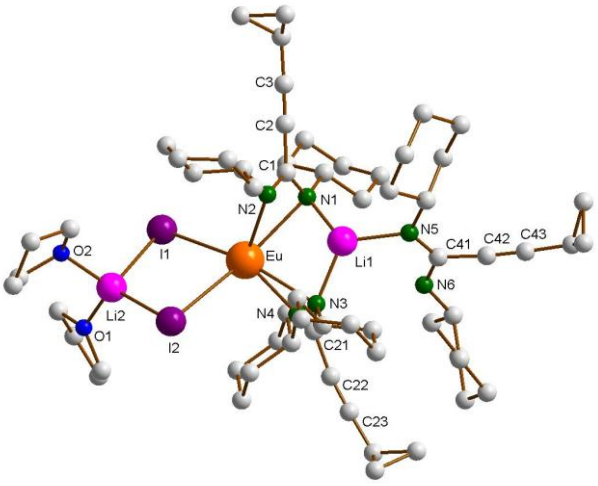

Figure 46. Molecular structure of **9**

The investigation of new Ce(III) complexes continues to be of significant current interest. The synthesis of the new Ce(III)diiminophosphinate complex [$Ph_2P(NSiMe_3)_2$]$_2$Ce(μ-Cl)$_2$Li(THF)$_2$ (**10**) (Figure 47) has been achieved by reaction of anhydrous $CeCl_3$ with Li[$Ph_2P(NSiMe_3)_2$] in a 1:2 molar ratio.

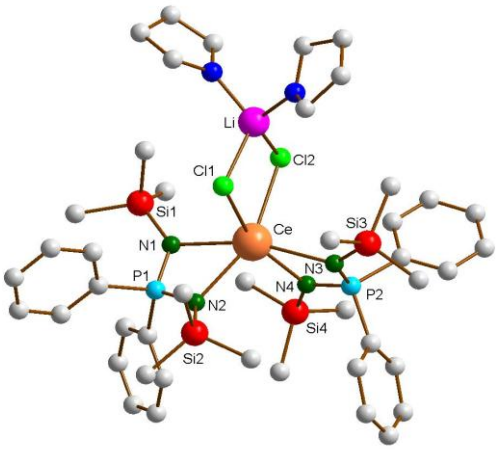

Figure 47. Molecular structure of **10**

Treatment of *N*,*N*′-dicyclohexylcarbodiimide with ^{n}BuLi in Et_2O *in situ* followed by addition of anhydrous $HoCl_3$ afforded the unexpected holmium(amidinato)guanidinate complex, [^{n}Bu-C(=NCy)(NCy)C(NCy)$_2$]Ho[^{n}Bu-C(NCy)$_2$](μ-Cl)$_2$Li(THF)$_2$ (**11**) (Figure 48).

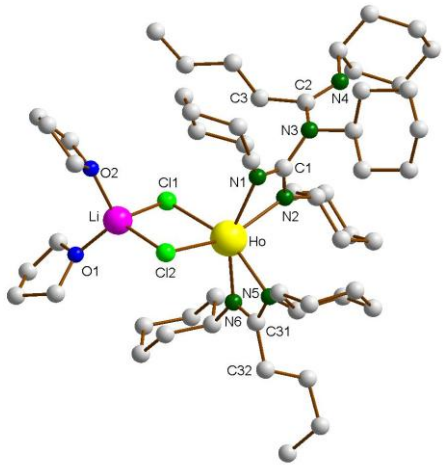

Figure 48. Molecular structure of (**11**)

A series of new homoleptic lanthanide(III) tris(cyclopropylethynylamidinate) complexes have been prepared, by reaction of anhydrous $LnCl_3$ (Ln = Nd, Sm or Ho) with **1a**, as well as the reaction of anhydrous $SmCl_3$ with **2a** in a 1:3 molar ratio. These reactions afforded the new lanthanide tris(cyclopropylethinylamidinates) [*c*-C_3H_5-C≡C-C(NR)$_2$]$_3$Ln (**12**: Ln = Nd, R = ^{i}Pr; **13**: Ln = Sm, R = ^{i}Pr; **14**: Ln = Sm, R = cyclohexyl (Cy); **15**: Ln = Ho, R = ^{i}Pr). The

structure of [*c*-C_3H_5-C≡C-C(N^{i}Pr)$_2$]$_3$Ho (**15**) was verified by a single-crystal X-ray diffraction study (Figure 49).

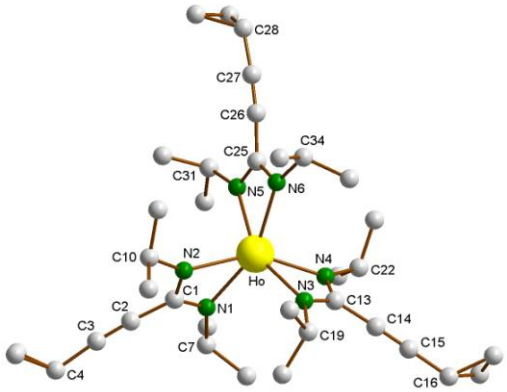

Figure 49. Molecular structure of **15**

In a similar manner, a series of new homoleptic lanthanide(III) tris(propiolamidinate) complexes were prepared by reaction of anhydrous $LnCl_3$ (Ln = Ce, Nd, Sm or Ho) with **3a** in a 1:3 molar ratio to give the new lanthanide tris(propiolamidinates) [Ph-C≡C-C(NCy)$_2$]$_3$Ln (**16**: Ln = Ce; **17**: Ln = Nd; **18**: Ln = Sm; **19**: Ln = Ho).

Lanthanide complexes containing Ln–N amide bonds have fundamental significance as catalysts for hydroamination reactions. Treatment of the chloro-bridged dimers (**5** – **7**) as well as the holmium "ate" complex **8** with KN(SiMe$_3$)$_2$ afforded unsolvated lanthanide bis(amidinato) amide complexes, [{*c*-C_3H_5-C≡C-C(NR)$_2$}$_2$LnN(SiMe$_3$)$_2$] (**20**: Ln = Ce, R = ^{i}Pr; **21**: Ln = Ce, R = Cy; **22**: Ln = Nd, R = Cy; **23**: Ln = Ho, R = Cy) (Figure 50).

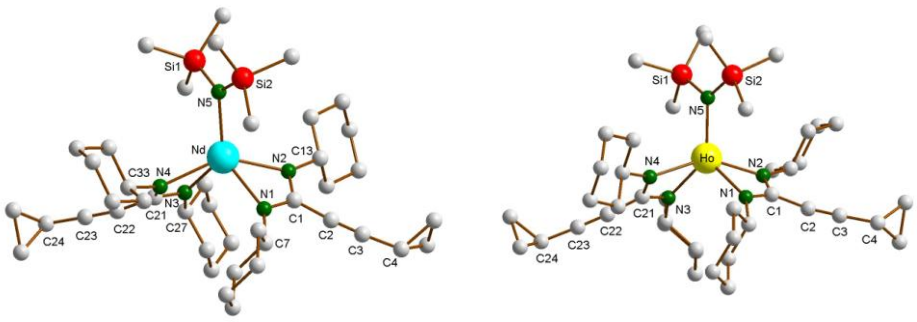

Figure 50. Molecular structures of **22** (left) and **23** (right)

The lithium-cyclopropylethinylamidinates Li[*c*-C_3H_5-C≡C-C(NR)$_2$] (**1a**: R = ^{i}Pr, **2a**: R = cyclohexyl (Cy)) ligands were also used as precursors for the preparation of a new series of half-sandwich complexes. These complexes contain the large flat cyclooctatetraenyl ligand ($C_8H_8^{2-}$, commonly abbreviated as COT), and were isolated as solvated, unsolvated and inverse sandwich complexes. Treatment of the halide precursors [(COT)Pr(μ-Cl)(THF)$_2$]$_2$ with **2a** and [(COT)Nd(μ-Cl)(THF)$_2$]$_2$ with **1a** and **2a** in THF in a 1:2 molar ratio respectively, afforded (COT)Ln(μ-*c*-C_3H_5-C≡C-C(NR)$_2$)$_2$Li(S) (**24**: Ln = Pr, R = Cy, S= Et_2O; **25**: Ln = Nd, R = ^{i}Pr, S = THF; **26**: Ln = Nd, R = Cy, S = THF), (Figure 51)

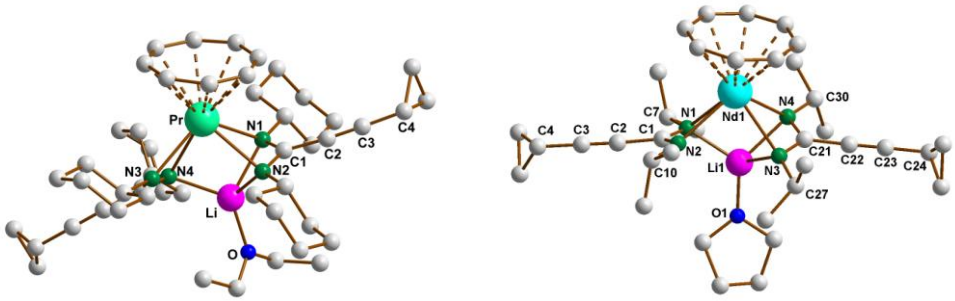

Figure 51. Molecular structures of **24** (left) and **25** (right)

Treatment of the dimers **5** and **6** *in situ* with $K_2C_8H_8$ in a 1:1 molar ratio in THF at room temperature afforded (μ-η^8:η^8-COT)[Ce{*c*-C_3H_5-C≡C-C(NR)$_2$}$_2$]$_2$ (**27**: R = ^{i}Pr; **28**: R = Cy) (Figures 52 and 53) as a novel method for encapsulation of a planar $(C_8H_8)^{2-}$ ring in lanthanide complexes containing amidinate ligands in the outer decks.

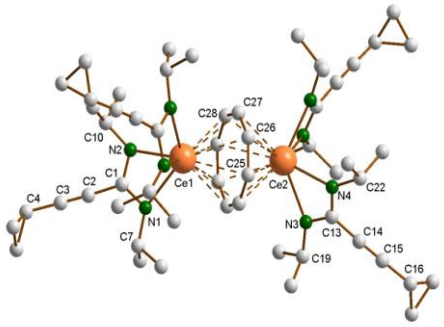

Figure 52. Molecular structure of **27**

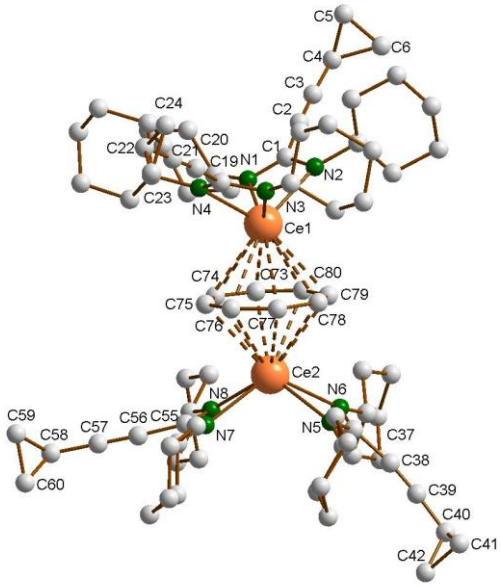

Figure 53. Molecular structure of **28**.

Novel unsolvated lanthanide half-sandwich complexes were prepared by using the precursors **1a**, **2a** and COT. Unlike the complexes **24** and **25**, the reaction of $[(COT)Pr(\mu\text{-}Cl)(THF)_2]_2$ with **1a** afforded the unsolvated centrosymmetric complex $[(COT)Pr(\mu\text{-}c\text{-}C_3H_5\text{-}C{\equiv}C\text{-}C(N^iPr)_2)]_2$ (**29**). These types of unprecedented dimeric strucures could be also accessed by reaction of $LnCl_3$ (Ln = Ce or Nd) with **1a** or **2a** and K_2COT in a 1:1:1 molar ratio as one-pot reaction to give novel $[(COT)Ln(\mu\text{-}c\text{-}C_3H_5\text{-}C{\equiv}C\text{-}C(NR)_2)]_2$ complexes (**30**: Ln = Ce, R = ^{i}Pr; **31**: Ln = Ce, R = Cy; **32**: L= Nd, R = ^{i}Pr) (Figures 54 and 55).

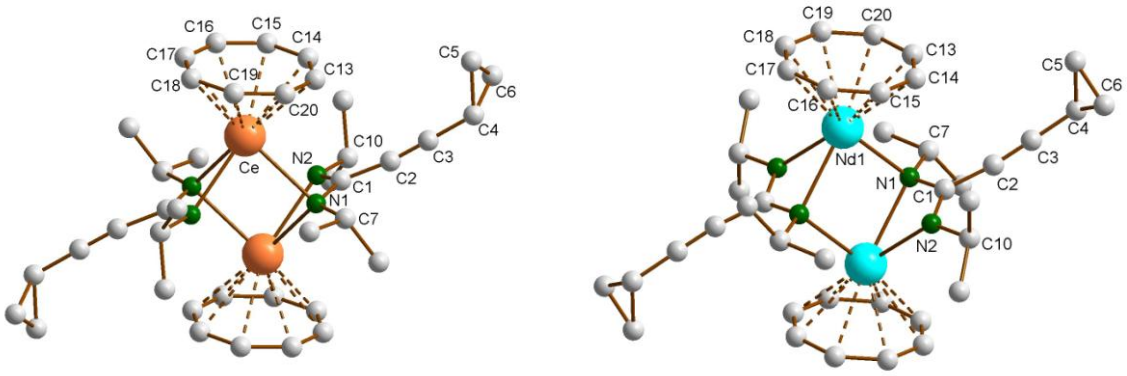

Figure 54. Molecular structures of **30** (left) and **32** (right).

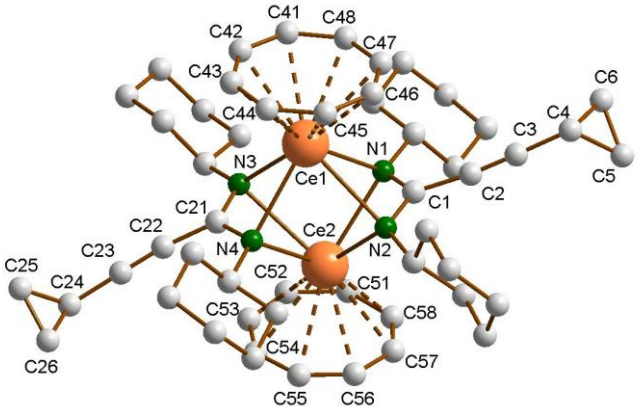

Figure 55. Molecular structure of **31**

Similar treatment of $HoCl_3$ with **1a** or **2a** and K_2COT as multi-component reaction in a 1:1:1 molar ratio afforded the solvated half sandwich complexes (COT)Ho(*c*-C_3H_5-C≡C-C$(NR)_2$)(THF) (**33**: R = ^{i}Pr; **34**: R = Cy) (Figure 56).

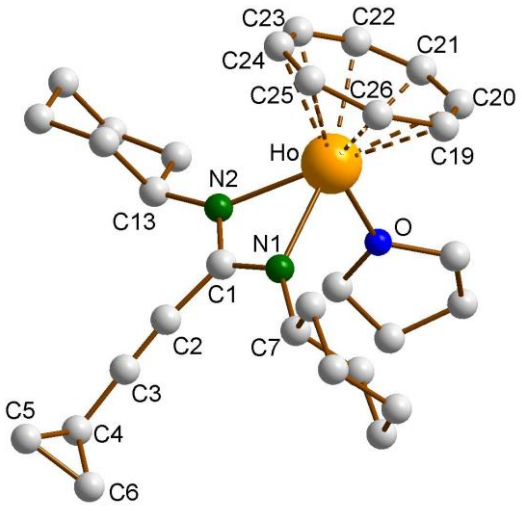

Figure 56. Molecular structure of **34**

A unique cyclic multidecker sandwich complex [(μ-η^8:η^8-COT){Nd(*c*-C_3H_5-C≡C-C$(NCy)_2$)(μ-Cl)}$_2$]$_4$ (**35**) was prepared by reaction of anhydrous $NdCl_3$ with K_2COT and **2a** as

one-pot reaction. The solid state structure of **35** reveals the presence of an unprecedented cyclic sandwich compound consisting of four COT rings sandwiched between eight Nd^{3+} ions, and each Nd^{3+} ion is bonded to one amidinate ligand and bridged by two chlorine atoms with the neighbouring Nd^{3+} atom (Figures 57 and 58)

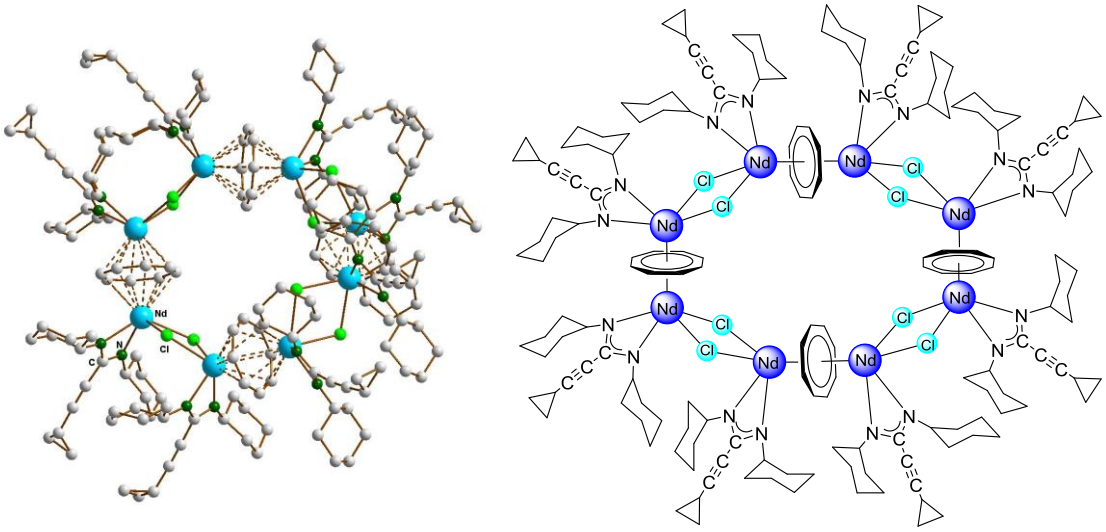

Figure 57. Molecular structure of **35** (left) and a schematic representation of **35** (right).

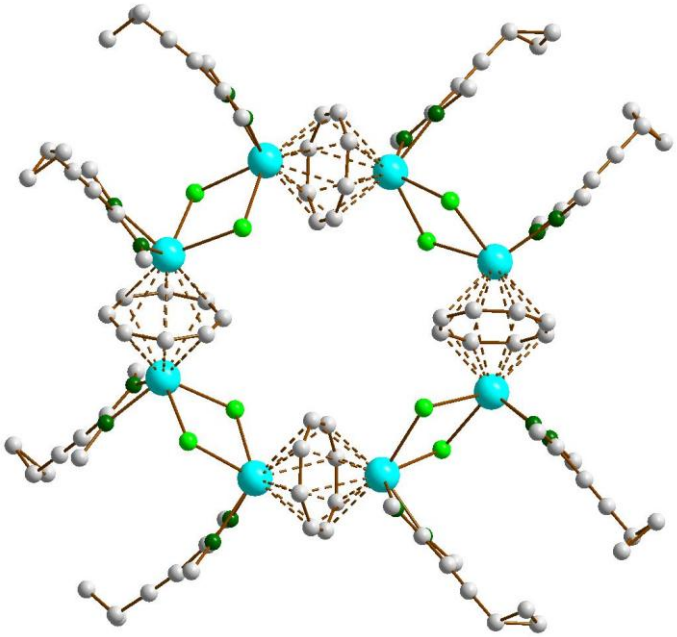

Figure 58. Molecular structure of **35** without cyclohexyl groups for clarity.

The new lanthanide bis- and tris(cyclopropylethinylamidinate) complexes were found to exhibit a catalytic activity towards C–C and C–N bond formation. All four new lanthanide bis(cyclopropylethinylamidinates) **5** – **8** were found to be extremely active precatalysts for the guanylation of *p*-phenylenediamine with 2 equiv. of *N*,*N*'-diisopropylcarbodiimide to give the bis-guanylation product. The isolated yields of the known compound 2,2'-(1,4-phenylene)-bis(2',3-diisopropylguanidine) (**36**) varied from 55 to >99% depending on the lanthanide metal used. This is a rare case of lanthanide chloro complexes being active catalysts for guanylation reactions. Because of its high catalytic activity even at room temperature, the complex **7** was used as precatalyst in the reaction of substituted anilines with both *N*,*N*′-diisopropylcarbodiimide and *N*,*N*′-dicyclohexylcarbodiimide to give the corresponding guanidine products. The reactions were carried out in concentrated THF solutions at room temperature or at 60 °C and catalyst loadings of 0.5 or 1.0%. The substituted anilines were *o*-, *p*- and *m*-phenylenediamine as well as *p*-chloroaniline. All the guanidine products (**36** – **42**) were fully characterized and two compounds (**40** and **42**) were structurally characterized by X-ray diffraction study (Figure 59).

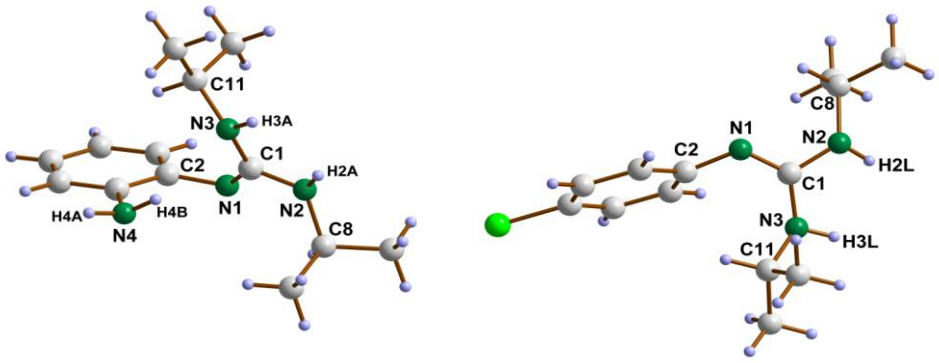

Figure 59. Molecular structures of 1,2-$C_6H_4(NH_2)[-N=C(NH^iPr)_2]$ (**40**) (left) and 1,4-$C_6H_4Cl[-N=C(NH^iPr)_2]$ (**41**) (right)

Likewise, the new homoleptic tris(cyclopropylethinylamidinates) **12** – **15** were used as precatalysts in C–C bond formation. The addition of phenylacetylene to *N*,*N*′-diisopropylcarbodiimide was catalyzed by the complexes **12** – **15** as precatalysts. The isolated yields of the known compound Ph-C≡C-$C(N^iPr)(NH^iPr)$ (**45**) varied from 27 to 85% depending on the lanthanide metal used. The reactions were carried out in concentrated THF

solutions at 60 °C and catalyst loadings of 0.5 or 1.0%. Complex **14** showed a higher catalytic activity than that found for the complexes **12**, **13** and **15**. Therfore, **14** used as precatalyst for the addition of three different terminal acetylenes to both *N*,*N*'-diisopropylcarbodiimide and *N*,*N*'-dicyclohexylcarbodiimide. Reactions of phenylacetylene with both *N*,*N*'-diisopropylcarbodiimide and *N*,*N*'-dicyclohexylcarbodiimide gave good yields of the propiolamidine products **45** and **46** (Figure 60), whereas cyclopropylacetylene could be added only to *N*,*N*'-dicyclohexylcarbodiimide affording a moderate yield of propiolamidine **47**. In sharp contrast, no reactions were observed when trimethylsilylacetylene used as alkyne component. Thus the use of the new homoleptic lanthanide(III) tris(cyclopropylethinylamidinates) as catalysts for the addition of terminal alkynes to carbodiimides appears to be quite limited.

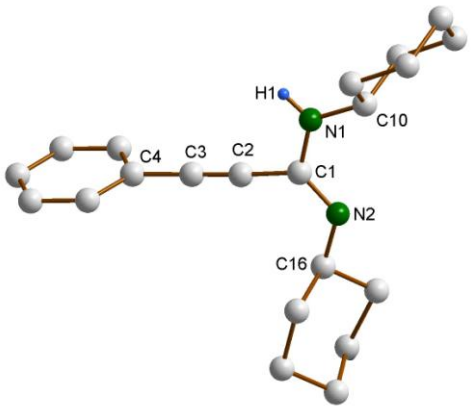

Figure 60. Molecular structure of Ph-C≡C-C(NCy)(NHCy) **46**

4. Experimental Section

General: All reactions were carried out in oven-dried or flame-dried glassware under an inert atmosphere of dry argon employing standard Schlenk and glovebox techniques. Et_2O, THF, DME, toluene and pentane were distilled from sodium/benzophenone under nitrogen atmosphere prior to use. All glassware was oven-dried at 120 ºC for at least 24 h, assembled while hot, and cooled under high vacuum prior to use. Cyclopropylacetylene, ^{n}BuLi, *N*,*N*′-dicyclohexylcarbodiimide and *N*,*N*′-diisopropylcarbodiimide were purchased from Aldrich. The starting marerials, $LnCl_3$ [186], $Li[Ph_2P(NSiMe_3)_2]$ [120, 121] and $[(COT)Ln(\mu\text{-}Cl)(THF)_2]_2$ [38] were prepared according to the literature methods. ^{1}H NMR (400 MHz) and ^{13}C NMR (100.6 MHz) spectra were recorded in THF-d_8, C_6D_6, toluene-d_8 or $(CD_3)_2SO$ solutions on a Bruker DPX 400 spectrometer at 25 ºC. Chemical shifts were referenced to TMS. IR spectra were recorded using KBr pellets on a Perkin Elmer FT-IR Spectrometer System 2000 between 4000 cm^{-1} and 400 cm^{-1}. Microanalyses of the compounds were performed using a Leco CHNS 923 apparatus.

Li[*c*-C_3H_5-C≡C-C(N^{i}Pr)$_2$]·THF (1a)

A diethyl ether (80 ml) solution of cyclopropylacetylene (4.2 ml, 50 mmol) in a Schlenk flask (250 ml) was cooled to –20 ºC and treated slowly with *n*-butyllithium (31.3 ml, 1.6 M solution in *n*-hexane). After 15 min, *N*,*N*′-diisopropylcarbodiimide (7.8 ml, 50 mmol) was added and the mixture was stirred for 10 min at –20 ºC. The solution was warmed to room temperature and stirred for 1h, and then concentrated under vacuum to a small volume (20 ml) and stored at –25 ºC in a freezer to obtain single-crystals of **1a**. Yield: 10.6 g, 78%. Elemental analysis for $C_{16}H_{27}LiN_2O$ (270.34 g·mol^{-1}): C, 71.09; H, 10.07; N, 10.36; found C, 70.78; H, 10.26; N, 11.14%. ^{1}H NMR (400 MHz, THF-d_8, 25 ºC): δ (ppm) 3.37 – 3.45 (m, 2H, C*H*, ^{i}Pr), 3.22 – 3.29 (m, 4H, THF), 1.37 – 1.45 (m, 4H, THF), 0.81 – 1.04 (m, 1H, C*H*, *c*-C_3H_5), 0.64 (d, 12H, CH_3, ^{i}Pr), 0.34 – 0.49 (m, 2H, CH_2, *c*-C_3H_5), 0.28 – 0.32 (m, 2H, CH_2, *c*-C_3H_5). ^{13}C NMR (100.6 MHz, THF-d_8, 25 ºC): δ (ppm) 157.0 (N*C*N), 97.1 (CH–*C*≡C), 69.0 (C≡*C*–C), 86.1 (THF), 49.8 (*C*H, ^{i}Pr), 26.8 (*C*H$_3$, ^{i}Pr), 26.3 (THF), 8.9 (*C*H$_2$, *c*-C_3H_5), 0.4 (*C*H, *c*-C_3H_5). MS (EI, M = 270.23): *m/z* (%) 191.2 (7) [M – {Li(THF)}]$^+$, 149.2 (12) [M – {Li(THF) + *c*-C_3H_5}]$^+$, 72.1 (100) [THF]$^+$. IR (KBr): ν (cm^{-1}) 3677 (w), 3209 (w), 3097 (m), 3016 (s), 2961 (vs), 2865 (s), 2609 (s), 2216 (s, C≡C), 1593 (s, NCN), 1385 (s), 1332 (m), 1170 (m), 1134

(s), 1052 (m), 964 (s), 918 (m), 871 (w), 840 (w), 812 (m), 729 (w), 716 (s), 687 (m), 663 (w), 529 (m), 507 (s), 436 (m).

Li[*c*-C_3H_5-C≡C-C(N^{i}Pr)$_2$]·Et_2O (1b)

Cyclopropylacetylene (4.2 ml, 50 mmol) was added to a Schlenk flask containing diethyl ether (80 ml) and the solution was cooled to –20 ºC, and *N,N'*-dicyclohexylcarbodiimide was added following the procedure for **1a**. The solvent was completely removed under vacuum to give a white precipitate, which was recrystallized from THF (30 ml) by storing in a freezer at –25 ºC to afford single crystals of **1b**. Yield: 10.2 g, 75%. Elemental analysis for $C_{16}H_{29}LiN_2O$ (272.36 g·mol^{-1}): C, 70.56; H, 10.73; N, 10.29; found C, 70.14; H, 9.33; N, 9.9%. ^{1}H NMR (400 MHz, THF-d_8, 25 ºC): δ (ppm) 3.74 – 3.81 (sept, 2H, C*H*, ^{i}Pr), 1.35 (sept, 1H, C*H*, *c*-C_3H_5), 0.99 (d, 12H, CH_3, ^{i}Pr), 0.76 – 0.81 (m, 2H, CH_2, *c*-C_3H_5), 0.62 – 0.66 (m, 2H, CH_2, *c*-C_3H_5). ^{13}C NMR (100.6 MHz, THF-d_8, 25 ºC): δ (ppm) 157.3 (N*C*N), 97.4 (CH–*C*≡C), 69.1 (C≡*C*–C), 50.0 (*C*H, ^{i}Pr), 26.9(*C*H_3, ^{i}Pr), 9.0 (*C*H_2, *c*-C_3H_5), 0.4 (*C*H, *c*-C_3H_5). MS (EI, M = 272.24): *m/z* (%) 271.29 (4) [M]$^+$, 191.22 (17) [M – Li(Et$_2$O)]$^+$. IR (KBr): ν (cm^{-1}) 3678 (w), 3337 (w), 3204 (w), 3095 (m), 3015 (m), 2963 (vs), 2866 (s), 2607 (m), 2217 (s, C≡C), 1989 (w), 1865 (w), 1592 (m, NCN), 1497 (s), 1385 (s), 1334 (m), 1263 (m), 1169 (s), 1132 (s), 1091 (m), 1028 (m), 965 (s), 871 (w), 840 (m), 811 (m), 729 (m), 715 (m), 694 (m), 663 (w), 531 (m), 439 (w), 407 (w).

Li[*c*-C_3H_5-C≡C-C(N^{i}Pr)$_2$]·DME (1c)

The compound was prepared by following the procedure described for **1a**. The solvent was completely removed under vacuum to give a white precipitate, which was recrystallized from 30 ml of DME by storing in a freezer at 5 ºC to obtain single-crystals of **1c**. Yield: 10.3 g, 72%. Elemental analysis for $C_{16}H_{29}LiN_2O_2$ (288.35 g·mol^{-1}): C, 66.64; H, 10.14; N, 9.71; found C, 66.28; H, 9.66; N, 9.67%. ^{1}H NMR (400 MHz, THF-d_8, 25 ºC): δ (ppm) 4.46 – 4.52 (m, 2H, C*H*, ^{i}Pr), 4.14 (s, DME), 3.98 (s, DME), 2.09 (sept, 1H, C*H*, *c*-C_3H_5), 1.71 (d, 12H, CH_3, ^{i}Pr), 1.51 – 1.53 (m, 2H, CH_2, *c*-C_3H_5), 1.36 – 1.42 (m, 2H, CH_2, *c*-C_3H_5). ^{13}C NMR (100.6 MHz, THF-d_8, 25 ºC): δ (ppm) 157.2 (N*C*N), 97.1 (CH–*C*≡C), 72.7 (*C*H_3, DME), 69.1 (C≡*C*–C), 58.2 (*C*H_2, DME),

49.9 (*C*H, ^{i}Pr), 26.9 (*C*H$_3$, ^{i}Pr), 9.0 (*C*H$_2$, *c*-C$_3$H$_5$), 0.4 (*C*H, *c*-C$_3$H$_5$). MS (EI, M = 288.24): *m/z* (%) 191.22 (9) [M – {Li(DME)}]$^+$, 92.1 (100) [DME]$^+$. IR (KBr): ν (cm^{-1}) 3677 (w), 3440 (w), 3320 (w), 3096 (w), 3016 (m), 2958 (vs), 2864 (s), 2699 (w), 2611 (w), 2475 (w), 2214 (s, C≡C), 2076 (w), 1991 (w), 1866 (w), 1780 (w), 1644 (m, NCN), 1596 (m), 1494 (vs), 1383 (m), 1353 (m), 1327 (s), 1284 (w), 1192 (m), 1168 (m), 1133 (s), 1120 (m), 1080 (s), 1050 (m), 1027 (m), 964 (s), 918 (m), 871 (w), 840 (w), 811 (m), 717 (m), 687 (w), 528 (m), 503 (m), 427 (m).

Li[*c*-C$_3$H$_5$-C≡C-C(NCy)$_2$]·THF (2a)

A solution of cyclopropylacetylene (4.2 ml, 50 mmol) in THF (90 ml) in a Schlenk flask (250 ml) was cooled to –20 ºC, and treated slowly with *n*-butyllithium (31.3 ml, 1.6 M solution in *n*-hexane). After 15 min, *N,N'*-dicyclohexylcarbodiimide (10.3 g, 50 mmol) was added and the mixture was stirred for 10 min at –20 ºC. The solution was warmed to room temperature and stirred for 1 h. The solution was reduced to a small volume (25 ml) under vacuum and stored at –25 ºC in a freezer to obtain single-crystals of **2a**. Yield: 4.1 g, 80%. Elemental analysis for $C_{22}H_{35}LiN_2O$ (350.47 g·mol^{-1}): C, 75.4; H, 10.07; N, 7.99; found C, 74.5; H, 10.33; N, 7.77%. ^{1}H NMR (400 MHz, THF-*d*$_8$, 25 ºC): δ (ppm) 3.56 (t, 4H, THF), 3.27 – 3.33 (m, 2H, C*H*, Cy), 1.72 (m, 4H, THF), 1.01 – 1.67 (m, 18H, C*H*$_2$, Cy), 1.27 – 1.35 (m, 1H, C*H*, *c*-C$_3$H$_5$), 0.74 – 0.80 (m, 2H, C*H*$_2$, *c*-C$_3$H$_5$), 0.57 – 0.63 (m, 2H, C*H*$_2$, *c*-C$_3$H$_5$). ^{13}C NMR (100.6 MHz, THF-*d*$_8$, 25 ºC): δ (ppm) 157.2 (N*C*N), 96.9 (CH–*C*≡C), 69.3 (C≡*C*–C), 86.1 (THF), 59.2 (*C*H, Cy), 37.8 (*C*H$_2$, Cy), 27-27.1 (*C*H$_2$, Cy), 26.3 (THF), 9.1 (*C*H$_2$, *c*-C$_3$H$_5$), 0.4 (*C*H, *c*-C$_3$H$_5$). MS (EI, M = 350.29): *m/z* (%) 272.4 (12) [M – {Li(THF)}]$^+$, 229.3 (18) [M – {Li(THF)+(*c*-C$_3$H$_5$)}]$^+$, 72.1 (100) [THF]$^+$. IR (KBr): ν (cm^{-1}) 3677 (w), 3438 (w), 3090 (m), 3010 (m), 2925 (vs), 2849 (vs), 2659 (w), 2589 (w), 2219 (s, C≡C), 1951 (w), 1599 (s, NCN), 1501 (vs), 1447 (s), 1425 (m), 1358 (s), 1341 (s), 1306 (m), 1254 (m), 1241 (m), 1181 (m), 1068 (s), 1056 (s), 1029 (m), 969 (vs), 918 (m), 898 (s), 887 (s), 857 (m), 842 (m), 812 (m), 796 (w), 785 (w), 713 (s), 672 (m), 544 (w), 497 (m), 476 (w), 451 (w), 433 (w), 403 (w), 417 (w).

Li[*c*-C$_3$H$_5$-C≡C-C(NCy)$_2$]·Et$_2$O (2b)

Cyclopropylacetylene (4.2 ml, 50 mmol) was dissolved in diethyl ether (80 ml) and the solution was cooled to –32 ºC. The reaction with *N,N'*-dicyclohexylcarbodiimide was carried

out by following the procedure described for **2a**. The solvent was completely removed under vacuum to give a white precipitate, which was recrystallized from 40 ml of THF by storing in a freezer at −25 ºC to obtain single-crystals of **2b**. Yield: 14.4 g, 82%. Elemental analysis for $C_{22}H_{37}LiN_2O$ (352.48 g·mol^{-1}): C, 74.96; H, 10.58; N, 7.95; found C, 73.96; H, 10.23; N, 8.66. ^{1}H NMR (400 MHz, C_6D_6, 25 ºC): δ (ppm) 3.66 – 3.99 (m, 2H, C*H*, Cy), 3.21 – 3.26 (q, 4H, C*H*$_2$, Et_2O), 0.94 – 2.27 (m, 18H, C*H*$_2$, Cy), 1.09 (t, 6H, C*H*$_3$, Et_2O) 0.82 – 0.89 (m, 1H, C*H*, *c*-C_3H_5), 0.68 (s, br, 2H, C*H*$_2$, *c*-C_3H_5), 0.41 (s, br, 2H, C*H*$_2$, *c*-C_3H_5); ^{13}C NMR (100.6 MHz, C_6D_6, 25 ºC): δ (ppm) 160.1 (N*C*N), 99.2 (CH–*C*≡C), 68.6 (C≡*C*–C), 65.9 (Et_2O), 59.3 (*C*H, Cy), 34.9 – 38.5 (*C*H$_2$, Cy), 26.6 -27.2 (*C*H$_2$, Cy), 15.2 (Et_2O), 9.3 (*C*H$_2$, *c*-C_3H_5), 0.4 (*C*H, *c*-C_3H_5). MS (EI, M = 352.31): *m/z* (%) 272.3 (73) [M – {Li(Et_2O)}]$^+$, 229.3 (100) [M – {Li(Et_2O)-*c*-C_3H_5}]$^+$. IR (KBr): ν (cm^{-1}) 3678 (w), 3439 (w), 3092 (w), 3012 (m), 2934 (vs), 2850 (s), 2665 (w), 2593 (w), 2220 (s, C≡C), 2074 (w), 1948 (w), 1890 (w), 1819 (w), 1598 (m, NCN), 1495 (vs), 1465 (s), 1448 (s), 1390 (s), 1361 (s), 1342 (s), 1309 (m), 1256 (m), 1242 (m), 1188 (w), 1160 (s), 1116 (m), 1089 (w), 1067 (s), 1027 (m), 971 (vs), 921 (w), 900 (m), 858 (m), 809 (m), 728 (m), 684 (m), 594 (m), 499 (m), 440 (m).

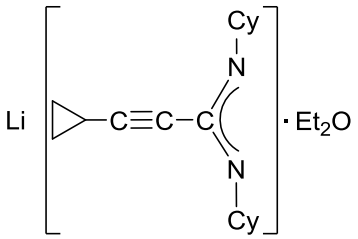

Li[*c*-C_3H_5-C≡C-C(NCy)$_2$]·DME (2c)

The compound was made by following the procedure for **2a**. The solvent was completely removed under vacuum to give a white precipitate, which was recrystallized from 30 ml of DME by storing in a freezer at −25 ºC to obtain single-crystals of **2c**. Yield: 16.1 g, 87%. Elemental analysis for $C_{22}H_{37}LiN_2O_2$ (368.49 g·mol^{-1}): C, 71.71; H, 10.12; N, 7.60; found C, 71.02; H, 9.88; N, 7.51. ^{1}H NMR (400 MHz, THF-d_8, 25 ºC): δ (ppm) 3.49 (s, DME), 3.37 – 3.44 (m, 2H, C*H*, Cy), 3.32 (s, DME), 1.12 – 1.79 (m, 18H, C*H*$_2$, Cy), 1.38 – 1.45 (m, 1H, C*H*, *c*-C_3H_5), 0.89 – 0.95 (m, 2H, C*H*$_2$, *c*-C_3H_5), 0.85 – 0.88 (m, 2H, C*H*$_2$, *c*-C_3H_5); ^{13}C NMR (100.6 MHz, THF-d_8, 25 ºC): δ (ppm) 157 (N*C*N), 96.8 (CH–*C*≡C), 72.7 (*C*H$_3$–DME), 69.4 (C≡*C*–C), 59.0 (*C*H, Cy), 58.8 (*C*H$_2$, DME), 38.0 (*C*H$_2$, Cy), 27.2 (*C*H$_2$, Cy), 9.1 (*C*H$_2$, *c*-C_3H_5), 0.4 (*C*H, *c*-C_3H_5). MS (EI, M = 368.30): *m/z* (%) 272.3 (65) [M – {Li(DME)}]$^+$, 229.2 (100) [M – {Li(DME) + *c*-C_3H_5 }]$^+$, 92.1 (73) [DME]$^+$. IR (KBr): ν (cm^{-1}) 3094 (w), 3015 (m), 2924 (vs), 2850 (s), 2662 (w), 2591 (w), 2224 (s, C≡C), 1605 (s, NCN), 1495 (vs), 1450 (s), 1361 (s), 1343 (m),

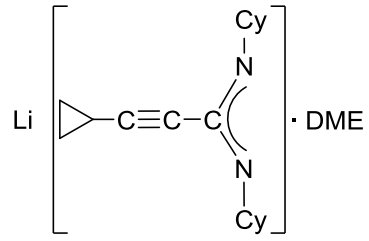

1306 (m), 1257 (m), 1239 (m), 1182 (m), 1161 (m), 1116 (m), 1070 (s), 1029 (m), 971 (m), 920 (w), 888 (m), 858 (m), 811 (w), 717 (m), 681 (m), 592 (m), 546 (w), 501 (m), 438 (w).

Li[Ph-C≡C-C(NCy)$_2$]·THF (3a)

A solution of phenylacetylene (3.30 ml, 30 mmol) in THF (80 ml) was cooled to –20 ºC and treated slowly with *n*-butyllithium (18.85 ml, 1.6 M solution in *n*-hexane). The solution was stirred for 15 min, before the *N,N'*-dicyclohexylcarbodiimide (6.20 g, 30 mmol) was added. The reaction mixture was stirred for 10 min at –20 ºC, and then warmed to room temperature and stirred for another 2 h. The solution was reduced to a small volume under vacuum (25 ml) and stored at –25 ºC in a freezer to obtain single-crystals of **3a**. Yield: 10.20 g, 88%. Elemental analysis for $C_{25}H_{35}LiN_2O$ (386.51 g·mol^{-1}): C, 77.69; H, 9.13; N, 7.25; found C, 77.15; H, 9.33; N, 7.08. ^{1}H NMR (400 MHz, toluene-d_8, 25 ºC): δ (ppm) 7.52 (d, J = 6.6 Hz, 2H, C_6H_5), 6.99 (m, 3H, C_6H_5), 3.96 (m, 2H, C*H*, Cy), 3.65 (m, 4H, THF), 1.44 (m, 4H, THF), 1.31 – 2.12 (m, 20H, CH_2, Cy); ^{13}C NMR (100.6 MHz, toluene -d_8, 25 ºC): δ (ppm) 159.3 (N*C*N), 158.5 (C≡*C*–C), 132.2 (C_6H_5), 123.8 (C_6H_5), 94.4 (C_6H_5), 82.4 (C_6H_5–*C*≡C), 68.2 (THF), 59.8 (*C*H, Cy), 37.6 (*C*H$_2$, Cy), 26.8 (*C*H$_2$, Cy), 25.6 (THF), 23.0 (*C*H$_2$, Cy). IR (KBr): ν (cm^{-1}) 3678 (w), 3438 (w), 3222 (m), 3081 (m), 3033 (m), 2926 (vs), 2852 (s), 2691 (w), 2663 (w), 2587 (w), 2363 (w), 2217 (m, C≡C), 1941 (w), 1891 (w), 1799 (w), 1635 (m), 1610 (vs, NCN), 1492 (vs), 1446 (m), 1388 (m),1360 (m), 1343 (m), 1311 (m), 1282 (m), 1213 (m), 1181 (m), 1156 (m), 1125 (m), 1101 (m), 1069 (m), 1027 (m), 912 (w), 889 (m), 843 (w), 797 (w), 755 (m), 709 (w), 690 (m), 639 (w), 616 (w), 555 (w), 527 (w), 448 (w), 428 (w).

Li[Ph-C≡C-C(NCy)$_2$]·Et$_2$O (3b)

The compound was prepared by following the procedure for **3a** using diethyl ether as solvent. The solvent was removed under vacuum affording **3b** as white solid. Yield: 8.85 g, 76%. Elemental analysis for $C_{25}H_{37}LiN_2O$ (388.52 g·mol^{-1}): C, 77.29; H, 9.60; N, 7.21; found C, 76.06; H, 9.52; N, 7.60. ^{1}H NMR (400 MHz, C_6D_6, 25 ºC): δ (ppm) 7.56 (d, J = 6.8 Hz, 2H, Ph), 6.95 (m, 3H, Ph), 4.01(s, br, 2H, C*H*, Cy), 3.25 (q, 4H, CH_2, Et$_2$O), 2.40 (m, 4H, CH_2, Cy), 1.93 (m, 6H, CH_2, Cy), 1.24 – 1.80 (m, 10H, CH_2, Cy), 1.15 (t, 6H, CH_3, Et$_2$O); ^{13}C NMR (100.6 MHz, C_6D_6, 25 ºC): δ (ppm) 132.3 (Ph), 123.8 (Ph), 94.3 (Ph), 83.1 (Ph–*C*≡C), 65.9 (Et$_2$O), 59.9

(*C*H, Cy), 37.7 (*C*H$_2$, Cy), 26.9 (*C*H$_2$, Cy), 26.5 (*C*H$_2$, Cy), 15.3 (Et$_2$O). IR (KBr): ν (cm^{-1}) 3676 (w), 3369 (w), 3213 (w), 3059 (m), 2961 (vs), 2865 (s), 2705 (w), 2610 (m), 2360 (w), 2211 (w, C≡C), 2126 (w), 1948 (w), 1879 (w), 1752 (w), 1592 (s, NCN), 1504 (vs), 1442 (s), 1372 (s), 1352 (s), 1323 (vs), 1226 (m), 1175 (s), 1133 (s), 1069 (m), 1051 (s), 1031 (s), 998 (m), 946 (m), 913 (s), 849 (m), 821 (m), 755 (vs), 714 (m), 690 (vs), 630 (w), 543 (m), 528 (s), 515 (m), 476 (w), 453 (w), 435 (w).

Li[^{n}Bu-C(=NCy)(NCy)C(NCy)$_2$]·THF (4)

A solution of *N*,*N*′-dicyclohexylcarbodiimide (10.30 g, 50 mmol) in 100 ml of THF at –20 °C was treated slowly with *n*-butyllithium (16 ml, 1.6 M solution in *n*-hexane). The reaction

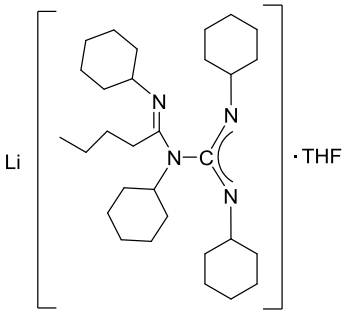

mixture was stirred for 10 min at –20 °C then warmed to room temperature and stirred over night to give a white suspension in THF. The solvent was removed under vacuum affording **4** as white solid. Yield: 16.4 g, 60%. Elemental analysis for $C_{34}H_{61}LiN_4O$ (548.83 g·mol^{-1}): C, 74.41; H, 11.20; N, 10.21; found C, 74.82; H, 10.85; N, 10.50. ^{1}H NMR (400 MHz, $(CD_3)_2SO$, 25 ºC): δ (ppm) 3.84 (m, 1H, C*H*, Cy), 3.60 (m, 4H, THF), 3.43 (m, 1H, C*H*, Cy), 3.04 – 3.18 (m, 2H, C*H*, Cy), 2.66 (m, 1H, C*H*$_2$, ^{n}Bu), 2.33 (m, 1H, C*H*$_2$, ^{n}Bu), 2.09 (m, 2H, C*H*$_2$, ^{n}Bu), 1.84 (m, 2H, C*H*$_2$, ^{n}Bu), 1.76 (m, 4H, THF), 1.65 (m, 8H, C*H*$_2$, Cy), 1.52 (m, 6H, C*H*$_2$, Cy), 1.26 (m, 26H, C*H*$_2$, Cy), 0.85 (m, 3H, C*H*$_3$, ^{n}Bu); ^{13}C NMR (100.6 MHz, C_6D_6, 25 ºC): δ (ppm) 155.3 (N*C*N), 145.1 (N*C*N), 67.0 (THF), 55.4 (*C*H, Cy), 54.2 (*C*H, Cy), 49.3(*C*H, Cy), 35.7 (*C*H$_2$, Cy), 35.1 (*C*H$_2$, Cy), 34.8 (*C*H$_2$, Cy), 34.5 (*C*H$_2$, ^{n}Bu), 30.7 (*C*H$_2$, ^{n}Bu), 29.5 (*C*H$_2$, ^{n}Bu), 25.8 (THF), 24.9 (*C*H$_2$, Cy), 22.6 (*C*H$_2$, Cy), 22.1 (*C*H$_2$, Cy), 13.8 (*C*H$_3$). MS (EI, M = 548.50): *m/z* (%) 125.2 (27) [Cy + C_3H_6]$^+$, 153.2 (88) [2Cy – Me]$^{2+}$, 183.3 (20) [2Cy + Me]$^{2+}$, 207.3 (12) [C(NCy)$_2$]$^+$, 222.3 (62) [C(NCy)$_2$ + Me]$^{2+}$, 235.4 (100) [C(NCy)$_2$ + C_2H_5], 264.4 (55) [^{n}Bu + C(NCy)$_2$]$^+$. IR (KBr): ν (cm^{-1}) 3449 (w), 3327 (w), 3225 (w), 2927 (vs), 2853 (s), 2666 (w), 2533 (w), 2354 (w), 2120 (w), 1959 (w), 1645 (m), 1578 (w), 1516 (m), 14450 (m), 1367 (w), 1339 (m), 1155 (w), 1128 (m), 1105 (w), 1053 (w), 1029 (w), 988 (w), 919 (w), 889 (w), 845 (w), 804 (w), 748 (w), 695 (w), 657 (w), 640 (w), 555 (w), 502 (w), 454 (w).

[{*c*-C_3H_5-C≡C-C(N^{i}Pr)$_2$}$_2$Ce(*μ*-Cl)(THF)]$_2$ (5)

A solution of anhydrous $CeCl_3$ (1.0 g, 4.1 mmol) in 30 ml of THF was added to a solution of **1a** (1.6 g, 8.2 mmol) in 70 ml of THF. The reaction mixture was heated to 65 ºC for 2 h and stirred at room temperature for 12 h. The solution color changed to yellow. The solvent was removed under vacuum followed by extraction with *n*-pentane (30 ml) to give a clear, bright yellow solution. The filtrate was concentrated under vacuum to ca. 10 ml. Crystallization at –30 ºC afforded **5** in the form of bright yellow, needle-like crystals. Yield: 1.6 g, 62%. Elemental analysis for $C_{56}H_{92}Ce_2Cl_2N_8O_2$ (1260.52 g·mol^{-1}): C, 53.31; H, 7.29; N, 8.88; found C, 53.29; H, 7.11; N, 8.79%. ^{1}H NMR (400 MHz, C_6D_6, 25 ºC): δ (ppm) 11.88 (m, 8H, C*H*(CH$_3$)$_2$), 3.42 (m, 4H, C*H*, *c*-C_3H_5), 2.67 (m, 8H, C*H*$_2$, *c*-C_3H_5), 1.75 (m, 8H, C*H*$_2$, *c*-C_3H_5), – 2.98 (s, br, 48H, C*H*$_3$) (THF signals not observed); ^{13}C{^{1}H} NMR (100.6 MHz, C_6D_6, 25 ºC): δ (ppm) 171.8 (N*C*N), 110.2 (C≡*C*-C), 79.1 (HC-*C*≡C) 55.6 (*C*H(CH$_3$)$_2$), 22.9 (CH(*C*H$_3$)$_2$), 11.3 (*C*H$_2$, *c*-C_3H_5), 3.0 (*C*H, *c*-C_3H_5) (THF signals not observed). IR (KBr): ν (cm^{-1}) 3852 (w), 3440 (w), 3282 (w), 3095 (w), 2963 (vs), 2867 (s), 2608 (w), 2221 (vs, C≡C), 1613 (s, C=N), 1465 (s), 1330 (m), 1182 (m), 966 (s), 812 (m), 688 (m), 527 (w).

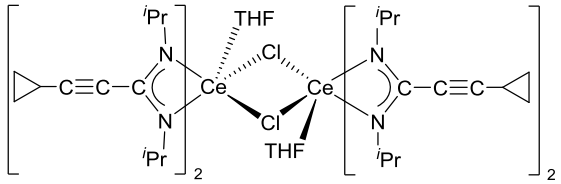

[{*c*-C_3H_5-C≡C-C(NCy)$_2$}$_2$Ce(*μ*-Cl)(THF)]$_2$ (6)

A solution of anhydrous $CeCl_3$ (1.0 g, 4.1 mmol) in 30 ml of THF was added to a solution of **2a** (2.3 g, 8.2 mmol) in 60 ml of THF following the procedure given for **5**. Crystallization at –30 ºC afforded **6** in the form of bright yellow, needle-like crystals. Yield: 1.7 g, 55%. Elemental analysis for $C_{80}H_{124}Ce_2Cl_2N_8O_2$ (1581.01 g·mol^{-1}): C, 60.72; H, 7.84; N, 7.08; found C, 60.86; H, 7.72; N, 7.53%. ^{1}H NMR (400 MHz, THF-d_8, 25 ºC): δ (ppm) 12.78 (m, 8H, C*H*, Cy), 4.02 (m, 4H, C*H*, *c*-C_3H_5), 3.58 (m, 8H, THF), 3.22 (m, 8H, C*H*$_2$, *c*-C_3H_5), 2.53 (m, br, 8H, C*H*$_2$, *c*-C_3H_5), 1.86 – 2.21 (m, 24H, C*H*$_2$, Cy), 1.71 – 1.80 (m, 8H, THF), 0.96 – 1.45 (m, 24H, C*H*$_2$, Cy), 0.86 – 0.97 (m, 8H, C*H*$_2$, Cy), – 0.54 (m, 8H, C*H*$_2$, Cy), – 3.02 (m, 16H, C*H*$_2$, Cy); ^{13}C{^{1}H} NMR (100.6 MHz, THF-d_8, 25 ºC): δ (ppm) 134.6 (N*C*N), 115.6 (C≡*C*-C), 71.5 (HC-*C*≡C), 68.1 (THF) 55.8 (*C*H, Cy), 37.2 (*C*H$_2$, Cy), 26.9 (*C*H$_2$, Cy), 26.5 (THF), 26.3 (*C*H$_2$, Cy), 11.5 (*C*H$_2$, *c*-C_3H_5), 3.8 (*C*H, *c*-C_3H_5). IR (KBr): ν (cm^{-1}) 3677 (s), 3438 (m), 2928

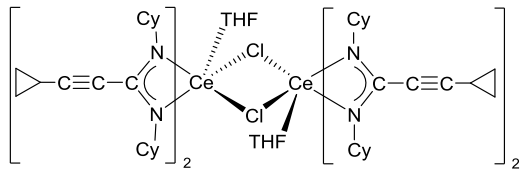

(vs), 2852 (vs), 2226 (s, C≡C), 1607 (vs, C=N), 1482 (m), 1390 (w), 1365 (w), 1254 (s), 1157 (w), 956 (s), 889 (s), 685 (m), 599 (w), 464 (w).

[{*c*-C_3H_5-C≡C-C(NCy)$_2$}$_2$Nd(*μ*-Cl)(THF)]$_2$ (7)

A 250 ml Schlenk flask was charged with anhydrous $NdCl_3$ (1.0 g, 4 mmol) and **2a** (2.2 g, 8 mmol). The reaction mixture in 100 ml THF was heated to 65 ºC for 3 h. The solution color changed to pale green. The solution was evaporated under vacuum followed by extraction with *n*-pentane (3 × 20 ml) to give a clear green solution. The filtrate was concentrated under vacuum to ca. 15 ml. Crystallization at –30 ºC afforded **7** in the form of deep green, needle-like crystals. Yield: 2.9 g, 85%. Elemental analysis for $C_{80}H_{124}Cl_2Nd_2N_8O_2$ (1589.25 g·mol^{-1}): C, 60.40; H, 7.80; N, 7.04; found C, 60.22; H, 7.30; N, 7.34%. ^{1}H NMR (400 MHz, C_6D_6, 25 ºC): δ (ppm) 21.84 (s, 8H, C*H*, Cy), 4.07 (m, 4H, C*H*, *c*-C_3H_5), 3.03 (m, 8H, CH_2, *c*-C_3H_5), 2.04 (m, 8H, CH_2, *c*-C_3H_5), 0.18 – 0.80 (m, 40H, CH_2, Cy), – 0.07 (m, 8H, CH_2, Cy), – 1.30 (m, 8H, CH_2, Cy), – 2.65 (m, 8H, CH_2, Cy), – 8.70 (m, 16H, CH_2, Cy) (THF signals not observed); ^{13}C{^{1}H} NMR (100.6 MHz, C_6D_6, 25 ºC): δ (ppm) 119.8 (N*C*N), 108.0 (C≡*C*-C), 74.1 (*C*H, Cy), 61.8 (HC-*C*≡C), 36.1 (*C*H$_2$, Cy), 26.3 (*C*H$_2$, Cy), 22.6 (*C*H$_2$, Cy), 12.2 (*C*H$_2$, *c*-C_3H_5), 2.6 (*C*H, *c*-C_3H_5) (THF signals not observed). IR (KBr): ν (cm^{-1}) 3438 (w), 3094 (w), 3012 (w), 2925 (vs), 2851 (vs), 2664 (w), 2221 (vs, C≡C), 1608 (m, C=N), 1473 (m), 1398 (m), 1362 (s), 1343 (m), 1307 (m), 1174 (s), 1120 (s), 973 (vs), 888 (m), 676 (s), 589 (s).

[*c*-C_3H_5-C≡C-C(NCy)$_2$]$_2$Ho(*μ*-Cl)$_2$Li(THF)(Et$_2$O) (8)

Anhydrous $HoCl_3$ (0.5 g, 1.8 mmol) and **2a** (1.0 g, 3.7 mmol) in 100 ml THF were charged into a 250 ml Schlenk flask. The reaction mixture was heated to 65 ºC for 3 h and stirred at room temperature for 12 h. The solvent was removed under vacuum followed by extraction with diethyl ether (2 × 20 ml) to give a clear, bright yellow solution. Crystallization at –30 ºC afforded **8** in the form of bright yellow, needle-like crystals. Yield: 1.3 g, 83%. Elemental analysis for $C_{44}H_{72}Cl_2HoLiN_4O_2$ (931.86 g·mol^{-1}): C, 56.71; H, 7.79; N, 6.01; found C, 56.79; H, 7.77; N, 6.11%. IR (KBr): ν (cm^{-1}) 3438 (w), 3279 (w),

3220 (w), 3010 (w), 2929 (vs), 2853 (s), 2227 (vs, C≡C), 1629 (m, C=N), 1593 (m), 1449 (vs), 1365 (m), 1254 (w), 974 (m), 690 (w).

[{*c*-C_3H_5-C≡C-C(NCy)$_2$}Li{*c*-C_3H_5-C≡C-C(NCy)$_2$}$_2$]Eu(*μ*-I)$_2$Li(THF)$_2$ (9)

A 250 ml Schlenk flask was charged with $EuI_2(THF)_2$ (1.1 g, 2 mmol) and **2a** (1.71 g, 6.1 mmol) in 60 ml of THF. The reaction mixture was stirred at room temperature over night. The

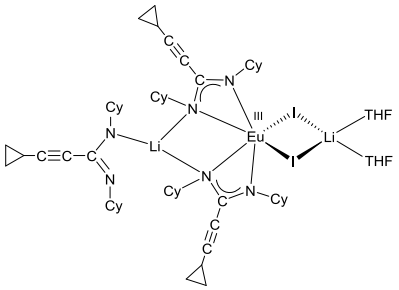

THF was removed under vacuum followed by extraction with 20 ml of *n*-pentane. Crystallization at 5 ºC afforded **9** in the form of bright yellow, needle-like crystals. Yield: 2.3 g, 85%. Elemental analysis for $C_{62}H_{97}EuI_2Li_2N_6O_2$ (1378.10 g·mol^{-1}): C, 53.98; H, 7.03; N, 6.09; found C, 52.86; H, 7.20; N, 6.30%. ^{1}H NMR (400 MHz, toluene-d_8, 25 ºC) δ (ppm) 6.33 – 3.75 (m, 60H, C*H*$_2$, Cy), – 1.75 (m, 6H, C*H*$_2$, *c*-C_3H_5), – 2.40 (m, 6H, C*H*$_2$, *c*-C_3H_5), – 3.18 (m, 3H, C*H*, *c*-C_3H_5), (THF signals has not observed). ^{13}C{^{1}H} NMR (100.6 MHz, C_6D_6, 25 ºC) δ (ppm) 30.2 (*C*H$_2$, Cy), 9.1 (*C*H$_2$, Cy), 4.6 (*C*H$_2$, *c*-C_3H_5), 0.1 (*C*H, *c*-C_3H_5). IR (KBr): ν (cm^{-1}) 3852 (m), 3438 (s), 3283 (m), 3092 (m), 3011 (m), 2928 (vs), 2853 (vs), 2666 (w), 2530 (w), 2227 (s, C≡C), 1959 (w), 1610 (vs, C=N), 1479 (m), 1449 (m), 1384 (w), 1363 (m), 1303 (m), 1253 (m), 1243 (m), 1180 (m), 1154 (w), 1120 (w), 1107 (w), 1074 (w), 1051 (w), 1029 (w), 974 (m), 957 (w), 890 (w), 861 (w), 811 (w), 747 (w), 701 (w), 668 (w), 626 (w), 588 (w), 554 (w), 503 (w), 465 (w).

[Ph$_2$P(NSiMe$_3$)$_2$]$_2$Ce(*μ*-Cl)$_2$Li(THF)$_2$ (10)

A solution of anhydrous $CeCl_3$ (1.0 g, 4.1 mmol) in 30 ml of THF was added to a solution of Li[Ph$_2$P(NSiMe$_3$)$_2$] (3 g, 8.2 mmol) in 60 ml of THF. The reaction mixture was stirred over

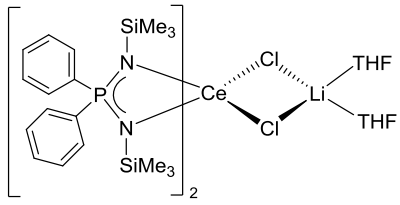

night at room temperature. The solution color changed to golden yellow. The solvent was removed under vacuum followed by extraction with *n*-pentane (30 ml) to give a clear, bright yellow solution. The filtrate was concentrated under vacuum to ca. 10 ml. Crystallization at 5 ºC afforded **10** in the form of bright yellow, blok-like crystals. Yield: 3.4 g, 78%. Elemental analysis for $C_{44}H_{72}CeCl_2LiN_4O_2P_2Si_4$ (1081.32 g·mol^{-1}): C, 48.82; H, 6.65; N, 5.17; found C, 42.10; H, 6.70; N, 5.30%. ^{1}H NMR (400 MHz, THF-d_8, 25 ºC): δ (ppm) 10.22 (m, 8H, C_6H_5), 9.50 (s, br, 4H, C_6H_5), 7.70 (m, 8H, C_6H_5), 1.44 (m, 8H, THF) – 4.80 (s, br, 3H, Si(C*H*$_3$)$_3$), –5.83 (s, br, 33H, Si(C*H*$_3$)$_3$); ^{13}C{^{1}H} NMR (100.6 MHz, THF-d_8, 25 ºC): δ (ppm) 144.0 (C_6H_5), 133.2

(C_6H_5), 132.5(C_6H_5), 131.2 (C_6H_5), 64.7 (THF), 24.1 (THF), – 1.3 (Si(CH_3)$_3$); ^{29}Si NMR (80 MHz, THF-d_8, 25 ºC): δ (ppm) – 13.90 (Si(CH_3)$_3$), – 21.24 (Si(CH_3)$_3$); ^{31}P NMR (162 MHz, THF-d_8, 25 ºC): δ (ppm) – 4.94. IR (KBr): ν (cm^{-1}) 3380 (m), 3222 (m), 3075 (s), 2952 (vs), 2897 (s), 2541 (w), 2029 (w), 1959 (w), 1821 (w), 1776 (w), 1638 (s), 1591 (m), 1437 (s), 1306 (s), 1246 (vs), 1154 (m), 1116 (m), 1044 (w), 1028 (w), 998 (m), 933 (m), 841 (s), 776 (m), 748 (s), 695 (s), 661 (w), 576 (w), 555 (w), 530 (s), 505 (m), 451 (w), 435 (w).

[^{n}Bu-C(=NCy)(NCy)C(NCy)$_2$]Ho[^{n}Bu-C(NCy)$_2$](μ-Cl)$_2$Li(THF)$_2$ (11)

A solution of anhydrous $HoCl_3$ (1.0 g, 3.6 mmol) in 50 ml THF was added to a stirred Et_2O solution (80 ml) of *in situ* prepared Li[^{n}Bu-C(=NCy)(NCy)C(NCy)$_2$] and Li[^{n}Bu-C(NCy)$_2$] (*N*,*N*′-dicyclohexylcarbodiimide (10.30 g, 50 mmol) in 80 ml of Et_2O at –20 °C was treated slowly with *n*-butyllithium (16 mL, 1.6 M solution in *n*-hexane)). The reaction mixture was stirred for 3 h at room temperature. The solvents were evaporated under vacuum, and the residue was extracted with 20 ml *n*-pentane. Concentration and cooling of the solution to 5 °C afforded **11** as yellow needle-like crystals. Yield: 2.8 g, 71%. Elemental analysis for $C_{55}H_{100}Cl_2HoLiN_6O_2$ (1120.22 g·mol^{-1}): C, 58.97; H, 9.00; N, 7.50; found C, 58.92; H, 8.98; N, 7.44%. IR (KBr): ν (cm^{-1}) 3321 (w), 3223 (w), 2929 (vs), 2857 (s), 2661 (w), 2525 (w), 2356 (w), 2118 (w), 1952 (w), 1577 (w), 1518 (m), 1367 (w), 1156 (w), 1129 (m), 1108 (w), 1085 (w), 1055 (w), 1045 (w), 983 (w), 922 (w), 892 (w), 865 (w), 820 (w), 715 (w), 657 (w), 643 (w), 553 (w), 505 (w), 456 (w).

[*c*-C_3H_5-C≡C-C(N^{i}Pr)$_2$]$_3$Nd (12)

A solution of anhydrous $NdCl_3$ (1.0 g, 4 mmol) in 30 ml of THF was added to a solution of **1a** (2.3 g, 12 mmol) dissolved in 70 ml of THF. The reaction mixture was heated to 65 ºC for 2 h and then stirred at r.t. over night, resulting in a blue solution. The solvent was evaporated under vacuum, and the residue was extracted with 30 ml *n*-pentane. The solvent was removed under vacuum affording **12** as green solid. Yield: 1.5 g, 54%. Elemental analysis for $C_{36}H_{57}NdN_6$ (718.12 g·mol^{-1}): C, 60.16; H, 7.93; N, 11.69; found C, 60.25; H, 7.92; N, 11.52%. ^{1}H NMR (400 MHz, C_6D_6, 25 ºC): δ (ppm) 22.3 (m, 6H, C*H*-(CH_3)$_2$), 4.10 (m, 3H, C*H*, *c*-C_3H_5), 2.97 (m, 6H, CH_2, *c*-C_3H_5), 2.02 (m, 6H, CH_2, *c*-C_3H_5), – 3.55 (m, 36H, CH_3);

$^{13}C\{^1H\}$ NMR (100.6 MHz, C_6D_6, 25 ºC): δ (ppm) 228.6 (N*C*N), 108.5 (C≡*C*-C), 65.3 (*C*H-$(CH_3)_2$), 59.8 (HC-*C*≡C), 23.1 (*C*H_3), 12.1 (*C*H_2, *c*-C_3H_5), 2.4 (*C*H, *c*-C_3H_5). MS (EI, M = 715.37): m/z (%) 631.6 (33) $[M - 2(^i Pr)]^+$, 396.4 (20) $[2(c\text{-}C_3H_5\text{-}C{\equiv}C\text{-}C(N^iPr)_2) + CH_3]^+$, 381.3 (15) $[2(c\text{-}C_3H_5\text{-}C{\equiv}C\text{-}C(N^iPr)_2)]^+$, 205.2 (50) $[(c\text{-}C_3H_5\text{-}C{\equiv}C\text{-}C(N^iPr)_2) + CH_3]^+$, 177.1 (34) $[c\text{-}C_3H_5\text{-}C{\equiv}C\text{-}C(N^iPr)_2 - CH_3]^+$, 149.1 (17) $[c\text{-}C_3H_5\text{-}C{\equiv}C\text{-}C(N^iPr)_2 - (c\text{-}C_3H_5)]^+$. IR (KBr): ν ($cm^{-1}$) 3678 (w), 3439 (w), 3220 (m), 3015 (m), 2963 (vs), 2867 (s), 2608 (w), 2220 (s, C≡C), 1865 (w), 1635 (m), 1591 (vs, NCN), 1498 (br), 1382 (m), 1332 (m), 1169 (m), 811 (w), 716 (w), 692 (w), 530 (w), 445 (w).

[*c*-C_3H_5-C≡C-C(N^iPr)$_2$]$_3$Sm (**13**)

A 250 ml Schlenk flask was charged with anhydrous $SmCl_3$ (1.0 g, 4 mmol) and **1a** (2.3 g, 12 mmol). Following the procedure described for **12**. The solvent was removed under vacuum affording **13** as yellow solid. Yield: 1.6 g, 55%. Elemental analysis for $C_{36}H_{57}N_6Sm$ (724.24 g·mol^{-1}): C, 59.70; H, 7.93; N, 11.60; found C, 59.80; H, 7.83, N, 11.55%. ^1H NMR (400 MHz, C_6D_6, 25 ºC): δ (ppm) 3.60 (m, 6H, C*H*-$(CH_3)_2$), 1.81 (m, 3H, C*H*, *c*-C_3H_5), 1.37 (m, 6H, CH_2, *c*-C_3H_5), 0.89 (m, 6H, CH_2, *c*-C_3H_5), – 0.47 (m, 36H, CH_3); $^{13}C\{^1H\}$ NMR (100.6 MHz, C_6D_6, 25 ºC): δ (ppm) 201.6 (N*C*N), 104.5 (C≡*C*-C), 73.5 (HC-*C*≡C), 48.3 (*C*H-$(CH_3)_2$), 25.1 (*C*H_3), 9.7 (*C*H_2, *c*-C_3H_5), 1.7 (*C*H, *c*-C_3H_5). MS (EI, M = 725.38): m/z (%) 726.4 (20) $[M]^+$, 710.5 (23) $[M - CH_3]^+$, 533.3 (10) $[M - c\text{-}C_3H_5\text{-}C{\equiv}C\text{-}C(N^iPr)_2]^+$, 343.1 (32) $[M - 2(c\text{-}C_3H_5\text{-}C{\equiv}C\text{-}C(N^iPr)_2)]$, 327.1 (22) $[M - 2(c\text{-}C_3H_5\text{-}C{\equiv}C\text{-}C(N^iPr)_2) - CH_3]^+$, 177.1 (58) $[c\text{-}C_3H_5\text{-}C{\equiv}CC(N^iPr)_2 - CH_3]^+$. IR (KBr): ν ($cm^{-1}$) 3653 (w), 3440 (w), 3096 (m), 3015 (w), 2963 (vs), 2866 (m), 2608 (w), 2221 (s, C≡C), 1612 (vs, NCN), 1466 (br), 1330 (s), 1263 (m), 1210 (m), 1185 (m), 1052 (w), 967 (s), 875 (w), 811 (m), 707 (m), 529 (w), 472 (w).

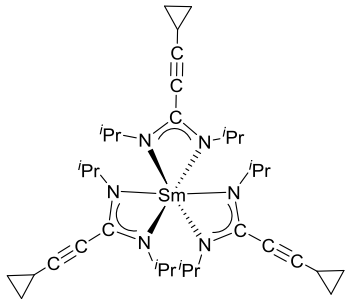

[*c*-C_3H_5-C≡C-C(NCy)$_2$]$_3$Sm (**14**)

Anhydrous $SmCl_3$ (1.0 g, 4 mmol) and **1b** (3.3 g, 12 mmol) were charged in a 250 ml Schlenk flask. 100 ml of THF were added and the reaction mixture was stirred over night at room temperature, resulting in a clear, yellow solution. The solvent was completely removed under vacuum to dryness followed by extraction with *n*-pentane (2 ×15 ml) to give a clear, yellow filtrate. Evaporation to dryness afforded **14** as a pale yellow solid. Yield: 3.0 g, 79%. Elemental analysis for $C_{54}H_{81}N_6Sm$ (964.62 g·mol^{-1}): C, 67.24; H, 8.46; N, 8.71; found C,

67.22; H, 8.51; N, 8.60%. ^{1}H NMR (400 MHz, C_6D_6, 25 ºC): δ (ppm) 3.34 (m, 6H, C*H*, Cy), 1.85 (m, 3H, C*H*, *c*-C_3H_5), 1.56 (m, br, 12H, CH_2, Cy), 1.40 (m, 6H, CH_2, *c*-C_3H_5), 0.97 – 1.32 (m, 18H, CH_2, Cy), 0.87 (m, 6H, CH_2, *c*-C_3H_5), 0.69 (br, 12H, CH_2, Cy), – 0.21 – – 0.12 (q, 6H, CH_2, Cy), – 2.31 (br, 12H, CH_2, Cy); ^{13}C{^{1}H} NMR (100.6 MHz, C_6D_6, 25 ºC): δ (ppm) 201.9 (N*C*N), 104.1 (C≡*C*-C), 73.7 (HC-*C*≡C), 56.9 (*C*H, Cy), 35.8 (*C*H_2, Cy), 25.5 (*C*H_2, Cy), 9.8 (*C*H_2, *c*-C_3H_5), 1.8 (*C*H, *c*-C_3H_5). MS (EI, M = 965.57): *m/z* (%) 965.7 (45) [M], 695.4 (70) [M – (*c*-C_3H_5-C≡C-C(NCy)$_2$)]$^+$, 272.2 (80) [*c*-C_3H_5-C≡C-C(NCy)$_2$]$^+$, 229.1 (58) [*c*-C_3H_5-C≡C-C(NCy)$_2$ – (*c*-C_3H_5)]$^+$, 190.1 (63) [*c*-C_3H_5-C≡C-C(NCy)$_2$ – (Cy)]$^+$, 177 (100) [*c*-C_3H_5-C≡C-C-NCy]$^+$. IR (KBr): ν (cm^{-1}) 3668 (w), 3438 (w), 3220 (w), 3012 (w), 2925 (vs), 2850 (s), 2665 (w), 2222 (m, C≡C), 1606 (m, NCN), 1469 (vs), 1398 (m), 1361 (s), 1174 (m), 1120 (m), 1028 (m), 972 (s), 888 (m), 703 (w), 676 (w), 588 (w).

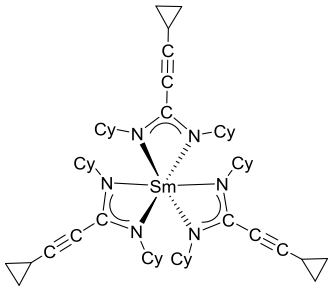

[*c*-C_3H_5-C≡C-C(N^{i}Pr)$_2$]$_3$Ho (**15**)

A solution of anhydrous $HoCl_3$ (1.0 g, 3.7 mmol) in 30 ml of THF was added to a solution of **1a** (2.2 g, 11.1 mmol) in 60 ml of THF. The reaction mixture was heated to 65 ºC for 3 h and then stirred over night. The solvent was removed under vacuum followed by extraction with *n*-pentane (2 × 15 ml) to give a clear, bright yellow solution. The filtrate was concentrated to ca. 5 ml. Crystallization at –32 ºC for afforded **15** as pale yellow crystals. Yield: 1.2 g, 45%. Elemental analysis for $C_{36}H_{57}HoN_6$ (738.81 g·mol^{-1}): C, 58.52; H, 7.78; N, 11.38; found C, 58.75; H, 7.33; N, 11.17%. Due to the strongly paramagnetic nature of the Ho^{3+} ion, the ^{1}H NMR resonances could not be assigned.^{13}C NMR (100.6 MHz, C_6D_6, 25 ºC): δ (ppm) 224.8 (N*C*N), 158.8 (C≡*C*-C), 62.7 (HC-*C*≡C), 50.4 (*C*H-(CH$_3$)$_2$), 29.8 (*C*H$_3$), 26.5 (*C*H$_3$), 8.7 (*C*H_2, *c*-C_3H_5), 0.35 (*C*H, *c*-C_3H_5). MS (EI, M = 738.39): *m/z* (%) 738.5 (35) [M], 723.5 (50) [M – CH$_3$]$^+$, 695.5 (32) [M – 2CH$_3$]$^+$, 547.3 (36) [M – *c*-C_3H_5-C≡C-C(N^{i}Pr)$_2$], 177.1 (100) [*c*-C_3H_5-C≡C-C(N^{i}Pr)$_2$ – CH$_3$]$^+$, 149.1 (43) [*c*-C_3H_5-C≡C-C(N^{i}Pr)$_2$ – (*c*-C_3H_5)]$^+$. IR (KBr): ν (cm^{-1}) 3440 (br), 3219 (m), 2964 (s), 2932 (m), 2869 (m), 2227 (m, C≡C), 1636 (m), 1612 (s, NCN), 1486 (m), 1375 (w), 1315 (w), 1260 (br), 1179 (w), 1031 (w), 984 (w), 879 (w), 812 (w), 505 (m), 468 (w).

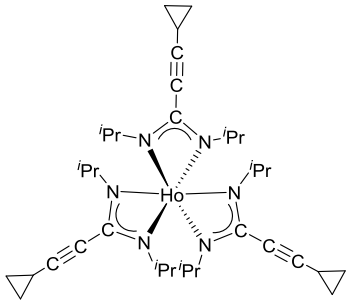

[Ph-C≡C-C(NCy)$_2$]$_3$Ce (16)

A solution of anhydrous $CeCl_3$ (1.0 g, 4 mmol) in 20 ml of THF was added to a solution of **3a** (4.6 g, 12 mmol) in 60 ml of THF. The reaction mixture was stirred over night at the room temperature. The solvent was removed under vacuum to dryness followed by extraction with *n*-pentane (3 × 10 ml) to give a clear, orange solution. The filtrate was evaporated under vacuum to afford **16** as yellow solid. Yield: 3.4 g, 81%. Elemental analysis for $C_{63}H_{81}CeN_6$ (1062.50 g·mol^{-1}): C, 71.22; H, 7.68; N, 7.91; found C, 71.36; H, 7.64; N, 7.90%. ^{1}H NMR (400 MHz, THF-d_8, 25 ºC): δ (ppm) 9.49 (s, br, 2H, C*H*, Cy), 8.81 (s, 3H, Ph), 7.83 – 8.05 (m, 6H, Ph), 7.29 – 7.56 (m, 6H, Ph), 3.76 (s, br, 2H, C*H*, Cy), 3.56 (m, 2H, C*H*, Cy), 0.93 – 2.12 (m, 50H, CH_2, Cy), – 0.05 (s, br, 4H, CH_2, Cy), – 1.82 (s, br, 6H, CH_2, Cy); ^{13}C{^{1}H} NMR (100.6 MHz, THF-d_8, 25 ºC): δ (ppm) 160.7 (N*C*N), 140.5 (Ph), 134 (Ph), 132.6 (Ph), 130.2 (Ph), 129.4 (Ph), 100.5 (C≡*C*-C), 90.1 (Ph-*C*≡C), 67.1 (*C*H, Cy), 61.1 (*C*H, Cy), 56.3 (*C*H, Cy), 36.4 (*C*H$_2$, Cy), 34.1 (*C*H$_2$, Cy), 26.2 (*C*H$_2$, Cy). IR (KBr): ν (cm^{-1}) 3439 (s), 3222 (s), 2973 (s), 2930 (vs), 2855 (w), 2217 (w, C≡C), 1637 (vs, NCN), 1448 (s), 1370 (m), 1309 (w), 1242 (s), 1180 (s), 1153 (s), 1079 (m), 1038 (m), 987 (m), 962 (w), 916 (w), 890 (m), 834 (w), 755 (s), 690 (s), 646 (w), 627 (w), 529 (w), 501 (w), 472 (w).

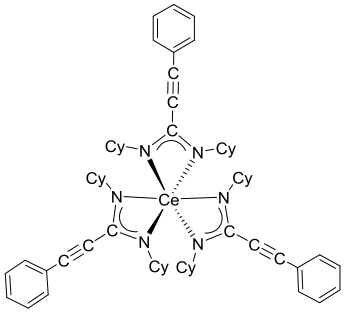
Ce
N
Cy
C
C
C

[Ph-C≡C-C(NCy)$_2$]$_3$Sm (18)

Reaction of anhydrous $SmCl_3$ (0.5 g, 2 mmol) with **3a** (2.3 g, 6 mmol). Following the procedure described for **16**, afforded **18** as pale yellow solid. Yield: 1.3g, 64%. Elemental analysis for $C_{63}H_{81}N_6Sm$ (1072.74 g·mol^{-1}): C, 70.54; H, 7.61; N, 7.83; found C, 69.62; H, 7.70; N, 7.60%. ^{1}H NMR (400 MHz, THF-d_8, 25 ºC): δ (ppm) 8.23 (d, 3H, Ph), 8.04 (s, br, 3H, Ph), 7.30 – 7.64 (m, 9H, Ph), 3.71 (s, br, 3H, C*H*, Cy), 3.30 (m, 3H, C*H*, Cy), 0.00 – 0.16 (m, 4H, CH_2, Cy), 0.30 – 2.06 (m, br, 50H, CH_2, Cy), – 1.70 (s, br, 6H, CH_2, Cy); ^{13}C{^{1}H} NMR (100.6 MHz, THF-d_8, 25 ºC): δ (ppm) 183.3 (N*C*N), 133.1 (Ph), 130.1(Ph), 129.6 (Ph), 124.4 (Ph), 97.7 (C≡*C*-C), 84.1 (Ph-*C*≡C), 59.5 (*C*H, Cy), 57.4 (*C*H, Cy), 36.6 (*C*H$_2$, Cy), 33.7 (*C*H$_2$, Cy), 26.9 (*C*H$_2$, Cy).

[Ph-C≡C-C(NCy)$_2$]$_3$Ho (19)

Reaction of anhydrous $HoCl_3$ (1.0 g, 3.7 mmol) with **3a** (4.3 g, 11.1 mmol). Following the procedure described for **16**, afforded **19** as pale yellow solid. Yield: 3.6 g, 91%. Elemental analysis for $C_{63}H_{81}HoN_6$ (1087.31 g·mol^{-1}): C, 69.59; H, 7.51; N, 7.73; found C, 69.45; H, 7.41; N, 7.73%. IR (KBr): ν (cm^{-1}) 3671 (w), 3362 (w), 3222 (w), 3063 (m), 2963 (vs), 2868 (s), 2710 (w), 2622 (m), 2363 (w), 2221 (w, C≡C), 2128 (w), 1952 (w), 1882 (w), 1754 (w), 1599 (s, NCN), 1518 (vs), 1452 (s), 1363 (s), 1318 (s), 1229 (m), 1072 (m), 1065 (s), 1036 (s), 999 (m), 949 (m), 854 (m), 822 (m), 758 (vs), 692 (vs), 652 (w), 534 (m), 531 (s), 512 (m), 479 (w), 451 (w).

[*c*-C$_3$H$_5$-C≡C-C(N^{i}Pr)$_2$]$_2$CeN(SiMe$_3$)$_2$ (20)

A solution of anhydrous $CeCl_3$ (1.0 g, 4.1 mmol) in 30 ml of THF was added to a solution of **1a** (1.6 g, 8.2 mmol) and KN(SiMe$_3$)$_2$ (0.8 g, 4.1 mmol) in 50 ml of THF. The reaction mixture was heated to 65 ºC for one hour and then stirred at r.t. over night. The solvent was removed under vacuum followed by extraction with *n*-pentane (30 ml) to give a clear, bright yellow solution. The filtrate was concentrated under vacuum to ca. 10 ml. Crystallization at –30 ºC afforded **20** in the form of bright yellow crystals. Yield: 0.97g, 37%. Elemental analysis for $C_{30}H_{56}CeN_5Si_2$ (683.10 g·mol^{-1}): C, 52.75; H, 8.26; N, 10.25; found C, 52.21; H,

8.27; N, 10.11%. ^{1}H NMR (400 MHz, C_6D_6, 25 ºC): δ (ppm) 11.93 (m, 4H, C*H*, C_3H_7), 3.50 (m, 2H, C*H*, *c*-C_3H_5), 2.74 (m, 4H, CH_2, *c*-C_3H_5), 1.83 (m, 4H, CH_2, *c*-C_3H_5), 0.04 (s, 18H, CH_3), − 2.95 (s, 24H, CH_3); ^{13}C{^{1}H} NMR (100.6 MHz, C_6D_6, 25 ºC): δ (ppm) 172.3 (N*C*N), 110.7 (C≡*C*-C), 79.4 (HC-*C*≡C), 56.1 (*C*H, C_3H_7), 22.9 (*C*H_3), 11.2 (*C*H_2, *c*-C_3H_5), 3.2 (*C*H_3), 2.3 (*C*H, *c*-C_3H_5); ^{29}Si NMR (80 MHz, C_6D_6, 25 ºC) δ (ppm) − 2.96. MS (EI, M = 682.31): *m/z* (%) 432.3 (100) [M –(*c*-C_3H_5-C≡C-C(N^{i}Pr)$_2$ + $SiMe_2$)]$^+$, 460.4 (20) [M –(*c*-C_3H_5-C≡CC(N^{i}Pr) + $SiMe_3$)]$^+$, 479.0 (38) [M –(^{i}Pr +N($SiMe_3$)$_2$)]$^+$.

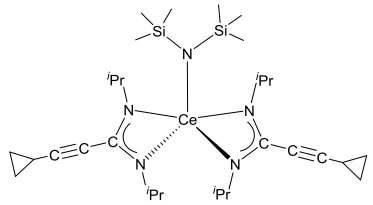

[*c*-C_3H_5-C≡C-C(NCy)$_2$]$_2$CeN($SiMe_3$)$_2$ (21)

A solution of anhydrous $CeCl_3$ (1.0 g, 4.1 mmol) in 20 ml of THF was added a solution of **2a** (2.3 g, 8.2 mmol) and KN($SiMe_3$)$_2$ (0.8 g, 4.1 mmol) in 60 ml of THF. The product was isolated following the procedure described for **20**. Crystallization at –30 ºC afforded **21** in the form of a bright yellow solid. Yield: 1.7 g, 52 %. Elemental analysis for $C_{42}H_{72}CeN_5Si_2$ (843.36 g·mol^{-1}): C, 59.82; H, 8.61; N, 8.30; found C, 59.72; H, 8.57; N, 8.32%. ^{1}H NMR (400 MHz, C_6D_6, 25 ºC): δ (ppm) 11.87 (m, 4H, C*H*, Cy), 3.56 (m, 2H, C*H*, *c*-C_3H_5), 2.85 (m, 4H, CH_2, *c*-C_3H_5), 1.77 – 1.87 (m, 4H, CH_2, *c*-C_3H_5), 0.52 (m, 24H, CH_2, Cy), 0.05 (s, 18H, CH_3), – 2.0 (m, 4H, CH_2, Cy), – 2.36 (m, 6H, CH_2, Cy), –7.2 (m, 6H, CH_2, Cy); ^{13}C{^{1}H} NMR (100.6 MHz, C_6D_6, 25 ºC): δ (ppm) 158.6 (N*C*N), 110.7 (C≡*C*-C), 80.3 (HC-*C*≡C), 65.2 (*C*H, Cy), 24.2 (*C*H_2, Cy), 23.9 (*C*H_2, Cy), 23.3 (*C*H_2, Cy), 11.5 (*C*H_2, *c*-C_3H_5), 3.5 (*C*H_3), 2.3 (*C*H, *c*-C_3H_5); ^{29}Si NMR (80 MHz, C_6D_6, 25 ºC): δ (ppm) 1.92. MS (EI, M = 842.44): *m/z* (%) 272.2 (100) [(*c*-C_3H_5-C≡C-C(NCy)$_2$]$^+$, 544.5 (78) [((*c*-C_3H_5-C≡C-C(NCy)$_2$)$_2$]$^+$, 703.6 (18) [M – Ce]$^+$, 761.8 (9) [M – (Cy)]$^+$, 814.7 (7) [M – 2Me]$^{2+}$, 825.8 (15) [M – Me]$^{2+}$.

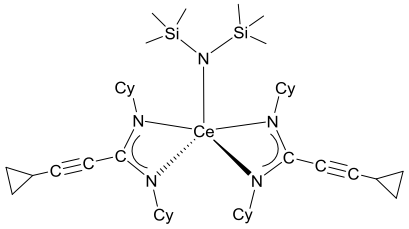

[*c*-C_3H_5-C≡C-C(NCy)$_2$]$_2$NdN($SiMe_3$)$_2$ (22)

A solution of anhydrous $NdCl_3$ (1.0 g, 4.0 mmol) in 20 ml of THF was added to a solution of **2a** (2.3 g, 8.0 mmol) and KN($SiMe_3$)$_2$ (0.8 g, 4.0 mmol) in 70 ml of THF. The reaction mixture was heated to 65 ºC for 1 h and then stirred at r. t. over night. The solvent was removed under vacuum to dryness followed by extraction of the residue with *n*-pentane (2 × 20 ml) to produce a clear, pale green solution. The filtrate was concentrated under vacuum to

ca. 10 ml. Crystallization at 5 ºC afforded **22** as pale green crystals. Yield: 2.2 g, 67 %. Elemental analysis for $C_{42}H_{72}N_5NdSi_2$ (847.48 g·mol^{-1}): C, 59.52; H, 8.56; N, 8.26; found C, 57.32; H, 8.76; N, 8.25%. ^{1}H NMR (400 MHz, toluene-d_8, 25 ºC): δ (ppm) 25.85 (m, 4H, C*H*, Cy), 4.80 (m, 2H, C*H*, *c*-C_3H_5), 3.78 (m, 4H, CH_2, *c*-C_3H_5), 2.58 (m, 4H, CH_2, *c*-C_3H_5), 0.34 – 1.82 (m, 12H, CH_2, Cy), 0.08 (s, 18H, CH_3), – 0.84 (m, 8H, CH_2, Cy), – 13.52 (m, 20H, CH_2, Cy); ^{13}C{^{1}H} NMR (100.6 MHz, Toluene-d_8, 25 ºC): δ (ppm) 109.6 (C≡*C*-C), 63.5 (HC-*C*≡C), 61.6 (*C*H, Cy), 25.4 (*C*H_2, Cy), 23.6 (*C*H_2, Cy), 22.8 (*C*H_2, Cy), 14.2 (*C*H_2, *c*-C_3H_5), 3.7 (*C*H_3), 2.6 (*C*H, *c*-C_3H_5); ^{29}Si NMR (80 MHz, C_6D_6, 25 ºC): δ (ppm) – 83.04.

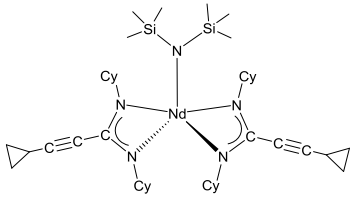

[*c*-C_3H_5-C≡C-C(NCy)$_2$]$_2$HoN(SiMe$_3$)$_2$ (23)

The reaction of anhydrous $HoCl_3$ (1.0 g, 3.6 mmol) with **2a** (2 g, 7.2 mmol) and KN(SiMe$_3$)$_2$ (0.72 g, 3.6 mmol) was carried out following the procedure described for **22**. Crystallization at 5 ºC afforded **23** as pale yellow crystals. Yield: 1.6 g, 51%. Elemental analysis for $C_{42}H_{72}HoN_5Si_2$ (868.17 g·mol^{-1}): C, 58.11; H, 8.36; N, 8.07; found C, 57.87; H, 8.61; N, 8.05 %. MS (EI, M = 867.46): *m/z* (%) 272.1 (80) [*c*-C_3H_5-C≡CC(NCy)$_2$]$^+$, 707.4 (100) [M – N(SiMe$_3$)$_2$], 785.5 (8) [M – (Cy)]$^+$, 796.5 (12) [M – SiMe$_3$]$^{2+}$, 852.5 (76) [M – Me]$^{2+}$, 867.6 (95) [M]. IR (KBr): ν (cm^{-1}) 3382 (m), 3096 (w), 3022 (m), 2926 (vs), 2850 (m), 2228 (s, C≡C), 1611 (s, NCN), 1469 (m), 1367 (m), 1325 (w), 1303 (w), 1260 (w), 1155 (w), 1118 (w), 1047 (w), 1031 (w), 999 (m), 965 (m), 834 (s), 771 (w), 700 (w), 688 (s), 652 (w), 571 (w), 552 (w), 532 (s), 512 (w), 457 (w), 428 (w).

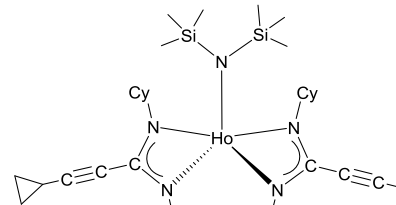

(COT)Pr[μ-*c*-C_3H_5-C≡C-C(NCy)$_2$]$_2$Li(Et$_2$O) (24)

A solution of [(COT)Pr(μ-Cl)(THF)$_2$]$_2$ (1.0 g, 1.15 mmol) in 20 ml THF was added to a solution of **2a** (0.8 g, 2.3 mmol) in 50 ml THF. The resulting orange reaction mixture was stirred over night at room temperature. After evaporation to dryness the residue was extracted with 30 ml of toluene. After filtration, the toluene was replaced by 10 ml of Et_2O to give a bright yellow solution.

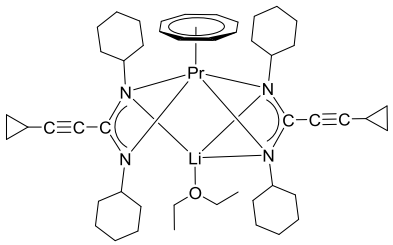

Crystallization at 5 ºC afforded **24** as bright yellow crystals. Yield: 0.85g, 53%. Elemental analysis for $C_{48}H_{72}LiN_4OPr$ (868.95 g·mol^{-1}): C, 66.24; H, 8.28; N, 6.42; found: C, 65.93; H, 8.14; N, 6.34%. ^{1}H NMR (400 MHz, THF-d_8, 25 ºC): δ (ppm) 5.50 – 5.90 (m, br, 8H, C_8H_8), 3.45 (s, br, Et_2O), 3.36 (m, br, 4H, C*H*, Cy), 1.39 (m, 2H, C*H*, *c*-C_3H_5), 1.05 – 1.61 (m, br, 40H, CH_2, Cy), 0.84 (s, br, 4H, CH_2, *c*-C_3H_5), 0.69 (s, br, 4H, CH_2, *c*-C_3H_5), 0.89 (s, br, Et_2O); ^{13}C{^{1}H} NMR (100.6 MHz, THF-d_8, 25 ºC): δ (ppm) 141.3 (N*C*N), 127.8 (C_8H_8), 94.9 (*C*≡C-C), 61.9 (CH_2, Et_2O), 60.5 (*C*H, Cy), 35.5 (*C*H_2, Cy), 27.1 (*C*H_2, Cy), 25.5 (*C*H_2, Cy), 14.4 (CH_3, Et_2O), 8.6 (*C*H_2, *c*-C_3H_5), – 0.3 (*C*H, *c*-C_3H_5). MS (EI, M = 868.35): *m/z* (%) 515.5 (10) [Pr(COT)(*c*-C_3H_5-C≡C-C(NCy)$_2$)], 378.4 (83) [(COT)(*c*-C_3H_5-C≡C-C(NCy)$_2$)]$^+$, 272.2 (87) [*c*-C_3H_5-C≡C-C(NCy)$_2$]$^+$, 243.2 (36) [Pr(COT)]$^+$. IR (KBr): ν (cm^{-1}) 3677 (w), 3440 (w), 3096 (w), 3015 (w), 2961 (s), 2865 (s), 2697 (m), 2217 (s, C≡C), 1593 (vs, NCN), 1495 (m), 1384 (m), 1333 (w), 1263 (w), 1169 (m), 1090 (w), 965 (w), 918 (w), 870 (w), 812 (w), 715 (w), 687 (w), 529 (w), 436 (w).

(COT)Nd[*μ*-*c*-C_3H_5-C≡C-C(N^{i}Pr)$_2$]$_2$Li(THF) (25)

A solution of [(COT)Nd(*μ*-Cl)(THF)$_2$]$_2$ (1.0 g, 1.16 mmol) in 20 ml THF was added to a solution of **1a** (0.62 g, 2.3 mmol) in 50 ml THF. The reaction mixture was stirred for 12 h at room temperature. The resulting solution blue was evaporated to dryness under vacuum, followed by extraction with *n*-pentane (30 ml) to give a clear pale blue solution. The filtrate was concentrated in vacuum to ca. 10 ml. Crystallization at 5 ºC afforded **25** in the form of pale blue crystals. Yield: 0.5 g 64%. Elemental analysis for $C_{36}H_{54}LiN_4NdO$ (710.01 g·mol^{-1}): C, 60.90; H, 7.67; N, 7.89; found C, 60.84; H, 7.10; N, 7.75%. MS (EI, M = 707.35): *m/z* (%) 701.5 (28) [M – Li]$^+$, 677.4 (17) [M – 2CH_3]$^+$, 524.3 (100) [Nd(*c*-C_3H_5-C≡C-C(N^{i}Pr)$_2$)$_2$]$^+$ or [(COT)Nd(*c*-C_3H_5-C≡C-C(N^{i}Pr)) + 2^{i}Pr]$^+$, 482.2 (15) [M – (*c*-C_3H_5-C≡C-C(N^{i}Pr)$_2$Li(THF))]$^+$, 398.1 (34) [(COT)Nd (C≡C-C(N^{i}Pr)$_2$)]$^+$. IR (KBr): ν (cm^{-1}) 3678 (w), 3439 (w), 3011 (w), 2932 (w), 2850 (s), 2664 (w), 2592 (w), 2219 (s, C≡C), 2074 (w), 1890 (m), 1818 (w), 1598 (s, NCN), 1447 (m), 1390 (m), 1361 (w), 1309 (w), 1255 (m), 1159 (m), 1116 (m), 1067 (w), 1027 (w), 971 (s), 858 (m), 728 (m), 593 (w), 499 (w), 439 (w).

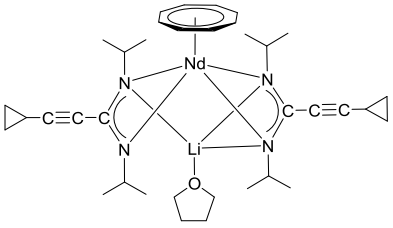

(COT)Nd[*μ*-*c*-C_3H_5-C≡C-C(NCy)$_2$]$_2$Li(THF) (26)

A solution of [(COT)Nd(*μ*-Cl)(THF)$_2$]$_2$ (1.0 g, 1.16 mmol) in 20 ml THF was added to a solution of **2a** (0.8 g, 2.3 mmol) in 50 ml THF, following the procedure for **25**, compound **26**

was isolated as a pale blue solid. Yield: 0.65 g, 41%. Elemental analysis for $C_{48}H_{70}LiN_4NdO$ (870.30 g·mol^{-1}): C, 66.20; H, 8.04; N, 6.43; found C, 66.08; H, 7.98; N, 6.10%. ^{1}H NMR

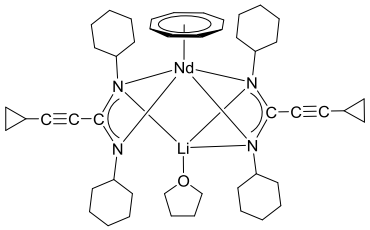

(400 MHz, THF-d_8, 25 ºC): δ (ppm) 32.78 (s, br, C*H*, 4H, Cy), 7.56 (s, 2H, C*H*, *c*-C_3H_5), 6.15 (s, 4H, CH_2, *c*-C_3H_5), 4.55 (s, 4H, CH_2, *c*-C_3H_5), 3.32 – 3.64 (m, br, 4H, CH_2, Cy), 1.30–1.40 (m, br, 16H, CH_2, Cy), – 1.33 (s, br, 4H, CH_2, Cy), – 4.63 (s, br, 16H, CH_2, Cy), – 11.56 (s, br, 8H, C_8H_8); ^{13}C NMR (100.6 MHz, THF-d_8, 25 ºC): δ (ppm) 183.5 (N*C*N), 160.8 (*C*$_8$H$_8$), 115.5 (C≡*C*-C), 92.2 (H-C-*C*≡C), 60.6 (*C*H, Cy), 40.7 (*C*H$_2$, Cy), 27.2 (*C*H$_2$, Cy), 26.0 (*C*H$_2$, Cy), 14.9 (*C*H$_2$, *c*-C_3H_5), 6.6 (*C*H, *c*-C_3H_5). MS (EI, M = 867.48): *m/z* (%) 517.3 (98) [M – (*c*-C_3H_5-C≡C-C(NCy)$_2$Li(THF))], 476.2 (37) [Nd(COT)(C≡C-C(NCy)$_2$)], 270.2 (43) [(*c*-C_3H_5-C≡C-C(NCy)$_2$]$^+$, 248.0 (59) [Nd(COT)]$^{2+}$. IR (KBr): ν (cm^{-1}) 3437 (w), 3225 (w), 3091 (w), 2928 (s), 2853 (m), 2536 (w), 2226 (vs, C≡C), 1635 (s, NCN), 1607 (m), 1479 (w), 1449 (w), 1366 (m), 1313 (m), 1254 (w), 1180 (w), 1157 (w), 1106 (m), 1030 (m), 975 (s), 890 (m), 841 (w), 700 (w), 566 (w), 465 (w).

(μ-η^8:η^8-COT)[Ce(*c*-C_3H_5-C≡C-C(N^{i}Pr)$_2$)$_2$]$_2$ (27)

A solution of [{*c*-C_3H_5-C≡C-C(N^{i}Pr)$_2$}$_2$Ce(μ-Cl)(THF)]$_2$ (**5**) (0.4 g, 0.33 mmol) in 50 ml THF was injected with K_2COT (0.6 ml of a 0.6 M solution in THF). The reaction mixture was

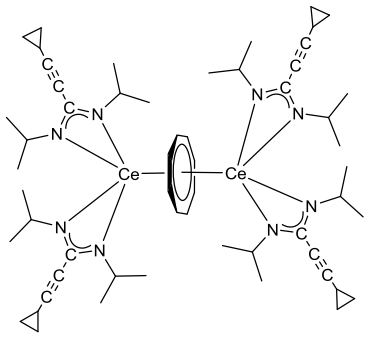

stirred for 12 h at room temperature. THF was removed under vacuum and the residue was extracted with 30 ml of *n*-pentane. The filtered solution was concentrated to 10 ml and then kept at 5 °C to afford **27** as yellow, needle-like crystals. Yield: 0.17g, 45%. Elemental analysis for $C_{56}H_{84}Ce_2N_8$ (1149.58 g·mol^{-1}): C, 58.51; H, 7.37; N, 9.75; found C, 58.59; H, 7.94; N, 9.72%. ^{1}H NMR (400 MHz, THF-d_8, 25 ºC): δ (ppm) 10.01 (s, br, 8H, C*H*, ^{i}Pr), 3.15 (s, br, 4H, C*H*, *c*-C_3H_5), 2.22 (s, 8H, CH_2, *c*-C_3H_5), 1.87 (s, 8H, CH_2, *c*-C_3H_5), – 0.32 (s, br, 48H, CH_3, ^{i}Pr), 1.15 (s, br, C_8H_8);^{13}C{^{1}H} NMR (100.6 MHz, THF-d_8, 25 ºC): δ (ppm) 161.2 (N*C*N), 108.1 (C≡*C*-C), 107.7 (*C*$_8$H$_8$), 77.1 (H-C-*C*≡C), 58.7 (*C*H, ^{i}Pr), 25.9 (*C*H$_3$, ^{i}Pr), 10.4 (*C*H$_2$, *c*-C_3H_5), – 0.4 (*C*H, *c*-C_3H_5).

(μ-η^8:η^8-COT)[Ce(*c*-C_3H_5-C≡C-C(NCy)$_2$)$_2$]$_2$ (28)

The reaction of [{*c*-C_3H_5-C≡C-C(N-*c*-C_6H_{11})$_2$}$_2$Ce(μ-Cl)(THF)]$_2$ (**6**) (0.5 g, 0.32 mmol) with K_2COT (0.6 ml of a 0.6 M solution in THF) was carried out as described for **27** and afforded **28** as yellow crystals. Yield: 0.23 g, 49%. Elemental analysis for $C_{80}H_{116}Ce_2N_8$ (1470.10 g·mol^{-1}): C, 65.36; H, 7.95; N, 7.62; found C, 65.61; H, 7.81; N, 8.80%. ^{1}H NMR (400 MHz, THF-d_8, 25 ºC): δ (ppm) 9.67 (s, br, 8H, C*H*, Cy), 3.22 (s, br, 4H, C*H*, *c*-C_3H_5), 2.28 (s, br, 8H, CH_2, *c*-C_3H_5), 1.92 (s, br, 8H, CH_2, *c*-C_3H_5), 0.97 – 1.60 (m, br, 82H, CH_2, Cy, C_8H_8), – 0.45 (s, br, 6H, CH_2, Cy); ^{13}C{^{1}H} NMR (100.6 MHz, THF-d_8, 25 ºC): δ (ppm) 163.2 (N*C*N), 114.5(C≡*C*-C), 106.9 (*C*$_8$H$_8$), 94.8 (C≡*C*-C), 67.1 (*C*H, Cy), 36.0 (*C*H$_2$, Cy), 33.5 (*C*H$_2$, Cy), 26.0 (*C*H$_2$, Cy), 10.6 (*C*H$_2$, *c*-C_3H_5), 2.4 (*C*H, *c*-C_3H_5).

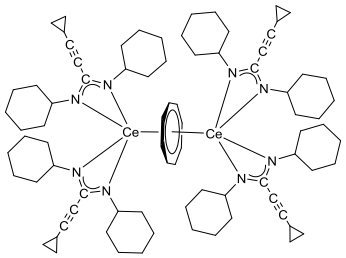

[(COT)Pr(μ-*c*-C_3H_5-C≡C-C(N^{i}Pr)$_2$)]$_2$ (29)

A solution of [(COT)Pr(μ-Cl)(THF)$_2$]$_2$ (1.0 g, 1.15 mmol) in 20 ml of THF was added to a solution of **1a** (0.31 g, 1.15 mmol) in 50 ml of THF. The resulting orange reaction mixture was stirred for 12 h at room temperature. Work-up as described for **28** using toluene (30 ml) for extraction gave **29** as yellow solid. Yield: 0.3 g, 47%. Elemental analysis for $C_{40}H_{54}N_4Pr_2$ (872.14 g·mol^{-1}): C, 55.04; H, 6.19; N, 6.42; found C, 55.14; H, 6.24; N, 6.29%. ^{1}H NMR (400 MHz, toluene-d_8, 25 ºC): δ (ppm) 10.57 (s, 4H, C*H*, ^{i}Pr), 1.94 (m, 2H, C*H*, *c*-C_3H_5), 1.70 (s, br, 4H, CH_2, *c*-C_3H_5), 1.22 (s, br, 4H, CH_2, *c*-C_3H_5), – 4.63 (s, br, 16H, C_8H_8), – 10.24 (s, br, 24H, CH_3, ^{i}Pr); ^{13}C{^{1}H} NMR (100.6 MHz, toluene-d_8, 25 ºC): δ (ppm) 186.1 (*C*$_8$H$_8$), 33.5 (*C*H, ^{i}Pr), 15.6 (*C*H$_3$, ^{i}Pr), 9.7 (*C*H$_2$, *c*-C_3H_5), 0.9 (*C*H, *c*-C_3H_5). IR (KBr): ν (cm^{-1}) 3833 (w), 3621 (w), 3221 (w), 3013 (w), 2964 (s), 2930 (m), 2537 (w), 2215 (vs, C≡C), 1836 (w), 1701 (w), 1612 (s, NCN), 1466 (w), 1381 (w), 1244 (m), 1179 (m), 1133 (m), 1080 (w), 1052 (w), 1032 (w), 983 (s), 966 (m), 946 (m), 841 (w), 732 (w), 702 (w), 646 (w), 587 (w), 442 (w).

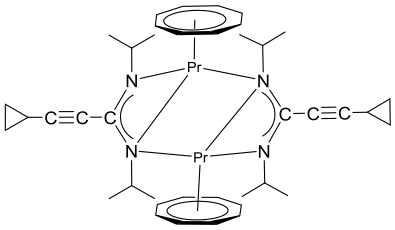

General procedure for the synthesis of [(COT)Ln(μ-*c*-C_3H_5-C≡C-C(NR)$_2$)]$_2$ or (COT)Ho(*c*-C_3H_5-C≡C-C(NR)$_2$)(THF) complexes

Anhydrous $LnCl_3$ (2 mmol) (Ln = Ce, Nd or Ho) in 40 ml THF was added to a mixture of the cyclopropylethinylamidinate (**1a** or **2a)** (2 mmol) and K_2COT (3.3 ml, 0.6 M solution in

THF), dissolved in 50 ml of THF. The reaction mixture was stirred for 12 h at room temperature. The solvent was removed under vacuum followed by extraction of the residue with 40 ml of toluene (*n*-pentane in the cases **33** and **34**) the solution was concentrated to 20 ml and then kept at 5 °C to afford **30 – 34**.

[(COT)Ce(*μ*-*c*-C_3H_5-C≡C-C(N^{i}Pr)$_2$)]$_2$ (30)

Compound **30** afforded as deep green, needle-like single-crystals suitable for X-ray diffraction. Yield: 0.96 g, 57%. Elemental analysis for $C_{40}H_{54}Ce_2N_4$ (871.13 g·mol^{-1}): C, 55.15; H, 6.25; N, 6.43; found C, 54.73; H, 6.25; N, 6.62%. ^{1}H NMR (400 MHz, THF-d_8, 25 ºC): δ (ppm) 12.32 (s, br, 4H, C*H*, ^{i}Pr), 3.43 (s, br, 2H, C*H*, *c*-C_3H_5), 2.60 (s, br, 4H, CH_2, *c*-C_3H_5), 2.11 (s, br, 4H, CH_2, *c*-C_3H_5), 0.91 – 1.53 (m, 40H, CH_3, ^{i}Pr, C_8H_8); ^{13}C{^{1}H} NMR (100.6 MHz, THF-d_8, 25 ºC): δ (ppm) 163.2 (N*C*N), 109.9 (C≡*C*-C), 108.6 (*C*$_8$H$_8$), 81.1 (H-C-*C*≡C), 60.8 (*C*H, ^{i}Pr), 27.3 (*C*H$_3$, ^{i}Pr), 10.6 (*C*H$_2$, *c*-C_3H_5), 3.4 (*C*H, *c*-C_3H_5). IR (KBr): ν (cm^{-1}) 3852 (w), 3743 (w), 3436 (w), 3224 (w), 3091 (w), 2965 (m), 2930 (m), 2870 (w), 2609 (w), 2533 (w), 2328 (w), 2318 (w), 2226 (s, C≡C), 2029 (m), 1976 (w), 1959 (w), 1634 (s, NCN), 1613 (w), 1560 (w), 1504 (w), 1449 (m), 1375 (w), 1307 (m), 1244 (m), 1180 (w), 1157 (w), 1029 (w), 985 (s), 945 (w), 895 (w), 878 (m), 844 (w), 813 (w), 747 (w), 700 (w), 667 (w), 615 (w), 588 (m), 555 (w), 504 (w), 466 (w), 458 (w).

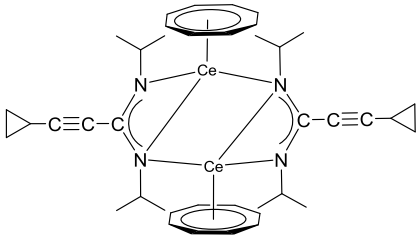

[(COT)Ce(*μ*-*c*-C_3H_5-C≡C-C(NCy)$_2$)]$_2$ (31)

Compound **31** afforded as green, needle-like single-crystals suitable for X-ray diffraction. Yield: 0.35 g, 17%. Elemental analysis for $C_{52}H_{70}Ce_2N_4$ (1031.36 g·mol^{-1}): C, 60.50; H, 6.78; N, 5.42; found C, 59.82; H, 6.63; N, 5.38%. ^{1}H NMR (400 MHz, THF-d_8, 25 ºC): δ(ppm) 12.22 (s, br, 4H, C*H*, Cy), 0.93 – 1.87 (m, br, 58H, CH_2, Cy, C_8H_8, C*H*, *c*-C_3H_5), 0.73 (m, br, 8H, CH_2, *c*-C_3H_5); ^{13}C{^{1}H} NMR (100.6 MHz, THF-d_8, 25 ºC): δ (ppm) 140.7 (N*C*N), 115.3 (*C*$_8$H$_8$), 94.7 (C≡*C*-C), 61.5 (*C*H, Cy), 35.8 (*C*H$_2$, Cy), 33.9 (*C*H$_2$, Cy), 26.8 (*C*H$_2$, Cy), 8.7 (*C*H$_2$, *c*-C_3H_5), 1.37 (*C*H, *c*-C_3H_5). IR (KBr): ν (cm^{-1}) 3833 (w), 3747 (w), 3435 (w), 3247 (w), 3090 (w), 2926 (s), 2853 (m), 2530 (w), 2356 (w), 2318 (w), 2225 (s, C≡C), 1959 (w), 1633 (vs, NCN), 1448 (m),

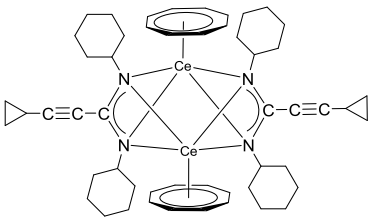

1310 (m), 1238 (w), 1180 (w), 1154 (w), 984 (s), 890 (w), 864 (w), 809 (w), 745 (w), 717 (w), 667 (w), 638 (m), 626 (w), 554 (w), 505 (w), 466 (w), 450 (w).

[(COT)Nd(*μ*-*c*-C_3H_5-C≡C-C(N^{i}Pr)$_2$)]$_2$ (32)

Compound **32** afforded as purple, needle-like single-crystals suitable for X-ray diffraction. Yield: 0.74 g, 43%. Elemental analysis for $C_{40}H_{54}N_4Nd_2$ (879.38 g·mol^{-1}): C, 54.63; H, 6.19; N, 6.37; found C, 54.39; H, 6.26; N, 6.49%. ^{1}H NMR (400 MHz, THF-d_8, 25 ºC): δ (ppm) 3.96 (s, br, 2H, C*H*, ^{i}Pr), 3.71 (s, br, 2H, C*H*, ^{i}Pr), 1.40 (s, br, 2H, C*H*, *c*-C_3H_5), 0.72 – 0.81 (s, br, 8H, CH_2, *c*-C_3H_5), 1.08 (s, br, 12H, CH_3, ^{i}Pr), 1.00 (s, br, 12H, CH_3, ^{i}Pr), – 11.75 (s, br, 16H, C_8H_8); ^{13}C{^{1}H} NMR (100.6 MHz, THF-d_8, 25 ºC): δ (ppm) 158.0 (N*C*N), 132.7 (C_8H_8), 52.2 (*C*H, ^{i}Pr), 42.3 (*C*H, ^{i}Pr), 22.7 (*C*H$_3$, ^{i}Pr), 8.8 (*C*H$_2$, *c*-C_3H_5), 0.4 (*C*H, *c*-C_3H_5). MS (EI, M = 874.25): *m/z* (%) 435.5 (20) [(COT)Nd(*c*-C_3H_5-C≡C-C(N^{i}Pr)$_2$)]$^+$. IR (KBr): ν (cm^{-1}) 3852 (w), 3438 (w), 3282 (w), 3222 (w), 3093 (w), 3012 (w), 2964 (m), 2929 (s), 2868 (s), 2610 (w), 2350 (w), 2350 (w), 2227 (s, C≡C), 1614 (vs, NCN), 1466 (w), 1375 (m), 1361 (m), 1315 (w), 1259 (w), 1179 (w), 1168 (m), 1133 (m), 1053 (w), 1031 (w), 984 (s), 966 (s), 944 (w), 880 (w), 845 (w), 812 (w), 774 (w), 745 (w), 701 (w), 668 (m), 607 (m), 506 (w), 467 (w), 450 (w).

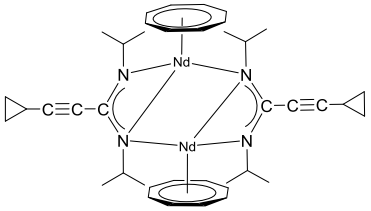

(COT)Ho[*c*-C_3H_5-C≡C-C(N^{i}Pr](THF) (33)

Compound **33** afforded as pale yellow solid. Yield: 0.84 g, 48%. Elemental analysis for $C_{24}H_{35}HoN_2O$ (532.49 g·mol^{-1}): C, 54.14; H, 6.63; N, 5.26; found C, 56.02; H, 6.00; N, 5.46%. MS (EI, M = 532.21): *m/z* (%) 460.4 (8) [M –THF], 531.5 (30) [M]$^+$, 547.5 (80) [M + CH_3)]$^+$. IR (KBr): ν (cm^{-1}) 3800 (w), 3571 (w), 3436 (w), 3317 (w), 3222 (w), 3091 (w), 3015 (w), 2960 (w), 2928 (s), 2865 (m), 2605 (w), 2221 (s, C≡C), 2108 (w), 1959 (w), 1843 (w), 1741 (w), 1718(m), 1611 (s, NCN), 1464 (w), 1402 (m), 1373 (m), 1356 (w), 1330 (w), 1262 (w), 1220 (m), 1186 (m), 1140 (w), 1121 (w), 1079 (w), 1053(w), 1029 (w), 968 (s), 891 (s), 843 (w), 811 (w), 788 (w), 745 (w), 712 (w), 702 (w), 644 (w), 595 (w), 530 (w), 472 (w), 453 (w), 440 (w).

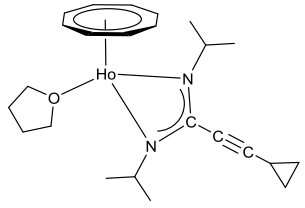

(COT)Ho[*c*-C_3H_5-C≡C-C(*c*-C_6H_{11}N](THF) (34)

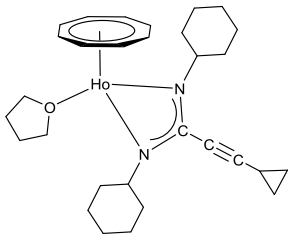

Compound **34** afforded as bright yellow, needle-like single-crystals suitable for X-ray diffraction. Yield: 0.65 g, 30%. Elemental analysis for $C_{30}H_{43}HoN_2O$ (612.62 g·mol^{-1}): C, 58.82; H, 7.08; N, 4.57; found C, 58.87; H, 6.53; N, 6.21%. MS (EI, M = 612.27): *m/z* (%) 269.1 (86) [M – (THF+(*c*-C_3H_5-C≡C-C(NCy)$_2$))]$^+$ or [*c*-C_3H_5-C≡CC(NCy)$_2$)]$^{2+}$, 433.3 (10) [M – (THF + COT)]$^{2+}$, 501.3 (33) [M – (THF + *c*-C_3H_5)]$^{2+}$, 540.4 (31) [M – THF]. IR (KBr): ν (cm^{-1}) 3436 (w), 3224 (w), 3092 (w), 3011 (w), 2927 (s), 2852 (s), 2666 (s), 2225 (vs, C≡C), 1959 (w), 1821 (w), 1603 (s, NCN), 1476 (w), 1449 (s), 1402 (w), 1363 (w), 1310 (w), 1253 (w), 1209 (m), 1180 (m), 1156 (m), 1123 (w), 1075 (w), 1053 (w), 1029 (w), 974 (s), 922 (s), 890 (m), 858 (w), 810 (w), 775 (w), 701 (w), 680 (w), 642 (w), 612 (w), 589 (w), 504 (w), 465 (w).

[(μ-η^8:η^8-COT)Nd_2(μ-Cl)$_2$(*c*-C_3H_5-C≡C-C(NCy)$_2$)$_2$]$_4$ (35)

Anhydrous $NdCl_3$ (1.0 g, 4 mmol) in 30 ml of THF was added to a mixture of **2a** (1.10 g, 4 mmol) and K_2COT (3.3 ml, 0.6 M in THF) in 50 ml of THF. The reaction mixture was stirred for 12 h at room temperature. THF was removed under vacuum, followed by extraction of the residue with 40 ml of toluene, the solution concentrated to 20 ml and then kept at 5 °C to afford **35** as blue crystals. Yield: 1.9 g, 20%. Elemental analysis for $C_{190}H_{264}Cl_8N_{16}Nd_8$(·6$C_7H_8$) ((4209.69 + 552.82) g·mol^{-1}): C, 58.45; H, 6.55; N, 4.70; found C, 57.28; H, 6.45; N, 5.20%. ^{1}H NMR ((400 MHz, THF-d_8, 25 ºC): δ (ppm) 3.61 (s, br, 8H, C*H*, Cy), 3.35 (s, br, 8H, C*H*, Cy), 1.35 (s, br, 18H, C*H*, *c*-C_3H_5), 0.84 (s, br, 16H, CH_2, *c*-C_3H_5), 0.71 (s, br, 16H, CH_2, *c*-C_3H_5), 1.01 – 2.01 (m, br, 160H, CH_2, Cy), – 11.34 (s, br, 32H, C_8H_8). ^{13}C{^{1}H} NMR (100.6 MHz, THF-d_8, 25 ºC): δ (ppm) 140.8 (N*C*N), 133.7 (C_8H_8), 61.1 (*C*H, Cy), 50.3 (*C*H, Cy), 35.9 (*C*H$_2$, Cy), 33.7 (*C*H$_2$, Cy), 26.7 (*C*H$_2$, Cy), 27.0 (*C*H$_2$, Cy), 8.9 (*C*H$_2$, *c*-C_3H_5), 0.1 (*C*H, *c*-C_3H_5). MS (EI, M = 4209.69): *m/z* (%) 229.3 (100) [C≡C-C(*c*-$C_6H_{11}N)_2$]$^+$, 272.4 (83) [*c*-C_3H_5-C≡C-C(*c*-$C_6H_{11}N)_2$]$^+$, 363.5 (75) [(COT) Nd (μ-Cl)(*c*-C_6H_{11})]$^+$, 446.6 (20) [Nd(μ-Cl)(*c*-C_3H_5-C≡C-C(*c*-$C_6H_{11}N)_2$)]$^{2+}$. IR

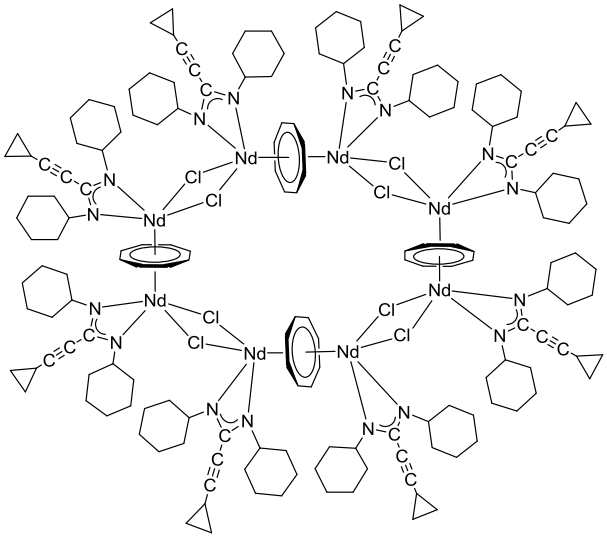

(KBr): ν (cm^{-1}) 3221 (w), 3091 (w), 3009 (w), 2929 (s), 2854 (s), 2668 (m), 2230 (s, C≡C), 1959 (w), 1627 (s, NCN), 1478 (w), 1450 (w), 1405 (w), 1365 (w), 1345 (m), 1310 (m), 1247 (w), 1190 (w), 1151 (m), 1001 (m), 1075 (m), 1030 (w), 974 (s), 959 (s), 926 (w), 891 (w), 862 (w), 842 (w), 811 (w), 793 (w), 754 (w), 697 (w), 668 (w), 628 (w), 588 (w), 502 (w), 466 (w).

General procedure for the catalytic reaction of 1,4-diaminobenzene with *N,N'*-diisopropylcarbodiimide by complexes 5 – 8

A 100 ml Schlenk flask was charged with 1,4-diaminobenzene (0.7 g, 6.4 mmol) and *N,N'*-diisopropylcarbodiimide (2.0 ml, 12.8 mmol) in 20 ml of THF. To the mixture was added the complex (**5**, **6**, **7**, or **8**) (0.5% mmol), dissolved in 5 ml of THF. The resulting mixture was stirred at 60 ºC or at room temperature for a fixed time, as shown in Table 8. The solvent was removed under vacuum and the product was purified by crystallization from a minimum amount of dry acetonitrile in air to give **36** in yields as shown in Table 8.

General procedure for the direct synthesis of guanidines from the reaction of primary amines with carbodiimides catalyzed by 7

Under dry argon a 50 ml Schlenk flask was charged with primary amines (1.0 equiv.) and carbodiimides (2.0 equiv.) in 20 ml of THF. To the mixture was added the complex **7** (0.005 equiv.), dissolved in 5 ml of THF. The resulting mixture was stirred at 60 ºC for a fixed time, as shown in Table 9. The solvent was removed under vacuum and the product was purified by recrystallization from dry acetonitrile in air affording the guanidines in yields as shown in Table 9.

NMR data of the known guanidine products 36 – 40:

36: ^{1}H NMR (400 MHz, $CDCl_3$, 25 ºC): δ (ppm) 6.75 (s, 4H), 3.73 (br, 4H), 1.13 (d, *J* = 6 Hz, 24H); ^{13}C NMR (100.6 MHz, $CDCl_3$, 25 ºC): δ (ppm) 150.7, 143.9, 124.4, 43.17, 23.3.

37: ^{1}H NMR (400 MHz, $CDCl_3$, 25 ºC): δ 6.6 (s, 4H), 3.16 – 3.47 (m, 4H), 1.08 –1.96 (m, 40H) (NH not observed); ^{13}C NMR (100.6 MHz, $CDCl_3$, 25 ºC): δ (ppm) 139.7, 138.4, 116.6, 55.7, 34.8, 25.4, 24.6.

38: ^{1}H NMR (400 MHz, $CDCl_3$, 25 ºC): δ 6.92 (t, 1H, J = 8 Hz), 6.21 (s, 1H), 6.07 (dd, 2H, *J* = 8 Hz, *J* = 2 Hz), 3.73 (m, 4H), 1.14 (d, 24H, *J* = 6 Hz) (NH not observed); ^{13}C NMR (100.6 MHz, $CDCl_3$, 25 ºC): δ (ppm) 151.22, 147.3, 129.8, 110.4, 101.8, 43.1, 23.3.

39: ^{1}H NMR (400 MHz, $CDCl_3$, 25 ºC): δ 6.93 (t, *J* = 8 Hz, 1H), 6.11 (dd, *J* = 8 Hz, *J* = 2 Hz, N*H*, 2H), 6.03 (s, 1H), 3.56 (m, br, 4H), 3.17 – 3.20 (m, 4H), 1.13 – 1.98 (m, 40H); ^{13}C NMR (100.6 MHz, $CDCl_3$, 25 ºC): δ (ppm) 147.5, 139.8, 130.1, 105.9, 101.8, 55.7, 34.9, 25.6, 24.6.
40: ^{1}H NMR (400 MHz, $CDCl_3$, 25 ºC): δ 6.79 (d, *J* = 7 Hz, *J* = 2 Hz, 1H), 6.71 – 6.74 (m, 2H), 6.67 (d, *J* = 7 Hz, *J* = 2 Hz, 1H), 3.76 (m, 2H), 1.16 (d, *J* = 6 Hz, 12H) (NH not observed); ^{13}C NMR (100.6 MHz, $CDCl_3$, 25 ºC): δ (ppm) 150.6, 140.7, 136.0, 122.6, 122.6, 118.8, 115.1, 43.1, 23.4.

General procedure for the direct synthesis of guanidines from the reaction of 4-chloroaniline with carbodiimides catalyzed by 7

Under argon, a 50 ml Schlenk flask was charged with 4-chloroaniline (1.0 equiv.) and carbodiimides (1.0 equiv.) in 10 ml of THF. To the reaction mixture was added the complex **7** (0.5 mmol %), dissolved in 5 ml THF. The resulting mixture was stirred at 60 ºC for a fixed time, as shown in Table 9. The solvent was removed under vacuum and the product was purified by recrystallization from acetonitrile in air affording the guanidines in very high yields as shown in Table 9.

NMR data of the known guanidine products 41 and 42:

41. ^{1}H NMR (400 MHz, DMSO-d_6, 25 ºC): δ (ppm) 7.15 – 7.17 (m, 2H), 6.74 – 6.76 (m, 2H), 4.80 (s, br, N*H*, 2H), 3.62 – 3.83 (m, 2H), 1.02 (d, *J* = 6 Hz, 12H); ^{13}C NMR (100.6 MHz, $CDCl_3$, 25 ºC): δ (ppm) 150.6, 150.1, 128.5, 123.9, 122.8, 42.1, 22.7.
42. ^{1}H NMR (400 MHz, $CDCl_3$, 25 ºC): δ (ppm) 7.21 – 7.19 (m, 2H), 6.79 – 6.75 (m, 2H), 3.62 (s, br, N*H*, 2H), 3.38 – 3.45 (m, 2H), 1.03 – 1.99 (m, 20H); ^{13}C NMR (100.6 MHz, $CDCl_3$, 25 ºC): δ (ppm) 150.1, 139.8, 129.1, 126.2, 124.8, 50.1, 33.7, 25.8, 24.8.

Formation of free the amidine 43 by controlled hydrolysis of 2a

A 0.5 g sample of **2a** was dissolved in acetonitrile and hydrolyzed by addition of one drop (*ca.* 30 mg) of water. Cooling to –20 °C afforded colorless crystals of **43** (*ca.* 100 mg) which were isolated by filtration, dried under vacuum and characterized by NMR spectroscopy. ^{1}H NMR (400 MHz, C_6D_6, 25 ºC): δ (ppm) 3.83 – 3.96 (s, br, 2H, C*H*, Cy), 1.03 – 1.76 (m, 20H, Cy), 0.96 – 1.03 (m, 1H *c*-C_3H_5), 0.55 – 0.60 (m, 2H, *c*-C_3H_5), 0.34 – 0.40 (m, 2H, *c*-C_3H_5) (NH not observed); ^{13}C NMR (100.6 MHz, C_6D_6, 25 ºC, TMS): δ (ppm) 140.7 (N*C*N), 94.9 (H-C-*C*≡C), 68.2(C≡*C*–C), 49.1 (*C*H, Cy), 34.8 (*C*H_2, Cy), 26.4 (*C*H_2, Cy), 25.1 (*C*H_2, Cy), 8.9 (*C*H_2, *c*-C_3H_5), 0.35 (*C*H, *c*-C_3H_5).

General procedure for the catalytic reaction of alkynyl with *N,N'*-diisopropylcarbodiimide by 12 – 15

A 100 ml-Schlenk flask was charged with phenylacetylene (1.40 ml, 12.8 mmol) and *N,N'*-diisopropylcarbodiimide (2.0 ml, 12.8 mmol) in 20 ml of THF. To the mixture was added the complex (**12**, **13**, **14**, or **15**) (0.5 or 1.0 mmol % as shown in Table 10), dissolved in 5 ml of THF. The resulting mixture was stirred at 60 ºC or at room temperature for a fixed time, as shown in Table 10. The solvent was removed under vacuum and the product was purified by crystallization from a minimum amount of dry acetonitrile in air to give **45** in yields as shown in Table 10.

General procedure for the catalytic reaction of alkynes with *N,N'*-diisopropylcarbodiimide using 14 as a catalyst

A 100 ml Schlenk flask was charged with alkyne (1.0 equiv. mmol) and *N,N'*-diisopropylcarbodiimide (1.0 eq. mmol) in 15 ml of THF. To the mixture was added the complex **14** (0.01 mmol equiv.), dissolved in 5 ml of THF. The resulting mixture was stirred at 60 ºC for a fixed time, as shown in Table 11. The solvent was removed under vacuum and the product was purified by crystallization from a minimum amount of dry acetonitrile in air to give:

45. ^{1}H NMR (400 MHz, $CDCl_3$, 25 ºC): δ (ppm) 7.45 – 7.54 (m, 2H), 7.31 – 7.38 (m, 3H), 3.96 (sept, 2H), 1.17 (d, J = 6.5 Hz, 12H); ^{13}C NMR (100.6 MHz, $CDCl_3$, 25 ºC): δ (ppm) 179.7, 141.8, 131.9, 129.4, 128.5, 121.4, 88.9, 23.9.

46. ^{1}H NMR (400 MHz, $CDCl_3$, 25 ºC): δ (ppm) 7.23 – 7.62 (m, 5H), 3.61 (m, 2H), 0.93 – 2.00 (m, 20H); ^{13}C NMR (100.6 MHz, $CDCl_3$, 25 ºC): δ (ppm) 141.9, 132.1, 129.4, 126.6, 121.5, 79.8, 34.9, 26.0, 25.2.

47. ^{1}H NMR (400 MHz, $CDCl_3$, 25 ºC): δ (ppm) 3.39 – 3.48 (m, 2H), 1.54 – 1.84 (m, 10H), 1.35 – 1.49 (m, 1H), 1.10 – 1.34 (m, 10H), 0.89 – 0.94 (m, 2H), 0.76 – 0.81 (m, 2H); ^{13}C NMR (100.6 MHz, $CDCl_3$, 25 ºC): δ (ppm) 141.9, 97.3, 77.3, 66.2, 34.2, 25.8, 24.9, 8.7, – 0.4.

5. Crystal data and refinement details

Table 12 Crystal data and structure refinement of **1a**

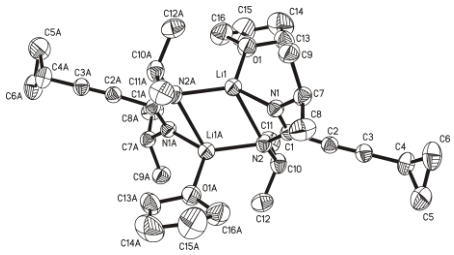

Identification code	ip295
Empirical formula	$C_{32}H_{54}Li_2N_4O_2$
Formula weight	540.67
Temperature	153(2) K
Wavelength	0.71073 Å
Crystal system	Triclinic
Space group	P-1
Unit cell dimensions	a = 9.787(2) Å α= 88.57(3)° b = 12.933(3) Å β= 73.60(3)° c = 14.055(3) Å γ = 82.34(3)°
Volume	1691.3(6) $Å^3$
Z	2
Density (calculated)	1.062 Mg/m^3
Absorption coefficient	0.065 mm^{-1}
F(000)	592
Crystal size	0.70 x 0.60 x 0.45 mm^3
Theta range for data collection	2.19 to 26.37°
Index ranges	$-12 \leq h \leq 12$, $-13 \leq k \leq 16$, $-17 \leq l \leq 17$
Reflections collected	14466
Independent reflections	6863 [R(int) = 0.0616]
Completeness to theta = 26.37°	99.3 %
Absorption correction	None
Refinement method	Full-matrix least-squares on F^2
Data / restraints / parameters	6863 / 0 / 377
Goodness-of-fit on F^2	1.026
Final R indices [I>2sigma(I)]	R1 = 0.0624, wR2 = 0.1582
R indices (all data)	R1 = 0.0854, wR2 = 0.1716
Largest diff. peak and hole	0.306 and -0.259 $e.Å^{-3}$

Table 13 Selected bond lengths [Å] and angles [°] of **1a**

Li(1)–O(1)	1.893(3)	N(1)–Li(1)–N(2)#1	126.96(16)
Li(1)–N(1)	1.975(3)	N(1)–Li(1)–N(2)	63.20(10)
Li(1)–N(2)#1	2.041(3)	N(2)#1–Li(1)–N(2)	112.29(14)
Li(1)–N(2)	2.336(4)	C(1)–N(1)–Li(1)	93.68(14)
N(1)–C(1)	1.318(2)	Li(1)#1–N(2)–Li(1)	67.71(14)
N(1)–C(7)	1.456(2)	C(1)–N(2)–Li(1)#1	124.73(14)
N(2)–C(1)	1.329(9)	C(1)–N(2)–Li(1)	78.38(12)
C(1)–C(2)	1.470(2)	N(1)–C(1)–N(2)	118.91(15)
C(2)–C(3)	1.193(2)	N(3)–Li(2)–N(4)#2	126.83(17)
C(3)–C(4)	1.446(3)	N(3)–Li(2)–N(4)	64.22(11)
Li(2)–O(2)	1.920(3)	Li(2)#2–N(4)–Li(2)	68.57(15)
Li(2)–N(3)	1.986(3)	N(3)–C(21)–N(4)	118.98(15)
Li(2)–N(4)#2	2.043(4)	N(3)–C(21)–Li(2)	54.66(12)

Table 14 Crystal data and structure refinement of **2a**

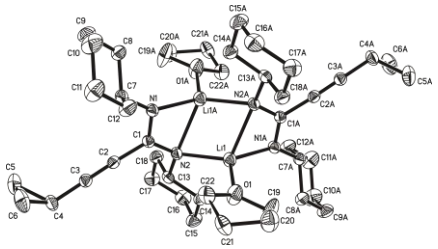

Identification code	ip240
Empirical formula	$C_{44}H_{70}Li_2N_4O_2$
Formula weight	700.92
Temperature	143(2) K
Wavelength	0.71073 Å
Crystal system	Monoclinic
Space group	$P2_1/n$
Unit cell dimensions	a = 10.799(2) Å α= 90° b = 20.431(4) Å β= 99.76(3)° c = 19.373(4) Å γ = 90°
Volume	4212.4(15) $Å^3$
Z	4
Density (calculated)	1.105 Mg/m^3
Absorption coefficient	0.066 mm^{-1}
F(000)	1536
Crystal size	0.40 x 0.30 x 0.30 mm^3
Theta range for data collection	2.13 to 26.37°
Index ranges	$-12 \leq h \leq 13$, $-24 \leq k \leq 25$, $-24 \leq l \leq 24$
Reflections collected	20709
Independent reflections	8519 [R(int) = 0.0497]
Completeness to theta = 26.00°	98.9 %
Absorption correction	None
Refinement method	Full-matrix least-squares on F^2
Data / restraints / parameters	8519 / 0 / 490
Goodness-of-fit on F^2	1.014
Final R indices [I>2sigma(I)]	R1 = 0.0565, wR2 = 0.1006
R indices (all data)	R1 = 0.1013, wR2 = 0.1119
Largest diff. peak and hole	0.222 and -0.198 $e.Å^{-3}$

Table 15 Selected bond lengths [Å] and angles [°] of **2a**

N(1)–C(1)	1.314(2)	N(1)#1–Li(1)–N(2)	129.62(17)
N(1)–C(7)	1.456(2)	N(1)#1–Li(1)–N(2)#1	65.10(10)
N(1)–Li(1)#1	1.986(3)	N(2)–Li(1)–N(2) #1	109.66(14)
N(2)–C(1)	1.341(2)	C(1)–N(1)–Li(1)#1	93.24(13)
N(2)–C(13)	1.4686(19)	C(1)–N(2)–Li(1)#1	81.66(12)
N(2)–Li(1)	2.052(3)	Li(1)–N(2)–Li(1)#1	70.34(14)
N(2)–Li(1)#1	2.245(3)	N(1)–C(1)–N(2)	118.91(14)
C(1)–C(2)	1.464(2)	Li(2)#2–N(4)–Li(2)	71.73(16)
C(2)–C(3)	1.193(2)	N(3)–C(31)–N(4)	118.19(15)
C(3)–C(4)	1.443(2)	N(3)–Li(2)–N(4)#2	121.01(17)
C(4)–C(5)	1.495(3)	N(3)–Li(2)–N(4)	66.16(11)
C(5)–C(6)	1.459(4)	N(4)#2–Li(2)–N(4)	108.27(16)
O(1)–Li(1)	1.887(13)		

Table 16 Crystal data and structure refinement of **3a**

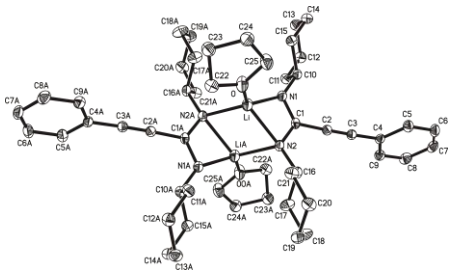

Identification code	magd78
Empirical formula	$C_{50}H_{70}Li_2N_4O_2$
Formula weight	772.98
Temperature	100(2) K
Wavelength	1.54184 Å
Crystal system	Triclinic
Space group	P-1
Unit cell dimensions	a = 9.8768(3) Å α= 104.144(3)°
	b = 10.2082(3) Å β= 90.248(3)°
	c = 11.6883(4) Å γ= 104.209(2)°
Volume	1105.18(6) $Å^3$
Z	1
Density (calculated)	1.161 Mg/m^3
Absorption coefficient	0.530 mm^{-1}
F(000)	420
Crystal size	0.12 x 0.10 x 0.10 mm^3
Theta range for data collection	3.91 to 76.97°
Index ranges	$-12 \leq h \leq 12$, $-12 \leq k \leq 12$, $-14 \leq l \leq 12$
Reflections collected	40575
Independent reflections	4628 [R(int) = 0.0274]
Completeness to theta = 76.97°	99.2 %
Absorption correction	Semi-empirical from equivalents
Max. and min. transmission	0.9490 and 0.9392
Refinement method	Full-matrix least-squares on F^2
Data / restraints / parameters	4628 / 0 / 262
Goodness-of-fit on F^2	1.027
Final R indices [I>2sigma(I)]	R1 = 0.0392, wR2 = 0.0964
R indices (all data)	R1 = 0.0403, wR2 = 0.0974
Largest diff. peak and hole	0.199 and -0.243 $e.Å^{-3}$

Table 17 Selected bond lengths [Å] and angles [°] of **3a**

N(1)–C(1)	1.3201(13)	N(1)–C(1)–N(2)	118.89(8)
N(2)–C(1)	1.3407(12)	N(1)–Li–N(2)	65.67(6)
N(1)–Li	2.031(2)	N(1)–Li–N(2)#1	118.44(9)
N(2)–Li	2.188(2)	N(2)#1–Li–N(2)	108.73(8)
C(1)–C(2)	1.4681(13)	Li#1–N(2)–Li	71.27(8)
C(2)–C(3)	1.2018(14)	C(1)–N(1)–Li	90.13(8)
O–Li	1.9518(19)	C(1)–N(2)–Li	83.13(7)
Li–N(2)#1	2.0580(19)	C(10)–N(1)–Li	149.12(8)
N(2)–Li#1	2.0580(19)	C(1)–N(2)–C(16)	118.73(8)
N(1)–C(10)	1.4560(12)		
N(2)–C(16)	1.4646(12)		

Table 18 Crystal data and structure refinement of **5**

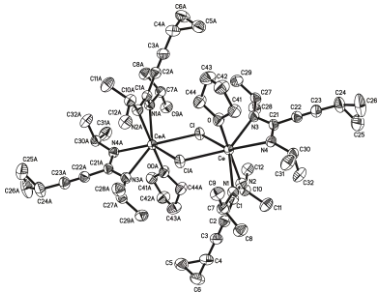

Identification code	ip310
Empirical formula	$C_{28}H_{46}CeClN_4O$
Formula weight	630.26
Temperature	153(2) K
Wavelength	0.71073 Å
Crystal system	Triclinic
Space group	P-1
Unit cell dimensions	a = 10.051(2) Å α= 82.71(3)°
	b = 11.371(2) Å β= 83.10(3)°
	c = 14.512(3) Å γ = 73.88(3)°
Volume	1574.3(5) $Å^3$
Z	2
Density (calculated)	1.330 Mg/m^3
Absorption coefficient	1.555 mm^{-1}
F(000)	650
Crystal size	0.60 x 0.50 x 0.46 mm^3
Theta range for data collection	2.12 to 28.28°
Index ranges	$-13 \leq h \leq 13$, $-14 \leq k \leq 15$, $-19 \leq l \leq 19$
Reflections collected	16986
Independent reflections	7771 [R(int) = 0.0620]
Completeness to theta = 28.00°	99.5 %
Absorption correction	None
Refinement method	Full-matrix least-squares on F^2
Data / restraints / parameters	7771 / 0 / 325
Goodness-of-fit on F^2	1.035
Final R indices [I>2sigma(I)]	R1 = 0.0404, wR2 = 0.1071
R indices (all data)	R1 = 0.0458, wR2 = 0.1100
Extinction coefficient	0.0452(19)
Largest diff. peak and hole	0.954 and -1.967 $e.Å^{-3}$

Table 19 Selected bond lengths [Å] and angles [°] of **5**

Ce–N(1)	2.516(3)	N(4)–Ce–N(3)	53.93(9)
Ce–N(2)	2.456(3)	N(2)–Ce–N(1)	54.14(9)
Ce–N(3)	2.515(3)	Cl–Ce–Cl#1	73.41(3)
Ce–N(4)	2.491(3)	O–Ce–Cl	100.51(7)
Cl–Ce	2.8335(11)	N(1)–C(1)–N(2)	116.2(3)
Ce–Cl#1	2.9223(12)	N(3)–C(21)–N(4)	116.8(3)
Ce–O	2.540(2)	N(2)–Ce–Cl	93.09(7)
N(1)–C(1)	1.328(4)	N(4)–Ce–Cl	135.95(7)
N(2)–C(1)	1.337(4)	N(3)–Ce–Cl	82.76(7)
N(3)–C(21)	1.332(4)	N(1)–Ce–Cl	127.98(7)
N(4)–C(21)	1.334(4)	N(2)–Ce–N(4)	91.70(9)
C(1)–C(2)	1.444(5)	N(2)–Ce–N(3)	105.88(10
C(2)–C(3)	1.189(5)		

Table 20 Crystal data and structure refinement of **6**

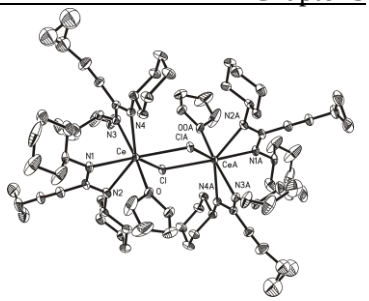

Identification code	magd76
Empirical formula	$C_{80}H_{124}Ce_2Cl_2N_8O_2$
Formula weight	1581.01
Temperature	293(2) K
Wavelength	1.54184 Å
Crystal system	Monoclinic
Space group	$P2_1/c$
Unit cell dimensions	a = 11.25710(10) Å α= 90°
	b = 19.86380(10) Å β= 99.3860(10)°
	c = 19.26360(10) Å γ = 90°
Volume	4249.84(5) $Å^3$
Z	2
Density (calculated)	1.235 Mg/m^3
Absorption coefficient	9.090 mm^{-1}
F(000)	1652
Crystal size	0.14 x 0.08 x 0.07 mm^3
Theta range for data collection	3.22 to 75.66°
Index ranges	$-14 \leq h \leq 12$, $-24 \leq k \leq 24$, $-24 \leq l \leq 24$
Reflections collected	146163
Independent reflections	8784 [R(int) = 0.0414]
Completeness to theta = 75.66°	99.7 %
Absorption correction	Semi-empirical from equivalents
Max. and min. transmission	0.5687 and 0.3626
Refinement method	Full-matrix least-squares on F^2
Data / restraints / parameters	8784 / 0 / 422
Goodness-of-fit on F^2	1.039
Final R indices [I>2sigma(I)]	R1 = 0.0274, wR2 = 0.0705
R indices (all data)	R1 = 0.0278, wR2 = 0.0709
Largest diff. peak and hole	0.595 and -0.851 $e.Å^{-3}$

Table 21 Selected bond lengths [Å] and angles [°] of **6**

Ce–N(4)	2.4616(17)	N(2)–Ce–N(1)	53.42(6)
Ce–N(2)	2.4873(17)	N(4)–Ce–N(3)	54.05(6)
Ce–N(3)	2.5196(17)	Cl–Ce–Cl#1	74.277(14)
Ce–O	2.5526(15)	N(4)–Ce–N(2)	137.05(6)
Ce–N(1)	2.5821(17)	N(4)–Ce–N(1)	87.57(6)
Ce–Cl#1	2.9057(4)	N(4)–Ce–Cl	124.40(4)
Cl–Ce#1	2.9057(4)	N(2)–Ce–Cl	84.75(4)
N(1)–C(1)	1.333(3)	N(3)–Ce–Cl	89.32(4)
N(1)–C(7)	1.471(3)	O–Ce–Cl	105.65(4)
N(2)–C(1)	1.335(3)	Ce–Cl–Ce#1	105.722(14)
C(1)–C(2)	1.459(3)	C(1)–N(1)–Ce	90.93(12)
C(2)–C(3)	1.195(3)	N(1)–C(1)–N(2)	117.44(18)

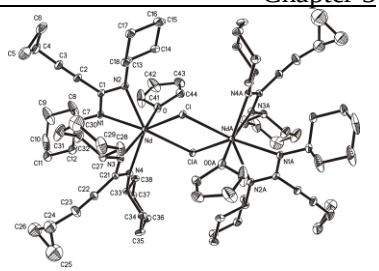

Table 22 Crystal data and structure refinement of **7**

Identification code	ip267
Empirical formula	$C_{80}H_{124}Cl_2N_8Nd_2O_2$
Formula weight	1589.25
Temperature	153(2) K
Wavelength	0.71073 Å
Crystal system	Monoclinic
Space group	$P2_1/c$
Unit cell dimensions	a = 11.290(2) Å α= 90° b = 19.824(4) Å β= 99.86(3)° c = 19.209(4) Å γ = 90°
Volume	4235.7(15) $Å^3$
Z	2
Density (calculated)	1.246 Mg/m^3
Absorption coefficient	1.321 mm^{-1}
F(000)	1660
Crystal size	0.60 x 0.43 x 0.37 mm^3
Theta range for data collection	2.05 to 29.25°
Index ranges	$-15 \leq h \leq 15$, $-27 \leq k \leq 26$, $-22 \leq l \leq 26$
Reflections collected	31182
Independent reflections	11375 [R(int) = 0.0356]
Completeness to theta = 29.25°	98.6 %
Absorption correction	None
Refinement method	Full-matrix least-squares on F^2
Data / restraints / parameters	11375 / 0 / 422
Goodness-of-fit on F^2	0.992
Final R indices [I>2sigma(I)]	R1 = 0.0341, wR2 = 0.0847
R indices (all data)	R1 = 0.0461, wR2 = 0.0882
Largest diff. peak and hole	0.624 and -2.455 $e.Å^{-3}$

Table 23 Selected bond lengths [Å] and angles [°] of **7**

Nd–N(4)	2.425(2)	N(4)–Nd–N(2)	137.12(7)
Nd–N(2)	2.450(2)	N(4)–Nd–N(3)	54.93(7)
Nd–N(3)	2.483(2)	N(2)–Nd–N(3)	100.90(8)
Nd–O	2.515(2)	N(4)–Nd–N(1)	86.91(7)
Nd–N(1)	2.555(2)	N(2)–Nd–N(1)	54.12(7)
Nd–Cl	2.8069(8)	Cl–Nd–Cl#1	73.88(2)
Nd–Cl#1	2.8730(7)	N(4)–Nd–Cl	124.80(6)
Cl–Nd#1	2.8730(7)	N(2)–Nd–Cl	84.72(5)
N(1)–C(1)	1.325(3)	N(3)–Nd–Cl	89.72(6)
N(1)–C(7)	1.464(3)	O–Nd–Cl	106.51(5)
N(2)–C(1)	1.339(3)	N(1)–C(1)–N(2)	117.6(2)
N(4)–C(21)	1.325(3)	N(4)–C(21)–N(3)	116.7(2)
N(3)–C(21)	1.336(3)	O–Nd–Cl#1	74.84(5)
C(1)–C(2)	1.457(4)	Nd–Cl–Nd#1	106.12(2)
C(2)–C(3)	1.186(4)		

Table 24 Crystal data and structure refinement of **8**

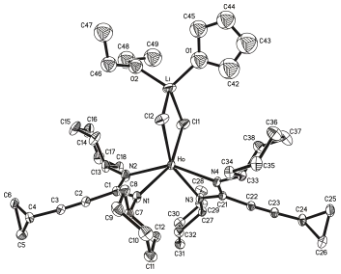

Identification code	ip288
Empirical formula	$C_{44}H_{72}Cl_2HoLiN_4O_2$
Formula weight	931.83
Temperature	153(2) K
Wavelength	0.71073 Å
Crystal system	Monoclinic
Space group	$P2_1/n$
Unit cell dimensions	a = 10.473(2) Å α= 90° b = 29.334(6) Å β= 91.61(3)° c = 15.009(3) Å γ = 90°
Volume	4609.2(16) $Å^3$
Z	4
Density (calculated)	1.343 Mg/m^3
Absorption coefficient	1.870 mm^{-1}
F(000)	1936
Crystal size	0.46 x 0.38 x 0.22 mm^3
Theta range for data collection	2.34 to 28.28°
Index ranges	$-13 \leq h \leq 13$, $-39 \leq k \leq 39$, $-20 \leq l \leq 20$
Reflections collected	31110
Independent reflections	11314 [R(int) = 0.0777]
Completeness to theta = 28.28°	99.2 %
Absorption correction	Sphere
Max. and min. transmission	0.2956 and 0.2774
Refinement method	Full-matrix least-squares on F^2
Data / restraints / parameters	11314 / 44 / 458
Goodness-of-fit on F^2	0.858
Final R indices [I>2sigma(I)]	R1 = 0.0428, wR2 = 0.0817
R indices (all data)	R1 = 0.0891, wR2 = 0.0902
Largest diff. peak and hole	0.941 and -1.514 $e.Å^{-3}$

Table 25 Selected bond lengths [Å] and angles [°] of **8**

Ho–N(1)	2.328(4)	N(1)–Ho–N(3)	100.14(14)
Ho–N(3)	2.331(4)	N(1)–Ho–N(2)	57.70(13)
Ho–N(2)	2.352(3)	N(3)–Ho–N(2)	101.10(13)
Ho–N(4)	2.359(3)	N(1)–Ho–N(4)	100.91(13)
Ho–Cl(1)	2.6428(14)	N(3)–Ho–N(4)	57.45(12)
Ho–Cl(2)	2.6574(1	Cl(1)–Ho–Cl(2)	83.70(5)
Cl(1)–Li	2.348(12)	Li–Cl(1)–Ho	89.6(3)
Cl(2)–Li	2.368(12)	Li–Cl(2)–Ho	88.8(3)
N(1)–C(1)	1.336(6)	O(1)–Li–O(2)	105.5(5)
N(2)–C(1)	1.335(6)	O(1)–Li–Cl(1)	112.9(5)
N(3)–C(21)	1.329(5)	O(2)–Li–Cl(1)	114.7(6)
N(4)–C(21)	1.342(5)	O(1)–Li–Cl(2)	111.6(7)
Li–O(1)	1.880(12)	O(2)–Li–Cl(2)	115.1(5)
Li–O(2)	1.954(12)	Cl(1)–Li–Cl(2)	97.2(4)

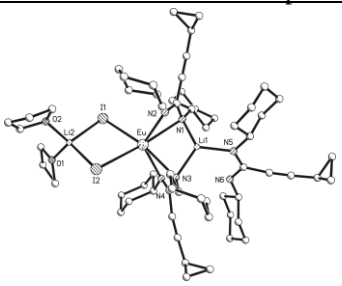

Table 26 Crystal data and structure refinement of **9**

Identification code	ip301
Empirical formula	$C_{62}H_{97}EuI_2Li_2N_6O_2$
Formula weight	1378.10
Temperature	153(2) K
Wavelength	0.71073 Å
Crystal system	Monoclinic
Space group	$P2_1/n$
Unit cell dimensions	a = 13.048(3) Å α= 90° b = 23.242(5) Å β= 99.78(3)° c = 22.028(4) Å γ = 90°
Volume	6583(2) $Å^3$
Z	4
Density (calculated)	1.390 Mg/m^3
Absorption coefficient	1.933 mm^{-1}
F(000)	2808
Crystal size	0.42 x 0.32 x 0.29 mm^3
Theta range for data collection	2.16 to 29.29°
Index ranges	$-17 \leq h \leq 17, -31 \leq k \leq 31, -30 \leq l \leq 30$
Reflections collected	49305
Independent reflections	17167 [R(int) = 0.0666]
Completeness to theta = 29.29°	95.5 %
Absorption correction	None
Refinement method	Full-matrix least-squares on F^2
Data / restraints / parameters	17167 / 51 / 668
Goodness-of-fit on F^2	0.892
Final R indices [I>2sigma(I)]	R1 = 0.0454, wR2 = 0.0968
R indices (all data)	R1 = 0.0802, wR2 = 0.1054
Largest diff. peak and hole	2.118 and -1.738 $e.Å^{-3}$

Table 27 Selected bond lengths [Å] and angles [°] of **9**

Eu–N(4)	2.556(3)	N(2)–Eu–N(1)	51.34(9)
Eu–N(2)	2.586(3)	N(4)–Eu–N(3)	52.21(9)
Eu–N(3)	2.655(3)	I(1)–Eu–I(2)	85.646(13)
Eu–N(1)	2.664(3)	N(3)–Eu–N(1)	82.48(9)
Eu–Li(1)	3.006(6)	N(1)–Li(1) –N(3)	118.4(3)
Eu–I(1)	3.2240(9)	I(2)–Li(2) –I(1)	105.9(2)
Eu–I(2)	3.2321(6)	N(5)–Li(1)–N(1)	119.2(4)
I(1)–Li(2)	2.781(7)	N(5)–Li(1)–N(3)	118.0(3)
I(2)–Li(2)	2.717(7)	N(5)–C(41)–N(6)	120.6(3)
Li(1)–N(5)	2.004(7)	N(2)–C(1)–N(1)	117.4(3)
Li(1)–N(1)	2.034(7)	N(4)–C(21)–N(3)	118.2(3)
Li(1)–N(3)	2.047(7)	O(2)–Li(2)–O(1)	107.4(4)
N(5)–C(41)	1.286(5)	Li(2)–I(2)–Eu	84.65(15)
N(6)–C(41)	1.356(5)	Li(2)–I(1)–Eu	83.80(15)

Table 28 Crystal data and structure refinement of **10**

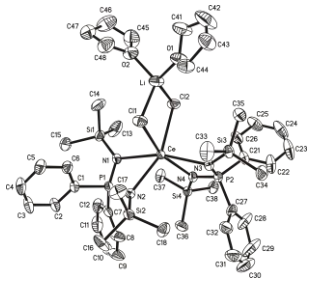

Identification code	ip223
Empirical formula	$C_{44}H_{72}CeCl_2LiN_4O_2P_2Si_4$
Formula weight	1081.32
Temperature	153(2) K
Wavelength	0.71073 Å
Crystal system	Monoclinic
Space group	$P2_1/n$
Unit cell dimensions	a = 11.117(2) Å α= 90° b = 36.425(7) Å β= 96.70(3)° c = 13.538(3) Å γ = 90°
Volume	5444.3(19) $Å^3$
Z	4
Density (calculated)	1.319 Mg/m^3
Absorption coefficient	1.118 mm^{-1}
F(000)	2244
Crystal size	0.40 x 0.40 x 0.30 mm^3
Theta range for data collection	1.88 to 29.18°
Index ranges	$-15 \leq h \leq 15$, $-45 \leq k \leq 49$, $-18 \leq l \leq 18$
Reflections collected	47566
Independent reflections	14020 [R(int) = 0.0758]
Completeness to theta = 29.18°	95.1 %
Absorption correction	None
Refinement method	Full-matrix least-squares on F^2
Data / restraints / parameters	14020 / 0 / 569
Goodness-of-fit on F^2	0.989
Final R indices [I>2sigma(I)]	R1 = 0.0394, wR2 = 0.0875
R indices (all data)	R1 = 0.0577, wR2 = 0.0937
Largest diff. peak and hole	0.692 and -1.064 $e.Å^{-3}$

Table 29 Selected bond lengths [Å] and angles [°] of **10**

Ce–N(4)	2.483(2)	N(2)–Ce–N(1)	60.96(7)
Ce–N(2)	2.501(2)	N(4)–Ce–N(3)	60.80(7)
Ce–N(1)	2.556(2)	Cl(2)–Ce–Cl(1)	79.01(3)
Ce–N(3)	2.558(2)	N(1)–P(1)–N(2)	107.21(12)
Ce–Cl(2)	2.8065(8)	N(4)–P(2)–N(3)	106.21(12)
Ce–Cl(1)	2.8088(9)	Cl(1)–Li–Cl(2)	97.7(2)
Li–O(1)	1.939(6)	O(1)–Li–O(2)	99.1(3)
Li–O(2)	1.946(7)	P(1)–N(1)–Si(1)	133.02(14)
Li–Cl(1)	2.358(6)	P(1)–N(2)–Si(2)	132.24(14)
Li–Cl(2)	2.385(6)	P(2)–N(3)–Si(3)	129.71(14)
P(1)–N(1)	1.593(2)	P(2)–N(4)–Si(4)	131.31(15)
P(1)–N(2)	1.594(2)	N(4)–Ce–N(2)	100.72(7)
P(2)–N(4)	1.593(2)	N(4)–Ce–N(1)	106.17(7)
P(2)–N(3)	1.597(2)	N(2)–Ce–N(3)	108.26(7)
Si(1)–N(1)	1.720(2)	N(1)–Ce–N(3)	162.73(7)

Table 30 Crystal data and structure refinement of **11**

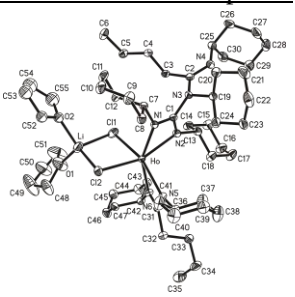

Identification code	ip360
Empirical formula	$C_{55}H_{100}Cl_2HoLiN_6O_2$
Formula weight	1120.18
Temperature	153(2) K
Wavelength	0.71073 Å
Crystal system	Triclinic
Space group	P-1
Unit cell dimensions	a = 12.909(3) Å α= 100.67(3)° b = 15.095(3) Å β= 97.20(3)° c = 16.786(3) Å γ = 109.50(3)°
Volume	2967.5(11) $Å^3$
Z	2
Density (calculated)	1.254 Mg/m^3
Absorption coefficient	1.465 mm^{-1}
F(000)	1184
Crystal size	0.34 x 0.20 x 0.12 mm^3
Theta range for data collection	2.32 to 26.37°
Index ranges	$-16 \leq h \leq 16$, $-17 \leq k \leq 18$, $-20 \leq l \leq 20$
Reflections collected	27555
Independent reflections	12090 [R(int) = 0.0747]
Completeness to theta = 26.37°	99.7 %
Absorption correction	None
Refinement method	Full-matrix least-squares on F^2
Data / restraints / parameters	12090 / 22 / 625
Goodness-of-fit on F^2	0.979
Final R indices [I>2sigma(I)]	R1 = 0.0473, wR2 = 0.0611
R indices (all data)	R1 = 0.0765, wR2 = 0.0652
Largest diff. peak and hole	0.947 and -1.512 $e.Å^{-3}$

Table 31 Selected bond lengths [Å] and angles [°] of **11**

Ho–N(5)	2.328(3)	N(5)–Ho–N(6)	57.38(11)
Ho–N(6)	2.340(3)	N(2)–Ho–N(1)	57.03(11)
Ho–N(2)	2.342(4)	Cl(1)–Ho–Cl(2)	85.19(5)
Ho–N(1)	2.355(3)	Cl(2)–Li–Cl(1)	99.9(3)
Ho–Cl(1)	2.6320(13)	O(1)–Li–O(2)	112.3(5)
Ho–Cl(2)	2.6438(15)	N(1)–C(1)–N(2)	115.3(4)
N(1)–C(1)	1.327(5)	N(6)–C(31)–N(5)	113.9(4)
N(2)–C(1)	1.328(5)	Li–Cl(1)–Ho	86.8(2)
N(3)–C(1)	1.430(5)	Li–Cl(2)–Ho	88.1(2)
N(3)–C(2)	1.403(5)	N(1)–C(1)–N(3)	121.6(3)
C(2)–C(3)	1.520(6)	N(2)–C(1)–N(3)	123.1(4)
C(3)–C(4)	1.530(5)	N(5)–Ho–N(2)	99.92(12)
C(31)–C(32)	1.521(6)	N(6)–Ho–N(2)	102.42(12)
Cl(1)–Li	2.369(10)	N(5)–Ho–N(1)	107.90(11)
O(1)–Li	1.907(9)	N(6)–Ho–N(1)	154.52(11)

Table 32 Crystal data and structure refinement of **15**

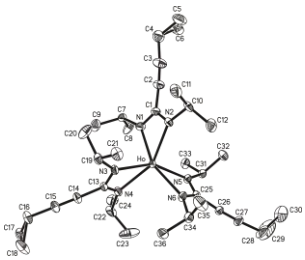

Identification code	ip298
Empirical formula	$C_{36}H_{57}HoN_6$
Formula weight	738.81
Temperature	153(2) K
Wavelength	0.71073 Å
Crystal system	Triclinic
Space group	P-1
Unit cell dimensions	a = 9.776(2) Å α= 101.28(3)° b = 13.149(3) Å β= 105.35(3)° c = 16.983(3) Å γ = 108.19(3)°
Volume	1905.6(7) $Å^3$
Z	2
Density (calculated)	1.288 Mg/m^3
Absorption coefficient	2.106 mm^{-1}
F(000)	764
Crystal size	0.40 x 0.40 x 0.20 mm^3
Theta range for data collection	2.31 to 29.21°
Index ranges	$-13 \leq h \leq 13$, $-18 \leq k \leq 18$, $-19 \leq l \leq 23$
Reflections collected	21302
Independent reflections	10209 [R(int) = 0.0600]
Completeness to theta = 29.21°	98.7 %
Absorption correction	None
Refinement method	Full-matrix least-squares on F^2
Data / restraints / parameters	10209 / 38 / 461
Goodness-of-fit on F^2	1.045
Final R indices [I>2sigma(I)]	R1 = 0.0343, wR2 = 0.0890
R indices (all data)	R1 = 0.0379, wR2 = 0.0907
Extinction coefficient	0.0091(7)
Largest diff. peak and hole	2.496 and -1.758 $e.Å^{-3}$

Table 33 Selected bond lengths [Å] and angles [°] of **15**

Ho–N(5)	2.342(2)	N(3)–Ho–N(4)	57.74(9)
Ho–N(3)	2.348(2)	N(2)–Ho–N(1)	57.08(9)
Ho–N(2)	2.351(3)	N(5)–Ho–N(6)	57.14(8)
Ho–N(4)	2.353(3)	N(5)–Ho–N(3)	153.11(10)
Ho–N(1)	2.359(3)	N(5)–Ho–N(2)	98.77(10)
Ho–N(6)	2.383(3)	N(3)–Ho–N(2)	103.76(10)
N(1)–C(1)	1.312(4)	N(5)–Ho–N(4)	106.03(10)
N(2)–C(1)	1.327(4)	N(2)–Ho–N(4)	150.92(10)
N(3)–C(13)	1.333(4)	N(5)–Ho–N(1)	104.51(10)
N(4)–C(13)	1.331(4)	N(3)–Ho–N(6)	101.51(9)
N(5)–C(25)	1.333(4)	N(2)–Ho–N(6)	107.47(10)
N(6)–C(25)	1.324(3)	N(1)–C(1)–N(2)	117.0(3)
C(1)–C(2)	1.461(5)	N(4)–C(13)–N(3)	116.9(3)
C(2)–C(3)	1.182(6)	N(6)–C(25)–N(5)	116.6(3)

Table 34 Crystal data and structure refinement of **22**

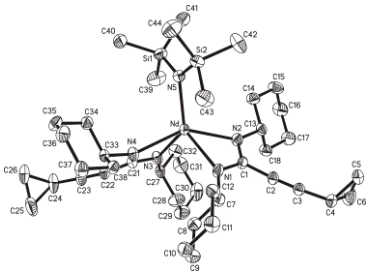

Identification code	ip377
Empirical formula	$C_{42}H_{72}N_5NdSi_2$
Formula weight	847.47
Temperature	153(2) K
Wavelength	0.71073 Å
Crystal system	Orthorhombic
Space group	Pbca
Unit cell dimensions	a = 17.981(4) Å α= 90° b = 30.061(6) Å β= 90° c = 16.598(3) Å γ = 90°
Volume	8972(3) $Å^3$
Z	8
Density (calculated)	1.255 Mg/m^3
Absorption coefficient	1.244 mm^{-1}
F(000)	3575
Crystal size	0.56 x 0.43 x 0.38 mm^3
Theta range for data collection	2.36 to 28.28°
Index ranges	$-22 \leq h \leq 23$, $-40 \leq k \leq 40$, $-22 \leq l \leq 20$
Reflections collected	48451
Independent reflections	10844 [R(int) = 0.0642]
Completeness to theta = 28.28°	97.4 %
Absorption correction	None
Refinement method	Full-matrix least-squares on F^2
Data / restraints / parameters	10844 / 0 / 451
Goodness-of-fit on F^2	0.963
Final R indices [I>2sigma(I)]	R1 = 0.0346, wR2 = 0.0790
R indices (all data)	R1 = 0.0576, wR2 = 0.0857
Largest diff. peak and hole	0.743 and -1.255 $e.Å^{-3}$

Table 34 Selected bond lengths [Å] and angles [°] of **22**

Nd–N(5)	2.323(2)	N(1)–Nd–N(2)	55.60(7)
Nd–N(3)	2.406(2)	N(3)–Nd–N(4)	55.56(7)
Nd–N(1)	2.420(2)	N(5)–Nd–N(3)	129.16(8)
Nd–N(2)	2.438(2)	N(5)–Nd–N(1)	129.62(8)
Nd–N(4)	2.440(2)	N(5)–Nd–N(4)	106.45(7)
Si(1)–N(5)	1.703(2)	N(5)–Nd–N(2)	109.86(7)
Si(2)–N(5)	1.705(2)	N(5)–Nd–N(4)	106.45(7)
N(1)–C(1)	1.332(3)	N(1)–Nd–N(4)	98.61(7)
N(2)–C(1)	1.336(3)	N(2)–Nd–N(4)	143.63(7)
N(3)–C(21)	1.328(3)	Si(1)–N(5)–Nd	117.23(11)
N(4)–C(21)	1.329(3)	Si(2)–N(5)–Nd	117.40(11)
C(1)–C(2)	1.447(4)	N(1)–C(1)–N(2)	116.2(2)
C(2)–C(3)	1.183(4)	N(3)–C(21)–N(4)	116.5(2)
C(3)–C(4)	1.438(4)		

Table36 Crystal data and structure refinement of **23**

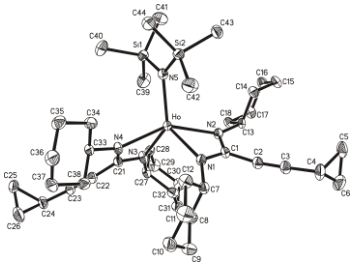

Identification code	ip439
Empirical formula	$C_{42}H_{72}HoN_5Si_2$
Formula weight	868.16
Temperature	133(2) K
Wavelength	0.71073 Å
Crystal system	Orthorhombic
Space group	Pbca
Unit cell dimensions	a = 16.537(3) Å α= 90°
	b = 17.882(4) Å β= 90°
	c = 29.726(6) Å γ = 90°
Volume	8791(3) $Å^3$
Z	8
Density (calculated)	1.312 Mg/m^3
Absorption coefficient	1.888 mm^{-1}
F(000)	3632
Crystal size	0.60 x 0.48 x 0.23 mm^3
Theta range for data collection	2.17 to 26.37°
Index ranges	$-19 \leq h \leq 20, -22 \leq k \leq 22, -28 \leq l \leq 37$
Reflections collected	19240
Independent reflections	8497 [R(int) = 0.0339]
Completeness to theta = 26.37°	94.5 %
Absorption correction	Sphere
Max. and min. transmission	0.2343 and 0.2129
Refinement method	Full-matrix least-squares on F^2
Data / restraints / parameters	8497 / 0 / 451
Goodness-of-fit on F^2	1.010
Final R indices [I>2sigma(I)]	R1 = 0.0305, wR2 = 0.0688
R indices (all data)	R1 = 0.0451, wR2 = 0.0728
Largest diff. peak and hole	0.629 and -0.944 $e.Å^{-3}$

Table 37 Selected bond lengths [Å] and angles [°] of **23**

Ho–N(5)	2.224(3)	N(5)–Ho–N(1)	126.46(9)
Ho–N(1)	2.303(2)	N(5)–Ho–N(3)	130.48(9)
Ho–N(3)	2.327(2)	N(1)–Ho–N(3)	103.06(10)
Ho–N(4)	2.344(2)	N(5)–Ho–N(4)	107.45(9)
Ho–N(2)	2.348(2)	N(1)–Ho–N(4)	101.05(8)
Si(1)–N(5)	1.712(3)	N(3)–Ho–N(4)	57.95(8)
Si(2)–N(5)	1.714(2)	N(5)–Ho–N(2)	105.49(9)
C(1)–N(2)	1.327(4)	N(1)–Ho–N(2)	58.20(8)
C(1)–N(1)	1.334(4)	N(3)–Ho–N(2)	99.26(8)
C(1)–C(2)	1.447(4)	N(4)–Ho–N(2)	147.06(9)
C(2)–C(3)	1.193(4)	N(2)–C(1)–N(1)	116.4(2)
C(3)–C(4)	1.436(4)	N(3)–C(21)–N(4)	115.7(2)
C(21)–N(3)	1.333(4)		
C(21)–N(4)	1.340(4)		

Table 38 Crystal data and structure refinement of **24**

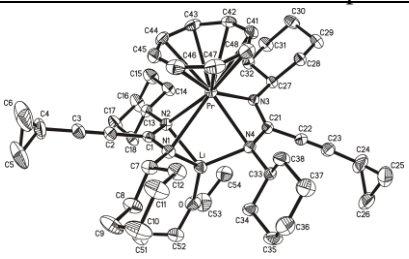

Identification code	ip400
Empirical formula	$C_{48}H_{72}LiN_4OPr$
Formula weight	868.95
Temperature	153(2) K
Wavelength	0.71073 Å
Crystal system	Orthorhombic
Space group	Pbca
Unit cell dimensions	a = 21.425(4) Å α= 90°
	b = 20.113(4) Å β= 90°
	c = 21.502(4) Å γ = 90°
Volume	9266(3) $Å^3$
Z	8
Density (calculated)	1.246 Mg/m^3
Absorption coefficient	1.089 mm^{-1}
F(000)	3664
Crystal size	0.46 x 0.35 x 0.14 mm^3
Theta range for data collection	2.15 to 26.37°
Index ranges	$-26 \leq h \leq 26$, $-25 \leq k \leq 21$, $-24 \leq l \leq 26$
Reflections collected	41749
Independent reflections	9346 [R(int) = 0.0663]
Completeness to theta = 26.37°	98.7 %
Absorption correction	Sphere
Max. and min. transmission	0.4912 and 0.4819
Refinement method	Full-matrix least-squares on F^2
Data / restraints / parameters	9346 / 0 / 496
Goodness-of-fit on F^2	1.014
Final R indices [I>2sigma(I)]	R1 = 0.0355, wR2 = 0.0790
R indices (all data)	R1 = 0.0515, wR2 = 0.0839
Largest diff. peak and hole	0.887 and -1.490 $e.Å^{-3}$

Table 39 Selected bond lengths [Å] and angles [°] of **24**

Pr–N(2)	2.569(2)	N(3)–Pr–N(4)	52.39(7)
Pr–N(3)	2.595(2)	N(2)–Pr–N(1)	49.79(7)
Pr–N(4)	2.599(2)	N(2)–Pr–N(3)	88.49(7)
Pr–N(1)	2.771(2)	N(2)–Pr–N(4)	83.43(7)
Li–N(4)	2.106(5)	N(3)–Pr–N(1)	116.65(7)
Li–N(2)	2.130(6)	N(4)–Pr–N(1)	74.53(7)
Li–N(1)	2.152(6)	O–Li–N(4)	125.5(3)
Pr–C(43)	2.697(3)	O–Li–N(2)	114.9(2)
Pr–C(44)	2.707(3)	N(4)–Li–N(2)	108.5(2)
Pr–C(47)	2.715(3)	O–Li–N(1)	128.1(3)
Pr–C(42)	2.731(3)	N(4)–Li–N(1)	99.7(2)
Pr–C(45)	2.734(3)	N(2)–Li–N(1)	63.56(16)
Pr–C(48)	2.735(3)	N(1)–C(1)–N(2)	115.7(2)
Pr–C(41)	2.742(3)	N(3)–C(21)–N(4)	118.5(2)

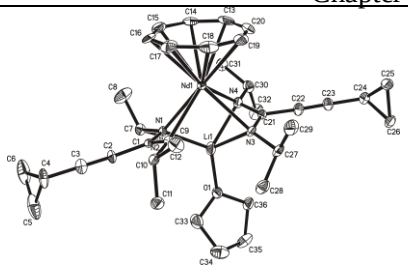

Table 40 Crystal data and structure refinement of **25**

Identification code	ip359
Empirical formula	$C_{36}H_{54}LiN_4NdO$
Formula weight	710.01
Temperature	153(2) K
Wavelength	0.71073 Å
Crystal system	Orthorhombic
Space group	$P2_12_12_1$
Unit cell dimensions	a = 17.592(3) Å α= 90°
	b = 20.156(4) Å β= 90°
	c = 20.206(4) Å γ = 90°
Volume	7165(2) $Å^3$
Z	8
Density (calculated)	1.316 Mg/m^3
Absorption coefficient	1.481 mm^{-1}
F(000)	2952
Crystal size	0.36 x 0.31 x 0.16 mm^3
Theta range for data collection	2.25 to 26.37°
Index ranges	$-21 \leq h \leq 21$, $-25 \leq k \leq 23$, $-23 \leq l \leq 25$
Reflections collected	40920
Independent reflections	14633 [R(int) = 0.0849]
Completeness to theta = 26.37°	99.9 %
Absorption correction	Sphere
Max. and min. transmission	0.4912 and 0.4819
Refinement method	Full-matrix least-squares on F^2
Data / restraints / parameters	14633 / 0 / 775
Goodness-of-fit on F^2	0.917
Final R indices [I>2sigma(I)]	R1 = 0.0442, wR2 = 0.0771
R indices (all data)	R1 = 0.0641, wR2 = 0.0815
Absolute structure parameter	0.490(14)
Largest diff. peak and hole	0.843 and -1.068 e.$Å^{-3}$

Table 41 Selected bond lengths [Å] and angles [°] of **25**

Nd(1)–N(3)	2.549(5)	N(2)–Nd(1)–N(1)	52.32(14)
Nd(1)–N(2)	2.555(5)	N(3)–Nd(1)–N(4)	49.78(16)
Nd(1)–N(1)	2.603(4)	N(2)–Nd(1)–N(4)	112.77(17)
Nd(1)–N(4)	2.771(5)	N(1)–Nd(1)–N(4)	75.56(16)
N(1)–Li(1)	2.048(13)	N(3)–Nd(1)–N(2)	82.71(18)
N(3)–Li(1)	2.175(12)	N(3)–Nd(1)–N(1)	84.62(17)
N(4)–Li(1)	2.152(14)	N(1)–Li(1)–N(4)	103.4(6)
Nd(1)–C(14)	2.684(7)	N(4)–Li(1)–N(3)	62.6(4)
Nd(1)–C(18)	2.701(6)	N(1)–Li(1)–N(3)	110.4(5)
Nd(1)–C(19)	2.702(6)	O(1)–Li(1)–N(1)	121.1(7)
Nd(1)–C(17)	2.709(7)	O(1)–Li(1)–N(4)	130.6(7)
Nd(1)–C(15)	2.709(7)	O(1)–Li(1)–N(3)	114.0(6)
Nd(1)–C(20)	2.720(7)		
Nd(1)–C(16)	2.724(7)		

Table 42 Crystal data and structure refinement of **27**

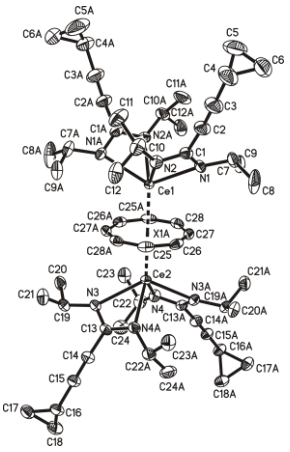

Identification code	ip447
Empirical formula	$C_{56}H_{84}Ce_2N_8$
Formula weight	1149.55
Temperature	153(2) K
Wavelength	0.71073 Å
Crystal system	Monoclinic
Space group	C2/c
Unit cell dimensions	a = 21.938(4) Å α= 90°
	b = 17.320(4) Å β= 112.97(3)°
	c = 16.644(3) Å γ = 90°
Volume	5823(2) $Å^3$
Z	4
Density (calculated)	1.311 Mg/m^3
Absorption coefficient	1.584 mm^{-1}
F(000)	2368
Crystal size	0.57 x 0.18 x 0.17 mm^3
Theta range for data collection	2.28 to 29.23°
Index ranges	$-29 \leq h \leq 30$, $-23 \leq k \leq 23$, $-21 \leq l \leq 22$
Reflections collected	35080
Independent reflections	7841 [R(int) = 0.0551]
Completeness to theta = 29.23°	99.1 %
Absorption correction	None
Refinement method	Full-matrix least-squares on F^2
Data / restraints / parameters	7841 / 0 / 299
Goodness-of-fit on F^2	1.155
Final R indices [I>2sigma(I)]	R1 = 0.0333, wR2 = 0.0806
R indices (all data)	R1 = 0.0367, wR2 = 0.0821
Largest diff. peak and hole	1.347 and -1.886 $e.Å^{-3}$

Table 43 Selected bond lengths [Å] and angles [°] of **27**

Ce(1)–N(2)#1	2.478(2)	Ce(2)–C(26)#1	2.882(3)
Ce(1)–N(2)	2.478(2)	Ce(2)–C(26)	2.882(3)
Ce(1)–N(1)#1	2.521(2)	Ce(2)–C(27)#1	2.890(3)
Ce(1)–N(1)	2.521(2)	Ce(2)–C(27)	2.890(3)
Ce(1)–C(28)	2.862(3)	N(1)–C(1)	1.327(4)
Ce(1)–C(28)#1	2.862(3)	N(2)–C(1)	1.331(4)
Ce(1)–C(27)	2.873(3)	N(2)–Ce(1)–N(1)	54.03(8)
Ce(1)–C(27)#1	2.873(3)	N(2)#1–Ce(1)–N(1)#1	54.03(8)
Ce(1)–C(25)#1	2.884(3)	N(4)#1–Ce(2)–N(3)#1	92.22(8)
Ce(1)–C(25)	2.884(3)	N(4)–Ce(2)–N(3)	92.22(8)
Ce(2)–N(4)	2.453(2)	N(1)–C(1)–N(2)	117.4(2)
Ce(2)–N(4)#1	2.453(2)	N(3)–C(13)–N(4)#1	117.3(2)
Ce(2)–N(3)#1	2.530(2)	N(3)–C(13)–C(14)	122.1(3)
Ce(2)–N(3)	2.530(2)		

Table 44 Crystal data and structure refinement of **28**

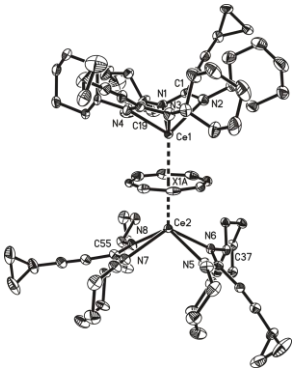

Identification code	ip448
Empirical formula	$C_{80}H_{116}Ce_2N_8$
Formula weight	1470.05
Temperature	143(2) K
Wavelength	0.71073 Å
Crystal system	Monoclinic
Space group	Pn
Unit cell dimensions	a = 21.084(4) Å α= 90° b = 13.758(3) Å β= 102.71(3)° c = 26.383(5) Å γ = 90°
Volume	7465(3) $Å^3$
Z	4
Density (calculated)	1.308 Mg/m^3
Absorption coefficient	1.251 mm^{-1}
F(000)	3072
Crystal size	0.48 x 0.34 x 0.33 mm^3
Theta range for data collection	2.04 to 25.68°
Index ranges	$-25 \leq h \leq 25$, $-14 \leq k \leq 16$, $-32 \leq l \leq 32$
Reflections collected	42721
Independent reflections	23075 [R(int) = 0.0356]
Completeness to theta = 25.68°	94.8 %
Absorption correction	Sphere
Max. and min. transmission	0.4303 and 0.4186
Refinement method	Full-matrix-block least-squares on F^2
Data / restraints / parameters	23075 / 2 / 1622
Goodness-of-fit on F^2	0.972
Final R indices [I>2sigma(I)]	R1 = 0.0268, wR2 = 0.0604
R indices (all data)	R1 = 0.0324, wR2 = 0.0624
Absolute structure parameter	0.530(7)
Largest diff. peak and hole	0.845 and -0.748 e.$Å^{-3}$

Table 45 Selected bond lengths [Å] and angles [°] of **28**

Ce(1)–N(4)	2.438(4)	Ce(2)–N(7)	2.504(4)
Ce(1)–N(2)	2.470(4)	Ce(2)–C(73)	2.852(4)
Ce(1)–N(1)	2.504(4)	Ce(2)–C(79)	2.874(4)
Ce(1)–N(3)	2.528(4)	Ce(2)–C(75)	2.877(4)
Ce(1)–C(80)	2.872(4)	Ce(2)–C(80)	2.881(4)
Ce(1)–C(74)	2.873(4)	Ce(2)–C(74)	2.887(4)
Ce(1)–C(73)	2.879(4)	Ce(2)–C(55)	2.899(4)
Ce(1)–C(19)	2.886(4)	Ce(2)–C(77)	2.904(4)
Ce(1)–C(79)	2.894(4)	Ce(2)–C(76)	2.904(4)
Ce(1)–C(75)	2.901(4)	N(2)–Ce(1)–N(1)	53.88(12)
Ce(1)–C(78)	2.908(4)	N(4)–Ce(1)–N(3)	54.48(12)
Ce(2)–N(5)	2.484(3)	N(8)–Ce(2)–N(7)	53.97(13)
Ce(2)–N(8)	2.502(4)	N(5)–Ce(2)–N(6)	53.90(12)

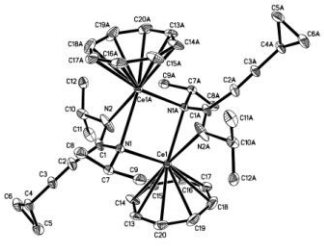

Table 46 Crystal data and structure refinement of **30**

Identification code	magd126
Empirical formula	$C_{40}H_{54}Ce_2N_4$
Formula weight	871.11
Temperature	100(2) K
Wavelength	1.54184 Å
Crystal system	Monoclinic
Space group	$P2_1/c$
Unit cell dimensions	a = 19.23876(16) Å α= 90°
	b = 19.87633(16) Å β= 99.8124(9)°
	c = 9.97581(10) Å γ = 90°
Volume	3758.90(6) $Å^3$
Z	4
Density (calculated)	1.539 Mg/m^3
Absorption coefficient	18.699 mm^{-1}
F(000)	1752
Crystal size	0.28 x 0.08 x 0.06 mm^3
Theta range for data collection	3.22 to 75.90°
Index ranges	$-24 \leq h \leq 24$, $-24 \leq k \leq 24$, $-12 \leq l \leq 10$
Reflections collected	157545
Independent reflections	7809 [R(int) = 0.0744]
Completeness to theta = 75.90°	99.6 %
Absorption correction	Semi-empirical from equivalents
Max. and min. transmission	0.4000 and 0.0775
Refinement method	Full-matrix least-squares on F^2
Data / restraints / parameters	7809 / 54 / 441
Goodness-of-fit on F^2	1.130
Final R indices [I>2sigma(I)]	R1 = 0.0442, wR2 = 0.1077
R indices (all data)	R1 = 0.0462, wR2 = 0.1091
Largest diff. peak and hole	1.229 and -1.555 $e.Å^{-3}$

Table 47 Selected bond lengths [Å] and angles [°] of **30**

Ce(1)–N(2)#1	2.625(5)	N(2)–Ce(1)#1	2.625(5)
Ce(1)–N(1)#1	2.634(4)	N(1)–C(1)	1.350(8)
Ce(1)–N(1)	2.664(4)	N(2)–C(1)	1.321(9)
Ce(1)–C(18)	2.694(7)	N(2)#1–Ce(1)–N(1)#1	51.08(19)
Ce(1)–C(19)	2.694(7)	N(2)#1–Ce(1)–N(1)	81.40(18)
Ce(1)–C(13)	2.702(5)	N(1)#1–Ce(1)–N(1)	89.93(14)
Ce(1)–C(17)	2.705(6)	Ce(1)#1–N(1)–Ce(1)	90.07(14)
Ce(1)–C(14)	2.706(6)	N(2)–C(1)–N(1)	116.2(5)
Ce(1)–C(16)	2.712(6)	N(4)–Ce(2)–N(3)	49.61(13)
Ce(1)–C(20)	2.712(6)	N(4)–Ce(2)–N(3)#2	76.33(14)
Ce(1)–C(15)	2.713(6)	N(3)–Ce(2)–N(3)#2	95.26(13)
N(1)–Ce(1)#1	2.635(4)	C(1)–N(1)–C(7)	117.2(4)

Table 48 Crystal data and structure refinement of **31**

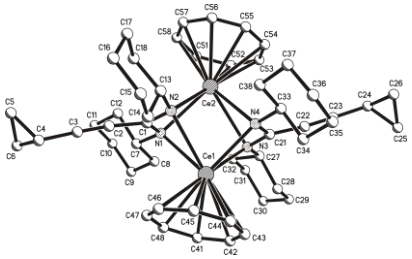

Identification code	magd100
Empirical formula	$C_{52}H_{70}Ce_2N_4$
Formula weight	1031.36
Temperature	100(2) K
Wavelength	1.54184 Å
Crystal system	Monoclinic
Space group	$P2_1/n$
Unit cell dimensions	a = 14.87097(10) Å α= 90°
	b = 20.01756(14) Å β= 93.5556(6)°
	c = 15.58600(8) Å γ = 90°
Volume	4630.72(5) $Å^3$
Z	4
Density (calculated)	1.479 Mg/m^3
Absorption coefficient	15.273 mm^{-1}
F(000)	2104
Crystal size	0.14 x 0.11 x 0.03 mm^3
Theta range for data collection	3.60 to 75.86°
Index ranges	$-18 \leq h \leq 18$, $-23 \leq k \leq 25$, $-19 \leq l \leq 19$
Reflections collected	214859
Independent reflections	9629 [R(int) = 0.0566]
Completeness to theta = 75.86°	99.7 %
Absorption correction	Semi-empirical from equivalents
Max. and min. transmission	0.6572 and 0.2236
Refinement method	Full-matrix least-squares on F^2
Data / restraints / parameters	9629 / 38 / 599
Goodness-of-fit on F^2	1.100
Final R indices [I>2sigma(I)]	R1 = 0.0379, wR2 = 0.0921
R indices (all data)	R1 = 0.0407, wR2 = 0.0939
Largest diff. peak and hole	1.097 and -1.122 $e.Å^{-3}$

Table 49 Selected bond lengths [Å] and angles [°] of **31**

Ce(1)–N(4)	2.648(3)	Ce(2)–N(4)	2.704(3)
Ce(1)–C(45)	2.693(4)	Ce(2)–N(3)	2.817(4)
Ce(1)–C(44)	2.697(4)	N(4)–Ce(1)–N(3)	50.04(10)
Ce(1)–C(48)	2.699(4)	N(4)–Ce(1)–N(1)	94.44(9)
Ce(1)–C(47)	2.699(4)	N(3)–Ce(1)–N(1)	79.18(11)
Ce(1)–N(3)	2.700(3)	N(3)–Ce(1)–N(2)	97.16(10)
Ce(1)–C(46)	2.704(4)	N(1)–Ce(1)–N(2)	48.32(10)
Ce(1)–C(41)	2.706(4)	N(1)–Ce(2)–N(2)	50.18(10)
Ce(1)–C(43)	2.718(4)	N(1)–Ce(2)–N(4)	95.22(9)
Ce(1)–C(42)	2.721(4)	N(2)–Ce(2)–N(4)	73.41(9)
Ce(1)–N(1)	2.731(3)	N(4)–Ce(2)–N(3)	48.33(10)
Ce(1)–N(2)	2.767(3)	C(1)–N(1)–Ce(2)	92.6(2)
Ce(2)–N(1)	2.642(3)	C(1)–N(1)–Ce(1)	85.8(2)
Ce(2)–N(2)	2.666(3	N(2)–C(1)–N(1)	114.1(3)

Table 50 Crystal data and structure refinement of **32**

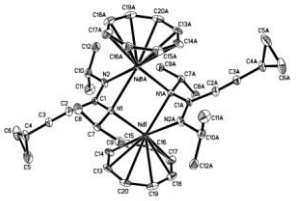

Identification code	magd125
Empirical formula	$C_{40}H_{54}N_4Nd_2$
Formula weight	879.35
Temperature	100(2) K
Wavelength	1.54184 Å
Crystal system	Monoclinic
Space group	$P2_1/c$
Unit cell dimensions	a = 19.11720(10) Å α= 90°
	b = 19.80540(10) Å β= 99.5500(10)°
	c = 9.95780(10) Å γ = 90°
Volume	3718.01(5) $Å^3$
Z	4
Density (calculated)	1.571 Mg/m^3
Absorption coefficient	21.293 mm^{-1}
F(000)	1768
Crystal size	0.12 x 0.10 x 0.06 mm^3
Theta range for data collection	3.24 to 75.80°
Index ranges	$-24 \leq h \leq 24$, $-24 \leq k \leq 24$, $-10 \leq l \leq 12$
Reflections collected	283708
Independent reflections	7724 [R(int) = 0.0652]
Completeness to theta = 75.80°	99.8 %
Absorption correction	Semi-empirical from equivalents
Max. and min. transmission	0.3615 and 0.1843
Refinement method	Full-matrix least-squares on F^2
Data / restraints / parameters	7724 / 48 / 443
Goodness-of-fit on F^2	1.113
Final R indices [I>2sigma(I)]	R1 = 0.0395, wR2 = 0.0960
R indices (all data)	R1 = 0.0398, wR2 = 0.0962
Largest diff. peak and hole	2.307 and -2.782 $e.Å^{-3}$

Table 51 Selected bond lengths [Å] and angles [°] of **32**

Nd(1)–N(2)#1	2.570(4)	Nd(2)–N(4)#2	2.761(4)
Nd(1)–N(1)#1	2.581(4)	N(1)–Nd(1)#1	2.581(4)
Nd(1)–N(1)	2.610(4)	N(2)–C(1)	1.329(6)
Nd(1)–C(18)	2.658(5)	N(1)–C(1)	1.361(6)
Nd(1)–C(19)	2.659(5)	N(1)–Nd(1)#1	2.581(4)
Nd(1)–C(13)	2.671(5)	N(2)–Nd(1)#1	2.571(4)
Nd(1)–C(17)	2.673(5)	N(4)–Nd(2)#2	2.761(4)
Nd(1)–C(15)	2.674(4)	N(2)#1–Nd(1)–N(1)#1	52.85(12)
Nd(1)–C(16)	2.675(5)	N(2)#1–Nd(1)–N(1)	85.93(12)
Nd(1)–C(20)	2.677(5)	N(1)#1–Nd(1)–N(1)	85.33(12)
Nd(1)–C(14)	2.679(5)	N(3)–Nd(2)–N(4)	50.33(13)
Nd(1)–C(1)#1	2.944(4)	N(3)–Nd(2)–N(3)#2	94.52(15)
Nd(2)–N(3)	2.634(6)	N(4)–Nd(2)–N(3)#2	76.10(15)
Nd(2)–N(4)	2.652(4)	N(2)–C(1)–N(1)	116.9(4)

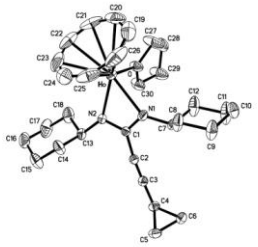

Table 52 Crystal data and structure refinement of **34**

Identification code	ip455
Empirical formula	$C_{30}H_{43}HoN_2O$
Formula weight	612.59
Temperature	133(2) K
Wavelength	0.71073 Å
Crystal system	Monoclinic
Space group	$P2_1/n$
Unit cell dimensions	a = 12.872(3) Å α= 90° b = 14.491(3) Å β= 100.37(3)° c = 15.056(3) Å γ = 90°
Volume	2762.4(10) $Å^3$
Z	4
Density (calculated)	1.473 Mg/m^3
Absorption coefficient	2.888 mm^{-1}
F(000)	1248
Crystal size	0.44 x 0.38 x 0.22 mm^3
Theta range for data collection	1.92 to 29.24°
Index ranges	$-17 \leq h \leq 17$, $-19 \leq k \leq 19$, $-18 \leq l \leq 20$
Reflections collected	30635
Independent reflections	7466 [R(int) = 0.0647]
Completeness to theta = 29.24°	99.2 %
Absorption correction	Sphere
Max. and min. transmission	0.1886 and 0.1648
Refinement method	Full-matrix least-squares on F^2
Data / restraints / parameters	7466 / 48 / 307
Goodness-of-fit on F^2	1.036
Final R indices [I>2sigma(I)]	R1 = 0.0362, wR2 = 0.0843
R indices (all data)	R1 = 0.0461, wR2 = 0.0881
Largest diff. peak and hole	1.899 and -2.651 $e.Å^{-3}$

Table 53 Selected bond lengths [Å] and angles [°] of **34**

Ho–N(2)	2.342(3)	C(2)–C(3)	1.197(4)
Ho–N(1)	2.349(3)	N(2)–Ho–N(1)	57.15(9)
Ho–O	2.397(2)	N(2)–Ho–O	84.13(9)
Ho–C(26)	2.552(5)	N(1)–Ho–O	84.63(10)
Ho–C(23)	2.557(4)	N(2)–Ho–C(26)	132.71(19)
Ho–C(25)	2.557(4)	N(1)–Ho–C(26)	95.80(13)
Ho–C(24)	2.558(4)	O–Ho–C(26)	135.5(2)
Ho–C(22)	2.569(4)	N(1)–C(1)–N(2)	115.5(3)
Ho–C(19)	2.570(5)	C(1)–N(1)–Ho	93.58(18)
Ho–C(21)	2.588(4)	C(1)–N(2)–Ho	93.72(19)
Ho–C(20)	2.598(4)		
C(1)–N(1)	1.324(4)		
C(1)–N(2)	1.329(4)		
C(1)–C(2)	1.453(4)		

Table 54 Crystal data and structure refinement of **35**

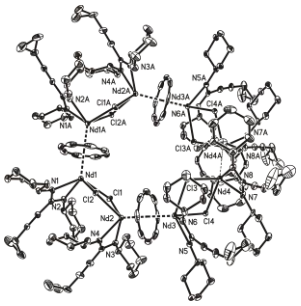

Identification code	magd112
Empirical formula	$C_{190}H_{264}Cl_8N_{16}Nd_8(6*C_7H_8)$
Formula weight	4209.69 + 552.82
Temperature	100(2) K
Wavelength	0.71073 Å
Crystal system	Monoclinic
Space group	C2/c
Unit cell dimensions	a = 44.794(9) Å α= 90° b = 21.617(4) Å β= 125.03(3)° c = 32.326(7) Å γ = 90°
Volume	25631(9) $Å^3$
Z	4
Density (calculated)	1.091 Mg/m^3
Absorption coefficient	1.712 mm^{-1}
F(000)	8528
Crystal size	0.18 x 0.12 x 0.11 mm^3
Theta range for data collection	1.51 to 26.56°
Index ranges	$-55 \leq h \leq 56$, $-26 \leq k \leq 27$, $-40 \leq l \leq 40$
Reflections collected	451720
Independent reflections	26581 [R(int) = 0.0925]
Completeness to theta = 26.56°	99.4 %
Absorption correction	Semi-empirical from equivalents
Max. and min. transmission	1.00000 and 0.52253
Refinement method	Full-matrix least-squares on F^2
Data / restraints / parameters	26581 / 0 / 1001
Goodness-of-fit on F^2	1.056
Final R indices [I>2sigma(I)]	R1 = 0.0478, wR2 = 0.1160
R indices (all data)	R1 = 0.0554, wR2 = 0.1205
Largest diff. peak and hole	2.533 and -1.664 $e.Å^{-3}$

Table 55 Selected bond lengths [Å] and angles [°] of **35**

Nd(1)–N(2)	2.403(4)	Nd(2)–C(42)	2.819(5)
Nd(1)–N(1)	2.424(4)	Nd(2)–C(23)	2.821(4)
Nd(1)–Cl(2)	2.7895(11)	Nd(2)–C(46)	2.824(5)
Nd(1)–C(22)	2.815(5)	Nd(2)–C(48)	2.831(5)
Nd(1)–C(19)#1	2.822(6)	Nd(2)–Cl(2)	2.8324(11)
Nd(1)–C(21)	2.822(5)	Nd(2)–C(47)	2.835(5)
Nd(1)–C(21)#1	2.827(5)	Nd(2)–C(43)	2.836(5)
Nd(1)–C(20)#1	2.829(5)	Nd(2)–C(44)	2.836(5)
Nd(1)–Cl(1)	2.8289(11)	Nd(2)–C(45)	2.851(5)
Nd(1)–C(20)	2.833(5)	N(2)–Nd(1)–N(1)	56.05(12)
Nd(1)–C(22)#1	2.839(5)	N(2)–Nd(1)–Cl(2)	112.87(10)
Nd(2)–N(4)	2.380(4)	N(1)–Nd(1)–Cl(2)	86.89(10)
Nd(2)–N(3)	2.434(4)	Nd(2)–Cl(1)–Nd(1)	104.02(4)
Nd(2)–Cl(1)	2.7684(12)	Nd(1)–Cl(2)–Nd(2)	103.38(4)

Table 56 Crystal data and structure refinement of **40**

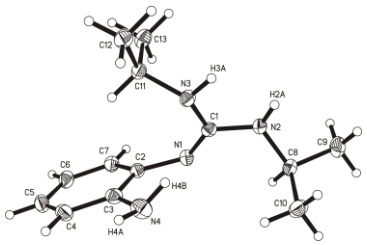

Identification code	magd92
Empirical formula	$C_{13}H_{22}N_4$
Formula weight	234.35
Temperature	100(2) K
Wavelength	1.54184 Å
Crystal system	Monoclinic
Space group	P 1 21/c 1
Unit cell dimensions	a = 13.9953(2) Å α= 90°
	b = 11.12560(10) Å β= 96.2330(10)°
	c = 8.57570(10) Å γ = 90°
Volume	1327.40(3) $Å^3$
Z	4
Density (calculated)	1.173 Mg/m^3
Absorption coefficient	0.565 mm^{-1}
F(000)	512
Crystal size	0.16 x 0.12 x 0.08 mm^3
Theta range for data collection	3.18 to 75.80°
Index ranges	$-17 \leq h \leq 17$, $-13 \leq k \leq 13$, $-10 \leq l \leq 10$
Reflections collected	44933
Independent reflections	2759 [R(int) = 0.0362]
Completeness to theta = 75.80°	99.7 %
Absorption correction	Semi-empirical from equivalents
Max. and min. transmission	0.9562 and 0.9150
Refinement method	Full-matrix least-squares on F^2
Data / restraints / parameters	2759 / 0 / 171
Goodness-of-fit on F^2	1.071
Final R indices [I>2sigma(I)]	R1 = 0.0362, wR2 = 0.0912
R indices (all data)	R1 = 0.0386, wR2 = 0.0930
Extinction coefficient	0.0026(4)
Largest diff. peak and hole	0.212 and -0.221 $e.Å^{-3}$

Table 57 Selected bond lengths [Å] and angles [°] of **40**

N(1)–C(1)	1.3011(13)	C(1)–N(1)–C(2)	123.84(8)
N(1)–C(2)	1.4142(12)	C(1)–N(2)–C(8)	122.83(8)
N(2)–C(1)	1.3704(12)	C(1)–N(3)–C(11)	123.75(8)
N(2)–C(8)	1.4634(12)	N(1)–C(1)–N(2)	119.35(9)
N(3)–C(1)	1.3796(12)	N(1)–C(1)–N(3)	127.33(9)
N(3)–C(11)	1.4733(12)	N(2)–C(1)–N(3)	113.32(8)
N(4)–C(3)	1.3994(14)	C(7)–C(2)–N(1)	118.17(9)
C(2)–C(7)	1.3984(14)	C(3)–C(2)–N(1)	123.05(9)
C(2)–C(3)	1.4138(14)	N(4)–C(3)–C(4)	120.26(10)
C(3)–C(4)	1.4015(15)		

Table 58 Crystal data and structure refinement of **41**

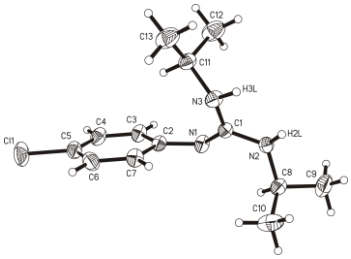

Identification code	ip379
Empirical formula	$C_{26}H_{40}Cl_2N_6$
Formula weight	507.54
Temperature	153(2) K
Wavelength	0.71073 Å
Crystal system	Monoclinic
Space group	$P2_1/n$
Unit cell dimensions	a = 8.5543(17) Å α= 90° b = 25.614(5) Å β= 91.17(3)° c = 13.077(3) Å γ = 90°
Volume	2864.6(10) $Å^3$
Z	4
Density (calculated)	1.177 Mg/m^3
Absorption coefficient	0.251 mm^{-1}
F(000)	1088
Crystal size	0.56 x 0.48 x 0.33 mm^3
Theta range for data collection	2.51 to 29.19°
Index ranges	$-9 \leq h \leq 11$, $-35 \leq k \leq 35$, $-17 \leq l \leq 17$
Reflections collected	21231
Independent reflections	7677 [R(int) = 0.0398]
Completeness to theta = 29.19°	99.1 %
Absorption correction	None
Refinement method	Full-matrix least-squares on F^2
Data / restraints / parameters	7677 / 0 / 323
Goodness-of-fit on F^2	1.036
Final R indices [I>2sigma(I)]	R1 = 0.0526, wR2 = 0.1283
R indices (all data)	R1 = 0.0758, wR2 = 0.1381
Largest diff. peak and hole	0.897 and -0.617 $e.Å^{-3}$

Table 59 Selected bond lengths [Å] and angles [°] of **41**

Cl(1)–C(5)	1.7416(17)	C(6)–C(7)	1.384(2)
N(1)–C(1)	1.3092(19)	C(1)–N(1)–C(2)	121.20(12)
N(1)–C(2)	1.3979(18)	C(1)–N(2)–C(8)	123.05(13)
N(2)–C(1)	1.3558(19)	C(1)–N(3)–C(11)	123.16(13)
N(2)–C(8)	1.4598(19)	N(1)–C(1)–N(2)	119.11(13)
N(3)–C(1)	1.3673(19)	N(1)–C(1)–N(3)	125.90(13)
N(3)–C(11)	1.4657(19)	N(2)–C(1)–N(3)	114.95(13)
C(2)–C(3)	1.398(2)	N(1)–C(2)–C(3)	119.17(14)
C(2)–C(7)	1.401(2)	N(1)–C(2)–C(7)	122.57(13)
C(3)–C(4)	1.384(2)	C(4)–C(5)–C(6)	121.18(15)
C(4)–C(5)	1.373(3)	C(4)–C(5)–Cl(1)	119.50(14)
C(5)–C(6)	1.386(3)		

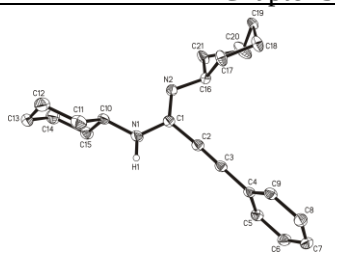

Table 60 Crystal data and structure refinement of **46**

Identification code	ip376
Empirical formula	$C_{21}H_{28}N_2$
Formula weight	308.45
Temperature	153(2) K
Wavelength	0.71073 Å
Crystal system	Triclinic
Space group	P-1
Unit cell dimensions	a = 9.7257(19) Å α= 70.77(3)° b = 10.383(2) Å β= 65.92(3)° c = 10.558(2) Å γ = 70.83(3)°
Volume	895.5(3) $Å^3$
Z	2
Density (calculated)	1.144 Mg/m^3
Absorption coefficient	0.067 mm^{-1}
F(000)	336
Crystal size	0.34 x 0.23 x 0.22 mm^3
Theta range for data collection	2.13 to 26.37°
Index ranges	$-12 \leq h \leq 11$, $-12 \leq k \leq 12$, $-13 \leq l \leq 12$
Reflections collected	7657
Independent reflections	3625 [R(int) = 0.0479]
Completeness to theta = 26.37°	99.0 %
Absorption correction	None
Refinement method	Full-matrix least-squares on F^2
Data / restraints / parameters	3625 / 157 / 267
Goodness-of-fit on F^2	1.071
Final R indices [I>2sigma(I)]	R1 = 0.0535, wR2 = 0.1411
R indices (all data)	R1 = 0.0717, wR2 = 0.1512
Largest diff. peak and hole	0.198 and -0.223 $e.Å^{-3}$

Table 61 Selected bond lengths [Å] and angles [°] of **46**

N(1)–C(1)	1.364(2)	C(1)–N(1)–C(10)	125.79(15)
N(1)–C(10)	1.451(3)	N(2)–C(1)–N(1)	121.93(17)
C(1)–N(2)	1.275(2)	N(2)–C(1)–C(2)	125.55(17)
C(1)–C(2)	1.451(2)	N(1)–C(1)–C(2)	112.52(15)
C(2)–C(3)	1.195(3)	C(3)–C(2)–C(1)	176.65(18)
C(3)–C(4)	1.436(2)	C(2)–C(3)–C(4)	179.07(18)
C(4)–C(5)	1.393(3)	C(5)–C(4)–C(9)	119.58(16)
C(4)–C(9)	1.394(2)	C(1)–N(2)–C(16)	117.4(4)
C(5)–C(6)	1.379(3)		
N(2)–C(16)	1.457(7)		

6. References

[1] S. Cotton, Lanthanide and Actinide Chemistry, John Wiley & Sons, Ltd., Chichester, UK, **2006**.

[2] T. J. Marks, *Organometallics*, **2013**, *32*, 1133.

[3] D. M. Yost, H. Russell, Jr, C. S. Garner, *The Rare Earths and Their Compounds*, Wiley, **1947**.

[4] N. E. Topp, *The Chemistry of the Rare Earth Elements*, Elsevier, **1965**.

[5] C. Elschenbroich, *Organometallics*, Wiley-VCH, ISBN: 3-527-29390-6, **2006**.

[6] F. M. A. Sroor, F. T. Edelmann, *Tetravalent Chemistry: Inorganic*, in: *The Rare Earth Elements: Fundamentals and Applications*, John Wiley & Sons, David A. Atwood, (Ed.), **2012**.

[7] F. M. A. Sroor, F. T. Edelmann, *Tetravalent Chemistry: Organometallic*, in: *The Rare Earth Elements: Fundamentals and Applications*, John Wiley & Sons, David A. Atwood, (Ed.), **2012**.

[8] F. M. A. Sroor, F. T. Edelmann, *Tetravalent Cerium Chemistry in Cerium: Molecular Structure, Technological Applications and Health Effects*, Nova Science Publishers Inc.: Hauppauge, NY, Aleksey Izyumov, Gulnaz Plaksin, (Eds.), **2012**.

[9] M. Gregson, E. Lu, J. Mcmaster, W. Lewis, A. J. Blake, S. T. Liddle, *Angew. Chem*. **2013**, *125*, 13254.

[10] N. A. Piro, J. R. Robinson, P. J. Walsh, E. J. Schelter, *Coord. Chem. Rev*. **2014**, *260*, 21.

[11] J. J. L. Roy, L. Korobkov, J. E. Kim, E. J. Schelter, M. Murugesu, *Dalton Trans*. **2014**, *43*, 2737.

[12] J.-C. Zhang, Y.-Z. Long, X. Wang, C.-N. Xu, *RSC Adv*. **2014**, *4*, 40665.

[13] O. M. D. Lutz, T. S. Hofer, B. R. Randolf, A. K. H. Weiss, B. M. Rode, *Inorg. Chem*. **2012**, *51*, 6746.

[14] A. Ikeda-Ohno, S. Tsushima, C. Hennig, T. Yaita, G. Bernhard, *Dalton Trans*. **2012**, *41*, 7190.

[15] J. R. Robinson, Z. Gordon, C. H. Booth, P. J. Carroll, P. J. Walsh, E. J. Schelter, *J. Am. Chem. Soc*. **2013**, *135*, 19015.

[16] P. B. Hitchcock, A. G. Hulkes, M. F. Lappert, *Inorg. Chem*. **2004**, *43*, 1031.

[17] S. Giessmann, S. Blaurock, V. Lorenz, F. T. Edelmann, *Inorg. Chem*. **2007**, *46*, 8100.

[18] M. P. Coles, P. B. Hitchcock, A. V. Khvostov, M. F. Lappert, Z. Li, A. V. Protchenko, *Dalton Trans*. **2010**, *39*, 6780.

[19] S. Deshpande, S. Patil, S. Kuchibatla, S. Seal, *Appl. Phys. Lett*. **2005**, *87*, 133113/1.

[20] S. Abanades, G. Flamant, *Solar Energy* **2006**, *80*, 1611.

[21] G. A. Silva, *Nat. Nanotechnol*. **2006**, *1*, 92.

[22] F. T. Edelmann, *Chem. Soc. Rev*. **2012**, *41*, 7657.

[23] P. L. Arnold, Z. R. Turner, N. Kaltsoyannis, P. Pelekanaki, R. M. Bellabarba, R. P. Tooze, *Chem. Eur. J*. **2010**, *16*, 9623.

[24] D. R. Lloyd, *J. Chem. Educ*. **1986**, *63*, 502.

[25] S. A. Cotton, *Compt. Rend. Chim*. **2005**, *8*, 129.

[26] V. F. Q. Norambuena, *The Reactivity of Rare-Earth Metallocenes towards Alkynes: Mechanism and Synthetic Applications*, PhD. Thesis, **2006**.

[27] G. Wilkinson, J. M. Birmingham, *J. Am. Chem. Soc*. **1954**, *76*, 6210.

[28] M. Tsutsui, H. J. Gysling, *J. Am. Chem. Soc*. **1969**, *91*, 3175.

[29] R. G. Hayes, J. L. Thomas, *J. Am. Chem. Soc*. **1969**, *91*, 6880.

[30] F. A. Hart, M. S. Saran, *Chem. Commun*. **1968**, 1614.

[31] F. A. Hart, A. G. Massaey, M. S. Saran, *J. Organomet. Chem*. **1970**, *21*, 147.

[32] S. A. Cotton, F. A. Hart, M. B. Hursthouse, A. J. Welch, *Chem. Commun*. **1972**, 1225.

[33] R. E. Maginn, S. Manastyrskyj, M. Dubeck, *J. Am. Chem. Soc*. **1963**, *85*, 672.

[34] M. Tsutsui, N. Ely, *J. Am. Chem. Soc*. **1974**, *96*, 4042.

[35] M. Tsutsui, N. Ely, *J. Am. Chem. Soc*. **1975**, *97*, 3551.

[36] M. Tsutsui, *J. Am. Chem. Soc*. **1975**, *97*, 1280.

[37] F. Mares, K. O. Hodgson, A. Streitwieser, *J. Organomet. Chem*. **1970**, *24*, C68.

[38] F. Mares, K. O. Hodgson, A. Streitwieser, *J. Organomet. Chem*. **1971**, *28*, C24.

[39] F. T. Edelmann, *Adv. Organomet. Chem*. **2008**, *57*, 183.

[40] F. T. Edelmann, *Chem. Soc. Rev*. **2009**, *38*, 2253.

[41] D. A. Kissounko, M. V. Zabalov, G. P. Brusova, D. A. Lemenovskii, *Russian Chemical Reviews*, **2006**, *75*, 351.

[42] A. R. Sadique, M. J. Heeg, C. H. Winter, *J. Am. Chem. Soc*. **2003**, *42*, 7951.

[43] P. B. Hitchcock, M. F. Lappert, D.-S. Liu, *J. Organomet. Chem*. **1995**, *488*, 241.

[44] P. B. Hitchcock, M. F. Lappert, P. G. Merle, *Dalton Trans*. **2007**, 585.

[45] D. M. Grove, G. van Koten, H. J. C. Ubbels, K. Vrieze, L. C. Niemann, C. H. Stam, *J. Chem. Soc. Dalton Trans*. **1986**, 717.

[46] D. J. Brown, M. H. Chisholm, J. C. Gallucci, *Dalton Trans.* **2008**, 1615.

[47] S. Dagorne, R. F. Jordan, V. G. Young, *Organometallics*, **1999**, *18*, 4619.

[48] W. W. Schoeller, A. Sundermann, M. Reiher, *Inorg. Chem*. **1999**, *38*, 29.

[49] S. Aharonovich, M. Kapon, M. Botoshanski, M. S. Eisen, *Organometallics*, **2008**, *27*, 1869.

[50] A. K. Nair, N. V. S. Harisomayajula, Y.-C. Tsai, *Dalton Trans*. **2014**, *43*, 5618.

[51] M. P. Coles, *Dalton Trans.* **2006**, 985.

[52] J. Barker, M. Kilner, *Coord. Chem. Rev.* **1994**, *133*, 219.

[53] K. A. Schug, W. Linder, *Chem. Rev*. **2005**, *105*, 76–113.

[54] M. D. Best, S. L. Tobey, E. V. Anslyn, *Coord. Chem. Rev*. **2003**, *240*, 3.

[55] A. R. Sanger, *Inorg. Nucl. Chem. Lett*. **1973**, *9*, 351.

[56] F. T. Edelmann, *Coord. Chem. Rev*. **1994**, 137, 403, and references cited therein.

[57] P. J. Baily, S. Pace, *Coord. Chem. Rev*. **2001**, *214*, 91.

[58] P. C. Junk, M. L. Cole, *Chem. Commun*. **2007**, 1579.

[59] Z. Zhang, L. Zahng, Y. Li, L. Hong, Z. Chen and X. Zhou, *Inorg. Chem*. **2010**, *49*, 715.

[60] T. Eisenmann, J. Khanderi, S. Schulz, U. Flörke, *Z. Anorg. Allg. Chem*. **2008**, *634*, 507.

[61] C. A.-Moreno, A. Antinolo, F. C.-Hermosilla, A. Otero, *Chem. Soc. Rev*. **2014**, *43*, 3406.

[62] C. Ergezinger, F. Weller, K. Dehnicke, *Z. Naturforsch*., Teil B, **1988**, *43*, 1119.

[63] F. Weller, F. Schmock, K. Dehnicke, *Z. Naturforsch*., Teil B, **1989**, *44*, 548.

[64] A. F. Wells, *Structural Inorganic Chemistry*, Clarendon Press, Oxford, **1984**.

[65] M. G. B. Drew, J. D. Wilkins, *J. Chem. Soc. Dalton Trans*. **1974**, 1579.

[66] R. Kempe, *Z. Anorg. Allg. Chem*. **2010**, *636*, 2135.

[67] F. T. Edelmann, *Homogeneous Catalysis Using Lanthanide Amidinates and Guanidinates*, Struct. Bond, **2010**, *137*, 109.

[68] R. Anwander, in: *Applied Homogeneous Catalysis with Organometallic Compounds*, B. Cornils, W. A. Herrmann, (Ed.), Wiley-VCH, Germany, **2002**, *2*, 974.

[69] Y. Luo, Y. Yao, Q. Shen, J. Sun, L. Weng, *J. Organomet. Chem*. **2002**, *662*, 144.

[70] S. Hamidi, L. N. Jende, H. M. Dietrich, C. Maichle-Mössmer, K. W. Törnroos, G. B. Deacon, P. C. Junk, R. Anwander, *Organometallics* **2013**, *32*, 1209.

[71] V. F. Q. Norambuena, A. Heeres, H. J. Heers, A. Meetsma, J. H. Teuben, B. Hessen, *Organometallics* **2008**, *27*, 5672.

[72] Y. Luo, P. Xu, Y. Lei, Y. Zhang, Y. Wang, *Inorg. Chim. Acta* **2010**, *363*, 3597.

[73] P. Benndorf, J. Jenter L. Zielke, P. W. Roesky, *Chem. Commun*. **2011**, *47*, 2574.

[74] J. Zhang, W. Yi, Z. Chen, X. Zhou, *Dalton Trans*. **2013**, *42*, 5826.

[75] Q. Li, S. Wang, S. Zhou, G. Yang, X. Zhu, Y. Liu, *J. Org. Chem*. **2007**, *72*, 6763.

[76] Z. Du, W. Li, X. Zhu, F. Xu, Q. Shen, *J. Org. Chem*. **2008**, *73*, 8966.

[77] Y. Cao, Z. Du, W. Li, J. Li, Y. Zhang, F. Xu, Q. Shen, *Inorg. Chem*. **2011**, *50*, 3729.

[78] W.-X. Zhang, M. Nishiura, Z. Hou, *J. Am. Chem. Soc*. **2005**, *127*, 16788

[79] S. Collins, *Coord. Chem. Rev*. **2011**, *255*, 118.

[80] T. Zessin, J. Anton, G. Linti, *Z. Anorg. Allg. Chem.* **2013**, *639*, 2224.

[81] D. Li, J. Guang, W.-X. Zhang, Y. Wang, Z. Xi, *Org. Biomol. Chem*. **2010**, 1816.

[82] V. K. Rai, M. Nishiura, M. Takimoto, S. Zhao, Y. Liu, Z. Hou, *Inorg. Chem*. **2012**, *51*, 822.

[83] V. K. Rai, M. Nishiura, M. Takimoto, Z. Hou, *J. Mater. Chem. C* **2013**, *1*, 677.

[84] M. R. Kelley, J.-U. Rohde, *Dalton Trans.* **2014**, *43*, 527.

[85] D. Elorriaga, F. Carrillo-Hermosilla, A. Antinolo, F. J. Suarez, I. Lopez-Solera, R. Fernandez-Galan, E. Villasenor, *Dalton Trans.* **2013**, *42*, 8223.

[86] D. Elorriaga, F. Carrillo-Hermosilla, A. Antinolo, I. Lopez-Solera, B. Menot, R. Fernandez-Galan, E. Villasenor, A. Otero, *Organometallics* **2012**, *31*, 1840.

[87] R. J. Schwamm, B. M. Day, Natalie, E. Mansfield, W. Knowlden, P. B. Hitchcock, M. P. Coles, *Dalton Trans*. **2014**, *43*, 14302.

[88] D. Chartrand, G. S. Hanan, *Inorg. Chem*. **2014**, *53*, 624.

[89] L. Zhang, L. Xiang, Y. Yu, L. Deng, *Inorg. Chem*. **2013**, *52*, 5906.

[90] T. Elkin, M. S. Eisen, *Catalysis Science & Technology*, **2014**.

[91] J. R. Hagadorn, J. Arnold, *Inorg. Chem*. **1997**, *36*, 132.

[92] W.-X. Zhang, M. Nishiura, Z. Hou, *J. Am. Chem. Soc*. **2005**, *127*, 16788.

[93] A. G. M. Barrett, M. R. Crimmin, M. S. Hill, P. B. Hitchcock, S. L. Lomas, M. F. Mahon, P. A. Procopiou, K. Suntharalingam, *Organometallics* **2008**, *27*, 6300.

[94] C. N. Roweley, T.-G. Ong, J. Priem, D. S. Richeson, T. K. Woo, *Inorg. Chem*. **2008**, *47*, 12024.

[95] P. Dröse, C. G. Hrib, F. T. Edelmann, *J. Organomet. Chem*. **2010**, *695*, 1953.

[96] M. L. Cole, G. B. Deacon, C. M. Forsyth, P. C. Junk, D. Polo-Ceron, J. Wang, *Dalton Trans.* **2010**, *39*, 6732.

[97] F. T. Edelmann, *New J. Chem*. **1995**, *19*, 535.

[98] W. W. Seidel, W. Dachtler, T. Pape, *Z. Anorg. Allg. Chem*. **2012**, *638*, 116.

[99] J. Richter, J. Feiling, H.-G. Schmidt, M. Noltemeyer, W. Brüser, F. T. Edelmann, *Z. Anorg. Allg. Chem.* **2004**, *630*, 1269.

[100] X. Zhang, W.-Z. Zhang, X. Ren, L.-L. Zhang, X.-B. Lu, *Org. Lett*. **2011**, *13*, 2402.

[101] X. Xu, J. Gao, D. Cheng, J. Li, G. Qiang, H. Guo, *Adv. Synth. Catal*. **2008**, *350*, 61.

[102] S. Zhou, S. Wang, G. Yang, Q. Li, L. Zhang, Z. Yao, Z. Zhou, H.-B. Song, *Organometallics* **2007**, *26*, 3755.

[103] L. Xu, Y.-C. Wang, W.-X. Zhang, Z. Xi, *Dalton Trans*. **2013**, *42*, 16466.

[104] Y. Wu, S. Wang, L. Zhang, G. Yang, X. Zhu, Z. Zhou, H. Zhu, S. Wu, *Eur. J. Org. Chem*. **2010**, 326.

[105] Z. Du, W. Li, X. Zhu, F. Xu, Q. Shen, *J. Organomet. Chem*. **2008**, *73*, 8966.

[106] W.-X. Zhang, M. Nishiura, Z. Hou, *J. Am. Chem. Soc*. **2005**, *127*, 16788.

[107] W.-X. Zhang, Z. Hou, *Org. Biomol. Chem*. **2008**, *6*, 1720.

[108] C. N. Rowley, T.-G. Ong, J. Priem, D. S. Richeson, T. K. Woo, *Inorg. Chem*. **2008**, *47*, 12024.

[109] R. Duchateau, C. T. van Wee, A. Meetsma, J. H. Teuben, *J. Am. Chem. Soc*. **1993**, *115*, 4931.

[110] F. T. Edelmann, J. Richter, *Eur. J. Solid State Inorg. Chem.* **1996**, *33*, 157.

[111] Z. P. Lu, G. P. A. Yap, D. S. Richeson, *Organometallics* **2001**, *20*, 706.

[112] Y. Luo, Y. Yao, Q. Shen, L. Weng, *Eur. J. Inorg. Chem*. **2003**, 318.

[113] A. A. Trifonov, E. A. Fedorova, G. K. Fukin, M. N. Bochkarev, *Eur. J. Inorg. Chem*. **2004**, 4396.

[114] Y.-M. Yao, Y.-J. Luo, Q. Shen, K.-B. Yu, *Jiegou Huaxue* **2004**, *23*, 391.

[115] X. Pang, H. Sun, Y. Zhang, Q. Shen, H. Zhang, *Eur. J. Inorg. Chem*. **2005**, 1487.

[116] A. A. Trifonov, D. M. Lyubov, E. A. Fedorova, G. K. Fukin, H. Schumann, S. Mühle, M. Hummert, M. N. Bochkarev, *Eur. J. Inorg. Chem*. **2006**, 747.

[117] Y. Yao, Y. Luo, J. Chen, Z. Zhang, Y. Zhang, Q. Shen, *J. Organomet. Chem*. **2003**, *679*, 229.

[118] P. Benndorf, J. Jenter, L. Zielke, P. W. Roesky, *Chem. Commun*. **2011**, *47*, 2574.

[119] G. K. Fukin, I. A. Guzei, E. V. Baranov, *J. Coord. Chem.* **2007**, *60*, 937.

[120] W. Wolfsberger, W. Hager, *Z. Anorg. Allg. Chem.* **1977**, *433*, 247.

[121] H. Schmidbaur, K. Schwirten, H. Pickel, *Chem. Ber*. **1969**, *102*, 564.

[122] A. Recknagel, A. Steiner, M. Noltemeyer, S. Brooker, D. Stalke, F. T. Edelmann, *J. Organomet. Chem*. **1991**, *414*, 327.

[123] V. Lorenz, A. Edelmann, S. Blaurock, F. Friese, F. T. Edelmann, *Organometallics* **2007**, *26*, 4708.

[124] D. Wood, G. P. A. Yap, D. S. Richeson, *Inorg. Chem.* **1999**, *38*, 5788.

[125] Y. Zhou, G. P. A. Yap, D. S. Richeson, *Organometallics* **1998**, *17*, 4387.

[126] J. Päiväsaari, C. L. Dezelah, D. Back, H. M. El-Kaderi, M. J. Heeg, M. Putkonen, L. Niinistö, C. H. Winter, *J. Mater. Chem.* **2005**, *15*, 4224.

[127] B. S. Lim, A. Rahtu, R. G. Gordon, *Nat. Mater.* **2003**, *2*, 749.

[128] B. S. Lim, A. Rahtu, J.-S. Park, R. G. Gordon, *Inorg. Chem.* **2003**, *42*, 7951.

[129] G. R. Giesbrecht, A. Shafir, J. Arnold, *J. Chem. Soc. Dalton Trans.* **1999**, 3601.

[130] W. J. Evans, T. A. Ulibarri, J. W. Ziller, *J. Am. Chem. Soc.* **1990**, *112*, 2314.

[131] L. Bourget-Merle, M. F. Lappert, J. R. Severn, *Chem. Rev.* **2002**, *102*, 3031.

[132] P. G. Hayes, W. E. Piers, R. McDonald, *J. Am. Chem. Soc.* **2002**, *124*, 3132.

[133] M. Schmid, S. M. Guillaume, P. W. Roesky, *Organometallics* **2014**, *33*, 5392.

[134] G. R. Giesbrecht, G. D. Whitener, J. Arnold, *J. Chem. Soc. Dalton Trans.* **2001**, 923.

[135] C. J. Schaverien, *Adv. Organomet. Chem.* **1994**, *36*, 283.

[136] F. T. Edelmann, *Angew. Chem.* **1995**, *107*, 2647; *Angew. Chem. Int. Ed. Engl.* **1995**, *34*, 2466.

[137] S. M. Cendrowski-Guillaume, M. Nierlich, M. Lance, M. Ephritikhine, *Organometallics* **1998**, *17*, 786.

[138] P. Poremba, U. Reißmann, M. Noltemeyer, H.-G. Schmidt, W. Brüser, F. T. Edelmann, *J. Organomet. Chem.* **1997**, *544*, 1.

[139] S. A. Kinsley, A. Streitwieser, A. Zalkin, *Organometallic*, **1985**, *4*, 52.

[140] K. O. Hodgson, F. Mares, D. Starks, A. Streitwieser, *J. Am. Chem. Soc*. **1973**, *85*, 8650.

[141] T. R. Boussie, D. C. Eisenberg, J. Rigsbee, A. Streitwieser, A. Zalkin, *Organometallic* **1991**, *10*, 1922.

[142] W. E. Evans, R. D. Clarck, M. A. Ansari, J. W. Ziller, *J. Am. Chem.Soc.* **1998**, *120*, 9555.

[143] K. O. Hodgson, K. N. Raymond, *Inorg. Chem.* **1972**, *11*, 3030.

[144] K. O. Hodgson, K. N. Raymond, *Inorg. Chem.* **1972**, *11*, 171.

[145] A. Jr. Streitwieser, In *Fundamental and Technological Aspects of Organo-f-Element chemistry*, T. J. Marks, I. L. Fragala, (Eds.); NATO ASI Series D. Reidel: Boston. MA. **1985**, Vol. 155, p. 77.

[146] A. Jr. Streitwieser, T. R. Boussie, *Eur. J. Solid State Inorg. Chem.* **1991**, *28*, 399.

[147] H. Schumann, J. Winterfeld, H. Hemling, F. E. Hahn, P. Reich, K.-W. Brezezinka, F. T. Edelmann, U. Kilimann, M. Schäfer, R. Herbst-Irmer, *Chem. Ber.* **1995**, *128*, 395.

[148] N. C. Burton, F. G. N. Cloke, P. B. Hitchcock, H. C. de Lemos, A. A. Sameh, *J. Chem. Soc. Chem. Commun.* **1989**, 1462.

[149] N. C. Burton, F. G. N. Cloke, S. C. P. Joseph, H. Karamallakis, A. A. Sameh, *J. Organomet. Chem.* **1993**, *462*, 39.

[150] M. Wedler, F. Knösel, U. Pieper, D. Stalke, F. T. Edelmann, H.-D. Amberger, *Chem. Ber.* **1992**, *125*, 2171

[151] V. Lorenz, S. Blaurock, C. G. Hrib, F. T. Edelmann, *Dalton Trans.*, **2010**, *39*, 6629.

[152] H. Schumann, J. Winterfeld, L. Esser, G. Kociok-Köhn, *Angew. Chem., Int. Ed. Engl.*, **1993**, *32*, 1208.

[153] A. Edelmann, V. Lorenz, C. G. Hrib, L. Hilfert, S. Blaurock, F. T. Edelmann, *Organometallics* **2013**, *32*, 1435.

[154] V. Lorenz, B. M. Schmiege, C. G. Hrib, J. W. Ziller, A. Edelmann, S. Blaurock, W. J. Evans, F. T. Edelmann, *J. Am. Chem. Soc.*, **2011**, *133*, 1257.

[155] W. J. Evans, M. A. Johnston, R. D. Clark, R. Anwander, J. W. Ziller, *Plyhedron*, **2001**, *20*, 2483.

[156] U. Reißmann, P. Poremba, M. Noltemeyer, H.-G. Schmidt, F. T. Edelmann, **2000**, *303*, 156.

[157] F. T. Edelmann, D. M. M. Freckmann, H. Schumann, *Chem. Rev.* **2002**, *102*, 1851.

[158] P. W. Roesky, *J. Organomet. Chem.* **2001**, *621*, 277.

[159] S. M. Cendrowski-Guillaume, G. Le Gland, M. Nierlich, M. Ephritikhine, *Organometallics.* **2000**, *19*, 5654.

[160] T. M. Gilbert, R. R. Ryan, A. P. Sattelberger, *Organometallics* **1988**, *7*, 2514.

[161] W. J. Evans, M. K. Takase, J. W. Ziller, A. L. Rheingold, *Organometallics* **2009**, *28*, 5802.

[162] M. K. Takase, N. A. Siladke, J. W. Ziller, W. J. Evans, *Organometallics* **2011**, *30*, 458.

[163] G. W. Rabe, M. Zhang-Preße, G. P. A. Yap, *Inorg. Chim. Acta* **2003**, *348*, 245.

[164] V. Lorenz, S. Blaurock, C. G. Hrib, F. T. Edelmann, *Organometallics* **2010**, *29*, 4787.

[165] M. Arrowsmith, M. R. Crimmin, M. S. Hill, S. L. Lomes, M. S. Heng, P. B. Hitchcock, G. K.-Köhn, *Dalton Trans.* **2014**, *43*, 14249.

[166] X. Gu, X. Zhu, Y. Wei, S. Wang, S. Zhou, G. Zhang, X. Mu, *Organometallics* **2014**, *33*, 2372.

[167] Y. Zhou, Y. Chi, F. Zhao, W-X, Zhang, Z. Xi, *Chem. Eur. J.*, **2014**, *20*, 2463.

[168] F. Zhang, J. Zhang, Y. Zhang, J. Hong, X. Zhou, *Organometallics* **2014**, *33*, 6186.

[169] X. You, S. Yu, Y. Liu, *Organometallics* **2013**, *32*, 5273.

[170] L. Hong, Y. Shao, L. Zhang, X. Zhou, *Chem. Eur. J.* **2014**, *20*, 8551.

[171] T. G. Ong, G. P. A. Yap, D. S. Richeson, *J. Am. Chem. Soc*. **2003**, *125*, 8100.

[172] Q. Li, S. Wang, S. Zhou, G. Yang, X. Zhu, Y. Liu, *J. Org. Chem.* **2007**, *72*, 6763.

[173] Z. Li, M. Xue, H. Yao, H. Sun, Y. Zhang, Q. Shen, *J. Organomet. Chem.* **2012**, *713*, 27.

[174] X. Zhu, Z. Du, F. Xu, Q. Shen, *J. Org. Chem.* **2009**, *74*, 6347.

[175] Y. Wu, S. Wang, L. Zhang, G. Yang, X. Zhu, C. Liu, C. Yin, J. Rong, *Inorg. Chim. Acta* **2009**, *362*, 2814.

[176] R. Jiao, M. Xue, X. Shen, Y. Zhang, Y. Yao, Q. Shen, *Eur. J. Inorg. Chem.* **2010**, *17*, 2523.

[177] C. Qian, X. Zhang, Y. Zhang, Q. Shen, *J. Organomet. Chem.* **2010**, *695*, 747.

[178] C. Liu, S. Zhou, S. Wang, L. Zhang, G. Yang, *Dalton Trans.* **2010**, *39*, 8994.

[179] Y. Cao, Z. Du, W. Li, J. Li, Y. Zhang, F. Xu, Q. Shen, *Inorg. Chem*. **2011**, *50*, 3729.

[180] P. H. Wei, L. Xu, L.-C. Song, W.-X. Zhang, Z. Xi, *Organometallics* **2014**, *33*, 2784.

[181] X. Zhang, C. Wang, C. Qian, F. Han, F. Xu, Q. Shen, *Tetrahedron* **2011**, *67*, 8790.

[182] L. Xu, Z. Wang, W.-X. Zhang, Z. Xi, *Inorg. Chem*. **2012**, *51*, 11941.

[183] J. Tu, W. Li, M. Xue, Y. Zhang, Q. Shen, *Dalton Trans*. **2012**, *42*, 5890.

[184] H. Shen, Y. Wang, Z. Xie, *Org. Lett.* **2001**, *13*, 4562.

[185] L. S. Mao, Q. Shen, J. Sun, *J. Organomet. Chem.* **1998**, *566*, 9.

[186] J. H. Freeman, M. L. Smith, *J. Inorg. Nucl. Chem*. **1958**, *7*, 224.

7. Liste der Veröffuntlichungen

Journals

- F. M. A. Sroor, C. G. Hrib, L. Hilfert, F. T. Edelmann, "*Lithium-cyclopropylethinylamidinates*" Z. Anorg. Allg. Chem. **2013**, *639*, 2390.

- F. M. Sroor, C. G. Hrib, L. Hilfert, P. G. Jones, F. T. Edelmann*, "Lanthanide(III)-bis(cyclopropylethinylamidinates): Synthesis, structure, and catalytic activity" J. Organomet. Chem.* **2015***, 785, 1.*

- F. M. Sroor, C. G. Hrib, L. Hilfert, S. Busse, F. T. Edelmann, *"Synthesis and Catalytic Activity of Homoleptic Lanthanide-tris(cyclopropylethinyl)amidinates" New J. Chem.* **2015**, in print.

- F. M. Sroor, C. G. Hrib, L. Hilfert, F. T. Edelmann, "*Synthesis and Structural Characterization of an Unusual Heterometallic Europium(III) Amidinate Complex*" *Z. Anorg. Allg. Chem.* **2015**, in print.

- F. M. Sroor, C. G. Hrib, L. Hilfert, F. T. Edelmann, "*Five different types of organolanthanide half-sandwich complexes from one ligand set*" *J. Am. Chem. Soc.* **2015**, in preparation.

- F. M. Sroor, C. G. Hrib, L. Hilfert, L. Hartenstein, P. W. Roesky, F. T. Edelmann, "*Synthesis and structural characterization of new bis(alkynylamidinato)-lanthanide(III)-amides*" *J. Organomet. Chem.* **2015**, in press.

- F. M. Sroor, C. G. Hrib, F. T. Edelmann, "*Synthesis and structure of* $[Ph_2P(NSiMe_3)_2]_2Ce(\mu\text{-}Cl)_2Li(THF)_2$" Acta Cryst. 2015, in press

Book (Chapters)

- F. M. A. Sroor, F. T. Edelmann, *Tetravalent Chemistry: Inorganic* In: *The Rare Earth Elements: Fundamentals and Applications*, John Wiley & Sons, **2012**, ISBN-10: 111995097X, David A. Atwood (Ed.).

- F. M. A. Sroor, F. T. Edelmann, *Tetravalent Chemistry: Organometallic* In: *The Rare Earth Elements: Fundamentals and Applications*, John Wiley & Sons, **2012**, ISBN-10: 111995097X, David A. Atwood (Ed.).

- F. M. A. Sroor, F. T. Edelmann, *Tetravalent Cerium Chemistry* In: *Cerium: Molecular Structure, Technological Applications and Health Effects,* Nova Science Publishers Inc.: Hauppauge, NY, **2012**, ISBN-10: 1522576705, Aleksey Izyumov, Gulnaz Plaksin (Eds.).

Lebenslauf

Persönliche Daten

Name	Farid Mohamed Ahmed Sroor
Geburtsdatum	01.04.1982
Geburtsort	Sohag, Ägypten
Familienstand	verheiratet
Staatsangehörigkeit	Ägyptisch

Schulausbildung

1988 – 1994	Khaled Ibn-Elwaleed Grundschule in Sohag
1994 – 1996	Al-Bindar Grundschule in Sohag
1996 – 1999	Abd-Elazez Abd-Elkareem-Gymnasium in Sohag
1999	Abitur am Abd-Elazez Abd-Elkareem-Gymnasium in Sohag

Studium

August 1999 – Mai 2003	Bachelorstudium der Chemie an der Universität Sohag
Mai 2003	Bachelor der Chemie mit Note "sehr gut" an der Universität Sohag
2003 – 2004	Diplomhauptprüfung in Chemie mit Note "sehr gut" an der Universität Minia
2004 – 2006	Masterarbeit in Chemie an der Universität Kairo und der Universität Minia
Januar 2007	Master der Chemie an der Universität Minia
2007–2010	Wissenschaftlicher Mitarbeiter am National Research Center (NRC) in Kairo
Seit April 2011	Arbeit an der Dissertation bei Prof. Dr. Frank. T. Edelamnn am Chemischen Institut der Otto-von-Guericke-Universität Magdeburg

Berufstätigkeit

Seit 2007	Wissenschaftlicher Mitarbeiter am National Research Center (NRC) in Kairo

Sonstiges

Oktober 2010 – März 2015	Graduiertenstipendiat des DAAD (Deutscher Akademischer Austausch-Dienst)